FAILURE CRITERIA AND CUMULATIVE DAMAGE IN FATIGUE UNDER MULTI-AXIAL STRESS CONDITIONS

DONALD LOWSON McDIARMID

A thesis presented for the degree
of Doctor of Philosophy of The
City University

Department of Mechanical Engineering
The City University, London.

June 1972

ABSTRACT

Previous investigations into fatigue under multiaxial stress, and also cumulative damage under uniaxial stress, are discussed in conjunction with the parameters relevant to the present experimental investigation.

A biaxial fatigue machine is described which can subject thin wall tubes to combinations of fluctuating internal pressure and either fluctuating longitudinal tension or compression covering the complete + + and + - stress quadrants. The machine is also provided with independent eight stage programmers in both pressure circuits.

Constant amplitude fatigue tests have been carried out on thin wall aluminium alloy (2L65) tubular specimens over the complete + + and + - stress quadrants.

A new equation for predicting the fatigue failure of ductile metals under multiaxial stress is proposed based on the maximum range of shear stress modified for the effects of the normal stress acting on the maximum shear stress plane and of anisotropy. This equation is shown to give excellent agreement with all published data on fatigue under uniaxial stress and multiaxial stress viz. combined bending and twisting and thin and thick wall cylinder data. A simplified equation, neglecting the effect of the range of normal stress, is suggested for design purposes.

Two level biaxial block programme tests, at constant and two step principal stress ratio, have also been carried out on the same aluminium alloy. The results of these tests are discussed with reference to the cumulative damage theories of failure developed for the case of uniaxial fatigue stress.

A new approach to fatigue analysis is suggested.

TABLE OF CONTENTS

LIST OF TABLES

LIST OF FIGURES

LIST OF PLATES

NOMENCLATURE

f	=	Amplitude of direct stress due to bending
q	=	Amplitude of shear stress due to twisting
b	=	Fatigue limit (direct stress) under reversed bending stress only
t	=	Fatigue limit (shear stress) under reversed torsional stress only
K	=	Ratio of transverse stress to longitudinal stress
k	=	Ratio of outer diameter to inner diameter of cylinder
σ	=	Normal stress
τ	=	Shear stress
τ_a	=	Shear stress amplitude on a maximum shear stress plane
$\sigma_1, \sigma_2, \sigma_3$	=	Principal stresses
$\sigma_H, \sigma_L, \sigma_R$	=	Principal stresses in the hoop, longitudinal and radial directions
HL, LR, RH	=	Maximum shear stress planes
$\tau_{HL}, \tau_{LR}, \tau_{RH}$	=	Maximum shear stresses in a cylinder
σ_τ	=	Normal stress amplitude on a maximum shear stress plane
$\sigma_{HL}, \sigma_{LR}, \sigma_{RH}$	=	Normal stress amplitudes on planes of maximum shear stress
$\sigma_{M\tau}$	=	Mean normal stress on the maximum shear stress plane
D	=	Fraction of damage; at failure $D = 1$
i	=	Particular step in sequence of steps of different stress amplitudes in a programme load test
n_i	=	Number of cycles of operation under conditions of the ith step of programme
N_i	=	Number of cycles required to produce failure under conditions of ith step of programme
n	=	Number of stress cycles
N	=	Number of stress cycles to failure
S_1, S_2, S_3	=	Stress amplitudes (maximum principal stress) in programme tests on thin wall tubes
n_1, n_2, n_3	=	Number of stress cycles at S_1, S_2, S_3

N_1, N_2, N_3	=	Number of stress cycles to failure at S_1, S_2, S_3
S_0, $S_{7.9}$, S_{-1}	=	Stress amplitudes (maximum principal stress) at K = 0, 7.9 and -1
N_0, $N_{7.9}$, N_{-1}	=	Number of cycles to failure at K = 0, 7.9 and -1
S	=	Maximum shear stress amplitude, under combined bending and twisting
S_G	=	Maximum shear stress amplitude as defined by the Gough ellipse quadrant equation
$S_{0.5,\ 1.0,\ldots.\ 5.0}$	=	Maximum shear stress amplitudes at values of n of 0.5, 1.0 ... 5.0
$P.D._n$	=	Percentage difference of calculated value of S_n with experimental value S
$C_{1,2\ldots}$	=	Material constants
σ_A	=	Reversed uniaxial fatigue strength
σ_D	=	Repeated (pulsating) tensile fatigue strength
τ_A	=	Reversed pure shear fatigue strength
n	=	Constant 0.5, 1.0 ... 5.0 in S_n
σ_u	=	Ultimate tensile strength (U.T.S.)
σ_y	=	Yield stress
$\bar{A}$	=	Anisotropy factor equal to the ratio of the fatigue strength in the transverse direction to the fatigue strength in the longitudinal direction
X	=	Damage exponent which varies with alternating stress level
F_1, F_2	=	Interaction factors
E	=	Young's Modulus of Elasticity
ν	=	Poisson's Ratio
ϵ	=	Strain
Endurance ratio	=	Reversed uniaxial fatigue strength/U.T.S.
θ	=	Angular orientation of loading measured from the bending direction in a combined bending and twisting test
L-H test	=	Single step test in which the pre-stress is lower than the test stress

H-L test = Single step test in which the pre-stress is higher than the test stress

Programme test = Test in which the stress amplitude is changed repeatedly according to a fixed sequence. The number of stress cycles between repetitions of the pattern is called the 'programme cycle'

Pulsating or repeated stress = Stress cycling from zero to a maximum

Subscripts

H, L, R = Principal stress directions in a cylinder

HL, LR, RH = Maximum shear stress planes

M = Mean or superimposed static stress

a = Stress amplitude

A = Stress amplitude with zero mean stress

Standard Deviation = $\frac{\sqrt{\bar{N}-1}}{\bar{N}}$ x (Mean percentage difference)

$\bar{N}$ = Number of combined bending and twisting conditions

GENERAL INTRODUCTION AND SUMMARY

The great majority of engineering components in service are subjected to complex non-constant states of stress. A survey of the literature shows that there is only a limited amount of data on fatigue under constant amplitude multiaxial stress and virtually none under non-constant amplitude multiaxial stress. The designer thus has to design for these service conditions using uniaxial fatigue data and the static properties of the material along with some criterion of fatigue failure. At the present time there are criteria of fatigue failure available for limited multiaxial stress conditions, such as the Gough ellipse quadrant for combined bending and twisting, but no general criterion which shows agreement with all the published multiaxial fatigue test data, including that under combined bending and twisting and the data on thin and thick wall tubes under internal pressure and end load. A new equation is developed and presented in this work which purports to remedy this situation.

Before any non-constant amplitude investigation under multiaxial fatigue stress can be contemplated, constant amplitude multiaxial fatigue stress data is required. The acquisition of constant amplitude fatigue data over the complete range of principal stress ratios of the + + and + - stress quadrants involves a formidable amount of testing but it also serves to substantiate, or otherwise, any criterion of fatigue failure developed. The testing of thin wall tubes under fluctuating internal pressure and fluctuating end load is at present the most convenient way of obtaining fatigue data over the widest range of principal stress ratio.

Thin wall tubes also offer other advantages in that the principal stresses are always in the same directions and the stress situation is almost biaxial, as the radial stress (internal pressure) is small compared with the other stresses, as is the case in many design situations. Also a relatively large volume of test material is subjected to the maximum stress conditions and stress gradient effects are small.

A special test machine had to be designed to subject thin wall tubes to this wide range of principal stress ratio. A servo hydraulic system was chosen for its good response to input signal and high operating speed, bearing in mind the contemplated non-constant amplitude tests and also the possible later extension to random load work. The longitudinal stress on the thin wall tubes was achieved using a differential piston device. The applied stress capability is essentially one way, that is none of the applied stresses can go through zero.

The proposed criterion of fatigue failure has been based on the physical concept of maximum shear stress amplitude as the main parameter with the effect of the normal stress acting on the maximum shear stress plane and anisotropy as secondary parameters. The relative effect of these parameters has been obtained using an empirical approach in analysing published test data.

As the field of non-constant amplitude multiaxial stress fatigue was unexplored it was decided to conduct a series of relatively simple two stage block programme tests at each of four principal stress ratios. The aluminium alloy tested was found to be anisotropic and two principal stress ratios were chosen where the maximum shear stress occurred on the isotropic and anisotropic

maximum shear stress planes respectively, thus investigating the effect of principal stress ratio and anisotropy under non-constant amplitude multiaxial fatigue stress. A small number of exploratory programme tests were also conducted where the principal stress ratio varied in a two stage manner.

The proposed criterion of fatigue failure is intended for use with any ductile metal under any multiaxial stress system including the effect of mean stress. Methods of allowing for material anisotropy have also been suggested. A simplified form of the criterion has also been proposed for design purposes. In both cases only one fatigue strength and the U.T.S. are required.

A first investigation of cumulative damage under multiaxial stress has been conducted and the results discussed with reference to published data and theory on cumulative damage under uniaxial stress.

A new approach to fatigue analysis has been suggested based on the work reported in this thesis.

The thesis is in three sections as follows:

PART I Summary of previous investigations into fatigue under multiaxial stress and discussion of cumulative damage in fatigue under multiaxial stress.

PART II Experimental work. Design and development of a biaxial fatigue machine, fatigue tests and discussion of results.

PART III Development of criteria of fatigue failure under multiaxial stress and comparison with published experimental data. Also comparison of cumulative damage results with uniaxial cumulative damage theories.

PART I

SUMMARY OF PREVIOUS INVESTIGATIONS INTO FATIGUE UNDER MULTIAXIAL STRESS AND DISCUSSION OF CUMULATIVE DAMAGE IN FATIGUE UNDER UNIAXIAL STRESS

Chapter 1 is a summary of previous investigations into fatigue under multiaxial stress covering combined bending and twisting and investigations using thin-wall and thick-wall tubular specimens. The various criteria of failure so far proposed are also discussed with special reference to the parameters considered and the generality, or otherwise, of their possible application.

As there has only been one very limited investigation of cumulative damage under multiaxial stress conditions the topic of cumulative damage under uniaxial stress is discussed in Chapter 2 with reference to the more important parameters involved and several of the more basic of the many cumulative damage theories proposed in the literature.

CHAPTER 1

PREVIOUS WORK ON FATIGUE UNDER MULTIAXIAL STRESS

1.1 Introduction

The general state of stress is as indicated in Fig. 1, where the stress histories in the three orthogonal directions at a point in a component are random, and can be reduced to a system of three principal stresses in three orthogonal directions at fixed orientations to the general stress planes at any instant in time. In the general case shown in Fig. 1 the principal stress axes will rotate with time.

It is only within the last ten years that the problem of fatigue under uniaxial random stress has seen more intensive investigation, due to the advent of the servo-hydraulic fatigue test machine with its high rate of response enabling random stress histories to be simulated in the laboratory.

At present only a very limited amount of fatigue testing has been conducted under multiaxial stress conditions, mainly due to the difficulties involved in testing under these more complex stress conditions. With one exception these tests have all been under conditions of constant stress amplitude.

Most service failures in fatigue start on a free surface, as in many cases the most severe conditions exist there and are of a biaxial stress nature such as a drive shaft under combined bending and twisting. This particular case of multiaxial stress fatigue, because of its importance in design, has seen considerable investigation although several aspects of the stress situation complicate the analysis of the test results with regard to the development of a general

criterion of fatigue failure under multiaxial stress. The principal stress axes rotate with variations in the ratio of bending to twisting and the shaft is subjected to a stress gradient. Only the extreme portions of the shaft in the plane of bending are under the maximum bending stress whereas the complete surface of the shaft is subjected to the maximum torsion stress. The stress gradient through the shaft will be a function of the shaft diameter and only a small volume of the test specimen is subjected to the maximum stress conditions. Further difficulties of analysis arise if the shaft is made of an anisotropic material as it is then difficult to separate the effects of state of stress from the effects of material anisotropy.

The testing of thin wall tubes under varying internal pressure and end load leads to a more simple state of stress and also allows a much larger range of biaxial stress ratio to be investigated. The principal stress axes are always radial, longitudinal and tangential and there is very little stress gradient through the thin wall of the tube. The most severely stressed position is at the inside face of the tube wall where a three-dimensional state of stress exists. For thin wall tubes the radial stress, which is equal to the internal pressure, will be small compared with the hoop and longitudinal stresses. Most test data on tubes is for pulsating stress conditions between zero and a maximum stress.

1.2 Combined Bending and Twisting

1.2.1 Alternating bending with superimposed static torsion

The first experiments of this type were reported by Ono (1) in 1921. The bending fatigue limits of ingot iron and a 0.3% carbon steel were raised slightly by the superimposition of a moderate torsion, but this had no effect on a 0.25% carbon steel.

Similar tests by Lea and Budgen (2) on three steels showed that the addition of a static torsion stress to reversed bending stresses causes a slight increase in endurance limit for nominal torsion stresses up to 50% above the yield stress followed by a marked reduction at higher stresses.

From the work of Nimhanminne (3) and Huitt (4) on two steels, it was suggested by Davies in the discussion of Gough and Pollard (5) that, up to the point where failure occurred by static yielding, the bending fatigue limit was reduced by the static torsional stress according to the equation

$$\frac{p^2}{P^2} + \frac{q}{Q} = 1 \qquad (1.1)$$

where $\pm P$ is the fatigue limit under reversed bending stress only, Q is the static ultimate shear strength of the material and $\pm p$ is the reversed bending fatigue limit when the superimposed static shear stress is q. The validity of the results of Nimhanminne and Huitt is questioned by Sines (6) who suggests that the equipment used also applied a static bending stress.

Capper (7) discusses a number of possible relations between alternating bending stress and static shear stress and compares them with the results of other experimenters.

Tests by Gough (8) on a high Ni Cr Mo steel showed that the alternating bending stress at the endurance limit decreased by about 8% for applied static torsion stress below the yield point.

1.2.2 Alternating torsion with superimposed static bending

Hohenemser and Prager (9) investigated a dead-mild steel under these stress conditions. The superimposed stress caused an increasing drop in the torsional fatigue limit, up to the point where yielding occurred, according to the ellipse quadrant relation

$$\frac{S^2}{q^2} + \frac{P^2}{f^2} = 1 \qquad (1.2)$$

where f is the ultimate tensile stress

P is the superimposed static tensile stress

$\pm q$ is the range of shear stress at the fatigue limit under reversed torsional stress, and

$\pm S$ is the range of shear stress at the fatigue limit under combined stresses.

They obtained about 25% reduction in the torsional fatigue limit with a static axial stress of approximately 75% of the ultimate tensile strength.

Sines (6) tested aluminium alloy under alternating torsion with a superimposed static compressive stress and found that a static compressive stress of approximately half the ultimate tensile strength increased the allowable alternating torsional stress by about 15%.

1.2.3 Alternating torsion with superimposed static torque

Although not combined bending and twisting the effects of this stress condition is included in this section for convenience.

Smith (10) has shown from the collected results of a large number of tests on both ferrous and non-ferrous materials that a static torque superimposed on an alternating shear stress has very little effect as long as the maximum stress does not exceed the yield stress.

1.2.4 Combined alternating bending and alternating twisting

The first tests of this type were conducted by Stanton and Batson (11) in 1916 on a dead mild steel using six combinations of cyclic bending and torsional stresses. The results of these tests were in good agreement with a constant value of the maximum shear stress amplitude.

Tests under combined bending and twisting were started by Gough, Pollard and Clenshaw in 1932, the final report (12) being published in 1951. Some of the work was published earlier in parts (5, 8, 13). This work is by far the most extensive test series so far conducted under conditions of multiaxial stress consisting of tests on twelve steels, ranging from a 30/35 tonf/in^2 low carbon nickel steel to a 95/105 tonf/in^2 air-hardening chromium steel, and two cast irons. The test programme covered notched and un-notched specimens with and without mean stress. It was found that the resistance of the ductile steels under combined bending and twisting fatigue stresses in the case of solid or hollow cylindrical specimens agreed with an empirical ellipse quadrant equation of the form

$$\frac{f^2}{b^2} + \frac{q^2}{t^2} = 1 \qquad (1.3)$$

where $\pm f$ is the range of direct stress due to bending

$\pm q$ is the range of shear stress due to torsion

$\pm b$ is the fatigue limit (direct stress) under reversed bending stress only and

$\pm t$ is the fatigue limit (shear stress) under reversed torsional stresses only.

The resistance of the cast irons and of the ductile steels with stress concentrations in the form of notches and holes was found to agree with an empirical ellipse arc equation of the form

$$\frac{q^2}{t^2} + \frac{f^2}{b^2}\left[\frac{b}{t} - 1\right] + \frac{f}{b}\left[2 - \frac{b}{t}\right] = 1 \qquad (1.4)$$

where the symbols have the same meaning as in the ellipse quadrant equation. In the case of tests on the ductile steels with superimposed static bending or torsional stresses it was found that, by interpolation, the range of stress correspondence to any required intermediate values of static bending and/or torsional stresses between the limits investigated could be deduced. The amount of the reduction, caused even by static stresses which were quite high in relation to the ultimate tensile strength of the material, was relatively small. The effect of superimposing static bending stresses on cyclic torsional stresses was more damaging than that of static torsional stresses imposed on cyclic bending stresses.

A study of SAE 4634 steel by Narmore (14) under combined bending and twisting alternating stresses showed that the test data gave good agreement with the ellipse quadrant equation.

Nishihara and Kawamoto (15) tested three carbon steels, an alloy steel, a cast-iron, two durals and a brass and developed mathematical relations for the fatigue strengths of the materials.

They also tested (16) two steels, a cast-iron and an aluminium alloy under alternating bending and torsion with a phase difference. The combined stress fatigue strengths with the torsion and bending out of phase were never less than the in-plane fatigue strengths. The maximum differences, occurring at a phase difference of 90° being about 10% for the steels, 30% for the cast irons, there being no difference for the aluminium alloy.

The results of tests by Sauer (17) on 14S-T aluminium alloy under one ratio of torsion to bending agreed with the maximum shear stress failure criterion.

Findley (18-29) has also been active in the field of fatigue under combined bending and twisting. This work consists largely of a theoretical study of theories of failure under static stress as applied to the case of fatigue stress conditions with correction for material anisotropy and experimental work attempting to corroborate some of the theoretical conclusions. The overall conclusion is that the maximum shear stress theory, modified for material anisotropy and the effect of the normal stress acting on the plane of maximum shear stress, gives the best correlation with test data. It was also shown theoretically that energy theories of failure were unlikely to be applicable to the fatigue situation and experiments conducted to prove the point (29).

1.3 Thin-walled tubes subjected to internal pressure

Combinations of bending and torsion give a limited range of biaxial principal stress ratio between 1 : 0 and 1 : -1. A much wider range of principal stress ratio can be investigated using thin wall tubes under fluctuating internal pressure and end load. Only a limited amount of test data under such stress conditions is available and most of this is in the ++ quadrant of the biaxial stress diagram where it is more difficult to differentiate between different criteria of fatigue failure. The thin wall tubular specimens required for such tests are expensive to produce in the quantity required for fatigue testing and also difficult to load in the desired manner; they do however offer several major advantages as mentioned in the introduction to this chapter. The tubes are subjected to fluctuating internal pressure and also a synchronised fluctuating axial load produced by either (a) a lever system (32, 33, 34, 36, 37) or

(b) by a longitudinal pressure load system (35, 39). Until recently all fatigue tests on thin wall tubes had been under conditions of pulsating stress.

The first reported fatigue tests on thin-walled tubes were those of Maier (30) in 1934 carried out on 33 mm diameter steel, brass and cast iron tubes under pulsating internal pressure at 330 c.p.m. up to 2×10^6 cycles. These tests were at K (equal to the ratio of transverse stress to longitudinal stress) values of 2 and ∞; in the latter case the longitudinal stress was suppressed by supporting the ends of the tube. Maier suggested from these tests that the principal stress ratio was not important and that the maximum principal stress theory may apply. As both the test conditions used are in the ++ quadrant the maximum shear stress theory would give the same result.

Marin (31) described a test machine of the type (a) mentioned above and reported the results of pulsating stress tests on SAE 1020 steel specimens of 1.1 inch diameter at a value of K = 1. From the few test results obtained it was suggested that "the fatigue strength is not influenced by the presence of a biaxial state of equal stress".

Morikawa and Griffis (32) used the same test machine as Marin to test SAE 1020 steel specimens of 1.0 inch inside diameter and 0.050 inch wall thickness in the welded, unwelded, annealed and normalised states. Tests were performed at values of K = 0, 1/5, ½, 1 and 2 under conditions of pulsating stress. The authors concluded that there was only a slight effect of principal stress ratio upon the endurance limit of this steel. The maximum principal stress criterion of failure (again the same as the maximum shear stress criterion for the range of K values used) was shown to apply for this material, modified by the anisotropy of the bar stock. The transverse endurance limit was found to be 15% lower than the longitudinal endurance limit. The slow speed, 300 c.p.m. of this machine was found to be a considerable handicap in running to 3×10^6 cycles.

Marin and Shelson (33), again using the same test machine tested 24S-T aluminium alloy at values of K = 0, ½, 1 and 2. They found that the uniaxial fatigue strength in the transverse direction could be as low as 60% that in the longitudinal direction and that the biaxial fatigue strength could be as low as 50% of the uniaxial longitudinal fatigue strength. Anisotropy was the predominant effect found in these tests which made it difficult to find agreement with any failure criterion.

Ros and Eichinger (34) used a machine of type (a) to test two steels, two weld metals, two aluminium alloys and a pure aluminium at values of K = 0, ½, 1, 2, ∞, -1 and -0. The tests, under pulsating

stress conditions were run at a speed of 250 c.p.m. up to 10^6 cycles. They concluded that the Coulomb-Mohr hypothesis gave the best agreement with test results.

A different type of loading system was used by Majors, Mills and McGregor (35). They used different configurations of pressure heads, so that only one pulsator was required, to test annealed SAE 1020 steel specimens of 1.00 inch inside diameter and 0.05 inch wall thickness under in-phase pulsating stress conditions at values of $K = 1.04$, 1.84, 40 and -1.27. Tests were conducted at 880 c.p.m. up to 10^7 cycles. They concluded that the distortion energy criterion gave the best agreement with the test results.

Marin and Hughes (36) tested 14S-T4 aluminium alloy specimens of 1.00 inch inside diameter and 0.05 inch wall thickness at values of $K = 0, \frac{1}{2}, 1$ and 2 in the Marin (31) test machine. Tests were conducted at 300 c.p.m. up to 5×10^6 cycles using pulsating stress conditions. The fatigue strength was affected by anisotropy, the transverse fatigue strength being approximately 65% of the longitudinal fatigue strength. The test results were found to give reasonable agreement with the maximum shear stress criterion modified for anisotropy. This work was continued by Bundy and Marin (37) for values of $K = \infty, -1$. A modified energy theory was proposed but the limited amount of test data available was insufficient to test the validity of the theory.

Cox and Owen (38) tested thin wall cyclinders subjected to static internal pressure with superimposed alternating direct stress, bending or torsion. Three aluminium alloys and a mild steel were tested, the specimens having an outside diameter of 0.625 inch and wall thickness of 0.015 inch. They concluded that in the case of alternating direct or bending stress that a high hoop stress due to internal pressure did not

reduce the endurance under high fatigue stresses; however under alternating torsion, internal pressure did markedly reduce the life of the specimens. The internal pressure was produced by either gas or oil.

A recent investigation on a low carbon steel by Rotvel (39) is particularly interesting as it used a pressure test rig capable of maintaining zero mean stress on both the transverse and the longitudinal stresses. The specimens used were 110 mm internal diameter and 2.2 mm wall thickness and tests were conducted over a range of K = 0, 0.8, 1.3 ∞, -0.75, -1.25 at a speed of 500 c.p.m. up to 2×10^6 cycles. It was found that the test data at zero mean stress did not give good agreement with failure criteria containing only one material constant, the best agreement being obtained with the total strain energy criterion. The test data was however found to give good agreement with both the octahedral stress criterion proposed by Crossland (40) and also a criterion proposed by Stanfield (41); both of these criteria contain two material constants and are discussed later.

Booth (42) tested aluminium alloy specimens of 0.875 inch internal diameter and 0.020 inch wall thickness in a test machine capable of imposing a fluctuating internal pressure at any phase relative to a fluctuating axial compressive load, with a variable pressure wave form. Tests were conducted under conditions of constant strain energy involving relatively large fluctuations in shear stress. Fatigue failures were experienced showing that energy conditions are not a criteria of fatigue failure.

Other examples of pressure testing equipment used to subject thin walled tubes to biaxial fatigue stress conditions are described by Crosby, Burns and Benham (43) and Havard and Topper (44). As both these items of test equipment are of slow operating speed, 1/6 Hz and 3 Hz

respectively, they have been used to investigate high-strain fatigue in the region of 10^3 to 10^5 cycles.

1.4 Thick-walled tubes subjected to internal pressure

Morrison and others (40, 45-49) have conducted extensive tests on thick cylinders of 1 inch bore and wall thickness varying from 0.1 to 1 inch in a special test machine (45) designed to apply the high pressures required. This machine applied pulsating internal pressure up to 25 tonf/in^2 to the thick wall cylinders under closed end conditions at 500 c.p.m. up to 10^7 cycles. The materials tested included a mild steel, a 3% chromium steel, an alloy steel (En 25), an austenitic steel, a nearly pure titanium and a light alloy. The results were found to depend mainly on the range of maximum shear stress applied. For both the thick cylinders tested here and the thin walled tube tests described earlier the allowable range of maximum shear stress is about one third of the tensile strength for steel and one quarter of the tensile strength for aluminium alloy. It was also found that the shear fatigue strength of the thick cylinders were only about half the values of the reversed torsion fatigue strength of solid specimens; this is partly due to the effect of the normal stress acting on the maximum shear stress planes in the case of the thick cylinders. The high pressure oil in direct contact with the inside wall of the thick cylinders has an effect which is difficult to quantify. Attempts have been made to protect the bores of the cylinders with plastic liners leading to considerable strengthening effects.

Tests on thick walled tubes have also been used to investigate the possible influence of the intermediate principal stress on fatigue under triaxial stress. Blass and Findley (50) conducted these tests on AISI 4340 steel using a Morrison type test machine modified to allow

a pulsating axial tension or compression to be applied in phase with the pulsating internal pressure. The maximum and minimum principal stresses were maintained constant while five different values of the intermediate principal stress were employed. The results showed no effect of the intermediate principal stress. It should however be noted that the steel used in these tests shows little effect of the normal stress acting on the critical shear plane, whereas some other metals such as aluminium alloys show a strong effect (28).

The effect of mean shear stress on the fatigue behaviour of thick-walled cylinders has been investigated by Burns and Parry (51) for EN 25 steel again using the Morrison type test machine. It was found that for the life range of 10^6 to 10^7 cycles the fatigue strength was dependent on the maximum range of bore shear stress and the associated mean shear stress, the fatigue strength increasing as the bore mean shear stress decreased. It was also noted that the lack of correlation of cylinder, torsion and push-pull fatigue data showed that other as yet unknown factors were involved. One of these factors is possibly the effect of the high pressure oil in contact with the cylinder bore surface.

Marsh and Haslam (52) describe equipment for applying pulsating internal oil pressure to thin-walled large diameter (8 inch) tubes and also other equipment for applying a much higher pulsating oil pressure as well as static or cyclic end loads to thick walled cylinders. The latter test machine is based on the Morrison (48) type test machine. Preliminary test results tend to agree with the maximum shear stress criterion at the fatigue limit as proposed by Morrison, but this criterion is only valid as long as the combined effect of the pressurised oil and the cyclic hoop stress, on the shear stress at the bore, is constant.

The problem of the effect of high pressure oil in the bore surface microcracks of thick walled cylinders is studied by Haslam (53). He proposed that the apparently low shear stress at the fatigue limit of thick-walled cylinders, as found by Morrison and other investigators is due to the cumulative effect of the high pressure oil and the combined stress conditions.

An empirical method of predicting the fatigue limit of such cylinders from a knowledge of the transverse uniaxial fatigue strength of the material and the diameter ratio of the cylinder is given in (54) and later developed (55) to provide complete theoretical fatigue curves, using fracture mechanics theory. In this method the oil effect is catered for by assuming that the effective hoop stress σ_e may be written as

$$\sigma_e = \sigma_t + n P$$

where σ_t is the hoop stress derived from the Lamé equation, and describes the effect of the oil in contact with the bore surface. The oil effect function n is determined from the empirical equation

$$n = \frac{5}{k+1}$$

where k = outer/inner diameter ratio of the cylinder. It should be noted that $n > 1$ where $k < 4$.

Crossland (40) investigated the effect of hydrostatic pressure up to 20 tonf/in^2 applied to solid steel (En 25) test specimens subjected to reversed torsion. The results for tests on unprotected specimens subjected to 20 tonf/in^2 pressure was almost the same as for specimens tested at atmospheric pressure in air or oil, except that there was no knee in the S-N curve. Specimens protected by a thin film of rubber under the same stress conditions gave an increase of 32% in the alternating torsional stress fatigue limit. Using the results of the

protected specimens it was suggested that the test data could be correlated on the basis of a Mises stress function modified by the maximum volumetric tensile stress acting.

Burns and Parry (56) extended these tests partly to investigate the results of dynamic yielding in the Crossland tests. Similar results to those of Crossland were obtained. Tests on protected specimens with hydrostatic pressures of 10, 15, 20 and 25 tonf/in^2 showed approximately a linear increase in torsional stress amplitude with increase in hydrostatic pressure. It was concluded that a hydrostatic pressure improves fatigue behaviour by applying a compressive stress on the planes of maximum shear stress thus inhibiting the growth of fatigue cracks.

White, Crossland and Morrison (47) subjected steel (En 25) specimens to fluctuating direct stress with tensile or compressive mean stress, at atmospheric pressure or with a superimposed fluid pressure of 20 tonf/in^2, the specimens being protected with a rubber coating in both cases. A fluid pressure of 20 tonf/in^2 increased the range of reversed stress to cause failure by 7% at the fatigue limit.

1.5 Miscellaneous Tests

Sawert (57) used different forms of specimens to obtain test results for a range of principal stress ratios. The specimen shapes used included notched shafts in bending and thin discs subjected to both alternating axial and transverse loads. These tests were under conditions of zero mean stress. Two steels were tested and it was concluded that the test data gave the best agreement with the distortion energy criteria of failure. The value of this work is difficult to determine due to the unknown size and stress gradient effects inherent in the tests.

Welter and Choquet (58) used a hydraulic machine to test cubic specimens with six threaded ends in three normal directions, under uniaxial, biaxial and triaxial stress conditions. Three structural steels were tested under pulsating stress conditions. The fatigue curves obtained for the triaxial stress case showed a direct relation to the uniaxial stress fatigue life, for the materials tested, the ratio of uniaxial to triaxial fatigue strength at 10^5 cycles being approximately equal to 2.

1.6 Fatigue Failure Criteria under Multiaxial Stress

The possible application of the theories of elastic failure under static stress to conditions of fatigue has been investigated by Findley (18) for the case of combined bending and twisting. He pointed out that the possible effect of anisotropy on the results of fatigue under combined bending and twisting had not been considered in any earlier work and showed that the following theories when corrected for anisotropy are equivalent to the Gough ellipse quadrant equation : maximum shear stress, maximum shear strain, distortion energy, octahedral shear stress and total deformation energy. Findley and Mathur (27) found that correcting the principal strain theory for anisotropy led to the ellipse arc equation.

Findley discusses the possible use of energy concepts in fatigue in references (18, 19). Microscopic studies of slip bands and fatigue crack formation have indicated that fatigue cracks develop in regions of heavy slip and so it would appear that the orientation of stress relative to slip planes is important in the initiation of fatigue cracks. Since energy is a scalar quantity its properties are independent of orientation of the principal stresses relative to the material, and hence it seems doubtful whether such a scalar quantity would be the determining factor

in fatigue. Further, if energy concepts were tenable material anisotropy should not affect the results of fatigue tests of specimens having variable orientation to material texture. The literature clearly shows that material anisotropy does have an effect in fatigue. The effect of mean stress on energy is shown in Fig. 2 reproduced from (19). A reversed sinusoidal cycle of stress produces an energy cycle varying from zero at zero stress, to a maximum at both maximum and minimum stress, which has a frequency twice that of the stress cycle. The effect of a moderate and a large mean stress on the energy cycle are also indicated in Fig. 2. The energy behaviour shown does not seem reasonable as a fatigue failure criterion under multiaxial stress. Findley et al (29) conducted tests to demonstrate that energy theories are not a satisfactory concept for fatigue failure. In these tests a circular disc was loaded along a diameter by means of pivot-pad bearings while the disc was rotated under a constant load to produce fluctuations of stress at the centre of the disc while the strain energy remained constant at the same position. As fatigue cracks were found in the region of constant strain energy it was concluded that a concept of fluctuating strain energy is not tenable as a theory of fatigue failure.

It has been pointed out that historically the distortion energy criteria was not proposed as an energy criterion, Von Mises proposing the formula as a mathematical modification to eliminate certain discontinuities in the maximum shear theory of static failure. The Von Mises criteria could be regarded as a possible empirical fatigue criteria and thus it would perhaps be more satisfactory to regard the energy type criteria of failure as empirical criteria of failure.

Stanfield (41) suggested that both the shear stress and the normal stress on the failure plane would be effective and proposed the relation

$$\tau_N = f - k\sigma_N \qquad (1.5)$$

where τ_N and σ_N are the shear stress and normal stress components on the critical plane and k and f are material constants. Stanfield also showed that if the constants in equation 1.5 are evaluated from the experimental values of bending and torsional fatigue strengths, the, criterion is identical with the ellipse arc equation. Stulen and Cummings (59) and Findley, Coleman and Handley (26) also used this form of criterion. Findley (28) developed this linear form of equation 1.5 to allow for mean stress in combined bending and twisting. Equation 1.5 then becomes

$$\tau_{CBA} = f - k\sigma_{BM} \qquad (1.6)$$

where τ_{CBA} is the allowable alternating shear stress on the critical plane

and σ_{BM} is the maximum normal stress on the critical plane, i.e. the sum of the normal stresses resulting from both the alternating and mean stresses.

A parabolic relationship for the effect of the normal stress was proposed by Coleman and Findley (24) but found to show little improvement on the linear theory of equation 1.5.

It should be noted that equations 1.5 and 1.6 apply to a critical shear stress plane which is not necessarily the plane of maximum shear stress. Applying equation 1.6 to Findley test data is complex and does not appear to give a significant improvement over the

application of equation 1.6 as applied to the plane of maximum shear stress.

Marin (60) has proposed a very general expression for fatigue failure under multiaxial stress including the effects of three dimensional anisotropy and mean stress. This expression is developed from the distortion energy criterion which has already been shown by Findley to have unlikely application, especially in the presence of mean stress, although the expression could be regarded as empirical. Marin claims good correlation with the results of combined bending and twisting fatigue tests but this is to be expected as it has been pointed out (61) that the Marin relation is equivalent to the Gough ellipse quadrant equation. According to the equation volumetric stresses have no effect, but the results of Crossland (40) and Burns and Parry (56) show that a volumetric compressive stress can increase the reversed torsional fatigue strength by over 30%. Also, Booth (42) has shown that if the anisotropic form of the Marin equation is used in the ++ quadrant of the biaxial stress diagram, the equation can lead to considerable errors due to the extremely high values of limiting stresses which it predicts. Thus it is apparent that the Marin relation has many serious limitations.

Sines (6) proposes a general criterion of failure for ductile metals tested below the yield stress which includes the effect of different combinations of alternating stress along with static stress. The criterion states that the permissible alternation of the octahedral shear stress is a linear function of the sum of the orthogonal normal static stresses. This criterion may be expressed as

$$\frac{1}{3}\left[(\sigma_1-\sigma_2)^2+(\sigma_2-\sigma_3)^2+(\sigma_3-\sigma_1)^2\right]^{\frac{1}{2}} \leqslant A-\alpha(S_x+S_y+S_z) \qquad (1.7)$$

where $\sigma_1, \sigma_2, \sigma_3$ = the amplitudes of the alternating principal stresses

S_x, S_y, S_z = the orthogonal static stresses

A = a material constant proportional to the reversed fatigue strength

α = a material constant giving the variation of the permissible range of stress with static stress

The justification for assuming that a linear relation exists between the amplitude of alternating stress and the static mean stress is indicated in Fig. 3, reproduced from (6). Consideration of the sum of the normal stresses on the planes of the greatest alternation of shear stress shows that when the sum $N_1 + N_2$ is positive, as it is for cases 1 and 5, an increase in the static stress reduces the permissible alternation of stress. When the sum is negative, as in case 2, the permissible alternation is increased. In the case of $N_1 + N_2$ zero, as in cases 3 and 4, then the static stress has no effect.

This criterion does not allow for the effect of anisotropy and requires the knowledge of two fatigue properties to be known before the constants A and α can be evaluated. Booth (42) points out that if this equation is applied to biaxial stress systems where the mean stresses are of opposite sign but the alternating stresses are applied algebraically in phase, then the equation predicts a fatigue strength equal to the uniaxial strength with zero mean stress, which does not agree with his test results.

Crossland (40) has suggested an equation similar to that of Sines (6), but using the maximum values of normal stresses instead of the mean values.

1.7 Cumulative Damage

Only one reference (62) can be found in the literature to work on non-constant amplitude fatigue under multiaxial stress conditions. Tests were conducted on SAE 1020 steel thin wall tubes having a wall thickness of 0.025 inch and an inside diameter of 0.878 inch subjected to a single principal stress ratio produced by combined alternating axial and torsional loads, with a single step change in the biaxial cyclic stress amplitude. Six L-H (low to high step) and eight H-L (high to low step) tests were conducted. It was concluded that the Miner (63) linear damage criterion was not accurate for these tests and that the Henry (64) non-linear theory gave reasonably accurate predictions of cycle ratio sums in the case of the H-L tests. A modification of the Henry criterion, using the concept of negative damage, was proposed to predict the L-H cycle ratio sums.

Cumulative damage theories for fatigue under uniaxial strcss are discussed in Chapter 2.

Table 1, reproduced from Forrest (84) shows the results of programme fatigue tests on unnotched aluminium alloy specimens under uniaxial stress conditions.

1.8 Summary

Although many investigations have been carried out on fatigue under multiaxial stress, these fall into three distinct groups, viz. combined bending and twisting, thin wall tubes and thick wall tubes, and up to now no general fatigue failure criteria satisfactorily explains the test results of all three groups.

In the case of combined bending and twisting, the empirical equations, the ellipse quadrant and arc (equations 1.3 and 1.4) are quite satisfactory, but although the effect of anisotropy under these conditions has been extensively discussed the suggestion that failure can be explained by the combined effects of the fluctuating shear and normal stresses acting on the maximum shear stress plane has so far not been systematically investigated. This has been done in this thesis in Chapter 7 where the Gough ellipse quadrant equation is further investigated and the extensive test data available under conditions of combined bending and twisting studied to this effect.

Combined bending and twisting tests cover only a limited range of biaxial stress ratio and the thin wall tube investigations so far conducted are also limited, only one investigation covering the complete ++ and +- stress quadrant, and that including only two conditions in the +- quadrant. The first main series of tests carried out in this thesis was to provide biaxial fatigue data for one material over the complete ++ and +- stress quadrants as a necessary preliminary to conducting cumulative damage tests.

CHAPTER 2

CUMULATIVE DAMAGE IN FATIGUE UNDER UNIAXIAL STRESS

2.1 Introduction

The term 'cumulative damage' is used for the effect of fluctuations in stress amplitude under fatigue conditions and many cumulative damage theories have been proposed in attempts to predict the lives of members under such conditions. The meaning of 'damage' can vary in the different theories proposed but the most generally accepted definition is that fatigue involves both crack initiation and propagation and the combined process can be described by a single damage function. Also the criterion of failure used is fracture.

Most of the theories proposed are of an empirical rather than a theoretical nature and in the following discussion only the theories with a possible practical application to the case of two stage block programme tests, as conducted in this investigation, will be dealt with.

It should be borne in mind that most cumulative damage theories rely on the use of pure sinusoidal fatigue data which is itself some 'central measure' of fatigue life with regard to scatter and probability of failure quite apart from the statistical aspects of the data to which these theories are applied. This point is rarely commented on in the development of cumulative damage theories and could be of particular importance with regard to the justification of the mathematical complexity involved in some theories.

Cumulative damage theories have been reviewed by Roylance (70), Kaechele (71) and most recently by O'Neill (72).

2.2 The Miner Rule

By far the most commonly used cumulative damage theory is that known as the Miner Rule (63), by virtue of its extreme simplicity of use, notwithstanding many attempts at modification and alternative theories. It is assumed that the damage caused by cycling at a given stress amplitude is directly proportional to the cycle ratio applied, that is to the ratio of cycles applies to cycles required to produce failure at the same stress. The damage caused by n_i cycles at stress amplitude S_i is then

$$D_i = \frac{n_i}{N_i} \qquad (2.1)$$

where N_i is the life in cycles at S_i. The criterion of failure under complex stress histories is then

$$D = \sum_{i=1}^{k} \frac{n_i}{N_i} = 1 \qquad \text{at failure} \qquad (2.2)$$

The ratio n/N is often referred to as the cycle ratio and the Miner Rule as the linear rule because of the linear rate of fatigue damage.

The linear rule was first mentioned by Palmgren (73) in connection with the life of ball bearings but without any suggestion of a theoretical or empirical basis. Langer (74) later proposed the linear rule in a more general form but it was Miner (63) who gave the rule some theoretical basis and conducted experiments to verify it, although these were of a very limited nature.

2.3 Stress Dependence and Interaction

A convenient classification of cumulative damage theories is that used by Kaechele (71) as follows:

(a) Cumulative fatigue damage theories can be stress dependent or stress independent. The amount of fatigue damage produced by a specified fraction of the number of cycles that would produce failure can be the same for all stress amplitudes (stress independence) or different (stress dependence).

(b) There can be interaction or interaction free theories. The course of damage at one stress amplitude may be changed by applying other stress amplitudes (interaction), or it may be unaffected (interaction-free).

Typical stress-independent and stress-dependent damage-cycle relationships are shown in Figs. 4 and 5.

The Miner theory can be shown to be stress independent and interaction free. Other theories (75, 76) that have these features are equivalent to the Miner theory.

The most simple cumulative damage test is the single-step test in which a certain number of stress cycles at one stress amplitude is applied and then the stress amplitude is stepped up, or down, and cycles at the second amplitude are applied until failure occurs. This type of test is not representative of service conditions.

If the stress amplitude is continually stepped between two stress levels at regular cycle intervals the test is known as an interval, spectrum or two stage block programme test and this is the next stage towards representing service loading. If this process is taken to the

limit we arrive at the random load test in which each cycle differs from the one before. However in this work we are only concerned with the two stage block programme type of test.

Stress dependent theories are only easily applied to single (or a small number of) step tests. Single step tests are likely to put an extreme emphasis on interaction effects which could be insignificant in a well mixed programme test.

2.4 Stress Dependent Theory

The Marco-Starkey (77) theory is an example of a stress dependent theory and specifies that the damage D arising from n cycles at stress condition S with an associated cycles to failure N is given by

$$D = \left(\frac{n}{N}\right)^{x_v} \qquad (2.3)$$

where the exponent x_v is a variable dependent on the applied stress condition. This damage specification is represented in Fig. 5, each stress condition requiring a separate curve. The exponent x_v is considered to have a value greater than one and approaches one as the stress condition becomes more severe. In Fig. 5 $S_1 > S_2 > S_3$.

Fig. 6 illustrates the effect of stress dependence in the case of single step tests. In the case of multi-level stress histories a step-by-step process of damage accumulation has to be employed which is very cumbersome excepting cases of simple stress histories.

Edwards (78) has used this damage relationship for a detailed study of the two-level programme type of test and considered the variation in $\sum \frac{n}{N}$ to be found using a range of the ratio X_2/X_1 where at stress level S_1 damage is

$$D = \left(\frac{n_1}{N_1}\right)^{X_1} \qquad (2.4)$$

and at stress level S_2 damage is

$$D = \left(\frac{n_2}{N_2}\right)^{X_2} \qquad (2.5)$$

under constant amplitude loading. Edwards found that $\sum \frac{n}{N}$ depends only on X_2/X_1 for two-level programme tests, the relationship being shown in Fig. 7.

2.5 Interaction Theory

Corten-Dolan Theory:

The Corten-Dolan (79) theory is an example of an interaction theory in which damage is dependent on previous stress history. The original presentation (79) of this theory included both stress-dependence and interaction effects. Later experimental work (80, 81) led to the formulation of a stress-independent, interaction theory.

The damage function proposed by Corten-Dolan is

$$D = m_i \; r_i \; n_i^{a_i} \qquad (2.6)$$

where for stress S_i, m_i is the number of damage nuclei

r_i is the damage rate coefficient

a_i is the damage rate exponent

and n_i is the number of cycles applied

The theory is developed in terms of a two-level programme S_1, S_2 $(S_1 > S_2)$ on the assumption that the number of damage nuclei, m, is determined by the higher stress level. The relation derived is

$$N_1 = N_g \alpha + R^{\frac{1}{a_1}} (1-\alpha) N_g^{\blacktriangle} \qquad (2.7)$$

where N_g = life under programme loading

N_1 = life at S_1, the first and highest applied stress

α = proportion of programme at S_1

R = r_2/r_1

A = a_2/a_1

From experimental work it was found that A was approximately unity thus the life under two-level programme loading is

$$N_g = \frac{N_1}{\alpha + R^{1/d}(1-\alpha)} \qquad (2.8)$$

Experimental work indicated that

$$R^{\frac{1}{d}} = \left(\frac{S_i}{S_1}\right)^d \qquad (2.9)$$

with d, a material constant, approximately constant over the range of S_i used.

It can be shown that the Corten-Dolan theory is a modification of the linear Miner theory accounting for interaction effects by a slope adjustment of the S-N curve as shown in Fig. 8a from b to d.

The Corten-Dolan theory has been criticised on several counts (71, 72, 82). The value of d has been derived using zero mean stress tests and it is possible that the value of d will be a variable dependent on mean stress. Also the reference condition used for damage accumulation is that of the most severe stress condition whereas a different stress condition used as reference would lead to a different result. The tests conducted in connection with this theory (80, 81) show that it would make little difference whether Miner's theory were used with the basic S-N curves or with the interaction curves derived, for the materials and stress spectra considered in these experiments.

Freudenthal-Heller Theory:

The Freudenthal-Heller (83) theory is based on the assumption

damage rates are not independent at different stress levels but dependent on the higher stress levels experienced in the previous stress history. The result is again a straight line modification of the S-N curve as shown in Fig. 8b. The interaction effects here are found using results from fatigue testing with simulated stress histories. In this case a defined reference stress level S_r with an associated number of cycles to failure N_r is used where S_r is unrelated to any stress condition in the applied stress history. N_r usually falls between 10^3 and 10^4 cycles. This eliminates the problem of the history related reference stress condition occurring in the Corten-Dolan theory. In their experimental work, Freudenthal-Heller found that interaction effects became more pronounced when the higher stress amplitudes were chosen for the test spectra, i.e. that the slope of the fictitious S-N curve tended to increase with increase of stress amplitudes used.

2.6 Summary

It is evident that the problem of cumulative damage in fatigue under uniaxial stress is far from resolved. The improvement in accuracy of fatigue life predictions found using cumulative damage theories other than the Miner theory are marginal and usually involve much more complicated computations and are also limited in their applicability to a particular material under particular stress conditions. In many cases the use of the Miner theory where $\sum \frac{n}{N} = C$ and $C \neq 1$ but is of the order of 0.4 to 0.6, decided by experience and any applicable test data, is found to give adequate life prediction.

As no previous work had been conducted on cumulative damage under multiaxial stress it was decided to investigate a limited number of biaxial stress cases under relatively simple two-stress level programme tests of three cycle block sizes and investigate the test data for the relevance of the basic parameters already discussed in this chapter.

PART II

EXPERIMENTAL WORK: DESIGN AND DEVELOPMENT OF A BIAXIAL FATIGUE MACHINE, FATIGUE TESTS AND DISCUSSION OF RESULTS

The main object of the test programme was a first study of cumulative damage in fatigue under multiaxial stress. As no comprehensive constant amplitude fatigue data was available for any material under the complete range of ++ and +- biaxial stress quadrants it was first necessary to obtain this data for the material to be used. In order to obtain this constant amplitude data a fatigue testing machine had to be designed, constructed and developed, capable of subjecting thin wall tubular specimens to a fluctuating internal pressure along with a fluctuating axial tensile or compressive load. The machine was further developed to operate in conjunction with a specially designed programmer capable of independent control of either or both the internal pressure or longitudinal load, thus enabling a wide range of multiaxial stress programme fatigue tests to be conducted.

CHAPTER 3

DESIGN OF BIAXIAL FATIGUE TEST MACHINE

3.1 Introduction

A survey of the literature indicated several machines designed to fatigue test thin wall cylinders. Marin (31) used a single hydraulic pulsator to apply a fluctuating internal pressure at 5 c.p.s. The pressure range was set by adjusting the throw of an eccentric which altered the stroke of a piston pump. Another eccentric mounted on the same shaft operated a lever mechanism which applied an in-phase longitudinal tensile load. This machine was modified by Bundy and Marin (37), by means of a compression adapter and an automatic pressure control system, to enable tension-compression biaxial fatigue tests to be conducted.

Majors, Mills and McGregor (35) used a fuel injection pump, which ran at 880 c.p.m. as a hydraulic pulsator. One pulsator was used, which could produce different fixed ratios of hoop to longitudinal stress by means of attaching suitably designed heads to the upper threaded ends of the tubular test specimens. A different pressure head was required for each principal stress ratio. Also the pump gave a very rapid rise and fall in pressure which took only about 15% of the cycle period time.

Booth (42) designed a test machine capable of applying various ratios of principal stress along with a variable time-phase relationship, the latter being achieved by the use of two separate pulsators, one for applying a fluctuating internal pressure and the other supplying a fluctuating pressure to a hydraulic ram which applied an axial compressive load to the specimen. This machine was

not capable of applying an axial tensile load.

. The first task was to design and develop a fatigue test machine capable of testing thin-wall tubes under tension-tension and tension-compression biaxial principal stress ratios. A servo hydraulic system was decided on as this would give good response to input signal, thus ensuring control of wave form and also enable a high operating speed to be maintained. Also a servo system would be more suitable than a mechanical system for the development of programme and random load capability. Two pressure systems were run from the one pump, one providing fluctuating internal pressure, the other providing fluctuating longitudinal tension or compression through a differential piston device.

The machine would have had a greater research capability had it been capable of testing with any biaxial mean stress. In the case of hoop stress this would have required external as well as internal hydraulic pressure, which could have been achieved by the use of an external thick sleeve fitted around the specimen. In the case of longitudinal stress the piston would have to have been pressurised on both the full bore and the annulus side, which again could be done. As it took some time to develop the machine to the condition described here, it is felt that the correct decision was made to leave this design improvement to a later stage.

The general layout of the complete test system is shown in Plate 1.

3.2 The Mechanical System

A photograph of the mechanical part of the test system is shown in Plate 2 and a general arrangement of the biaxial fatigue machine is shown in Fig. 9.

The test specimen is screwed into a lower housing which is attached to a base plate. The piston housing is screwed onto the upper end of the test specimen, the piston shaft passing through the test specimen and being screwed into the lower housing. The piston has square section oil seals and backing rings; the piston shaft passes through a similar sealing arrangement in the piston housing. The piston housing is restrained laterally but free to move axially in a ball bushing mounted in a block supported by side plates which are attached to the base plate.

One hydraulic oil circuit supplies internal pressure to the specimen through an inlet port in the lower housing. A second hydraulic oil circuit supplies pressure either (a) to the full bore side of the piston through an inlet port in the piston housing plug or (b) to the annulus side of the piston directly through an inlet port in the piston which is plugged in case (a). Case (a) produces tension in the test specimen while case (b) produces compression.

3.3 The Hydraulic System

The hydraulic pump used is a Fairey Type 6-3000, capable of delivering 6 gallons per minute at a pressure of 3000 p.s.i. The pump is fitted with an accumulator, a filter capable of filtering to 5 microns and a fan for cooling. The oil used is Shell Tellus 27; specification given in Table 2. For pump specification see Table 3.

The complete unit is enclosed in a double skin ½ inch thick blockboard housing, the cavity between the skins being filled with "Stillite" sound proofing material. The housing is provided with an air inlet at one side and a small extractor fan at the other to assist the flow of cooling air through the housing.

A circuit diagram of the test system is shown in Fig. 10. The pressure line from the pump is connected to a valve mounting block which supplies pressure to each of the two Dowty Moog servo control valves, one for each pressure circuit. The return line is connected from the valve block back to the pump. The Moog control valves are provided with fan air cooling. The Moog valves are Series 22 (8 g.p.m.).

Needle stop valves and pressure gauges used for calibration, setting up tests and control purposes are situated as shown in Fig. 11.

The pressure switch shown in the circuit is used as a specimen failure cut-off device. The operation of this switch is described later.

3.4 The Control System

A block diagram of the control system is shown in Fig. 10.

The control system uses an oscillator as the signal generator. The oscillator has two outputs whose relative phase difference can be adjusted. These outputs operate the two pressure circuits through a controller where static and dynamic pressure levels can be set for both pressure circuits. Each pressure circuit is controlled by a Dowty Moog electro-hydraulic servo valve. The control loop is closed by pressure transducer signals, taken in each pressure circuit as close as possible to the test specimen and fed back to the controller via amplifiers.

A mechanical cycle counter is wired to the oscillator output and has a divide by four control.. Further controls provided are pump on/off, pump filter clog warning and emergency cut-out switch.

3.5 The Programmer

The original intention was to conduct random load biaxial fatigue tests. However when a literature survey indicated that there was a very limited amount of data available on constant amplitude biaxial fatigue, and most of that under the limited conditions of combined bending and twisting, and virtually none under non constant amplitude conditions, it was realised that the original intention was over ambitious. As a first step towards investigating non-constant amplitude biaxial fatigue it was decided to build an eight stage block programmer for each pressure circuit capable of providing blocks of 10^3, 10^4 and 10^5 cycles of load.

The programmer operates by changing the input resistors to an operational amplifier. The sin signal from the oscillator is fed to the operational amplifier via a preset resistance which determines the amplification, and a preset potentiometer which determines the d.c. level, of the output signal. By means of relays eight such pairs of controls are connected in twin to the amplifier thus giving an eight stage programmer in which each stage is a specific combination of static and dynamic voltage conditions. The relays are driven by the eight outputs of an eight bit register, so that the eight relays are sequentially energised. Associated with each stage there is a three position switch, the wiper on each switch being commonly connected to the clock inputs by the register, via its associated relay. A five decade counter which is driven by the sin signal has its third, fourth and fifth decades connected to the first, second and third

positions of each switch, thus making it possible to programme each stage for either 10^3, 10^4 or 10^5 cycles. The register has switches connected between each stage which permit the operation of from two to eight stages.

The two pressure circuits of the machine are driven by the two output sin signals from the oscillator and there are two channels as described above, each with its own operational amplifier. The register and the counting circuits are common to both channels. One sin signal is taken to an electro-mechanical counter to give the total cycles count.

3.6 Material and Thin Wall Tubular Fatigue Test Specimens

The material tested was a copper alloy of aluminium to specification 2L65 (HE 15 WP) supplied by James Booth Aluminium Ltd. in 30 x 10 ft lengths of 1¼ inch extruded bar.

This material was used as it is a commonly used high strength aluminium alloy, is easily machined and there is some fatigue data available. Also it has a low ratio of fatigue strength to proof stress which is a necessary requirement in the case of fluctuating fatigue stress testing with relatively high mean stresses. This is especially true in the case of biaxial fatigue testing of thin wall tubes under longitudinal compressive stress and hoop tensile stress where instability problems arise as discussed in Chapter 6.

The chemical composition and general mechanical properties of the alloy to this specification are given in Table 4.

The dimensions of the test specimen are shown in Fig. 12. The method of manufacture was to first rough machine the specimen blanks to the form shown in Fig. 13. The blank was drilled 55/64 in dia. and then bored out to the finished inside diameter of ⅞ in. using

two cuts of 0.005 in followed by two cuts of 0.002 in followed by final cuts of 0.001 in to size. The specimen was then mounted on an expanding mandrel in a lathe fitted with a profile copying attachment and the end threads cut. The end locating diameters were then cut and the centre portion machined to size using a master profile. The final cuts on the centre portion were two of 0.010 in, two of 0.006 in and finishing cuts of 0.002 in and 0.001 in respectively, to size. In this way as much care as possible was used to obtain concentricity, good surface finish and consistancy of manufacturing process.

The longitudinal surface roughness from two specimens selected at random from approximately every second bar machined, was 15 to 25 micro inch C.L.A. along the outside diameter and 15 to 35 micro inch C.L.A. along the inside diameter, confirming the consistancy of surface finish.

The wall thickness used was a compromise between avoiding buckling instability problems and overall size of specimen.

A special device, shown in Plate 3, was used to measure the specimen wall thickness. This consisted of a mandrel mounted as a cantilever from a base plate and fitted with a dome headed screw. A micrometer head was rigidly attached to the base of the measuring device immediately over the dome headed screw. The difference in micrometer readings when the spindle was screwed down to touch the dome headed screw and that when the specimen was in position on the mandrel gave the specimen wall thickness. By this means the specimen wall thickness could be measured to an accuracy of 0.0001 inch. All specimen wall thicknesses were measured at four radial stations at each of three longitudinal stations.

The stress concentration effect of the 1.5 in fillet radius is not known. No data can be found in the literature for the stress concentration effect of circular fillets in stepped wall cylinders subjected to internal pressure. Lee and Ades (65) have investigated the stress concentration factor for cylinders subjected to axial tension for a range of fillet radius to wall thickness $\frac{1}{4} \leqslant r/t \leqslant 2$ whereas the specimen tested had an r/t ratio of 75. However, only two cases of the failure crack running into the fillet radius occurred in the complete test programme, and these could be explained by the fact that the spanner flats had been machined incorrectly.

3.7 Strain Measuring Equipment

The dynamic hydraulic pressures were measured by means of Coutant Electronic pressure transducers connected to Boulton Paul Transducer Meters. The output signals from the pressure transducers were fed to a four trace oscilloscope after being demodulated and amplified by the strain meter.

Shinkoh foil resistance strain gauges, type F1083, having a gauge length of 8 mm were used on the specimens during calibration. The strain gauges were fed with a carrier frequency of 1 kc/s from a Boulton Paul 'Multimeter'. Static strain measurements were read directly off the meter and dynamic measurements were made by feeding the demodulated signal to the oscilloscope. When more than one strain gauge was being used an Apex unit was used for switching purposes. In the later stages of the testing, a recalibration was necessary after fitting new oil seals. The static strain recording, in this case, was greatly facilitated by the use of a Modulog data recording system. Calibration details are given in Appendix 2.

CHAPTER 4

DEVELOPMENT OF BIAXIAL FATIGUE TEST MACHINE

4.1 The Mechanical System

The use of test specimens with threaded ends can lead to problems of bending stress caused by misalignment of end fittings in the test machine. In an attempt to circumvent this difficulty the test specimen was originally designed with a close tolerance spigot at each end locating in suitable housings in the test machine. Assembly tests with strain gauged specimens showed that the specimens were being subjected to assembly bending strains of an unacceptable magnitude. Attempts to reduce these strains led to the mechanical system being stripped and re-aligned, and also to the test specimens being modified with further close tolerance locating regions at the inner ends of the threaded portions. Further assembly tests with eight strain gauged specimens indicated that these modifications limited assembly bending stresses to a maximum of 1 tonf/in^2. The effect of a possible error in applied longitudinal mean stress of the order of 1 tonf/in^2 maximum was regarded as being not significant. Attempts to devise a mechanical method of measuring assembly strains using Huggenberger extensometers were abandoned as being impractical. Static and dynamic pressure tests, even at high pressures, showed only small differences in strain distribution around the specimens which could be accounted for by the small variations in wall thickness of the test specimens. These tests also showed that piston seal friction was absorbing some of the longitudinal pressure effort. The necessary corrections to allow for this effect are given in Appendix 2.

4.2 The Hydraulic System

Initial operation of the hydraulic system showed that only a relatively small range of pressure could be achieved in either circuit before the pressure waveform became unstable and no further increase of amplitude could be realised. This was to prove to be a major development difficulty, although having a simple solution as was eventually found.

After checking the electronics and servo valves and interchanging components in both pressure circuits it appeared that the trouble lay in the mechanical part of the test machine. This was also indicated by the fact that the longitudinal pressure circuit was affected more than the internal pressure circuit. Among the variables investigated were the piston seals, the volume of oil in the circuit, the type of piping (rigid or flexible), the position of the valves relative to the specimen and the oil delivery porting. As no significant improvement was obtained by any of these measures it was decided to try to run some tests within the limitations of the equipment.

After a few tests it was noticed that one of the servo valves was erratic in operation and also giving an improved wave form at infrequent intervals. Also the oil which was lost into the drip tray, when a fatigued specimen was removed from the test machine contained a measure of fine sediment. These facts led to an investigation of the small sintered bronze disc filters which were situated in the valve block between the servo valves and the test specimen, and regarded as necessary, due to the fact that the oil circuit was broken each time a specimen was changed. It was found that these discs had eroded at the edges (probably during the system flushing and cleaning operation) and hence particles of disc material had found their way into

the servo valves. Removal of these filters led to an immediate improvement in performance and after a little difficulty with sticking servo valves the system cleansed itself and operated as originally intended. As now realised, if any particles of dirt should get into the oil system when a specimen is removed from the machine it is unlikely to reach the servo valves as there is very little oil flow and this dirt will probably be purged from the system when the specimen is next changed.

It was also found during tests that the servo valves were running very hot, leading to control difficulties. The fitting of a cooling fan and ducting, as shown in Plate 1, greatly alleviated this difficulty.

The sound proof housing around the pump installation decreased the noise level in the laboratory but led to overheating problems in the case of longer tests (greater than approximately 70,000 cycles or about ½ hour running) which in turn led to control problems. During the longer life tests an access panel was left partly open to allow greater airflow around the pump and this overcame the problem, at the cost of an increase in noise level.

4.3 The Control System

Before the start of a test the machine was run for 20 minutes at a dynamic pressure range of about half the maximum required in both pressure circuits. During this period the test specimen was isolated from pressure by means of needle valves. In order to accelerate this oil warm up procedure the servo valve and pump auxiliary fans were not used during this period and the sound proof housing was kept completely closed. This procedure brought the oil to an operating temperature of 30°C. The cooling fans were used during

tests and the access panel in the sound proof housing kept partly open. Minor adjustments to pressure were required during the first 30 minutes (72,000 cycles at 40 c.p.s.) of a test and thereafter the internal pressure required very little adjustment but the longitudinal pressure required small adjustments at approximately 30 minute intervals, as it tended to run at a slowly increasing temperature. All tests were manually controlled for the first two hours (288,000 cycles at 40 c.p.s.) and thereafter at 20 minute intervals. All programme tests were manually controlled throughout.

The pressure transducer signals were continuously monitored on a four trace oscilloscope; two of the traces being used for marking purposes. These pressure transducer signals had been previously calibrated, statically and dynamically, using the test pressure gauge and strain gauged test specimens. During pressure calibration strain signals from the two pressure circuits were found to have a phase difference and the phase adjustment on the oscillator was adjusted accordingly.

The static pressures could also be read on dial gauges. These dial gauges had needle valves in their supply lines so that the dynamic pressure fluctuations could be damped out by almost closing the needle valves.

A pressure switch operating in the mean internal pressure line was used to switch the machine off when specimen failure occurred. This switch was set to operate on a pressure drop of 50 p.s.i. When the specimen developed a crack large enough to allow a mean internal pressure drop of this magnitude the pressure switch operated to switch the machine off. Generally, providing that the pressure switch had been set as finely as this and for the medium and low pressure ranges,

the switch would operate on the pressure drop though a crack sufficiently small to be difficult to detect with the naked eye. In this case only a fine spray of oil was emitted before the machine switched off. In the case of tests at the higher pressure levels, larger cracks occurred and the escaping oil was deflected into a drip tray.

The detailed procedure for setting up a test is given in Appendix 3.

4.4 Accuracy of the Applied Stresses

Errors could arise in the applied stresses due to the following causes:

(1) Stresses applied during assembly of the specimen in the test machine.

(2) Measurement of specimens.

(3) Method of calculating the stresses.

(4) Method of reading the applied pressures.

4.4.1 Assembly stresses

This problem was discussed in Chapter 4.1.

4.4.2 Measurement of specimens

The wall thickness could be measured to an accuracy of 0.0001 inch, which could introduce an error of ½% on a wall thickness of 0.020 inch. The error in measuring the diameter of 0.915 inch would be about 0.01% and thus negligible.

Thus the maximum error from this source is $\pm$ ½%.

4.4.3 Method of calculating the stresses

As discussed in Appendix 1 the general method of calculating stresses was that the longitudinal stress was based on the minimum mean thickness at the transverse stations considered and the hoop stress was calculated from the Lamé equation using the minimum wall thickness and the outside diameter at this station. For the eccentric bore conditions found in the specimens tested and for the free ends of the closed end case ($K = 2$) these assumptions would lead to negligible errors in longitudinal stress and a maximum error of 1.5% in the hoop stress.

From the calibration tests of Appendix 2 a maximum bending stress effect of 4% was found, assuming that all of the stress difference was due to bending which is definitely on the pessimistic side, for all other cases where the piston assembly is fitted.

In axial load fatigue tests no allowance is normally made for changes in lateral dimensions due to applied stresses. If the same assumption is made here and only change in diameter is considered under hoop stress then the error involved in the hoop stress is σ_H / E which for the maximum hoop stress used of 24 tonf/in^2 amounts to an error of 0.5%.

Thus the maximum error from this source will be 4%.

4.4.4 Method of reading the applied pressures

The oscilloscope used had an 8 cm screen, divided into 0.2 cm divisions. The position of the bottom of the pressure wave was arranged to coincide with the bottom division on the oscilloscope screen and the position of the top of the pressure wave could be estimated to ½ of a screen division, i.e. 0.05 cm. With the gain adjusted to give a minimum wave height of 4 cm the maximum error which could be introduced is thus ± 1½%.

Pressure gauges and transducers were calibrated using a 3,000 p.s.i. standard test Bourdon type gauge, on which the pressure could be estimated to within 2 p.s.i. This gauge was supplied with a calibration certificate and was periodically checked on a dead weight testing machine. The calibration of the oscilloscope and the pressure transducers was checked before and after testing each day.

4.4.5 Maximum errors

Thus in the worst possible case if all the maximum errors occur at the same time, the maximum error will be ± (0.5 + 4.0 + 1.25)%, i.e. ± 5.75%. It is however unlikely that all of these errors would occur at the same time and be additive in stress effect.

In discussing the accuracy of testing machines Weibull (89) points out that "an accuracy of ± 3% seems to be generally accepted as satisfactory", and that accuracies better than this require considerable skill.

CHAPTER 5

DETAILS OF FATIGUE TEST PROGRAMME

5.1 Object of Fatigue Tests

The object of the tests was to study cumulative damage effects in fatigue under biaxial stress. As no previous data was available it was first necessary to conduct constant amplitude fatigue tests under a range of biaxial stress conditions.

5.2 Details of Tests

5.2.1 Uniaxial Fatigue Tests on Solid Specimens - Series 1

The object of these tests was to enable an estimation to be made of the effects of anisotropy and polishing. Uniaxial direct load fatigue tests were conducted on solid specimens of the form shown in Fig. 14, cut in the longitudinal direction from the bar stock in the position shown in Fig. 15, so that the axis of the specimens corresponded with the same radial position as the wall of the tubular fatigue specimens. Pulsating fatigue tests were carried out on polished and unpolished specimens, corresponding to the stress conditions in Series 2 ($K = 0$). These tests were carried out on an Amsler 2 tonf Vibrophore machine using a 0.4 tonf dynamometer. The specimens were polished on a Morrison polishing machine. The polishing machine was run at its slowest speed using grade 0 emery paper for the first six minutes followed by four minutes with grade 000. Oil was used to lubricate the specimen during the final stage of polishing.

Rotating bending zero mean stress tests were also conducted on solid specimens of the form shown in Fig. 17, cut longitudinally and transversely from the bar stock in the position shown in Fig. 15. These tests were conducted on a Gill type machine.

As the standard size of rotating bending specimen used in this machine is 2.21 in long and the transverse specimens had to be cut from 1.25 in diameter bar, both full size and short, with packing pieces, longitudinal specimens were used for test comparison purposes with the short transverse test specimens.

5.2.2 Biaxial Constant Amplitude Fatigue Tests on Tubular Specimens - Series 2

These tests were conducted for a number of ratios of hoop stress to longitudinal stress (= K) viz. K = 0, 0.5, 1.0, 2.0, 7.9, -2.0, -1.0, -0.5 and -0, in order to obtain S-N data over the life range from 10^4 to 10^6 cycles. These tests were nominally pulsating from zero to a maximum. As a small degree of mean pressure drift was experienced during the development of the machine the mean pressures in the internal, longitudinal tension and longitudinal compression pressure circuits were maintained at 100 p.s.i. greater than the pressure amplitudes, leading to mean stresses of 1 tonf/in^2, 1.8 tonf/in^2 and 1.5 tonf/in^2 in the hoop, longitudinal tension and longitudinal compression stresses respectively, greater than the stress amplitudes. This measure ensured that the full stress amplitude would always be maintained.

For each value of K, the greatest algebraic stress conditions are shown in Fig. 18 in the form of Mohr stress circles, and the stress-time relationships in Fig. 19.

5.2.3 Biaxial Programme Fatigue Tests at Constant Principal Stress Ratio K - Series 3

Programme fatigue tests were conducted at four principal stress ratios K = 0, 2, 7.9 and -1. Various combinations of pairs of cycle blocks of 10^3, 10^4 and 10^5 were used between pairs of stress levels chosen from three levels in each case. The stress levels and

cycle block combinations used are shown in Fig. 20.

5.2.4 Biaxial Programme Fatigue Tests at Two Principal Stress Ratios - Series 4

A limited number of programme tests at two principal stress ratios was conducted as a preliminary investigation under more complex stress conditions, of the dual isotropic/anisotropic fatigue mechanism and interaction effects found in the earlier test series.

Principal stress ratio combinations of K = 0/7.9 and 7.9/-1 were chosen as in each case the maximum shear stress planes alternated between the isotropic and anisotropic. Cycle blocks were all of 10^4 cycles.

Four tests were conducted at K = 0/-1 and -1/0 where the maximum shear stress always occurred on the isotropic shear planes. These tests were necessarily of the single stress step change type as the different values of K required different test machine configurations.

The test stress conditions are illustrated in Fig. 21.

CHAPTER 6

DISCUSSION OF RESULTS

6.1 Static Tests

The results of the static tests are shown in Table 5 and Fig. 22.

The Hounsfield tests show that the U.T.S. in the transverse direction was within 1% of that in the longitudinal direction. These transverse test specimens were cut from a radial direction whereas in the fatigue tests the 'transverse' stress acts in the hoop direction. The ductility, measured by % reduction in area, was 8% in the transverse direction and 24% in the longitudinal direction.

6.2 Fatigue Fracture Details and Scatter in Results

6.2.1 Fracture Details

In cases where the hoop stress was the maximum the fatigue fractures were longitudinal cracks, either about ½ to ¾ inch long or very fine cracks difficult to see with the naked eye. Longitudinal cracks also occurred in cases where the longitudinal stress was equal to the hoop stress, i.e. $K = \pm 1$, as the material tested was weaker in the transverse direction. In cases where the longitudinal tensile stress was greater than the hoop stress the fatigue fractures were either fine cracks or the specimens broke in two parts. For the cases of longitudinal compression buckling problems were experienced and the fractures obtained in the cases of $K = -\frac{1}{2}$ and -0 are discussed in detail in Chapter 6.4 Plate 4 shows examples of the large and small fatigue cracks.

The surface of the large cracks were largely at 45° to the surface of the specimen except at the crack initiation position where

the crack surface was in a radial direction for longitudinal cracks and in a transverse direction for transverse cracks. Evidence of plastic flow at the ends of the cracks was indicated by surface wrinkling. The crack appearance was similar at the inner and outer surfaces of the specimens. In some cases it was possible, with the aid of a microscope, to see that the cracks had initiated at the inner surface, for both longitudinal and transverse cracks as shown in Plate 5.

Table 6 shows that the positions of the fractures in the test rig are reasonably evenly distributed in a radial direction, giving 30%, 21%, 26% and 23% in the four quadrants indicated. There is no indication of the test machine exerting any influence on the position of failure in the specimens. The specimen failures tended to be nearer one end of the test region than the middle as any machining non-uniformity usually derived from a slight taper in the wall thickness. Table 6 also shows that 47% of the specimens failed at the position of minimum wall thickness, meaning that about half the specimens tested failed at positions where the calculated stresses would be higher than those at the actual failure positions. Appendix 1 shows that, for the wall thickness limits achieved, the maximum difference in actual and calculated stress is 1.5%.

6.2.2 Scatter

The comparison of bar strengths shown in Table 6 indicates that bars B and E were weaker, and bar D stronger, than the average. Examination of the test data for the cases of K = 0 and 2 (Table 9) tend to substantiate that bar D was stronger but not that bars B and E were weaker. It is difficult to make any quantitative assessment of the greater strength of bar D.

An examination of fatigue test data in the literature for heat treated aluminium alloys (68) shows a relatively large degree of scatter as has also been found in the work reported in this thesis. The above reference shows, for the same material as tested here, several instances of fatigue strength variation at 10^6 cycles of the order of $\pm$ 15%, which agrees approximately with the greatest scatter found in this work.

The volume of material subjected to the maximum stress conditions in thin wall tubes falls between the cases of rotating bending and direct stress, while the surface area, where fatigue cracks normally initiate, subjected to the maximum stress conditions will be relatively greater than in the other two cases. The photomicrographs shown in Plate 6, show that there is a large number of grains existing across the thin wall thickness. The use of thin wall tubes, in which the crack propagation stage will not last as long as in the more usual solid specimens, may lead to greater scatter as it is generally accepted that there is less scatter in the propagation stage than in the initiation stage of fatigue failure. Tests in which the predominant stress is in the weaker transverse direction have a greater scatter possibly due to the greater possibility of non uniform grain structure in this direction.

The degree of scatter experienced is also a function of variation in specimen manufacture and testing technique, both of which are difficult to quantify, but which have been maintained as consistent as possible.

6.3 Uniaxial Fatigue Tests - Series 1

The results of the rotating bending fatigue tests are shown in Table 7 and Fig. 23. The test results from the longitudinal types of specimen, full size and short, fall within the same scatter band, indicating that there is no machine effect due to using short specimens. The results of the transverse tests are seen to give shorter lives than the longitudinal tests at the same stress level. The estimated curves show the fatigue strengths at 10^6 cycles as being $\pm$ 11.2 tonf/in^2 and $\pm$ 12.9 tonf/in^2 for the transverse and longitudinal tests respectively. Thus the transverse fatigue strength is approximately 85% of the longitudinal fatigue strength at 10^6 cycles. The longitudinal fatigue curve is almost identical with that given in the Royal Aeronautical Society Data Sheet E.07.01 Fig. 3 for the aluminium alloy L65.

The results of axial load fatigue tests on polished and unpolished specimens are shown in Table 8 and Fig. 24. These tests were carried out on the Vibrophore machine. The scatter of results for the unpolished specimens is seen to be much greater than for the polished specimens. For this reason it is difficult to estimate the difference in fatigue strength between the polished and unpolished specimens. The estimated curves indicate that at 10^6 cycles the fatigue strengths of the polished and unpolished specimens are 9.4 $\pm$ 9.4 tonf/in^2 and 8.9 $\pm$ 8.9 tonf/in^2 respectively, i.e. a reduction of 5%. The result for the polished specimen is similar to results obtained by Woodward et al (93), who carried out uniaxial mean stress tests on specimens machined from two batches of 1 inch diameter HE15WP extruded bar and obtained strengths of 10 $\pm$ 12 tonf/in^2 and 7.5 $\pm$ 10 tonf/in^2. Table 9, reproduced from Forrest (84) shows the results

of several investigations into the effect of surface roughness on the fatigue strength of a number of different materials. It shows that Siebel and Gaier obtained a 7% reduction in fatigue strength between polished and smooth turned specimens of Al. Cu alloy specimens, which is similar to the results obtained in Fig. 24.

The difference of fatigue strength between polished and unpolished specimens can also be due in part to residual stresses which may be incurred due to polishing the specimen surface.

From Fig. 25a, showing the results of repeated longitudinal fatigue stress tests ($K = 0$) on tubular specimens, the fatigue strength at 10^6 cycles is seen to be 8.6 ± 8.6 tonf/in^2. which is in good agreement with the unpolished uniaxial test result of 8.9 ± 8.9 tonf/in^2.

A comparison of the Vibrophore axial load tests and the thin wall tube axial load tests may also be influenced by the size and shape of specimens, speed of testing and the effects of oil. From an analysis of test data in the literature Forrest (84) concludes that there is no size effect on plain specimens under direct fatigue stress, but there is a size effect in bending tests on plain specimens; an increase in fatigue strength being obtained for specimens less than 1 inch diameter. The Vibrophore tests were conducted at 3500 cycles per minute whereas the thin wall tube tests were run at 2400 cycles per minute. This relatively small difference in speeds of cycling would not be expected to affect the fatigue strength. In the case of thick wall tube fatigue tests the high hydraulic pressures used, of the order of 20 tonf/in^2, are known to have a detrimental effect on the fatigue strength of the tube material. However in the case of thin wall tube fatigue tests the hydraulic pressure used, of the order of 1 tonf/in^2, is small compared with the stresses in the tube and is not likely to

have any considerable stress effect though it may have a corrosive, or protective, effect on the material surface depending on the type of oil used. Banin (85) conducted rotating bending tests on 2L65 aluminium alloy specimens in air and in a Shell Tellus 27 oil environment and at 10^6 cycles found a 10% increase in fatigue life in the case of specimens protected in the oil environment.

In the work reported in this thesis all tests were conducted with oil in the specimen, though in the case of K = 0 and K = -0 this oil was not pressurised. Thus all tests are subject to the same oil environment conditions.

6.4 Biaxial Constant Amplitude Fatigue Tests - Series 2

The results of this test series are shown in Table 10 and Fig. 25. Figs. 25a to 25j are in terms of the maximum principal stress amplitude whereas Fig. 25k, the comparison figure showing all results, is in terms of maximum shear stress amplitude for correlation purposes.

It should be noted that the test cycling speed was increased from 15 c/s to 40 c/s as experience was gained on the test machine. Also that the uniaxial fatigue tests conducted on the Vibrophore machine were run at 60 c/s. Wyss (69) has shown that there is no frequency effect on aluminium-copper alloys of the type tested here over the range 6 to 130 c/s. These tests were carried out on plain specimens in pulsating tension.

Due to the expense of the thin walled specimens used in these investigations it was intended to conduct only three tests at each of four stress levels for each principal stress ratio. Because of the effects of scatter this was not always possible. Also because of the small slope of the S-N curves at 10^6 cycles it was often necessary to

carry out further tests in this region in order to determine the fatigue strength at this life. The tests were carried out in increasing order of complexity and difficulty i.e. K = 0, 7.9, 2, 1, 0.5, -2, -1, -0.5 and -0.

The curves shown in Fig. 25 are the best fit, drawn by eye, through the log mean of cycles to failure at the different stress levels used. Attempts were made at mathematical curve fitting but these were found to be impractical for the small number of tests conducted at each value of K; especial difficulty was experienced at the longer life end of the curve in coping with not failed test results. The test data has however been plotted on a best straight line fit, using the method of least squares, to log S - log N axes as shown in Fig. 26.

The scatter in test results is seen to be somewhat greater in the cases where the hoop stress is the maximum principal stress as would be expected from the anisotropic effects produced during bar manufacture. In the cases of K = -1, -½ and -0 the range of test stress levels was limited by buckling problems which are discussed later in this section.

Fig. 25k shows that the results of cases K = 0 and 0.5 are very similar over the range 4×10^4 to 10^6 cycles, the pulsating stress levels at these lives being $\pm$ 6.0 and $\pm$5.8 tonf/in^2, and $\pm$ 4.3 tonf/in^2 respectively on a maximum shear stress basis. Over the same life range the results of cases K = 1, 2 and 7.9 are also very similar, the curve for K = 2 being slightly lower than the other two. The pulsating stress levels in the case of K = 1 and 7.9 are $\pm$ 5.0 tonf/in^2 and $\pm$ 3.6 tonf/in^2 at the lives of 4×10^4 and 10^6 cycles again on a maximum shear stress basis. In the case of tensile-tensile biaxial stress the maximum principal stress and the maximum shear stress failure criteria

lead to the same result. In these tests the third principal stress, the internal pressure, is not zero being in the order of 0.50 tonf/in^2 compressive at the higher test stress levels; this internal pressure effect is included in the values of maximum shear stress. These results can be explained on a basis of maximum range of shear stress, modified for the effects of anisotropy, being the criteria of failure. This is illustrated in Fig. 18 which shows that, in the cases of K = 1, 2 and 7.9, the maximum shear stress occurs on the HR shear plane which is the anisotropic shear plane and weaker than the HL and RL shear planes as it can contain extruded grains which can act as stress raisers. In this case the anisotropic plane is 16% weaker than the isotropic planes.

In the case of tensile-compressive biaxial stress Fig. 25k shows, over the life ranges achieved, that the fatigue strength increases progressively from the case of K = -2 through K = -1 to K = -0.5. Again referring to Fig. 18 these results can also be explained on a basis of maximum range of shear stress being the criterion of failure, but now modified for the effect of normal stress acting on the maximum shear stress plane. In the case of tensile-tensile biaxial stress the normal stress acting on the maximum shear stress plane was always equal to the maximum shear stress. When K is negative the normal stress acting on the maximum shear stress plane decreases from a tensile value when K = -2, through zero when K = -1 to a compressive value when K = -½ and -0. Once a crack has initiated in a maximum shear stress plane it will propagate more rapidly the greater the tensile normal stress acting on that plane and likewise be inhibited from propagating in the case of compressive normal stress acting on the maximum shear stress plane. In the case

of tensile-compressive biaxial stress the maximum shear stress acts on the isotropic HL plane.

The rather untypical results in the case of $K = -2$, where there is low scatter in test results at two test stress levels and high scatter at other test stress levels, could be explained by the fact that this test case falls near the transition region where the fatigue strengths of the HR and HL maximum shear stress planes are nearly the same under their respective fatigue stress conditions.

Instability effects in the thin-wall tubes under the combined effects of internal pressure and end load were first encountered while testing at $K = -1$. It was found that attempts to fatigue test at hoop stress ranges giving a maximum hoop stress of 17 $tonf/in^2$ led to buckling failure. This experimental value of hoop stress producing buckling at $K = -1$ agrees with the theoretical value of 17 $tonf/in^2$ as discussed in Appendix 4 and shown in Fig. 45. This limitation on hoop stress restricts the S-N curve obtainable for $K = -1$ to life values of the order of 10^5 cycles and greater.

In the case of $K = -\frac{1}{2}$ buckling effects were experienced at stress conditions giving a maximum hoop stress of 9 $tonf/in^2$ although the theoretical instability value of hoop stress is 10.5 $tonf/in^2$. These tests had to be continuously monitored for signs of buckling as failure occurred by specimen collapse very shortly after a fatigue crack formed and it was then impossible to tell whether the specimen had in fact failed in fatigue or by buckling. Specimens G13 and T15 showed no evidence of buckling before failure and specimen G18 was unbroken at 10^6 cycles. Specimens D2 and M3 failed early by buckling. Of the other results at $K = -1$ most showed some evidence of the onset of buckling before failure. Thus for $K = -\frac{1}{2}$ buckling instability

effects restrict the obtainable region of the S-N curve to life values of the order of 10^6 cycles or greater.

Under conditions of longitudinal compressive fatigue stress, failure occurred by specimen collapse shortly after the formation of a fatigue crack. A small static internal pressure of 150 p.s.i. was maintained in the specimens in this case in order to operate the pressure switch at failure and oil seepage through the fatigue crack was observed before failure by collapse. In some cases the machine was switched off by hand after formation of the fatigue crack but before collapse. Attempts to run fatigue tests at a value of maximum compressive stress of 26 tonf/in^2 led to immediate specimen collapse when load was applied.

The form of a typical buckled specimen is shown in Plate 7.

The log S - log N plot shown in Fig. 21 also indicates the grouping of the test results as already suggested and also shows that the slope of the plot for K = -2 should perhaps be steeper to fit with the overall data.

6.5 Biaxial Programme Fatigue Tests at Constant Principal Stress Ratio K - Series 3

The results of this test series are shown in Table 11 and Fig. 27.

The variable amplitude data are plotted as a bar graph in Fig. 27, each bar representing the data from one individual test. The mean cycle ratio sums of three tests at each test stress and programme condition, in most cases, are also shown and compared with the Miner prediction of unity where

$$D = \sum \frac{n}{N} = 1$$

The range of cycle ratio sums found are as follows

K = 0 0.32 to 1.53 (24 tests at 8 programme conditions)

K = 2 0.24 to 1.82 (26 tests at 8 programme conditions but neglecting 4 very high results and one premature failure)

K = 7.9 0.13 to 1.46 (24 tests at 8 programme conditions but neglecting 1 very high result)

K = -1 0.27 to 1.48 (9 tests at 3 programme conditions)

The mean cycle ratio sums for all tests are shown in Table 11e which shows that the overall mean is 0.77. The Miner prediction is seen to be unconservative.

In the case of K = 0 the lowest cycle ratio sums occur in the $S_2 - S_3$ and $S_1 - S_3$ test conditions. In only one test condition $S_1 - S_2$ ($10^3 - 10^4$) is D significantly greater than unity, viz. 1.39, and apart from the cycles at S_1 the specimens withstood a larger number of cycles at S_2 than in the case of constant amplitude testing at S_2. In most cases the damage caused by the higher stress level was sufficient to cause accelerated damage at the lower stress level and hence produce values of $D < 1$. An overall value of D = 0.4 would be safe for the majority of K = 0 tests, only four test results falling below this value.

A comparison of the $S_2 - S_3$ test results for K = 0 and -1, shown in Figs. 23a and 23d, shows that the trend is the same and the results very similar for similar test conditions. This might be expected as the same isotropic maximum shear stress planes are concerned.

The test results for K = 2 and 7.9, shown in Figs. 27b and 27c, show greater scatter as might be expected in the case of the anisotropic maximum shear stress plane and already found for the

constant amplitude tests. Results, for the same programme conditions, for K = 2 and 7.9 are very comparable, neglecting untypical values, except in the case of S_1 - S_3 tests. Again a value of D = 0.4 would be safe for K = 2 and 7.9 tests except for the case of S_2 - S_3 (10^4 - 10^5) where in both instances test results are consistantly of the order of D = 0.2. Indeed in this case the number of cycles to failure in the programme tests is lower than if the tests had been run to failure at the higher stress level only. No explanation can be suggested for this behaviour. These tests were effectively high to low single step tests which, generally speaking, give $D < 1$ but not as low as 0.2.

The main variables involved in this series of tests are as follows:

1. K, the principal stress ratio
2. Stress levels used. Here S_1 - S_2, S_2 - S_3, S_1 - S_3.
3. Programme block sizes.
   Here 10^4 - 10^4, 10^3 - 10^4, 10^4 - 10^5.
4. The 'mix' of the programme i.e. how many blocks occur in the tests. Here the number of blocks varied from less than one to twenty.

For the limited number of tests conducted it is only possible to suggest general qualitative results as discussed above. The possible relevance of cumulative damage theories, proposed for the case of uniaxial fatigue stress, to these results is investigated in Chapter 9.

6.6 Biaxial Programme Fatigue Tests at Two Principal Stress Ratios - Series 4

6.6.1 Cumulative Damage Tests κ = 0/7.9

All cycle blocks are 10^4 cycles.

The results of these tests are given in Table 12a and the stress conditions illustrated in Fig. 21.

In the interests of clarity and as an assistance in following the text selected parts of the above information is given in the diagrams shown for each particular test stress case.

K = 0/7.9

CASE 1

At K = 0

Test stress, S_o = 12 ± 12 tonf/in^2

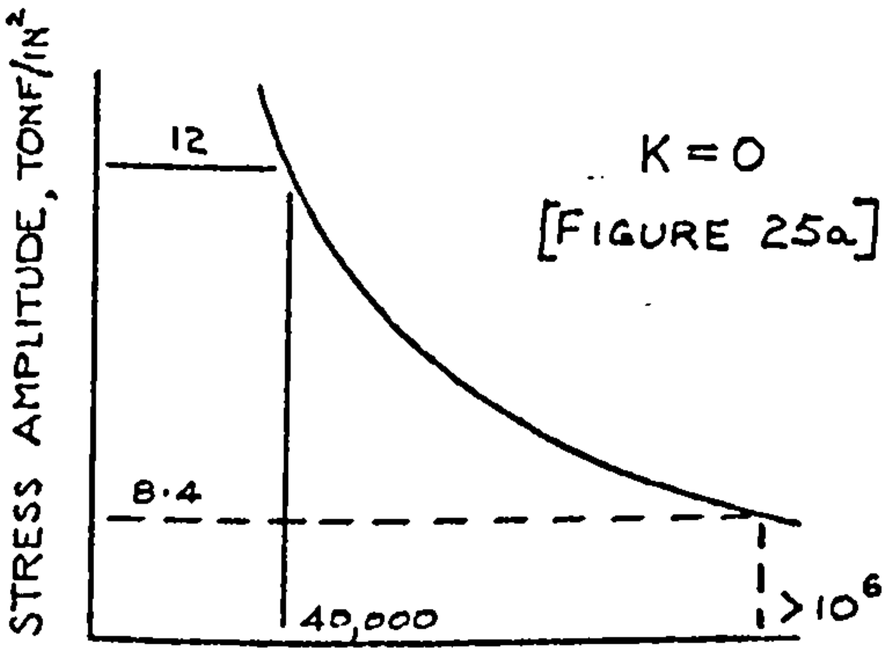

At K = 7.9

Test stress, $S_{7.9}$ = 9.5 ± 9.5 tonf/in^2

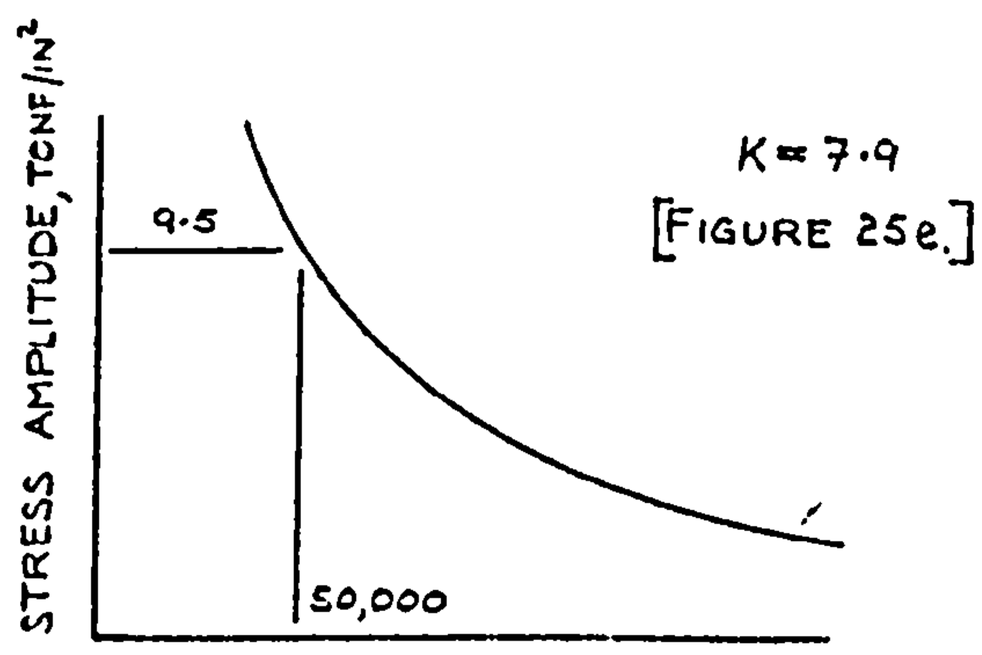

Stress conditions

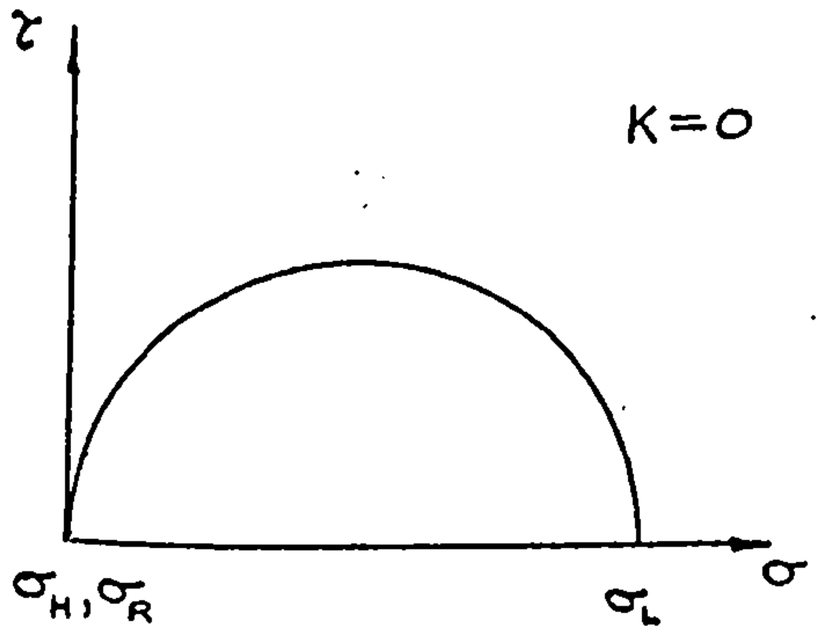

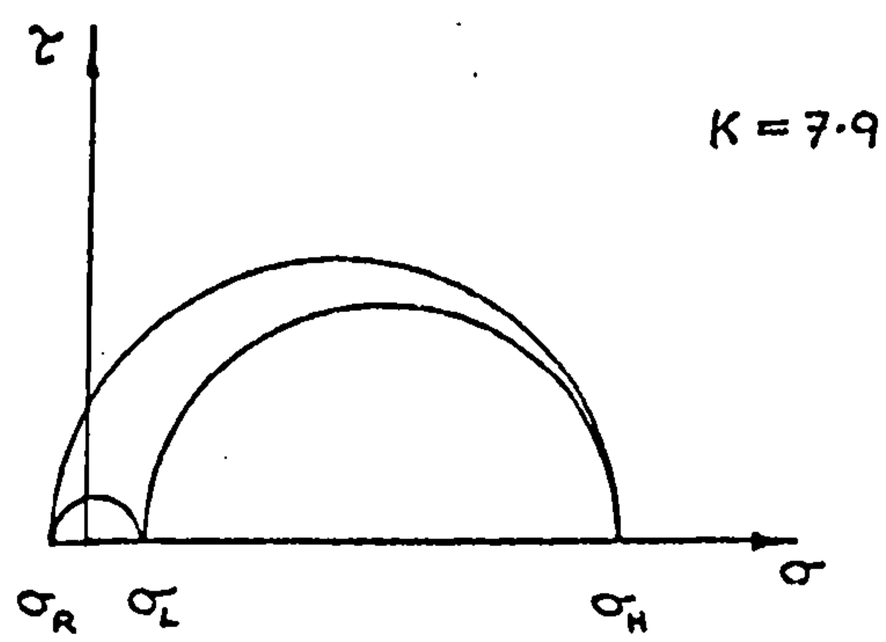

Conditions on maximum shear stress planes:

LR, LH	:	High shear stress amplitude	:	HR(HL, see text)
HR	:	Low (or zero) shear stress amplitude	:	LR

Note: HR is the anisotropic (weaker) shear stress plane

DIAGRAM 1

K = 0/7.9

CASE 1:

S_o = 12 ± 12 tonf/in^2 N_o = 40,000 cycles

$S_{7.9}$ = 9.5 ± 9.5 tonf/in^2 $N_{7.9}$ = 50,000 cycles

At stress condition S_o damage was expected on the LR and LH maximum shear stress planes and zero damage on the HR plane. The life found at constant stress amplitude S_o = 12 ± 12 tonf/in^2 was N_o = 40,000 cycles.

At stress condition $S_{7.9}$ damage was expected on the HR maximum shear stress plane. The life found at constant stress amplitude $S_{7.9}$ = 9.5 ± 9.5 tonf/in^2 was $N_{7.9}$ = 50,000 cycles. On the HL maximum shear stress plane the maximum shear stress equals a pulsating value of ½(9.5 - 9.5/7.9) i.e. 4.7 ± 4.2 tonf/in^2 while the normal stress on the maximum shear stress plane is 5.4 ± 5.4 tonf/in^2; diagram 1 shows the expected life for this stress condition to be greater than 10^6 cycles and thus little or no damage was expected on the LR and HL planes.

The mean life of two tests was approximately 40,000 cycles and failure occurred on a transverse plane. If the damage mechanisms on the isotropic LR/LH and anisotropic HR planes had acted separately at S_o and $S_{7.9}$ respectively then a life of the order of 80,000 cycles would have resulted. The tests show that the damage started at S_o has been continued at $S_{7.9}$.

$K = 0/7.9$

CASE 2

At K = 0

Test stress, $S_o = 10 \pm 10$ tonf/in^2

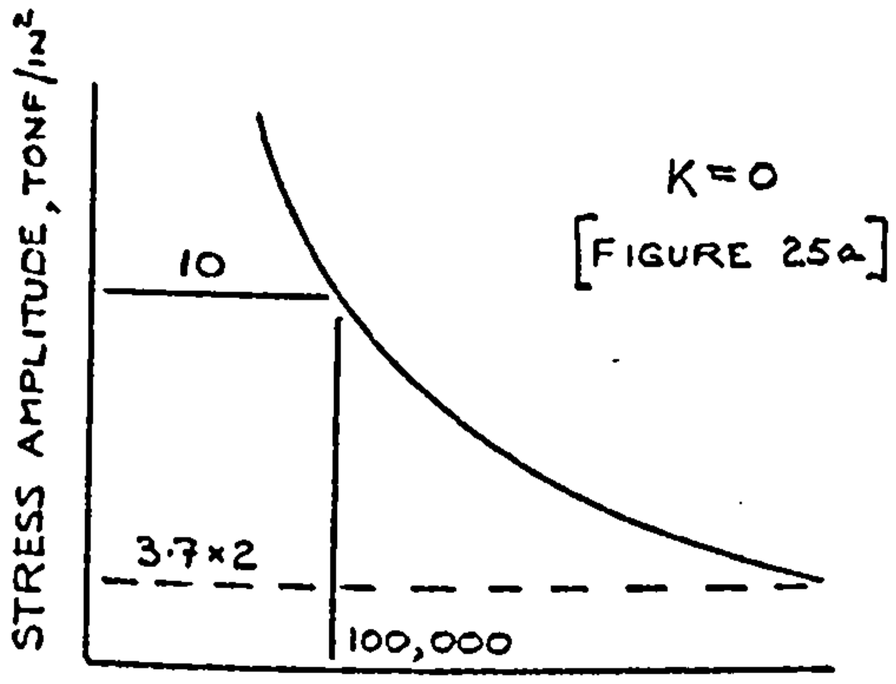

At K = 7.9

Test stress, $S_{7.9} = 8.5 \pm 8.5$ tonf/in^2

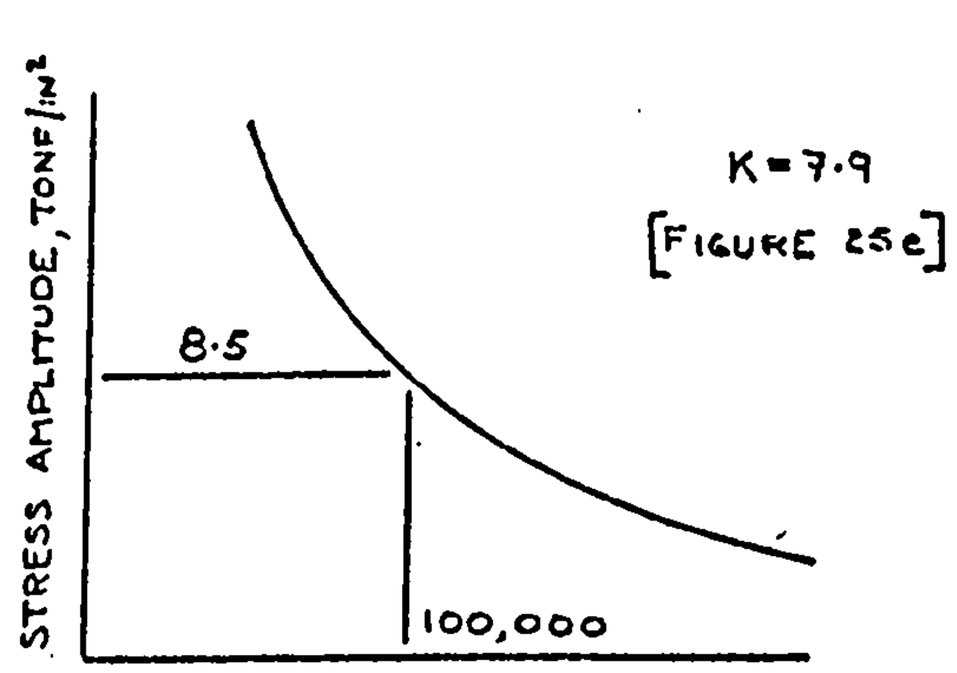

Stress conditions

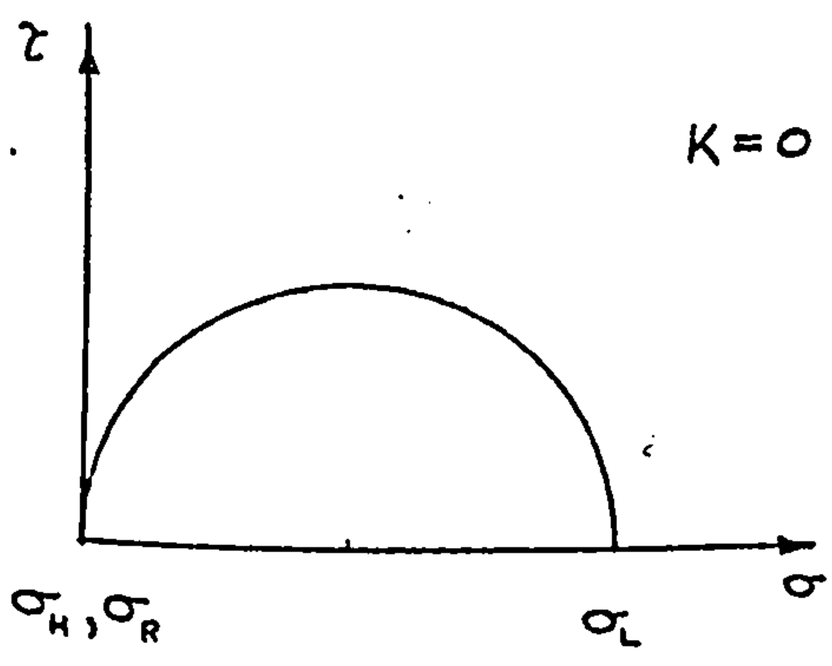

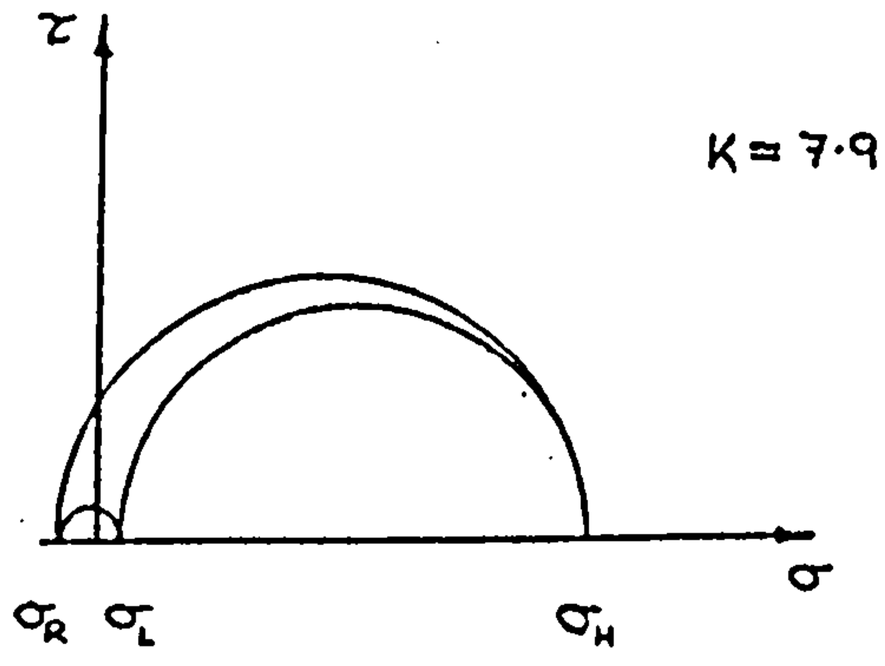

Conditions on maximum shear stress planes:

LR, LH	:	High shear stress amplitude	:	HR
HR	:	Low (or zero) shear stress amplitude	:	LR, LH

Note: HR is the anisotropic (weaker) shear stress plane.

DIAGRAM 2

K = 0/7.9

CASE 2:

S_o = 10 ± 10 tonf/in^2 N_o = 100,000 cycles

$S_{7.9}$ = 8.5 ± 8.5 tonf/in^2 $N_{7.9}$ = 100,000 cycles

The stress levels were reduced to determine whether the interaction effect found in Case 1 still occurred.

Again at stress conditions S_o damage was expected on the LR and LH maximum shear stress planes and zero damage on the HR plane. The life found at constant stress amplitude S_o = 10 ± 10 tonf/in^2 was N_o = 100,000 cycles.

At stress condition $S_{7.9}$, damage was expected on the HR maximum shear stress plane. The life found at constant stress amplitude $S_{7.9}$ = 8.5 ± 8.5 tonf/in^2 was $N_{7.9}$ = 100,000 cycles. On the HL maximum shear stress plane the maximum shear stress equals a pulsating value of ½ (8.5 - 8.5/7.9) i.e. 4.2 ± 3.7 tonf/in^2 while the normal stress on the maximum shear stress plane is 4.8 ± 4.8 tonf/in^2; diagram 2 shows the expected life for this stress condition to be very much greater than 10^6 cycles and thus no damage was expected on the LR and LH planes.

The mean life of two tests was 175,000 cycles and failure occurred in a longitudinal plane. If the damage mechanisms had acted separately a life of the order of 200,000 cycles would have resulted as was the case here.

K = 0/7.9

CASE 3

At K = 0

Test stress, S_o = 9.5 ± 9.5 tonf/in^2

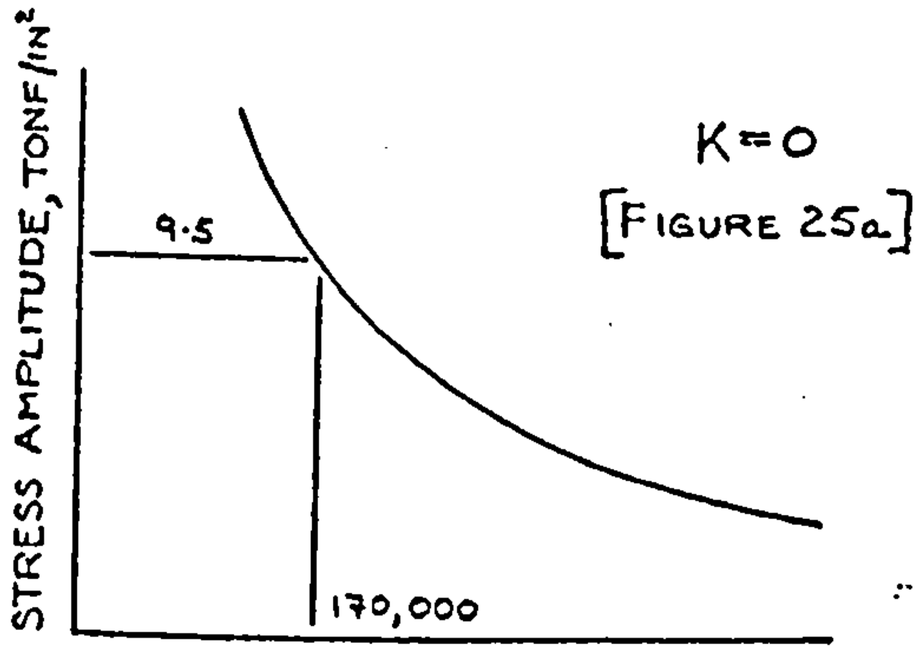

At K = 7.9

Test stress, $S_{7.9}$ = 9.5 ± 9.5 tonf/in

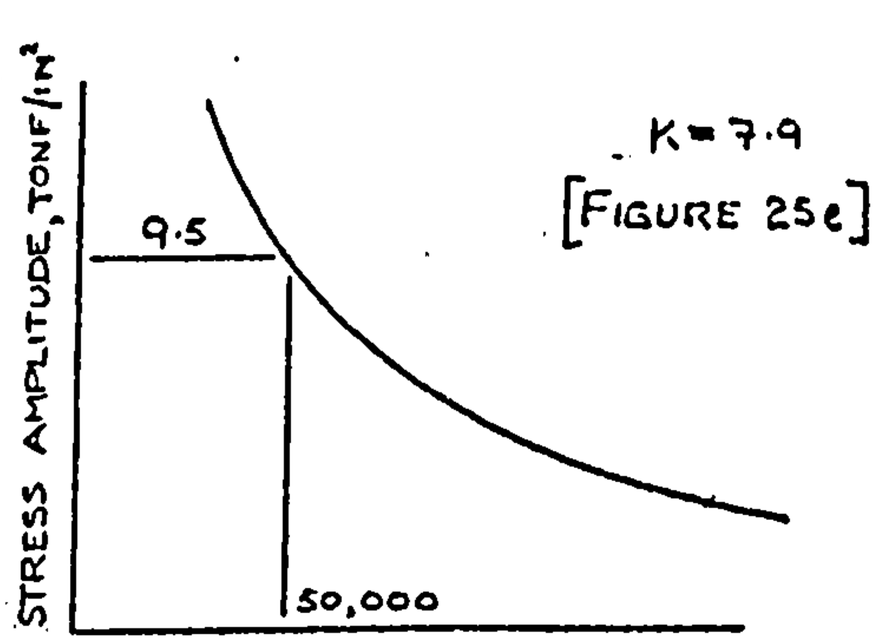

Stress conditions

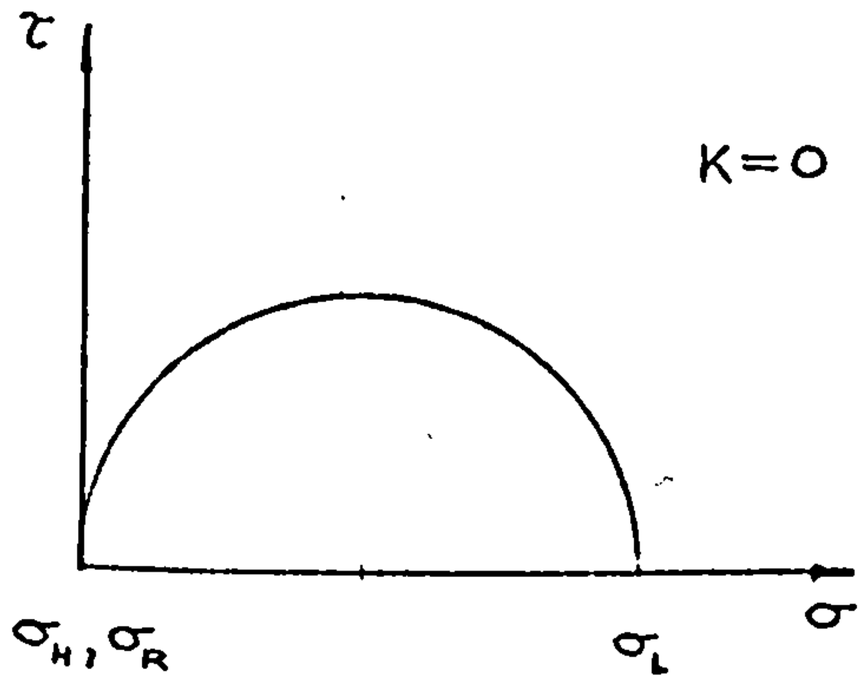

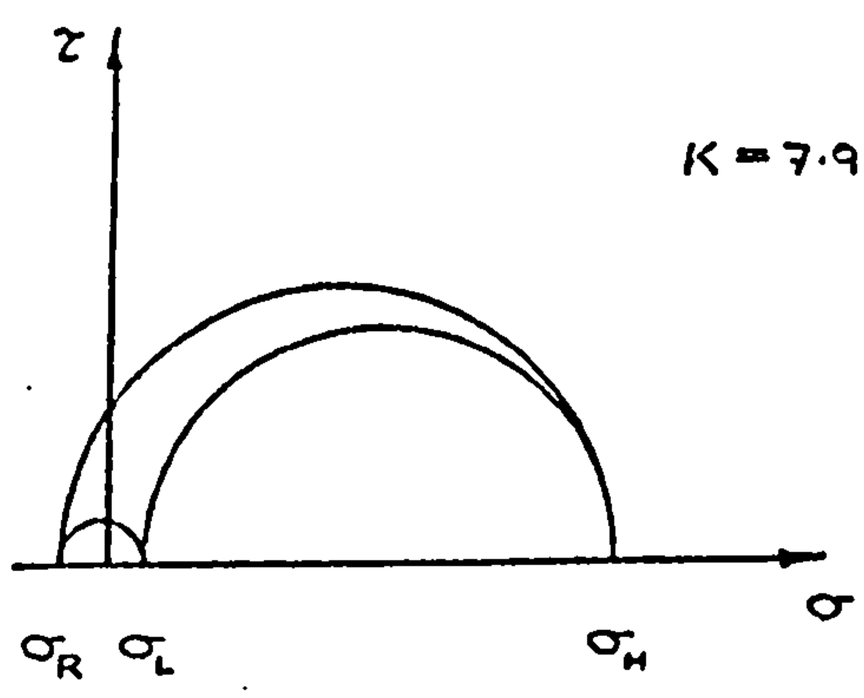

Conditions on maximum shear stress planes:

LR, LH : High shear stress amplitude : HR

HR : Low (or zero) shear stress amplitude : LR, LH

Note: HR is the anisotropic (weaker) shear stress plane.

DIAGRAM 3

K = 0/7.9

CASE 3

S_o = 9.5 ± 9.5 tonf/in^2 N_o = 170,000 cycles

$S_{7.9}$ = 9.5 ± 9.5 tonf/in^2 $N_{7.9}$ = 50,000 cycles

In this case stress conditions between cases 1 and 2 were chosen. Again at stress condition S_o damage was expected on the LR and LH maximum shear stress planes and zero damage on the HR plane. The life found at constant stress amplitude S_o = 9.5 ± 9.5 tonf/in^2 was N_o = 170,000 cycles.

At stress condition $S_{7.9}$ damage expectations were as for case 1, i.e. damage on the HR plane and no damage on the LR and LH planes.

The results of three tests gave lines of 37,000 80,000 and 154,000 cycles, showing a greater degree of scatter than in cases 1 and 2 and giving a mean life of 90,000 cycles. Failure again occurred in a longitudinal plane. If the damage mechanisms had acted separately a life of the order of 100,000 cycles would have resulted as was indicated by the mean life found.

Summary of K = 0/7.9 cumulative damage test results:

Case	Stress levels $tonf/in^2$ $S_o - S_{7.9}$	Expected life cycles	Mean test life cycles
1	12 - 9.5	80,000	40,000
2	10 - 8.5	200,000	175,000
3	9.5 - 9.5	100,000	90,000

Note: The expected life is based on the isotropic and anisotropic, damage mechanisms acting separately.

6.6.2 Cumulative Damage Tests K = -1/7.9

All cycle blocks are 10^4 cycles.

The results of these tests are given in Table 12b and the stress conditions illustrated in Fig. 21.

In the interests of clarity and as an assistance in following the text selected parts of the above information is given in the diagrams shown for each particular test stress case.

K = -1/7.9

CASE 1

At K = -1

Test stress, S_{-1} = 7 ± 7 tonf/in^2

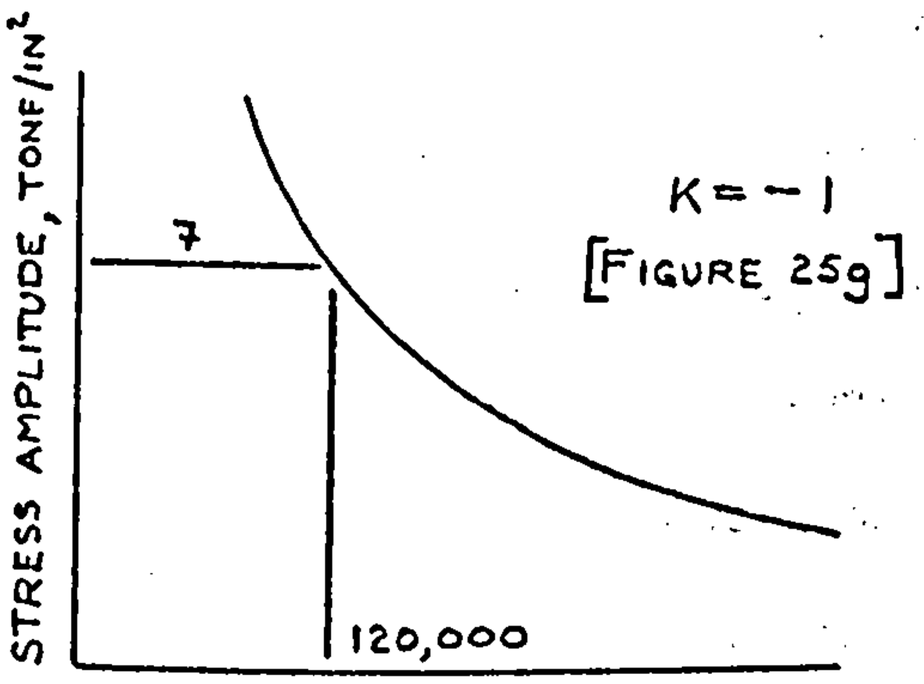

K = -1
[FIGURE 25g]

At K = 7.9

Test stress, $S_{7.9}$ = 8 ± 8 tonf/in^2

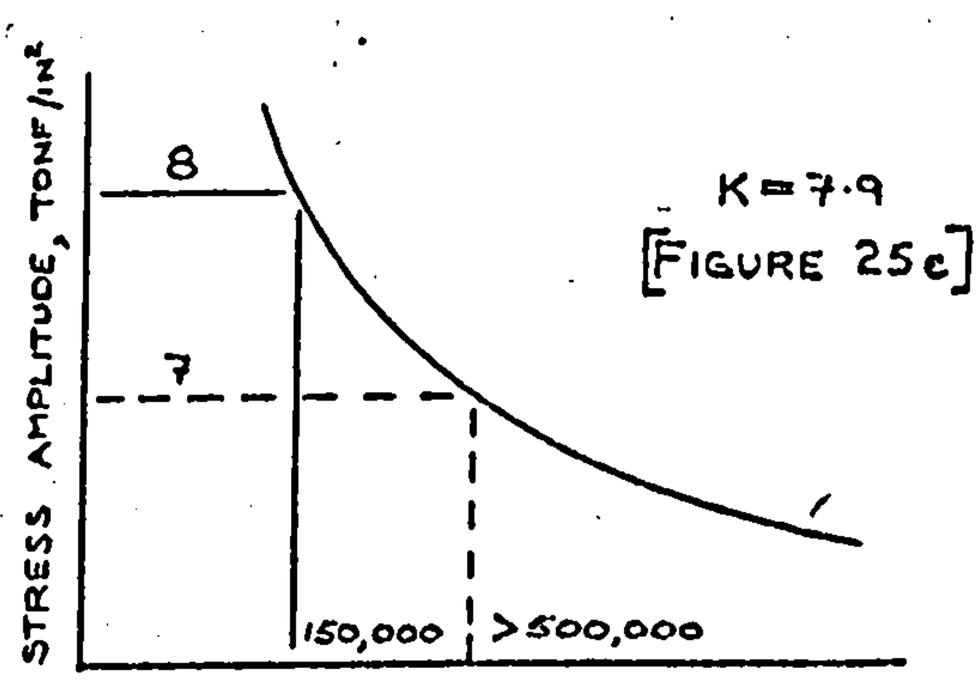

K = 7.9
[FIGURE 25c]

Stress conditions

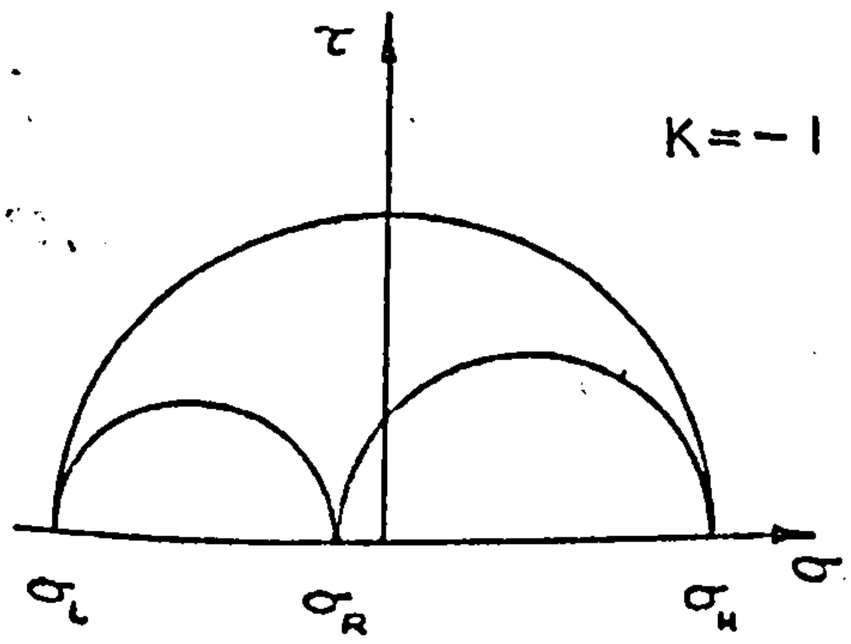

K = -1

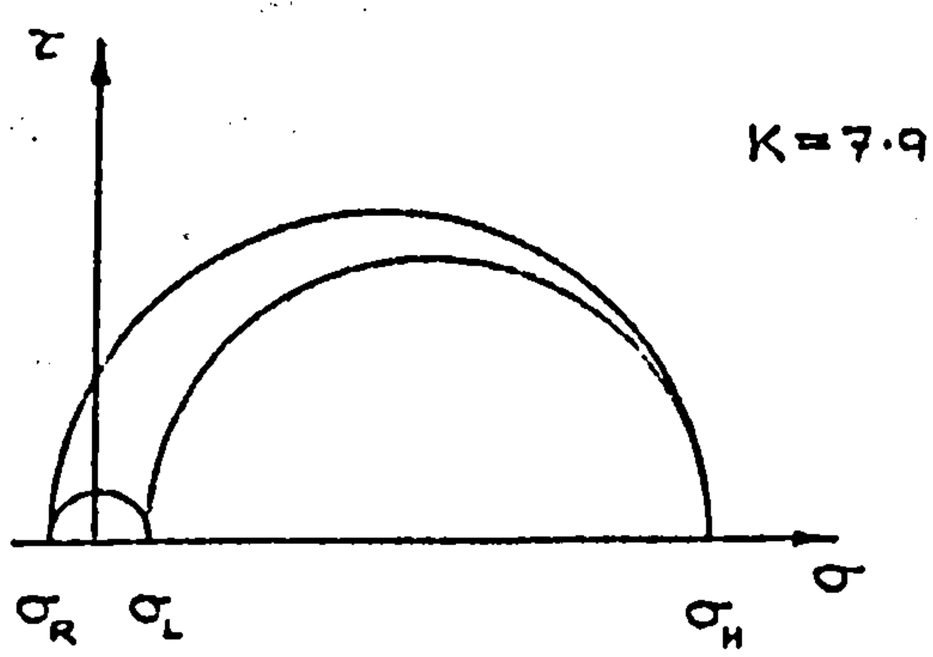

K = 7.9

Conditions on maximum shear stress planes:

LH : High shear stress amplitude : HR

LR, HR : Low shear stress amplitude : LR, LH

Note: HR is the anisotropic (weaker) shear stress plane.

DIAGRAM 4

$K = -1/7.9$

CASE 1:

$S_{-1} = 7 \pm 7$ tonf/in^2 $\quad N_{-1} = 120{,}000$ cycles

$S_{7.9} = 8 \pm 8$ tonf/in^2 $\quad N_{7.9} = 150{,}000$ cycles

At stress condition S_{-1} damage was expected on the HL maximum shear stress plane. The life found at constant stress amplitude $S_{-1} = 7 \pm 7$ tonf/in^2 was $N_{-1} = 120{,}000$ cycles. The stress condition on the HR plane was 7 ± 7 tonf/in^2 and diagram 4 shows the expected life for this stress condition to be greater than 500,000 cycles.

At stress condition $S_{7.9}$ damage was expected on the HR plane. The life found at constant stress amplitude $S_{7.9} = 8 \pm 8$ tonf/in^2 was $N_{7.9} = 150{,}000$ cycles. On the HL plane the stress condition was less than 8 ± 8 tonf/in^2 and from diagram 1 no damage was expected.

If the damage mechanisms had acted separately the expected life would have been of the order of 240,000 cycles. Test lives were 51,000 and 114,000 cycles, and failure occurred in a longitudinal plane, thus indicating the presence of interaction effects.

$K = -1/7.9$

CASE 2:

At K = -1

Test stress, $S_{-1} = 6 \pm 6$ tonf/in^2

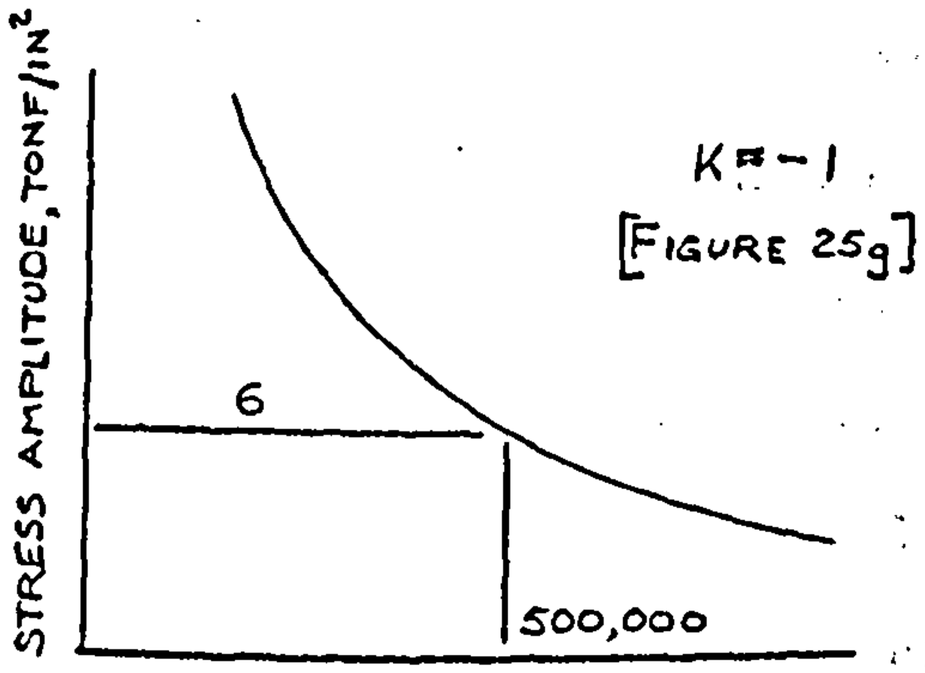

At K = 7.9

Test stress, $S_{7.9} = 8 \pm 8$ tonf/in^2

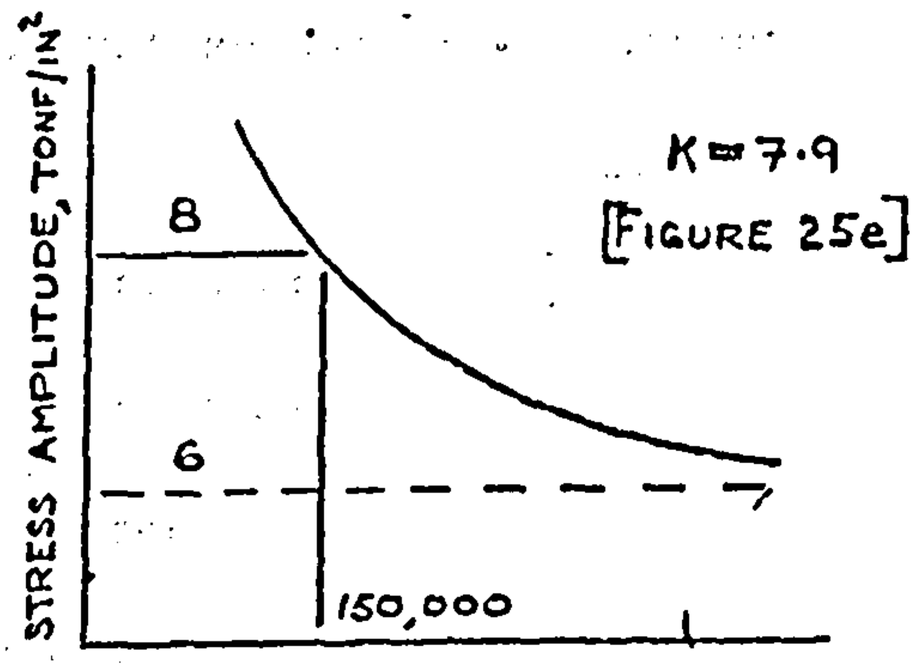

Stress conditions:

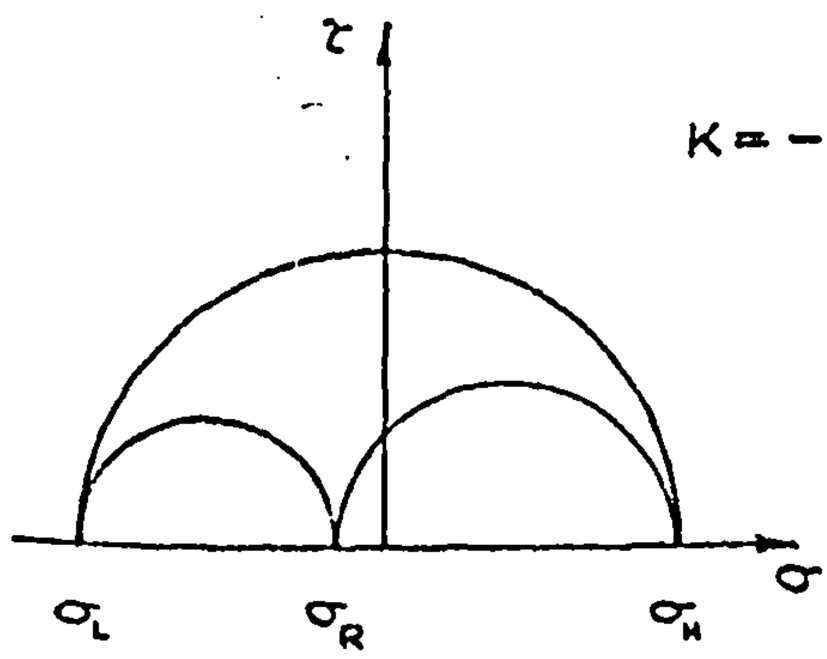

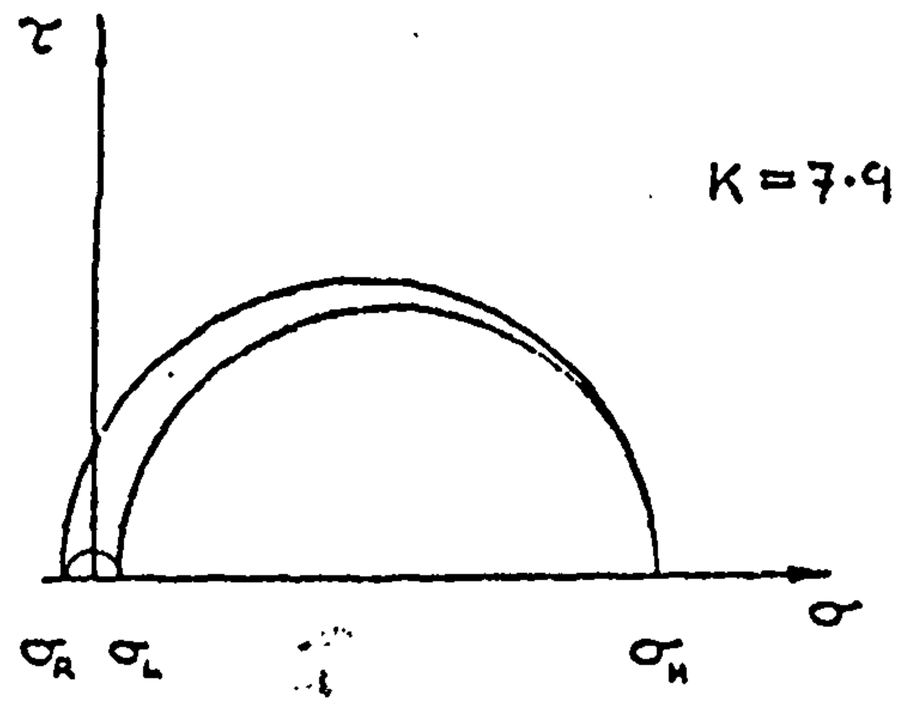

Conditions on maximum shear stress planes:

LH : High shear stress amplitude : HR

LR, HR : Low shear stress amplitude : LR, LH

Note: HR is the anisotropic (weaker) shear stress plane.

DIAGRAM 5

$K = -1/7.9$

CASE 2:

$S_{-1} = 6 \pm 6$ tonf/in^2 $\quad N_{-1} = 500{,}000$ cycles

$S_{7.9} = 8 \pm 8$ tonf/in^2 $\quad N_{7.9} = 150{,}000$ cycles

The level of S_{-1} was reduced so that no damage was expected on the HR plane, as indicated in diagram 5.

The expected life, barring interaction effects, was now of the order of 300,000 cycles. However test lives were 76,000 and 152,000, both substantially lower than expected, indicating the presence of interaction effects. Failure occurred in a longitudinal plane.

K = -1/7.9

CASE 3:

At K = -1

Test stress, S_{-1} = 5 ± 5 tonf/in^2

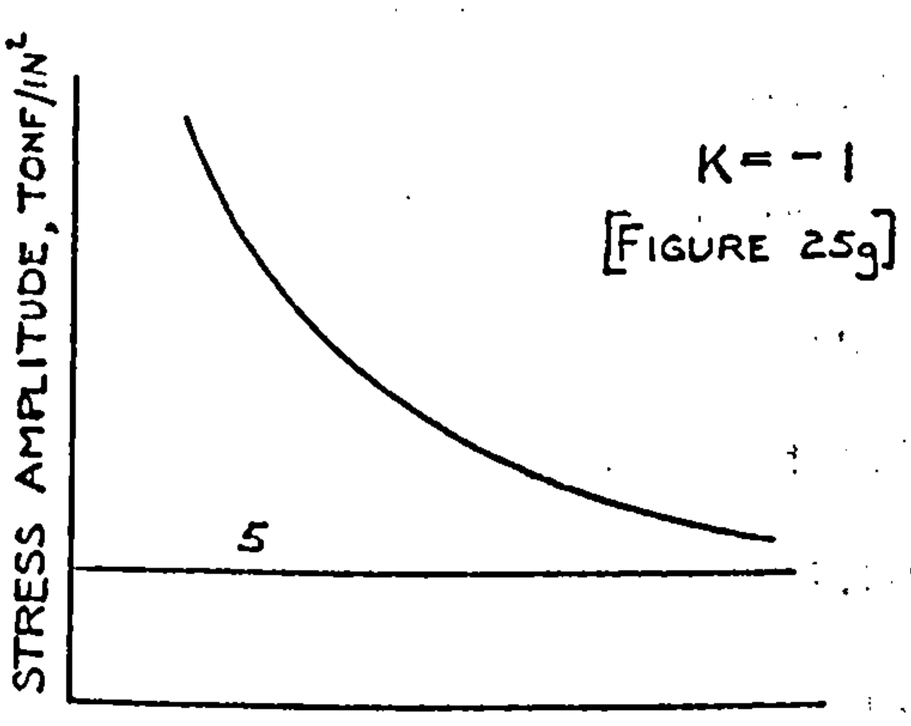

At K = 7.9

Test stress, $S_{7.9}$ = 8 ± 8 tonf/in^2

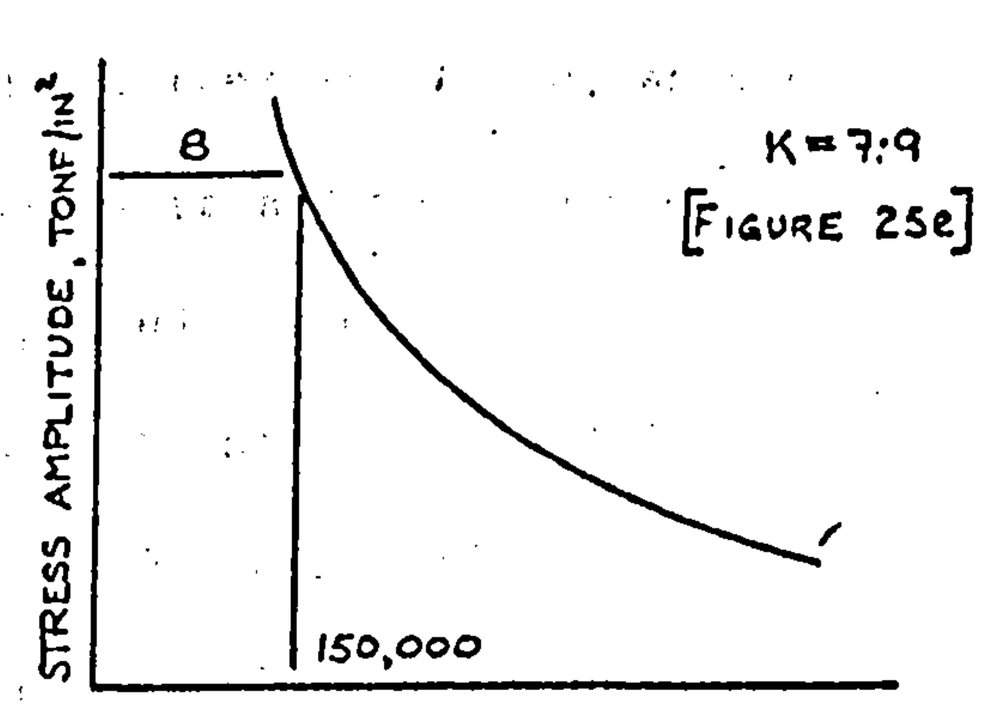

Stress conditions:

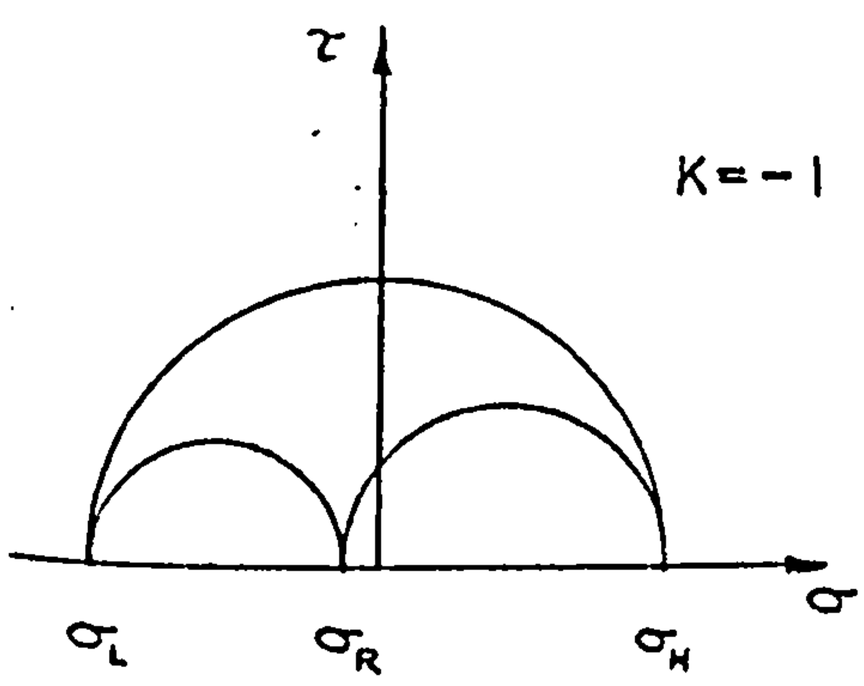

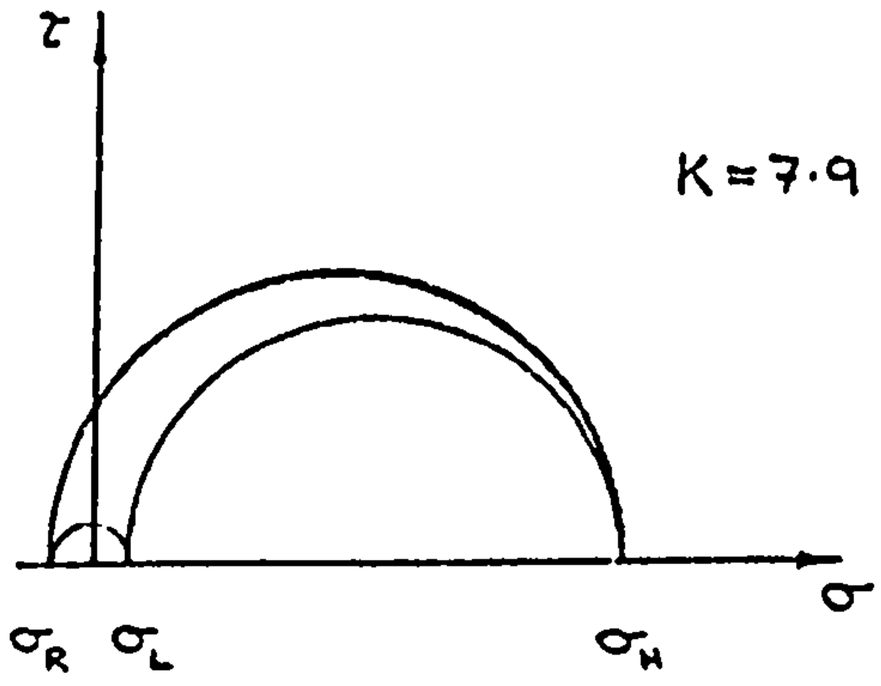

Conditions on maximum shear stress planes:

: High shear stress amplitude : HR

LH, LR, HR : Low shear stress amplitude : LR, LH

Note: HR is the anisotropic (weaker) shear stress plane.

DIAGRAM 6

$K = -1/7.9$

CASE 3:

$S_{-1} = 5 \pm 5$ tonf/in^2 $\quad N_{-1} = 10^7$ cycles

$S_{7.9} = 8 \pm 8$ tonf/in^2 $\quad N_{7.9} = 150{,}000$ cycles

Further reduction of S_{-1} to 5 ± 5 tonf/in^2 would, as seen from diagram 6, give effectively infinite life and no damage on either the isotropic HL or the anisotropic HR planes.

Thus the expected life is again of the order of 300,000 cycles. Test lives were 131,000 and 155,000 cycles indicating the continued presence of interaction effects. Failure again occurred in a longitudinal plane.

K = -1/7.9

CASE 4:

At K = -1

Test stress, S_{-1} = 4 ± 4 tonf/in^2

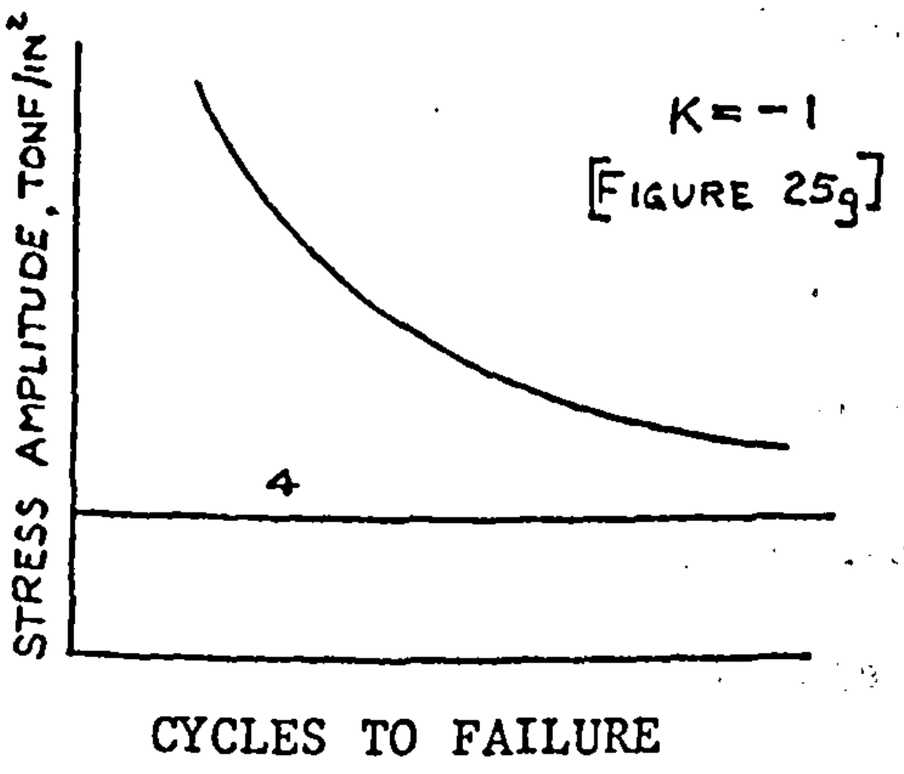

At K = 7.9

Test stress, $S_{7.9}$ = 8 ± 8 tonf/in^2

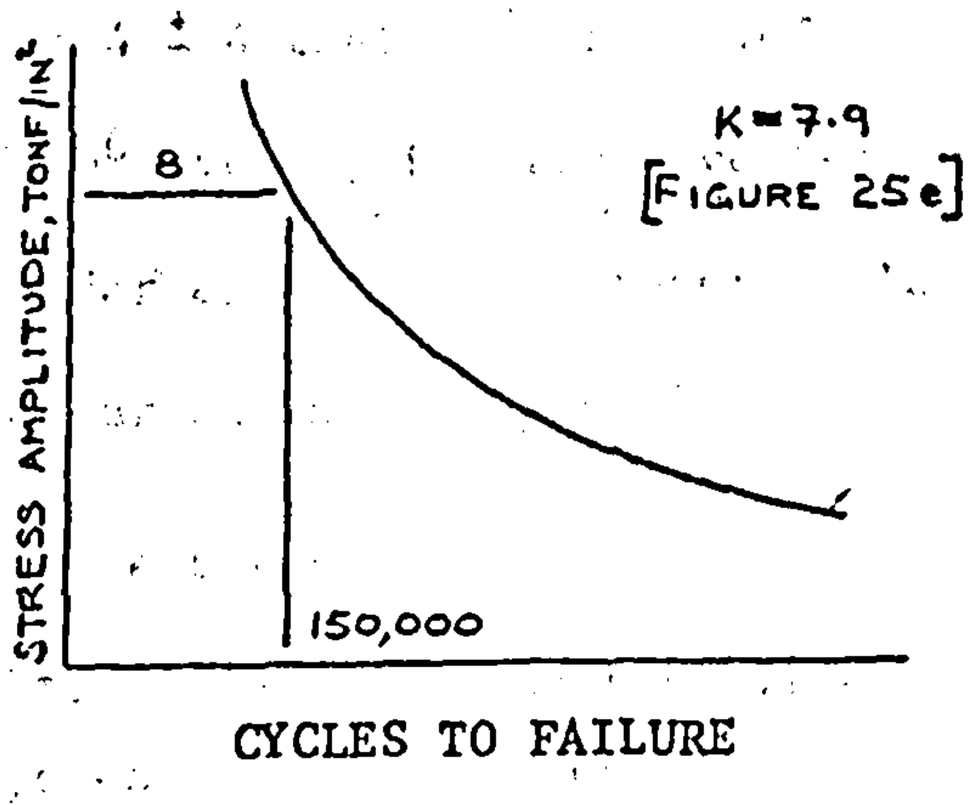

Stress conditions:

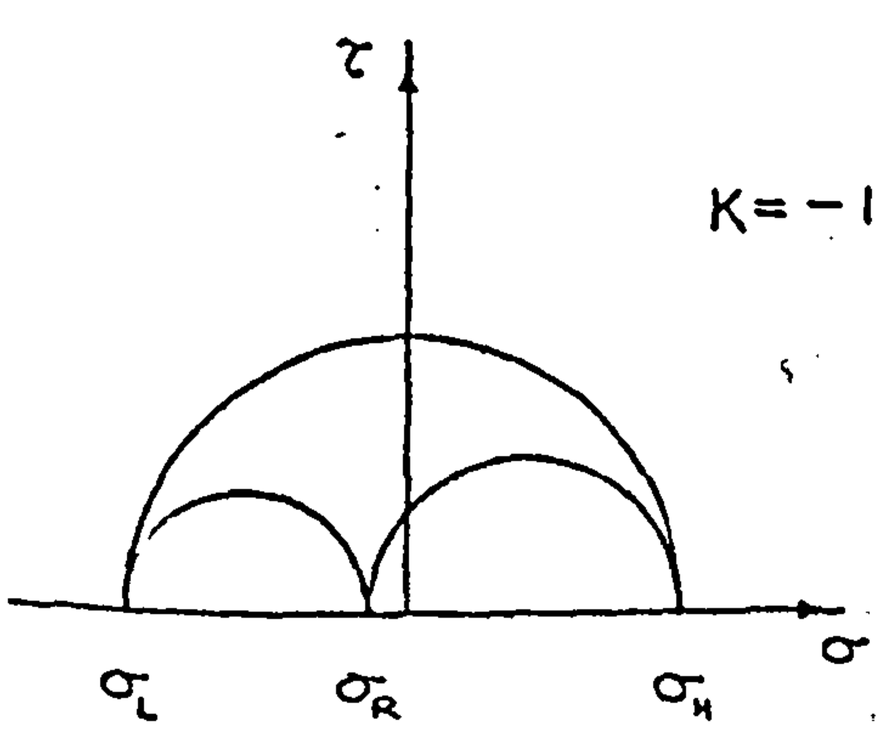

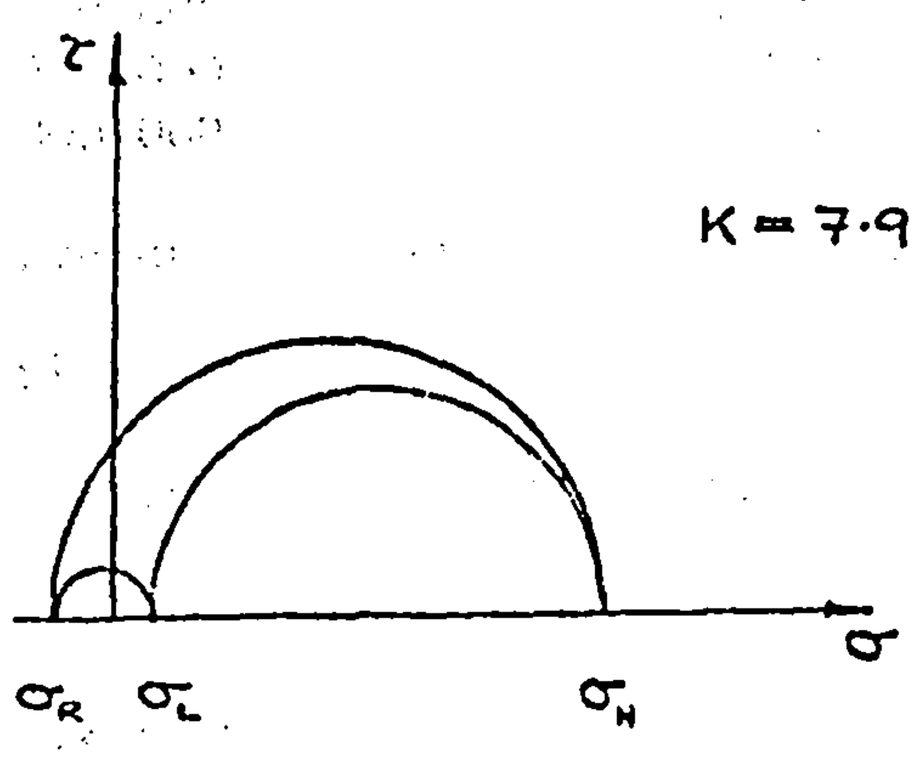

Conditions on maximum shear stress planes:

	:	High shear stress amplitude	: HR
LH, LR, HR	:	Low shear stress amplitude	: LR, LH

Note: HR is the anisotropic (weaker) shear stress plane.

DIAGRAM 7

$K = -1/7.9$

CASE 4:

$S_{-1} = 4 \pm 4$ tonf/in^2 $\quad N_{-1}$ = Infinite life

$S_{7.9} = 8 \pm 8$ tonf/in^2 $\quad N_{7.9}$ = 150,000 cycles

A further reduction of S_{-1} to 4 ± 4 tonf/in^2, i.e. 70% of the stress level to give a life of 10^6 cycles, finally gave test lives of 271,000 and 432,000, of the order expected when interaction effects do not exist. Failure again occurred in a longitudinal plane.

Summary of $K = -1/7.9$ cumulative damage test results:

Case	Stress levels tonf/in^2 $S_{-1} - S_{7.9}$	Expected life Cycles	Mean test life Cycles
1	7 - 8	240,000	80,000
2	6 - 8	300,000	110,000
3	5 - 8	300,000	140,000
4	4 - 8	300,000	350,000

These exploratory cumulative damage tests at two principal stress ratios indicate that interaction effects are occurring. A fatigue crack started at a particular stress level at the first value of principal stress ratio will continue to propagate at a second value of principal stress ratio, at a stress level which would produce no damage if applied only at the second value of principal stress ratio. In case 4 above it was necessary to reduce S_{-1} to 70% of the stress level to give a life of 10^6 cycles, in order to eliminate interaction effects. It has been suggested elsewhere (86), in connection with cumulative damage rotating bending tests that to neglect cycles of amplitude less than 80% of the fatigue limit gives results which agree closely with experiment.

6.6.3 Cumulative Damage Tests K = -1/0 and 0/-1

The results of these tests are given in Tables 12c and 12d.

As K values of -1 and 0 required the use of different configurations of the test machine these tests were run for 50,000 cycles at S_{-1}, followed to failure at S_o.

$S_{-1} = 7 \pm 7$ tonf/in^2 $\quad N_{-1} = 120{,}000$ cycles

$S_o = 10 \pm 10$ tonf/in^2 $\quad N_o = 100{,}000$ cycles

These stress conditions imposed the most severe shear stress on the HL planes in both cases. Thus, 50,000 cycles at S_{-1} represented 50,000/120,000 i.e. 0.42 of the life at S_{-1} leaving 0.58 of the life at S_o remaining, i.e. 0.58 x 100,000 = 58,000 cycles.

Test results were 58,000 and 95,000 cycles, failure occurring in the transverse direction.

Similarly for K = 0/-1, 20,000 cycles at S_o were followed to failure at S_{-1}.

$S_o = 12 \pm 12$ tonf/in^2 $\quad N_o = 40{,}000$ cycles

$S_{-1} = 7 \pm 7$ tonf/in^2 $\quad N_{-1} = 120{,}000$ cycles

Thus 20,000 cycles at S_o represented 0.50 of life, leaving 0.5 x 120,000 i.e. 60,000 cycles remaining at S_{-1}.

Test results were 77,000 cycles and unbroken at 100,000 cycles. The latter test could not be completed due to an oil leak at the specimen end.

6.7 Summary of Results

The results obtained for the various test Series are summarised below.

6.7.1 Uniaxial Fatigue Tests on Solid Specimens - Series 1

Rotating bending tests showed that the transverse fatigue strength at 10^6 cycles was 85% of the longitudinal fatigue strength.

Axial load fatigue tests showed that the fatigue strength of specimens with a good turned finish was 5% less than the fatigue strength of polished specimens at 10^6 cycles.

The repeated tensile fatigue strength of the solid specimens was found to be in good agreement with the repeated tensile fatigue strength of the thin-wall tube specimens.

6.7.2 Biaxial Constant Amplitude Fatigue Tests - Series 2

The results of these tests indicate a possible correlation with a theory of failure based on the maximum shear stress amplitude modified for the effects of the normal stress amplitude acting on the maximum shear stress plane and also the effects of mean stress and anisotropy.

The repeated tensile transverse fatigue strength at 10^6 cycles was found to be 82% of the repeated tensile longitudinal fatigue strength.

6.7.3 Biaxial Programme Fatigue Tests at Constant Principal Stress Ratio K - Series 3

The range of cycle ratio sums was found to be of the order of 0.2 to 1.5 for the four values of K at which tests were conducted.

No significant difference could be detected between the results of tests, whether the maximum shear stress amplitude occurred in the isotropic or anisotropic shear stress planes.

Strong interaction effects were found between cycles at different stress levels. The overall mean cycle ratio sum found was 0.77 with a lowest value of 0.13.

The lowest values of cycle ratio sums were found for K = 2 and 7.9 at $S_2 - S_3$ ($10^4 - 10^5$), reducing the tests to single step tests.

6.7.4 Biaxial Programme Fatigue Tests at Two Principal Stress Ratios - Series 4

A small number of exploratory tests indicated strong interaction effects and also that cycles at stress levels greater than the order of 70% of the fatigue strength at 10^6 cycles had to be taken into account.

PART III

DEVELOPMENT OF CRITERIA OF FATIGUE FAILURE UNDER MULTIAXIAL STRESS AND COMPARISON WITH PUBLISHED EXPERIMENTAL DATA. ALSO COMPARISON OF CUMULATIVE DAMAGE RESULTS WITH UNIAXIAL CUMULATIVE DAMAGE THEORIES

A study of the literature showed that none of the existing general fatigue failure equations satisfactorily explained the results of published multiaxial stress fatigue tests. It was decided to attempt to develop such an equation taking the fluctuating shear stress on the plane of maximum shear stress as the criterion of failure modified for the effect of the mean and fluctuating normal stresses on the same plane and also considering the effect of anisotropy. It was intended that this fatigue failure criteria should be general in so far as explaining the results of all multiaxial stress fatigue investigations so far conducted on ductile materials including combined bending and twisting and tests on thin and thick wall tubes.

The results of the cumulative damage tests conducted in this thesis were studied with a view to the possible extension of theories so far developed for the case of uniaxial stress cumulative damage to the multiaxial stress cumulative damage condition.

A new approach to fatigue analysis has been suggested based on the work reported in this thesis.

CHAPTER 7

DEVELOPMENT OF CRITERIA OF FATIGUE FAILURE

7.1 Introduction

As the constant amplitude fatigue tests progressed it became apparent that the test data could possibly be correlated on the basis of maximum shear stress modified for the effect of the normal stress on the maximum shear stress plane as already discussed in Chapter 1. In this work the results could also be affected by material anisotropy and mean stress, as pulsating stress conditions are used. The effect of material anisotropy is discussed later in this Chapter.

A re-examination of the literature indicated that no detailed study had been made of the case of combined bending and twisting with regard to a possible failure criteria based on maximum shear stress modified by the effect of the normal stress on the maximum shear stress plane. Findley, as already discussed in Chapter 1.6, has worked in this field and suggested a failure criterion based on maximum shear stress modified for the effects of anisotropy andnormal stress acting on the maximum shear stress plane (26). This criterion requires the use of the least squares method on test data to solve for three material constants which has been carried out for the one material tested. In this test series only three conditions of combined bending and twisting were tested. No attempt has been made to apply the criterion to the more extensive work of Gough (12) who tested 14 materials at five conditions of combined bending and twisting.

It is difficult to separate the effects of anisotropy and normal stress acting on the maximum shear stress plane. Findley (18) showed that the maximum shear stress failure criterion when modified for the effect of anisotropy led to the Gough ellipse quadrant equation.

There is however no evidence to indicate that anisotropy was present in any of the materials tested by Gough, although it is only fair to say that no tests were conducted to determine the degree of anisotropy. On this particular point Gough (87) states

> "The regularity of the variation in fatigue resistance as the principal stress changes from the direction of the specimen axis to one making 45 degrees with that axis does not suggest that this variation can be due, to any appreciable extent, to anisotropy of the material, but is primarily a real stress effect. For this regularity of variation is a feature observed with all the materials tested, whereas the degree of anisotropy present in the various materials would be expected to differ considerably."

In the particular case of combined bending and twisting the ellipse quadrant equation was found by empirically fitting the combined stress data between the end points of bending only and torsion only which were assumed to lie on the curve. This procedure will automatically account for any anisotropic effect occurring.

It is now proposed to re-examine combined bending and twisting data from the view point of a maximum shear stress failure criterion modified for the effect of normal stress on the maximum shear stress plane assuming that either there is no anisotropy or that its effect is included by virtue of taking the bending only and torsion only data points as end points on the curve.

7.2 A Further Study of Fatigue Failure under Combined Bending and Twisting

The Gough ellipse quadrant equation

$$\frac{f^2}{b^2} + \frac{q^2}{t^2} = 1 \qquad (7.1)$$

may be written as

$$\left(\frac{f}{2}\right)^2 \frac{4t^2}{b^2} + q^2 = t^2$$

and thus

$$\left(\frac{f}{2}\right)^2 + q^2 = t^2 - \left(\frac{f}{2}\right)^2 \frac{4t^2}{b^2} + \left(\frac{f}{2}\right)^2$$

$$= t^2 - \left(\frac{f}{2}\right)^2 \left[\frac{4t^2}{b^2} - 1\right]$$

Now $\left[\left(\frac{f}{2}\right)^2 + q^2\right]^{\frac{1}{2}} = \tau_a$, the shear stress amplitude on the maximum shear stress plane

and $\frac{f}{2} = \sigma_r$, the normal stress amplitude on the maximum shear stress plane

$$\therefore \quad \tau_a^2 = t^2 - \left[\frac{4t^2}{b^2} - 1\right] \sigma_r^2 \qquad (7.2)$$

or $$\tau_a^2 = C_1 - C_2 \sigma_r^2 \qquad (7.3)$$

where C_1 = a material constant $= t^2$

C_2 = " " " $= \left[\frac{4t^2}{b^2} - 1\right]$

The Gough ellipse quadrant equation shows that the maximum allowable shear stress amplitude is a function of the normal stress amplitude acting on the maximum shear stress plane and two material constants, themselves a function of the reversed bending and reversed torsion fatigue strengths of the material.

In order to investigate the relationship between τ_a and σ_τ which best fits the Gough test data it is assumed that

$$\tau_a = C_3 - C_4 \sigma_\tau^n \qquad (7.4)$$

where C_3, C_4 = material constants

and n = a constant

This possible relationship between τ_a and σ_τ is chosen for initial investigation as it is the most simple non linear effect of σ_τ on τ_a, including a single power function of stress rather than the more complex expression of equation 7.3 which includes two stress power functions.

Assuming, as in the Gough ellipse quadrant equation, that the curve passes through the points $(f = o, q = t)$ and $(f = b, q = o)$ then from

$$\left[\left(\frac{f}{2}\right)^2 + q^2\right]^{\frac{n}{2}} = C_3 - C_4\left(\frac{f}{2}\right)^n$$

when $f = o, q = t$

$$\therefore \quad C_3 = t$$

and when $f = b, q = o$

$$\therefore \quad C_4 = \frac{t - \frac{b}{2}}{\left(\frac{b}{2}\right)^n}$$

$$= \left(\frac{2}{b}\right)^n t - \left(\frac{b}{2}\right)^{1-n}$$

thus

$$\tau_a = t - \left[\left(\frac{2}{b}\right)^n t - \left(\frac{b}{2}\right)^{1-n}\right]\left(\frac{f}{2}\right)^n \qquad (7.5)$$

Fig. 28 shows the solution of equation 7.5 for a range of n = 0.5, 1.0, 1.5, 2.0 and 2.5 and also equation 7.2, for values of b/t = 1.0, 1.5 and 2.0. As b/t increases from 1.0 to 2.0 the value of τ_a becomes less dependent on the value of n and is independent of n when b/t = 2.0. The maximum principal stress failure criterion predicts a value of b/t = 1.0 while the maximum shear stress failure criterion predicts a value of b/t = 2.0.

Tables 13 to 15 and Fig. 29 show the analysis of the Gough (12) test data for equation 7.2 and equation 7.5 for a range of n = 0.5 to 2.5 in increments of 0.1. Fig. 29a shows that for the solid and hollow specimen tests where b/t is less than 1.70 a value of n = 1.5 gives a standard deviation* within 0.2% for five materials and 0.7% for the other two. When b/t is greater than 1.70 Fig. 28 has shown that the curves are almost independent of n. The Gough ellipse quadrant equation has an equivalent value of n = 2.2 and gives a standard deviation within 0.9% for six materials and 1.5% for the other one, with b/t less than 1.70. (* See Nomenclature.)

In the case of the two cast irons and the notched materials the position is not quite so clear. A value of n = 1.25 gives a standard deviation within 1.4% for all cases with the exception of one cast iron as shown in Fig. 29c.

Frith (88) conducted combined bending and twisting fatigue tests on high-tensile alloy steels. The analysis of this data is shown in Tables 16 and 17 and Fig. 30. Again a value of n = 1.5 is found for the solid and hollow specimens and a lower value of 1.0 to 1.25 found for the specimens with stress raising oil holes.

Finally the data of Nishihara and Kawamoto (15), who tested several ferrous and non-ferrous materials under combined bending and twisting fatigue, has been analysed and the results are shown in Tables 18 and 19 and Fig. 31. Again, for the ductile materials a value of n = 1.5 gives a standard deviation within 0.5% for all materials.

The above analysis indicates that for ductile materials

$$\tau_a = C_3 - C_4 \sigma_\tau^{1.5} \qquad (7.6)$$

where

$$C_3 = t$$

$$C_4 = \frac{t - \frac{b}{2}}{\left(\frac{b}{2}\right)^{1.5}}$$

The values of the material constants C_3 and C_4 for the materials tested by Gough are given in Table 15.

This analysis has shown that the fatigue behaviour of materials under completely reversed combined bending and twisting can be predicted to a high degree of accuracy in terms of the bending only and twisting only fatigue strengths. Equation 7.6 is based on the physical interpretation of the effect of the normal stress acting on the maximum shear stress plane whereas the Gough ellipse quadrant was proposed as a purely empirical relationship. Both equations allow for the possible effect of material anisotropy by taking the bending only and torsion only results as end points of the curve.

7.3 General Reversed Stress Systems

Equation 7.6 has been derived for the case of combined bending and twisting. Extending this equation to the general case we have

$$\tau_a = C_5 - C_6 \sigma_\tau^{1.5} \qquad (7.7)$$

where $\pm \tau_a$ is allowable range of shear stress on the maximum shear stress plane

$\pm \sigma_\tau$ is the range of normal stress on the maximum shear stress plane

and C_5, C_6 are material constants.

To solve for the material constants C_5 and C_6, from the case of uniaxial reversed stress where $\tau_a = \sigma_A/2$,

$$\frac{\sigma_A}{2} = C_5 - C_6\left(\frac{\sigma_A}{2}\right)^{1.6} \qquad (7.8)$$

and from the case of reversed pure shear stress where $\tau_a = \tau_A$

$$\tau_A = C_5 \qquad (7.9)$$

It should be noted that if τ_A is found from reversed torsion it will include the effect of any anisotropy occurring in the material whereas if τ_A is found from thin wall cylinder tests at K = -1 no anisotropic effect is included as the maximum shear stress does not act on the anisotropic maximum shear stress plane.

Then using equations 7.8 and 7.9

$$C_6 = \frac{\tau_A - \frac{\sigma_A}{2}}{\left(\frac{\sigma_A}{2}\right)^{1.5}} \qquad (7.10)$$

Thus, substituting for C_5 and C_6 in equation 7.7

$$\tau_a = \tau_A - \left[\frac{\tau_A - \frac{\sigma_A}{2}}{\left(\frac{\sigma_A}{2}\right)^{1.5}}\right] \sigma_\tau^{1.5} \qquad (7.11)$$

Assuming that τ_A is the reversed torsion fatigue strength t and that σ_A , the reversed axial fatigue strength is equal to the reversed bending fatigue strength b .then the relationship between t and b for structural materials is as shown in Table 20, reproduced from Forrest (84). The most widely used structural materials are steels and aluminium alloys having average values of t/b of 0.60 and 0.55 respectively. An average value of 0.58 is used which allows direct comparison with expressions derived in (42). It has to be borne in mind that this average value of t/b of 0.58 is derived from values ranging from 0.52 to 0.74.

Then using $\frac{t}{b} = 0{\cdot}58 = \frac{\tau_A}{\sigma_A} = \frac{1}{\sqrt{3}}$ in equations 7.9 and 7.10 gives

$$C_6 = \frac{0{\cdot}58\,\sigma_A - 0{\cdot}5\,\sigma_A}{\left(\frac{\sigma_A}{2}\right)^{1.5}} = \frac{0{\cdot}225}{\sigma_A^{0.5}} \qquad (7.12)$$

and $$C_5 = 0{\cdot}58\,\sigma_A \qquad (7.13)$$

Then equation 7.7 becomes

$$\tau_a = 0{\cdot}58\,\sigma_A - \frac{0{\cdot}225}{\sigma_A^{0.5}}\,\sigma_\tau^{1.5} \qquad (7.14)$$

The limiting reversed biaxial stresses obtained from equation 7.14 are shown in Fig. 32 in terms of the reversed fatigue strength σ_A .

7.4 Effect of Mean Stress

Many components in structures are subjected to stresses which fluctuate between different values of tension and compression. Only a limited amount of data on the effect of static mean stress is available and most of this data concerns the case of uniaxial tensile mean stress. Uniaxial mean stress tests show considerable variation in results (84) and a number of empirical relations have been proposed (89) to enable an estimate to be made of the fluctuating fatigue strength if the alternating fatigue strength and the tensile strength of the material are known. The most commonly used uniaxial mean stress equations are those of Gerber and Goodman in the forms known as the Gerber Parabola and the Modified Goodman Line as shown in Fig. 33. These equations are perfectly adequate in the case of tensile mean stress, the Modified Goodman Line being more conservative than the Gerber Parabola, most results for ductile materials falling above the Modified Goodman Line. In the case of compressive mean stress these equations are found to be inadequate, as the presence of a compressive mean stress has been found to increase the allowable alternating fatigue strength, rather than cause a decrease as predicted by the equations. Data involving the effect of a compressive mean stress is very limited but the point is illustrated in the results shown in Figs. 34 and 35, where the results are plotted as a function of the ultimate tensile stress as is the case in the use of the Gerber Parabola and the

Modified Goodman Line. In order to cope with this difficulty Booth (42) has suggested an equation of the form

$$\left(\frac{\sigma_a}{\sigma_A}\right)^2 + \frac{\sigma_M}{\sigma_U} = 1 \qquad (7.15)$$

As shown in Fig. 33 this is a parabola with the apex at unity on the abscissa whereas the Gerber Parabola has the apex at unity on the ordinate. Fig. 33 also shows the limiting static failure stresses for a range of values of the endurance ratio. Booth also pointed out that his proposed equation would tend to give higher values than could be obtained in a static test, in the case of shorter life tests at high mean stress with high values of endurance ratio. This is also the case with the Gerber Parabola.

Equation 7.15 when written in terms of the shear and normal stress conditions on the maximum shear stress plane gives

$$\left(\frac{\tau_a}{\sigma_A/2}\right)^2 + \frac{\sigma_{mr}}{\sigma_U/2} = 1 \qquad (7.16)$$

This predicts no decrease in torsional stress amplitude with an increase in static torque and a value of $\tau_A/\sigma_A = 0.5$ The results collected by Smith (90) and shown in Fig. 36 show that for ductile metals a superimposed static shear stress has little effect on the reversed shear stress provided that the maximum stress in the cycle does not exceed the yield stress. Tests conducted by Gough (12) further indicated that a superimposed bending stress on reversed torsion (so that the superimposed principal bending stress is on the plane of maximum reversed shear stress) has a large weakening effect. These results indicate that the mean normal stress acting on the maximum fluctuating shear stress plane has an effect on the fatigue strength.

For the effect of the mean normal stress acting on the plane of maximum fluctuating shear stress, from equation 7.16

$$\tau_a = \frac{\sigma_A}{2}\left[1 - \frac{\sigma_{MT}}{\sigma_U/2}\right]^{\frac{1}{2}} \qquad (7.17)$$

The combined effect of the mean normal stress and the amplitude of normal stress acting on the maximum fluctuating shear stress plane is obtained from equations 7.11 and 7.17 as

$$\tau_a = \left\{\tau_A - \left[\frac{\tau_A - \sigma_A/2}{(\sigma_A/2)^{3/2}}\right]\sigma_\tau^{3/2}\right\}\left[1 - \frac{\sigma_{MT}}{\sigma_U/2}\right]^{\frac{1}{2}} \qquad (7.18)$$

and in the case of $\tau_A/\sigma_A = t/b = 0.58$

$$\tau_a = \left[0.58\sigma_A - \frac{0.225}{\sigma_A^{1/2}}\sigma_\tau^{3/2}\right]\left[1 - \frac{\sigma_{MT}}{\sigma_U/2}\right]^{\frac{1}{2}} \qquad (7.19)$$

The limiting biaxial repeated stresses (zero minimum stresses) obtained from equation 7.19 are shown in Figs. 32 and 37 which illustrate the effect of the endurance ratio on the limiting stresses. The equation is plotted in terms of both the reversed (σ_A in Fig. 32) and the repeated tensile (σ_D in Fig. 37) fatigue strengths for convenience later when comparing the equation with published test results.

Another possible method of dealing with the effect of mean stress is suggested by Fig. 38 reproduced from Forrest (84). The ratio σ_a/σ_A is shown to vary linearly with σ_M/σ_Y according to

$$\sigma_a = \sigma_A\left[1 - \frac{0.4\sigma_M}{\sigma_Y}\right] \qquad (7.20)$$

giving a mean stress correction factor of

$$\left[1 - \frac{0.4\,\sigma_{mr}}{\sigma_Y}\right]$$

and in the case of $\tau_A/\sigma_A = t/b = 0.58$ then

$$\tau_a = \left[0.58\,\sigma_A - \frac{0.225}{\sigma_A^{1/2}}\,\sigma_\tau^{3/2}\right]\left[1 - \frac{0.4\,\sigma_{mr}}{\sigma_Y}\right] \qquad (7.21)$$

Table 22 shows a comparison of the results obtained from equations 7.19 and 7.21 for σ_{-D}/σ_D in the case of the Ros and Eichinger (34) test data. No significant improvement in the correlation of test data is found and it is proposed that equation 7.19 in terms of σ_U is used as fatigue data is more commonly related to σ_U than σ_Y.

The effect of mean stress may be better expressed in terms of the true fracture stress rather than the ultimate tensile strength, but at present test data on true fracture stress is limited (42).

7.5 Effect of Anisotropy

Many materials exhibit a considerable degree of anisotropy and this effect has to be allowed for in considering fatigue strength under multiaxial stress. Table 21, reproduced from Findley and Mathur (22) shows that the reduction in fatigue strength between the strongest and weakest directions may be up to 45%. Most of this data was obtained from fatigue tests made in bending on specimens cut parallel and perpendicular to the grain of the bar stock. Not only is there very little data on anisotropy with regard to multi-axial stress fatigue, no data can be found on the uniaxial fatigue strengths of anisotropic materials with regard to mean stress effects in both the longitudinal and transverse directions.

Anisotropy at the macroscopic level can be attributed to

effects such as alignment in the direction of metal flow, non-metallic inclusions, cavities and preferential grain orientation. These result in two types of anisotropy: firstly location anisotropy where properties vary according to position in the bar or billet of material and secondly direction anisotropy which can appear in a material containing stringer type inclusions or preferential grain direction due to rolling or extruding.

Frith (88) has shown that anisotropy increases as reduction in diameter from ingot to bar is increased. For steels treated to 110 tonf/in^2 tensile strength he obtained a reduction in fatigue strength in the transverse direction of 21 to 36% for steel reduced 86% from ingot bar and 41% for a steel reduced 95%. The results of other investigators are also quoted showing that the reduction of fatigue strength in the transverse direction increases with the strength of the steel. These results are in agreement with those of Boyd (94) who tested one steel tempered at seven different temperatures to produce a tensile strength ranging from 60 to 130 tonf/in^2. He found that the reduction in the fatigue limit from the longitudinal to transverse direction increased from 15% for a tensile strength of 60 tonf/in^2 to 50% for a tensile strength of 130 tonf/in^2. The longitudinal fatigue limit increased with the U.T.S. but there was only a small change in the transverse fatigue limit.

Templin et al (95) tested four aluminium alloys but found little difference between the transverse and longitudinal fatigue strengths. Findley and Mathur (22) however, testing two aluminium alloys, obtained up to 20% reduction in bending fatigue strength.

In the case of combined bending and twisting, as already discussed in Chapter 7.1, the effect of any anisotropy present in the

material is catered for in using the reversed bending and reversed torsion fatigue strengths as end points in the derived relations.

In the case of tests on thin wall tubes the effect of anisotropy can be allowed for by using a reduction factor $\overline{A}$ applied to the limiting alternating shear stress when this occurs on the anisotropic maximum shear stress plane, where

$$\overline{A} = \frac{\text{fatigue strength in the transverse direction}}{\text{fatigue strength in the longitudinal direction}}$$

$$= \frac{\sigma_{HP}}{\sigma_{LP}}$$

and it is assumed that mean stress effects are the same in the longitudinal and transverse directions.

In other cases where the plane of maximum alternating shear stress falls between the maximum and minimum strength shear planes it would be safer to use the anisotropic fatigue strength at present till further information is obtained. The results of Findley and Mathur (22) indicate that a simple linear relationship between fatigue strength and angle of rotation between the maximum and minimum strength directions would give a reasonable approximation.

7.6 Summary

The derived general expression for fatigue failure of ductile metals under multiaxial stress based on the maximum shear stress theory of failure modified for the effects of the fluctuating and mean normal stresses acting on the plane of maximum shear stress is

$$\tau_a = \left\{ \tau_A - \left[\frac{\tau_A - \frac{\sigma_A}{2}}{\left(\frac{\sigma_A}{2}\right)^{3/2}} \right] \sigma_\tau^{3/2} \right\} \left[1 - \frac{\sigma_{mt}}{\sigma_u/2} \right]^{\frac{1}{2}} \qquad (7.18)$$

Where τ_A/σ_A is assumed equal to $1/\sqrt{3}$ then equation 7.18 becomes

$$\tau_a = \left[0.58\,\sigma_A - \frac{0.225}{\sigma_A^{1/2}}\,\sigma_\tau^{3/2}\right]\left[1 - \frac{\sigma_{mx}}{\sigma_u/2}\right]^{\frac{1}{2}} \qquad (7.19)$$

in terms of σ_A and σ_u.

If the effect of σ_τ is neglected the simplified form of equation 7.19 becomes

$$\left[\frac{\tau_a}{\sigma_A/\sqrt{3}}\right]^2 + \frac{\sigma_{mx}}{\sigma_u/2} = 1 \qquad (7.22)$$

In the case of uniaxial stress, equation 7.18 simplifies to the form given in equation 7.15,

$$\left(\frac{\sigma_a}{\sigma_A}\right)^2 + \frac{\sigma_m}{\sigma_u} = 1 \qquad (7.15)$$

CHAPTER 8

COMPARISON OF PROPOSED EQUATIONS WITH EXPERIMENTAL RESULTS

8.1 Introduction

Due to the inherent scatter in the experimental data so far available and also the different forms of presentation of this data, the most satisfactory method of comparing fatigue test results with various proposed failure criteria is of a diagrammatic nature. In this way any correlation, or otherwise, is immediately apparent.

The only other general equations so far proposed for fatigue failure under multiaxial stress are those of Marin (60) and Booth (42). The Marin equation has already been discussed (Chapter 1.6) and rejected as inadequate. A further inadequacy of the Marin equation not already mentioned is the fact that it predicts equal fatigue strengths for repeated tension and compressive stress. It is quite clear from test data that this is not so. At this stage it is necessary to discuss the Booth equations in greater detail.

8.2 The Booth Equations

Booth (42) proposed the following equations.

(a) For all metals:

$$A\tau_a + C\sigma_{m\tau} + B\sigma_a + D\sigma_m = 1 \qquad (8.1)$$

where the constants A, B, C and D are found from the reversed torsion and axial load fatigue strengths and the fatigue strength under reversed torsion with a superimposed static torque together with the true fracture strength. σ_a is the principal stress amplitude.

It is not possible to compare this equation with test results as it involves the true fracture strength which can not be calculated from the results reported.

Further this equation, when used for the case of combined bending and torsion, reduces to the Ellipse Arc used by Gough (12) which is known to apply to brittle but not ductile materials.

(b) For most structural metals, where only one fatigue strength and the U.T.S. are required

$$8\tau_a^2 + \sigma_a^2 + 6\frac{\sigma_A^2}{\sigma_u}\cdot\sigma_{m\tau} = 3\sigma_A^2 \qquad (8.2)$$

This equation is derived from the equation

$$A\tau_a^2 + B\hat{\sigma}_a^2 + C\sigma_{m\tau} = 1 \qquad (8.3)$$

relating alternating shear strength, τ_a, maximum principal stress amplitude, $\hat{\sigma}_a$, and the mean normal stress, $\sigma_{m\tau}$, acting on the same plane as τ_a. The constants A, B and C are found from the reversed torsion and axial load fatigue strengths and the U.T.S. Also τ_A/σ_A is assumed equal to 0.58.

(c) A simpler equation is proposed for design purposes, neglecting the effect of the maximum principal stress amplitude

$$\left(\frac{\tau_a}{\sigma_A/2}\right)^2 + \left(\frac{\sigma_{m\tau}}{\sigma_u/2}\right) = 1 \qquad (8.4)$$

This predicts $\tau_A/\sigma_A = 0.5$

In equation 8.2 a relationship has been assumed between τ_a^2, $\hat{\sigma}_a^2$ and $\sigma_{m\tau}$. In this thesis a relationship has been derived between

τ_a^2, σ_τ^3 and $\sigma_{m\tau}$ resulting in equation 7.19. If the Booth approach in the manner of equation 8.3 is used such that

$$A\,\tau_a^2 + B\,\sigma_\tau^3 + C\,\sigma_{m\tau} = 1 \qquad (8.5)$$

the equation derived is

$$3\,\tau_a^2 + \frac{2}{\sigma_A}.\sigma_\tau^3 + 2\,\sigma_A^2.\frac{\sigma_{m\tau}}{\sigma_u} = \sigma_A^2 \qquad (8.6)$$

The simplified expression found from equation 8.6 when the effect of σ_τ is neglected is equivalent to

$$\left(\frac{\tau_a}{\sigma_A/\sqrt{3}}\right)^2 + \frac{\sigma_{m\tau}}{\sigma_u/2} = 1 \qquad (8.7)$$

8.3 Combined Bending and Torsion (In phase)

Test data for the case of reversed combined bending and twisting stress has been analysed in Chapter 7.2 and found to give very close agreement with equation 7.6. For design purposes negligible errors would be introduced by using the Gough ellipse quadrant for ductile materials. Equation 7.2 gives a physical explanation of the fatigue process under combined bending and twisting whereas the Gough ellipse quadrant is empirical.

Gough also conducted combined cyclic and static stress tests on a 65 tonf nickel-chromium steel to specification S65A (8,12). It is pointed out (8) that this steel, with its high ratio of yield to ultimate tensile strength, shows relatively small decreases in fatigue strength under even very high values of applied static stresses of similar kind and thus equation 7.18 would overestimate the decrease in fatigue strength due to the application of superimposed static stresses.

It was found that the application of static bending and torsional stresses affected the values of the "end points" b and t, the relation remaining the ellipse quadrant.

Findley (18,19) also investigated the effect of "range of stress" in combined bending and torsion, meaning the effect of mean stress. For the materials tested and the high mean stress values used the data analysis involved corrections for the influence of yielding at the maximum stress.

8.4 Thin Wall Tubes

A greater range of principal stress combinations can be obtained using thin wall tubes subjected to fluctuating internal pressure with superimposed fluctuating axial load than can be obtained from combined bending and twisting. Due to the difficulty in conducting such tests, particularly in the + - quadrant as shown in Fig. 32, only a few investigations have so far been attempted. Until the work of Rotvel (39) all such tests had been for the case of pulsating, zero to maximum stress.

It is clear from Fig. 39a, that if the actual ratio of $\tau_A/\sigma_A = 0.64$ as found for the material used by Rotvel were applied in equation 7.14 that almost exact correlation would be obtained with experimental data. As noted by Rotvel it is unfortunate that the test cases chosen in the + - quadrant are symmetrically disposed about K = -1 thus giving the same results.

Until the work reported in this thesis only Ros and Eichinger (34) had conducted tests over the full range of the ++ and +- quadrants i.e. from uniaxial pulsating longitudinal tension, through uniaxial pulsating hoop tension to uniaxial pulsating longitudinal compression. Only two test cases are reported in the + - quadrant. Seven metals were tested, but the results in the cases of Reinaluminium and Avional D

include neither the uniaxial fatigue strength in the longitudinal or hoop direction. In these cases the uniaxial pulsating longitudinal tensile fatigue strength is assumed equal to that found for K = ½. The test data is compared with the derived equations 7.19 and 7.22 and the Booth equations 8.2 and 8.4 in Figs. 39b to h. The predicted limiting fatigue strengths have been calculated using one fatigue result and the U.T.S. of the material. In all cases, with one exception, the uniaxial pulsating longitudinal tensile fatigue strength has been used. In the case of Arcos Ductilend the uniaxial pulsating hoop fatigue stress has been used as the data given for the longitudinal strength is approximate and appears to be low. In the + + quadrant only the curve for equation 7.19 is shown as all four equations give values within 2% of that predicted by equation 7.22.

As the four equations 7.19, 7.22, 8.2 and 8.4 give results in the + - quadrant which are not widely different and test data is available only for the cases of K = -1 and -0 it is difficult to state that any one equation gives better agreement than another. Further it is difficult to assess the reliability of the test data at K = -0 as axial compression tests are notoriously difficult to conduct without introducing bending effects especially in the case of repeated load application. In the case of Arcos Stabilend, Arcos Ductilend and Perunal the actual values are much greater than those predicted by any of the equations in the + - quadrant. In each of these cases closer agreement between the derived expressions would have been obtained if the fatigue result at K = -1 had been used instead of the uniaxial longitudinal fatigue result and also if the mean stress effect equation had been assumed to

be a straight line rather than the parabola used. There is evidence of an anisotropic effect in the case of the aluminium alloy Perunal, an anisotropic factor of the order of 0.8 would be applicable to the case of transverse hoop stress.

The test data of Majors et al (35) has been criticised by Findley (18) for accepting the bending fatigue strength as being precisely determined and assuming that any uncertainties must occur in the data under other stress conditions. Further the method of testing possibly induces bending stresses and the pressure waveform applied to the specimens is saw toothed rather than sinusoidal. From the rotating bending stress data quoted the transverse reversed fatigue strength is 85% the longitudinal reversed fatigue strength. This anisotropic factor applied to the results in Fig. 39j would give better agreement between the actual and predicted fatigue strengths, though the one value in the + - quadrant is low.

The results of Bundy and Marin are in quite good agreement with the derived equations except in the case of K = 2 which has been questioned by the authors themselves.

The limiting stress values shown in the hoop direction are lower than in the longitudinal direction as allowance has been made in each case for the small radial stress occurring.

8.5 Thick-wall Tubes

In the two multiaxial fatigue stress situations already considered, combined bending and twisting and thin cylinders under combined internal pressure and end load, the stress situation was essentially biaxial. However, in the case of thick wall cylinders under internal pressure the most severe stress conditions occur at the inner wall face and are of a triaxial nature as the internal pressure

is appreciable in magnitude compared with the hoop and longitudinal stresses it generates.

Morrison, Crossland, Parry and co-workers (40, 45-49) have conducted an extensive series of investigations of the fatigue strength of thick walled cylinders subjected to pulsating internal oil pressure. The results of these tests showed that the fatigue strength of the thick cylinders, in terms of maximum shear stress amplitude, was about half that suggested from solid torsion fatigue tests. They suggested that the pulsating high pressure oil in intimate contact with the cylinder bore may cause a decrease in fatigue strength and showed, in a small number of tests, in which the cylinder bores were protected by a neoprene coating that the fatigue strength was increased.

This oil effect has as yet not been satisfactorily explained. Haslam (54) has attempted to allow for it in an empirical fashion as discussed in Chapter 1.4. Frost (96) has suggested that the stress causing a fatigue crack to open in the case of a pressurised and unprotected cylinder will be the sum of the hoop stress and the internal pressure in the crack; the crack propagating, in the case of the pressurised thick cylinder, in a direction normal to the hoop stress.

If this concept is applied using the general expression derived for fatigue failure, equation 7.18,

$$\tau_a = \left\{ \tau_A - \left[\frac{\tau_A - \frac{\sigma_A}{2}}{\left(\frac{\sigma_A}{2}\right)^{3/2}} \right] \sigma_r^{3/2} \right\} \left[1 - \frac{\sigma_{mr}}{\frac{\sigma_u}{2}} \right]^{\frac{1}{2}} \qquad (7.18)$$

in the case of a thick cylinder under internal pressure where the principal stresses at the inner bore are as shown in Diagram 8, the radial stress being compressive and equal to the internal pressure in the cylinder,

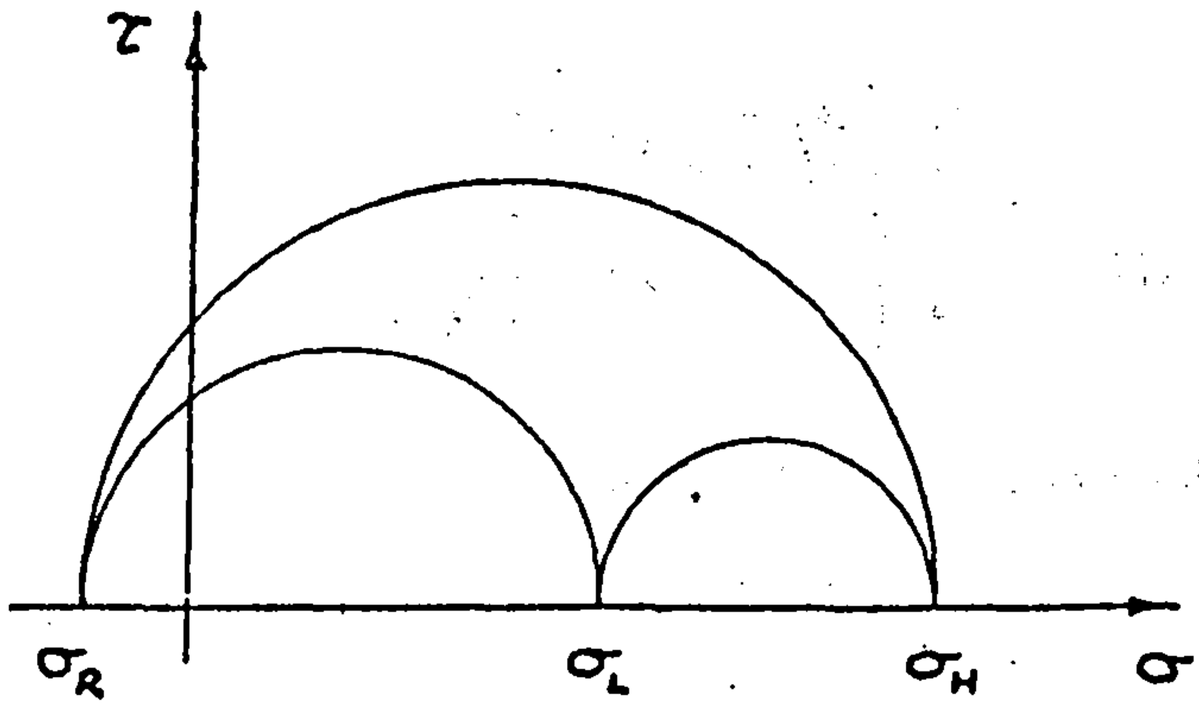

DIAGRAM 8

$$= -p$$

and if it is assumed, in the case of unprotected cylinder bores, that the hoop stress is augmented by the pressure then equation 7.18 can be written as

$$\frac{(\sigma_H+p)-(-p)}{4} = \left\{\tau_A - \left[\frac{\tau_A - \frac{\sigma_A}{2}}{\left(\frac{\sigma_A}{2}\right)^{3/2}}\right]\left[\frac{(\sigma_H+p)+(-p)}{4}\right]^{3/2}\right\}\left\{1-\frac{\left[\frac{(\sigma_H+p)+(-p)}{2}\right]}{\frac{\sigma_U}{2}}\right\}^{1/2} \qquad (8.8)$$

where σ_H = the range of hoop stress at the fatigue limit

p = the range of internal pressure at the fatigue limit

Hence,

$$\frac{\sigma_H + 2p}{4} = \left\{\tau_A - \left[\frac{\tau_A - \frac{\sigma_A}{2}}{\left(\frac{\sigma_A}{2}\right)^{3/2}}\right]\left(\frac{\sigma_H}{4}\right)^{3/2}\right\}\left[1 - \frac{\sigma_H}{\sigma_U}\right]^{1/2}$$

Now

$$\sigma_H = p\frac{k^2+1}{k^2-1} = p\,\overline{k}$$

where $k = \dfrac{\text{outer diameter of cylinder}}{\text{inner diameter of cylinder}}$

$$\overline{k} = \frac{k^2+1}{k^2-1}$$

Hence the following equation is applicable to thick cylinders with unprotected bores

$$\frac{p(\bar{k}+2)}{4} = \left\{ \tau_A - \left[\frac{\tau_A - \frac{\sigma_A}{2}}{\left(\frac{\sigma_A}{2}\right)^{3/2}} \right] \left(\frac{p\bar{k}}{4} \right)^{3/2} \right\} \left[1 - \frac{p\bar{k}}{\sigma_u} \right]^{1/2} \qquad (8.9)$$

In a similar manner, if it is assumed in the case of protected cylinder bores that the hoop stress is not augmented by the pressure then equation 7.18 can be written as

$$\frac{\sigma_H - (-p)}{4} = \left\{ \tau_A - \left[\frac{\tau_A - \frac{\sigma_A}{2}}{\left(\frac{\sigma_A}{2}\right)^{3/2}} \right] \left[\frac{\sigma_H + (-p)}{4} \right]^{3/2} \right\} \left\{ 1 - \frac{\left[\frac{\sigma_H + (-p)}{2} \right]}{\frac{\sigma_u}{2}} \right\}^{1/2} \qquad (8.10)$$

Hence,

$$\frac{\sigma_H + p}{4} = \left\{ \tau_A - \left[\frac{\tau_A - \frac{\sigma_A}{2}}{\left(\frac{\sigma_A}{2}\right)^{3/2}} \right] \left[\frac{\sigma_H - p}{4} \right]^{3/2} \right\} \left\{ 1 - \frac{\sigma_H - p}{\sigma_u} \right\}^{1/2}$$

Then, substituting for $\sigma_H = p\,k$ the following equation is applicable to thick cylinders with protected bores

$$\frac{p(\bar{k}+1)}{4} = \left\{ \tau_A - \left[\frac{\tau_A - \frac{\sigma_A}{2}}{\left(\frac{\sigma_A}{2}\right)^{3/2}} \right] \left[\frac{p(\bar{k}-1)}{4} \right]^{3/2} \right\} \left\{ 1 - \frac{p(\bar{k}-1)}{\sigma_u} \right\}^{1/2} \qquad (8.11)$$

As an illustration of the use of equations 8.9 and 8.11 they are used in conjunction with test data from Morrison et al (48) on EN 25 steel using both protected and unprotected cylinder bores, as follows:

For EN 25 steel,

$\tau_A = \pm 19.5$ tonf/in^2 = torsion fatigue strength of solid specimens (shear)

$\sigma_A = \pm 28.0$ tonf/in^2 = reversed uniaxial fatigue strength

$\sigma_u = 56.2$ tonf/in^2 = ultimate tensile strength

$k = 1.4$

$\bar{k} = k^2+1 / k^2-1 = 3.08$

Substitution of this data in equation 8.9 and solving for p gives for the unprotected bore case a value of p = 9.5 tonf/in^2 i.e. the range of pulsating internal pressure (10^7 cycles).

The nominal (not allowing for augmented hoop stress due to internal pressure) shear fatigue strength range is given by $\frac{1}{2}(\sigma_H + p) = p/2\ (\bar{k} + 1) = 2.04\ p$ in this case. Thus the predicted shear fatigue strength range is 2.04 x 9.5 = 19.4 tonf/in^2 which is in good agreement with the experimental shear fatigue strength range of 18.0 tonf/in^2. Note that the actual (allowing for augmented hoop stress due to internal pressure) shear fatigue strength range is $\frac{1}{2}p\ (\bar{k} + 2) = 24.2$ tonf/in^2.

Substitution of the material data in equation 8.11 and solving for p gives for the protected bore case a value of p = 12.5 tonf/in^2 i.e. the range of pulsating internal pressure (10^7 cycles).

The nominal shear fatigue strength range is again given by $\frac{1}{2}(\sigma_H + p) = p/2\ (\bar{k} + 1) = 2.04\ p$ in this case. Thus the predicted shear fatigue strength range is 2.04 x 12.5 = 25.6 tonf/in^2 which is again in very good agreement with the experimental shear fatigue strength range of 24.0 tonf/in^2 and the actual shear fatigue strength range of 24.2 tonf/in^2 for the unprotected bore case.

The results of using equation 8.9, in the case of unprotected bores, and equation 8.11, in the case of protected bores, to predict the fatigue strengths of the materials tested by Morrison et al (48), as given in Table 24, and other investigators, is shown in Table 25 and Fig. 41, where the predicted results can be compared with the experimental results.

Morrison has pointed out that the results, in the case of stainless steel and titanium are affected by plastic deformation at

the bore of these cylinders. In the case of the Haslam (54) tests on EN 26 steel the reversed shear fatigue strength is not quoted and this has been derived from the pulsating transverse tensile fatigue strength using the Gerber parabola. In all other cases, with the exception of the tests on DTD 364 aluminium alloy which were of a limited nature and subject to a large degree of scatter, the predicted values of shear fatigue strength fall within 5% of the experimental values. The Morrison data includes extensive results of auxiliary tests including the reversed torsion and reversed transverse tensile fatigue strengths and thus the effects of anisotropy can be included in the use of equations 8.9 and 8.11.

It is believed that the theory presented here is the first to (1) explain satisfactorily the low fatigue strength of thick cylinders under pulsating internal pressure and

(2) predict satisfactorily fatigue strength under the three conditions of multiaxial fatigue stress experienced in

(a) combined bending and twisting

(b) thin wall tubes under the combined effects of pulsating internal pressure and end load and

(c) thick wall cylinders under pulsating internal pressure,

as well as satisfying uniaxial fatigue test data.

Frost and Burns (99) previously attempted a correlation of fatigue test data on the basis of the critical range of shear stress being a function of the maximum normal stress on the plane of maximum range of shear stress, but found poor agreement, particularly with the thick cylinder test data. Jones and Tomkins (100) showed that improved agreement for the thick cylinder data could be obtained using the Frost and Burns hypothesis when the cylinder hoop stress

was augmented by the effect of the oil pressure.

A further series of tests were conducted by the Bristol University investigators on the effect of large superimposed hydrostatic pressure in the case of Vibrac Ni Cr Mo steel under axial load or torsional fatigue conditions. In these tests the cylinders were protected by rubber coatings. Crossland (40) found an increase of 32% in the reversed torsional fatigue strength of solid specimens subjected to a hydrostatic pressure of 20 tonf/in^2 and Burns and Parry (56) obtained a 46% increase in the torsional fatigue limit of both solid and hollow specimens due to a pressure increase of 25 tonf/in^2. In the case of axial load fatigue tests White, Crossland and Morrison (47) obtained only a 7% increase in the reversed axial fatigue strength under a pressure increase of 20 tonf/in^2. As the specimen surfaces are protected in these tests there is no tensile increase in the normal stress acting on the maximum shear stress plane due to oil pressure penetration of the fatigue crack and hence the increases in fatigue strength found are due to the beneficial effect of a compressive mean stress as predicted by the parabolic expression of equation 7.17. In the case of reversed torsion and reversed axial load, an increase of pressure of 20 tonf/in^2 and 25 tonf/in^2 will give 31% and 38% increases in strength respectively according to equation 7.17. These predicted values are in good agreement with the test results of Crossland, and of Burns and Parry. In the case of the low increase found by White et al it is thought that the test results were affected by gross yielding.

Crowther in the discussion of the Morrison et al (48) work would not subscribe to the view that the hydraulic oil could enter the fatigue crack and hence assist the crack to propagate and cause earlier failures in unprotected than in protected bores. He argued that by the time the discontinuity or crack had grown to such a size that it admitted sufficient oil to cause pressure on its faces, then the specimen was bound to fail and a rubber protective coating would be as effective as oil in entering the cavity and transmitting the pressure. Nevertheless when the additional stress effect of the hydraulic oil in the case of unprotected cylinder bores is not allowed for the predicted shear stress amplitudes are 25 to 80% in excess of those found by test whereas allowance for the additional stress effect due to the oil gives very good correlation, within 5%, when using equation 7.18.

8.6 Comparison of Series 2 Experimental Results with the Proposed Equations

Fig. 40 shows that equation 7.19 is in excellent agreement with the experimental results. The material used in the tests is seen to be anisotropic, the fatigue strength in the transverse direction being 0.82 the fatigue strength in the longitudinal direction. It is also clear that the case of $K = -2$ falls in the transition region where the failure plane changes from the anisotropic to the isotropic maximum shear stress plane as was suggested as a possible explanation for the different pattern of results obtained in this case. The experimental result for the case of $K = -0$ is 7% lower than predicted but the difficulties of testing under compressive stress only have already been discussed in Chapter 6.4.

The simpler equation 7.22, which neglects the effect of

the fluctuating normal stress on the maximum shear stress plane, is seen to agree with the experimental results within 6% excepting the $K = -0$ case.

The fact that the mean stresses are slightly greater than the stress amplitudes, as detailed in Chapter 5.2.2, has a maximum effect of 3% in the application of the failure equations and has been allowed for in Fig. 40.

CHAPTER 9

COMPARISON OF BIAXIAL PROGRAMME FATIGUE TEST RESULTS AT CONSTANT PRINCIPAL STRESS RATIO WITH UNIAXIAL CUMULATIVE DAMAGE THEORIES

9.1 Introduction

Cumulative damage theories have already been discussed in Chapter 2 and the test results have already been compared with the Miner predictions in Chapter 6.

In this chapter the test data is analysed for the possible applicability of cumulative damage theories based on

(1) stress dependence (as in Edwards (78))

(2) interaction (as in Corten and Dolan (79))

(3) interaction factors based on either the higher or lower programme stress level.

9.2 Stress Dependence

For comparison with the expressions found by Edwards (78) for two-level programme tests the linear damage at the first stress level is plotted versus the cycle ratio sum as shown in Fig. 42.

For this theory to be applicable the test results for programme tests between two stress levels should fall on curves of the form shown in Fig. 7. On a very tentative basis one might suggest that

(a) the $S_1 - S_2$ results for $K \approx 2, 7.9$ lie on programme test curve for $X_2/X_1 = 5$

(b) the $S_2 - S_3$ results for $K \approx 7.9$ lie on programme test curve for $X_2/X_1 = 10$

and (c) the $S_1 - S_3$ results for $K \approx 0$ lie on programme test curve for $X_2/X_1 = 8$.

9.3 Interaction

Using the highest programme stress level for each K value the cycle ratio sums have been found for a range of values of slope of the log S - log N curve, zero slope being taken from Fig. 26. The results are shown in Table 23 and Fig. 43. For this theory to be applicable Fig. 43 would have to show the same value of % increase in reverse slope of the log S - log N curve to be required for each K value to give the cycle ratio sum as unity. It is obvious from Fig. 43 that this is not the case and thus an interaction theory based on increasing the reverse slope of the log S - log N diagram is not applicable.

9.4 Interaction Factor (F_1) based on Higher Test Stress Level

The interaction factor F_1 is defined as follows

$$\frac{n_{HIGH}}{N_{HIGH}} + \frac{F_1 n_{LOW}}{N_{HIGH}} = 1$$

$$\therefore \quad F_1 = \frac{N_{HIGH} - n_{HIGH}}{n_{LOW}}$$

where n_{HIGH} = cycles at higher stress level

N_{HIGH} = cycles to failure at higher stress level

n_{LOW} = cycles at lower stress level

N_{LOW} = cycles to failure at low stress level

This factor F_1 can be interpreted as a measure of the effectiveness of cycles at the lower stress level on life at the higher stress level.

The results, based on the mean value at any particular programme stress condition, are shown in Fig. 44a. This concept does not appear to give any overall consistent result, values of F_1 varying from -0.4 to 2.08.

9.5 Interaction Factor (F_2) based on Lower Test Stress Level

The interaction factor F_2 is defined as follows:

$$\frac{n_{HIGH}}{N_{HIGH}} + \frac{n_{LOW}}{F_2 N_{LOW}} = 1$$

$$\therefore \quad F_2 = \frac{N_{LOW}}{1 - \frac{n_{HIGH}}{N_{HIGH}}}$$

This factor F_2 can be interpreted as a correction to the lower stress level cycle ratio.

The results are shown in Fig. 44b. Again this concept does not appear to give any overall consistent result, values of F_2 varying from -0.15 to 2.32.

9.6 A proposed New Approach to Fatigue Analysis

It is not surprising that the uniaxial cumulative damage theories do not agree with the biaxial test data. Many of these theories require the use of parameters found from particular tests and are thus only applicable to those particular conditions. Despite many attempt no cumulative damage theory has been found to be generally better than the Miner rule for predicting life under uniaxial fatigue stress conditions.

Even today, for design purposes, the Miner rule is usually used with modifying factors applied according to the service conditions likely to be met and using knowledge gained from past similar experience; but in all cases tests have to be conducted on the actual components under conditions as close as possible to those likely to occur in service in order to confirm the safety of the design.

In the work reported here, constant amplitude fatigue has been found to be dependent on four main parameters.

(i) shear stress amplitude on the maximum shear stress plane;

(ii) normal stress amplitude on the maximum shear stress plane;

(iii) mean stress;

and (iv) anisotropy

in terms of equation 7.18 for long life at the fatigue limit or 10^6 cycle. This equation has been found to be valid for long life regardless of differences in crack initiation and propagation conditions existing under the difference test conditions analysed.

Further investigation is required to find whether equation 7.18 is applicable in the life range of 10^4 to 10^6 cycles. The combined bending and torsion test data available was aimed mainly at the determination of fatigue limit conditions although there is some data between 10^5 and 10^6 cycles. Only a very limited amount of thin wall tube data at only a few principal stress ratios is available at lives between 10^4 and 10^6 cycles.

The cumulative damage tests at two principal stress ratios, the first of their kind, conducted in this work have indicated the necessity to differentiate between the four effects enumerated above in an effort to understand the interaction effects occurring.

The effect of anisotropy can be eliminated by the choice of materials which show the same bending and the same torsion fatigue strengths regardless of the direction of orientation of material specimens taken from the bulk material.

The majority of combined bending and torsion fatigue tests have been conducted at zero mean stress and these are the most simple test conditions. There is a need for extensive testing under combined bending and twisting with mean stress to further confirm

the applicability of equation 7.18. In the case of tests on thin wall tubes under the combined effect of longitudinal stress and internal pressure it is much more difficult to test under conditions of zero mean stress as the tube has to be pressurised both externally and internally. Only Rotvel (39) has so far conducted such tests.

Alternating torsion tests offer the most simple means of studying the effect of range of shear stress on the maximum shear stress plane where the normal stress on the maximum shear stress plane is zero.

Cumulative damage tests under alternating torsion also offer the most simple method of studying interaction effects under conditions of shear stress only acting on the maximum shear stress plane. No such test data is known in the fatigue literature.

An extension of the study of interaction effects in cumulative damage on the maximum shear stress plane under both shear stress amplitude and normal stress amplitude, would best be conducted on thin wall tubes, where the principal stress planes remain the same under internal pressure and longitudinal stress, and do not rotate as in the case of various combinations of bending and twisting. These cumulative damage tests would be at constant principal stress ratios and would require the longitudinal stress to go through zero and the tubes to be pressurised internally and externally.

Further extensions of this work would involve cumulative damage tests at zero mean stress but different principal stress ratios and then the study of mean stress and anisotropy.

These cumulative damage tests would progress from single

step tests to programme tests and finally to random load tests.

The test programme proposed above is undoubtedly of an extremely daunting nature but it offers the possibility of studying the fundamental nature of the fatigue problem, rather than the mere collection of material test data, under particular, rather than general stress conditions which comprises the great majority of the vast amount of fatigue testing conducted over the last hundred or so years.

This work would be preliminary to a similar study, but under notched conditions, and eventually to the consideration of the effects of size, surface treatment, temperature, fretting and the many complex effects found under service conditions.

CONCLUSIONS

Fatigue tests on thin wall aluminium alloy tubes over a wide range of principal stress ratio have led to the development of a criterion of fatigue failure under multiaxial stress based on maximum shear stress amplitude modified for the effects of the normal stress acting on the maximum shear stress plane and also of anisotropy. Published test data has been analysed to determine the relative influences of these parameters.

The equation developed for ductile, isotropic metals is

$$\tau_a = \left[0{\cdot}58\sigma_A - \frac{0{\cdot}225}{\sigma_A^{\frac{1}{2}}}\sigma_\tau^{\frac{3}{2}}\right]\left[1 - \frac{\sigma_{M\tau}}{\sigma_U/2}\right]^{\frac{1}{2}}$$

where only one fatigue strength and the U.T.S. are required.

This form of equation is shown to be in excellent agreement with all the available test data under conditions of multiaxial stress fatigue, viz.

(i) combined bending and twisting; where agreement is better than that obtained using the Gough ellipse quadrant equation;

(ii) thin wall tubes; including the experimental data on 2L65 aluminium alloy of this thesis;

(iii) thick wall tubes; when the additional effect of the high pressure oil is taken into account;

and also with uniaxial fatigue test data where the equation simplifies to

$$\left(\frac{\sigma_a}{\sigma_A}\right)^2 + \frac{\sigma_M}{\sigma_U} = 1$$

The simplified equation

$$\left[\frac{\tau_a}{\sigma_A/\sqrt{3}}\right]^2 + \frac{\sigma_{nr}}{\sigma_u/2} = 1$$

neglecting the effect of the range of normal stress on the maximum shear stress plane is suggested for design purposes where the small loss of accuracy is balanced by the greater simplicity of application.

Methods of allowing for anisotropy under the states of multiaxial stress mentioned above have been suggested.

The results of two level block programme cumulative damage tests on the same aluminium alloy at four values of constant principal stress ratio show no significant effect of principal stress ratio whether the maximum shear stress amplitude occurs on the isotropic or anisotropic shear stress planes. Values of cycle ratio sums were found between 0.13 and 1.82 with an overall mean of 0.77. A stress dependent theory was found to have possible application to these results whereas no correlation could be found with present uniaxial interaction theories.

The results of exploratory programme tests at several combinations of two different principal stress ratios indicated the presence of strong interaction effects and also that cycles at stress levels greater than the order of 70% of the fatigue strength at 10^6 cycles have to be taken into account.

A new approach to fatigue analysis has been suggested based on the progressive study of each of the following effects in turn

(i) shear stress amplitude on the maximum shear stress plane;

(ii) normal stress amplitude on the maximum shear stress plane;

(iii) mean stress

and (iv) anisotropy,

firstly under constant amplitude stress conditions followed by cumulative damage conditions of increasing complexity.

ACKNOWLEDGEMENTS

The author wishes to thank Professor J.C. Levy, Head of the Department of Mechanical Engineering, The City University, London, for his support, advice, guidance and encouragement throughout this project.

The author also wishes to thank the technicians of the Materials Section of the Department of Mechanical Engineering, The City University, London, for their willing assistance throughout this project. Especial thanks are due to Mr. R. Castle and Mr. M. Walshe who manufactured the test specimens and to Mr. J. Heaphy who built the programmer.

BIBLIOGRAPHY

1. ONO, A.
"Fatigue of Steel under Combined Bending and Torsion",
Memoirs, College of Engineering, Kyushi, Imperial University, Japan, Vol. 2, pp. 117-142, 1921.

2. LEA, F.C. and BUDGEN, H.P.
"Combined Torsional and Repeated Bending Stresses",
Engineering, Vol. 122, pp. 242-245, 1926.

3. NIMHANMINNE, S.K.
"Static Torque Combined with Cyclic Bending",
M.Sc. thesis, University of London, July 1931.

4. HUITT, W.J.
"The Failure of Nickel Alloy Steel under Torsion by the Addition of Alternating Bending",
M.Sc. thesis, University of London, May, 1935.

5. GOUGH, H.J. and POLLARD, H.V.
"The Strength of Metals under Combined Alternating Stresses",
Proc. Inst. Mech. E. Vol. 131, pp. 3-103, November 1935.

6. SINES, G.
"Failure of Materials under Combined Repeated Stresses",
N.A.C.A. T.N. 3495, November 1955.

7. CAPPER, P.L.
"Fatigue under Combined Bending and Torsion",
The Engineer (London) Vol. 164, pp. 150-152, August 6, 1937.

8. GOUGH, H.J.
"Engineering Steels under Combined Cyclic and Static Stresses",
The Engineer (London), Oct. 28, 1949, pp. 497-500; Nov. 4, 1949, pp. 510-514; November 11, 1949, pp. 540-543; Nov. 18, 1949, pp. 570-573. See also: Proc. I.Mech.E., Vol. 160, No. 4, pp. 417-440 and J. App. Mechanics, Vol. 17, No. 2, pp. 113-125, June 1950.

9. HOHENEMSER, K and PRAGER, W.
"The Problem of Fatigue Strength under Complex Stresses",
Metallwirtschaft, Vol. 12, pp. 342-343, 1933.

10. SMITH, J.O.
"The Effect of Range of Stress on the Torsional Fatigue Strength of Steel",
Univ. of Illinois Eng. Exp. Stn., Vol. 37, Bulletin No. 316, Sept. 26, 1939.

11. STANTON, T.E. and BATSON, R.G.
"The Fatigue Resistance of Mild Steel under Various Conditions of Stress Distribution",
Engineering, Vol. 102, pp. 269-270, Sept. 15, 1916.

12. GOUGH, H.J., POLLARD, H.V. and CLENSHAW, W.J.
"Some Experiments on the Resistance of Metals to Fatigue under Combined Stresses",
Aero Res. Council Rep., R and M 2522, 1951.

13. GOUGH, H.J. and POLLARD, H.V.
"The Effect of Specimen Form on the Resistance of Metals to Combined Alternating Stresses",
Proc. I.Mech.E., Vol. 132, pp. 549-573, December 1936.

14. NARMORE, P.B.
"A Fatigue Study of Strong Steel under Combined Alternating Stresses", Ph.D. thesis, University of Michigan, Nov. 1937.

15. NISHIHARA, T. and KAWAMOTO, M.
"The Strength of Metals under Combined Alternating Bending and Torsion",
Memoirs College of Engineering, Kyoto Imperial University, Japan, Vol. 10, No. 6, pp. 177-201, 1941.
Also abstract, The Journal Inst. Metals, Vol. 10, p. 124, April 1943.

16. NISHIHARA, T. and KAWAMOTO, M.
"The Strength of Metals under Combined Alternating Bending and Torsion with Phase Difference",
Memoirs College of Engineering, Kyoto Imperial University, Japan, Vol. 11, No. 5, pp. 85-112, 1945.

17. SAUER, J.
"A Study of Fatigue Phenomena under Combined Stress"
Proc. 7th Int. Congress of Applied Mechanics, Vol. 4, pp. 150-164, 1948.

18. FINDLEY, W.N.
"Combined Stress Fatigue Strength of 76S-T61 Aluminium Alloy with Superimposed Mean Stresses and Corrections for Yielding", N.A.C.A. T.N. 2924, May 1953.
Also see Proc. A.S.T.M., Vol. 52, pp. 818-836, 1952.

19. FINDLEY, W.N.
"Effect of Range of Stress in Fatigue of 76S-T61 Aluminium Alloy under Combined Stresses which Produce Yielding",
Trans. A.S.M.E., J. App. Mech., Vol. 20, No. 3, pp. 365-374, 1953.

20. FINDLEY, W.N.
"Experiments in Fatigue under Ranges of Stress in Torsion and Axial Load from Tension to Extreme Compression",
Proc. A.S.T.M., Vol. 54, pp. 836-852, 1954.

21. FINDLEY, W.N., MITCHELL, W.I. and MARTIN, D.E.
"Combined Bending and Torsion Fatigue Tests of 25S-T Aluminium Alloy", Proc. Second U.S. National Congress of Applied Mechanics, pp. 585-593, 1954.

22. FINDLEY, W.N., and MATHUR, P.N.
"Anisotropy of Fatigue Strength of a Steel and Two Aluminium Alloys in Bending and Torsion", Proc. A.S.T.M., pp. 924-941, 1955.

23. FINDLEY, W.N., MITCHELL, W.I. and STROHBECK, D.D.
"Effect of Range of Stress in Combined Bending and Torsion Fatigue Tests of 25S-T6 Aluminium Alloy", Trans. A.S.M.E., Vol. 78, No. 7, pp. 1481-1487, October 1956.

24. FINDLEY, W.N. and COLEMAN, J.J.
"A Theory of the Non-Linear Influence of Normal Stress on Fatigue under Combined Stresses", Proc. 2nd Conf. on the Mechanics of Elasticity and Plasticity, Office of Ord. Res. p. 214, February 1957.

25. FINDLEY, W.N.
"Fatigue of Metals under Combined Stresses", Trans. A.S.M.E., Vol. 79, pp. 1337-1348, August 1957.

26. FINDLEY, W.N., COLEMAN, J.J. and HANLEY, B.C.
"Theory for Bending and Torsion Fatigue with Data for SAE 4340 Steel", Proc. I. Mech. E. Fatigue Conference pp. 150-157, 1956.

27. FINDLEY, W.N. and MATHUR, P.N.
"Modified Theories of Fatigue Failure under Combined Stress", Proc. S.E.S.A., Vol. XIV, No. 1, pp. 35-46, 1956.

28. FINDLEY, W.N.
"A Theory for the Effect of Mean Stress on Fatigue of Metals under Combined Torsion and Axial Load or Bending", Trans. A.S.M.E., Series B.J. Eng. For Industry, Vol. 81, No. 4, pp. 301-306, November 1959.

29. FINDLEY, W.N., MATHUR, P.M., SZCZEPANSKI, E, and TEMEL, A.W.
"Energy versus Stress Theories for Combined Stress - A Fatigue Experiment using a Rotating Disk", Trans. A.S.M.E., Series D, Vol. 83, pp. 10-14, March 1961.

30. MAIER, A.F.
"Stress Reversal in Tubes under Internal Pressure", Stahl und Eisen, Bd. 54, Heft 50, pp. 1289-1291, Dec. 13, 1934.

31. MARIN, J.
"Strength of Steel Subjected to Biaxial Fatigue Stresses", Welding Research Journal, pp. 554-9, November 1942.

32. MORIKAWA, G.K. and GRIFFITHS, L.V.
"Biaxial Fatigue Strength of Low Carbon Steels", Welding Journal Research Supplement, Vol. 24, pp. 167-174, 1945.

33. MARIN, J. and SHELSON, W.
"Biaxial Fatigue Strength of 24 S-T Aluminium Alloy",
N.A.C.A. T.N. 1889, May 1949.

34. ROS, M. and EICHINGER, A.
"Die Bruchgefahr Fester Korper bei weiderholter Beanspruchung Ermudung"
Metalle, Bericht 173, Eidgenossische Material-Prufungs- und Versuchsanstalt fur Industries, Bauwesan und Gewerbe (Zürich), Sept. 1950.

35. MAJORS, H., MILLS, B.D. and McGREGOR, C.W.
"Fatigue under Combined Pulsating Stresses",
Trans. A.S.M.E., (J. App. Mechanics), Vol. 17, No. 2, pp. 218-221, 1950.

36. MARIN, J. and HUGHES, W.P.
"Fatigue Strength of 14S-T4 Aluminium Alloy under Biaxial Tensile Stress", N.A.C.A. T.N. 2704, June 1952.

37. BUNDY, R.W. and MARIN, J.
"Fatigue Strength of 14S-T4 Aluminium Alloy under Biaxial Tensile Stress",
Proc. A.S.T.M., Vol. 54, pp. 755-768, 1954.

38. COX, H.L. and OWEN, N.B.
"The Influence of Biaxial Mean Stress on the Failure of Tubes by Fatigue"
Aero. Quart., Vol. 12, Part I, February 1961.

39. ROTVEL, F.
"Biaxial Fatigue Tests with Zero Mean Stresses using Tubular Specimens",
Int. J. Mech. Sci., Vol. 12, pp. 597-613, 1970.

40. CROSSLAND, B.
"Effect of Large Hydrostatic Pressures on the Torsion Fatigue Strength of an Alloy Steel",
Proc. Int. Conf. on Fatigue of Metals, I.Mech.E., London, p. 138, 1956.

41. STANFIELD, G.
Written discussion.
Proc. I.Mech.E., Vol. 131, p. 93, 1935.

42. BOOTH, S.E.
"Fatigue Failure Criteria using Two Load Systems out of Phase",
M.Sc. thesis, University of London, 1970.

43. CROSBY, J.R., BURNS, D.J. and BENHAM, P.P.
"Effect of Stress Biaxiality on the High Strain Fatigue of an Aluminium-copper Alloy",
Experimental Mechanics, pp. 305-312 July 1969.

44. HAVARD, D.G. and TOPPER, T.H.
"New Equipment for Cyclic Biaxial Testing",
Experimental Mechanics, pp. 550-557, December 1969.

45. MORRISON, J.L.M., CROSSLAND, B. and PARRY, J.S.C.
"Fatigue under Triaxial Stress: Development of a Testing Machine and Preliminary Results",
Proc. I.Mech.E., Vol. 170, pp. 697-712, 1956.

46. PARRY, J.S.C.
"Further Results of Fatigue under Triaxial Stress",
Proc. Int. Conf. on Fatigue of Metals, I.Mech.E., London, p. 132, 1956.

47. WHITE, D.J., CROSSLAND, B. and MORRISON, J.L.M.
"Effect of Hydrostatic Pressure in the Direct Stress Fatigue Strength of an Alloy Steel",
J.Mech.Eng. Sci., Vol. 1, pp. 39-49, 1959.

48. MORRISON, J.L.M., CROSSLAND, B. and PARRY, J.S.C.
"Strength of Thick Cylinders Subjected to Repeated Internal Pressure,
Proc. I.Mech.E., Vol. 174 (2), pp. 95-117, 1960.

49. PARRY, J.S.C.
"Fatigue of Thick Cylinders: Further Practical Information",
Proc. I.Mech.E., Vol. 180 (1), p.387, 1965.

50. BLASS, J.J. and FINDLEY, W.N.
"The Influence of the Intermediate Principal Stress on Fatigue under Triaxial Stresses",
Mat. Res. and Stand., Vol. 7, No. 6, pp. 254-261, 1967.

51. BURNS, D.J. and PARRY, J.S.C.
"Effect of Mean Shear Stress on the Fatigue Behaviour of Thick-Walled Cylinders",
Conf. on High Pressure Eng., I.Mech.E., London, pp. 217-225, 1967.

52. MARSH, K.J. and HASLAM, G.H.
"Fatigue of Cylinders Subjected to Pulsating Internal Oil Pressure",
N.E.L. Report No. 381, East Kilbride, Glasgow, Jan. 1969.

53. HASLAM, G.H.
"The Fatigue Strength of Thick-Walled Steel Cylinders Subjected to Pulsating Internal Pressures",
N.E.L. Report No. 444, East Kilbride, Glasgow, Feb. 1970.

54. HASLAM, G.H.
"The Fatigue Limit of Cylinders Subjected to Repeated Internal Pressures",
High Temperatures-High Pressures, Vol. 1, pp. 705-711, 1969.

55. HASLAM, G.H.
"Estimation of the Fatigue Life of a Thick-Walled Cylinder Subjected to Repeated Internal Pressure",
J.Mech.Eng.Sci., Vol. 13, No. 3, pp. 130-136, 1971.

56. BURNS, D.J. and PARRY, J.S.C.
"Effect of Large Hydrostatic Pressure on the Fatigue Strength of Two Steels",
J. of Mech. Eng. Sci., pp. 293-305, September 1964.

57. SAWERT, W.
"Fatigue Strength under Multiaxial Stress",
Z.V.D.I. Bd. 87, No. 39, pp. 609-615, 1943.

58. WELTER, G. and CHOQUET, J.A.
"Triaxial Tensile Stress Fatigue Testing",
Welding Journal, Vol. 42, pp. 565s - 570s, Dec. 1963.

59. STULEN, F.B. and CUMMINGS, H.N.
"A Failure Criterion for Multiaxial Fatigue Stresses",
Proc. A.S.T.M., Vol. 54, p. 822, 1954.

60. MARIN, J.
"Interpretation of Fatigue Strengths for Combined Stresses",
Proc. Int. Conf. on Fatigue, I.Mech.E., London, pp. 184-194, 1956.

61. SOPWITH, D.G.
"Reporters Introduction",
Proc. Int. Conf. on Fatigue, I.Mech.E., London, p.15, 1956.

62. BLATHERWICK, A.A. and VISTE, N.D.
"Cumulative Damage under Biaxial Fatigue Stress",
Mat. Res. and Stand., Vol. 7, No. 8, pp. 331-336, August 1967.

63. MINER, M.A.
"Cumulative Damage in Fatigue"
J. of App. Mech., A.S.M.E., Vol. 12, No. 3, pp. A159-A164, September 1945.

64. HENRY, D.L.
"A Theory of Fatigue-Damage Accumulation in Steel",
Trans. A.S.M.E., Vol. 77, No. 6, pp. 913-918, August 1955.

65. LEES, L.H.N. and ADES, C.S.
"Stress concentration factors for circular fillets in stepped wall cylinders subjected to axial tension",
Proc. Soc. Exp. Stress Analysis, Vol. 14, No. 1, pp. 99-108, 1955.

66. JEFFREY, G.B.
"Plane Stress and Plane Strain in Bi-polar Co-ordinates",
Phil. Trans. A, Vol. CCXXI, pp. 265-293, 1920.

67. COKER, E.G. and FILON, L.N.G.
"A Treatise on Photoelasticity",
2nd Ed., p. 313, Cambridge University Press.

68. MANN, J.Y.
"A Survey of Data on the Fatigue Properties of D.T.D. 363 and L.65 (D.T.D. 364) Aluminium Alloys", Aero. Res. Labs., Melbourne, S. and M. Note 248, 1958.

69. WYSS, T.
"Influence of Testing Frequency on the Fatigue Strength of Steels and Light Alloys"
Amer. Soc. Test. Mat., Bull. 188, p.31, 1953.

70. ROYLANCE, T.F.
"Review of Cumulative Damage in Fatigue",
M.O.S. S. and T. Memo. 8/57, 1957.

71. KAECHELE, L.
"Review and Analysis of Cumulative Damage Theories",
Rand Comp. Memo. RM-3650-PR, August 1963.

72. O'NEILL, M.J.
"A Review of Some Cumulative Damage Theories",
Aero Res. Lab., Structures and Materials Rep. 326,
Melbourne, Australia, June 1970.

73. PALMGREN, A.
"The Life of Ball Bearings",
Zeutschaft das Vereins deutsches Ingenieure,
Vol. 68, No. 14, pp. 339-341, April 1924.

74. LANGER, B.F.
"Fatigue Failure from Stress Cycles of Varying Amplitude",
Trans. A.S.M.E., Vol. 59, pp. A160-162, 1937.

75. SHANLEY, F.R.
"A Proposed Mechanism of Fatigue Failure",
I.U.T.A.M. Colloquium on Fatigue, Weibull and Odquist, Eds. Stockholm, p. 251, 1955.

76. VALLURI, S.R.
"A Unified Engineering Theory of High Stress Level Fatigue",
Aerospace Engineering, p. 18, October 1961.

77. MARCO, S.M. and STARKEY, W.L.
"A Concept of Fatigue Damage",
Trans. A.S.M.E., Vol. 76, No. 4, pp. 627-632,
May 1954.

78. EDWARDS, P.R.
"Cumulative Damage in Fatigue with Particular Reference to the Effects of Residual Stresses",
Royal Aircraft Establishment, Tech. Rep. 69237, November 1969.

79. CORTEN, H.T. and DOLAN, T.J.
"Cumulative Fatigue Damage",
International Conference on Fatigue of Metals", I.Mech.E., and A.S.M.E., London, 1956.

80. LIU, H.W. and CORTEN, H.T.
"Fatigue Damage during Complex Stress Histories",
N.A.S.A. T.N. D-256, November 1959.

81. LIU, H.W. and CORTEN, H.T.
"Fatigue Damage under Varying Stress Amplitudes",
N.A.S.A. T.N. D-647, November 1960.

82. SCHJELDERUP, M.C.
"Cumulative Fatigue Damage"
J. Aerospace Science, Vol. 26, June 1959.

83. FREUDENTHAL, A.M. and HELLER, R.A.
"On Stress Interaction in Fatigue and a Cumulative Damage Rule",
J. Aerospace Sci., Vol. 26, pp. 431-442, July 1959.

84. FORREST, P.G.
"Fatigue of Metals",
Pergamon Press, London, 1962.

85. BANIN, E.
"The Effect of an Oil Environment on the Fatigue Life of a Duralumin Alloy",
Project Report 286, Department of Mechanical Engineering, The City University, London, 1968.

86. MARSH, K.J.
"Cumulative Fatigue Damage under a Symmetrical Saw-tooth Loading Programme",
N.E.L. Report No. 136, East Kilbride, Glasgow, March 1964.

87. GOUGH, H.J.
"Engineering Steels under Combined Cyclic and Static Stresses", Discussion.
J. of Applied Mechanics, A.S.M.E., Vol. 18, No. 2, p. 211, June 1951.

88. FRITH, P.H.
"Fatigue of Wrought High-Tensile Alloy Steels",
Int. Conf. on Fatigue, Inst. Mech. Eng., p. 462, 1956.

89. WEIBULL, W.
"Fatigue Testing and Analysis of Results",
Pergamon Press 1961.

90. SMITH, J.O.
"Effect of Range of Stress on Fatigue Strength",
Univ. Illinois Eng. Expt. Station Bulletin 334 (1942).

91. NISHIHARA, T. and SAKURAI, T.
"Fatigue Strength of Steel for Repeated Tension and Compression",
Trans. Soc. Mech. Eng. (Japan), Vol. 5, No. 18, pp. 25-29, February 1939 (in Japanese). pp. 58-59 (English summary).

92. O'CONNOR, H.C. and MORRISON, J.L.M.
"The Effect of Mean Stress on the Push-Pull Fatigue Properties of an Alloy Steel",
I.Mech.E. and A.S.M.E., Int. Conf. on Fatigue of Metals, pp. 102-109, 1956.

93. WOODWARD, A.R., GUNN, K.W. and FORREST, G.
"The Effect of Mean stress on the Fatigue of Aluminium Alloys", I.Mech.E. and A.S.M.E., Int. Conf. on Fatigue of Metals, pp. 158-170, 1956.

94. BOYD, R.K.
"Fatigue Strength of an Alloy Steel: Effect of Tempering Temperature and Directional Properties",
Proc. I.Mech.E., Vol. 179, Part I, 1964-65.

95. TEMPLIN, R.L., HOWELL, F.M. and HARTMANN, E.C.
"Effect of Grain Direction on Fatigue Properties of Aluminium Alloys",
Product Engineering, Vol. 21, pp. 126-130, July 1950.

96. FROST, N.E.
"A Note on the Behaviour of Fatigue Cracks",
J.Mech. Phys. Solids, 9, p. 143, 1961.

97. JONES, B.H. and MELLOR, P.B.
"Plastic Flow and Instability Behaviour of Thin-Walled Cylinders Subjected to Constant Ratio Tensile Stress",
Jnl. Strain Analysis, 2 (1), pp. 62-67, 1967.

98. WEIL, N.A.
"Tensile Instability of Thin Walled Cylinders of Finite Length",
Int. Jnl. Mech. Sci., 5, pp. 487-506, 1963.

99. FROST, W.J. and BURNS, D.J.
"Effect of Oil and Mercury at High Pressure on the Fatigue Behaviour of Thick-Walled Cylinders of En25 Steel",
Proc. Inst. Mech. Eng., London, Vol. 182, Part 3c, "High Pressure Engineering", pp. 65-71, 1967-68.

100. JONES, P.M. and TOMKINS, B.
Discussion.
Proc. Inst. Mech. Eng., London, Vol. 182, Part 3C, "High Pressure Engineering", pp. 309-311, 1967-68.

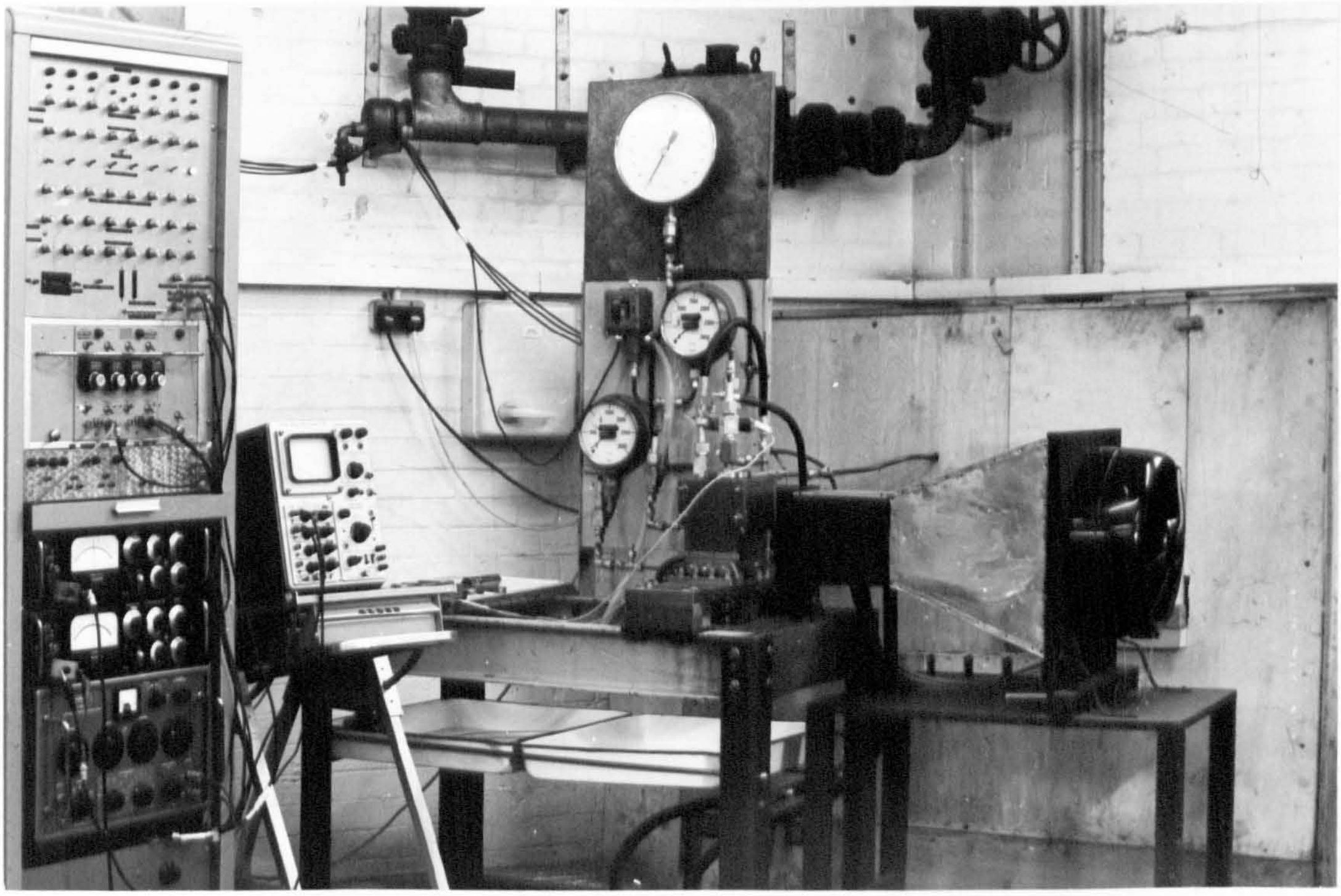

PLATE 1. COMPLETE TEST SYSTEM.

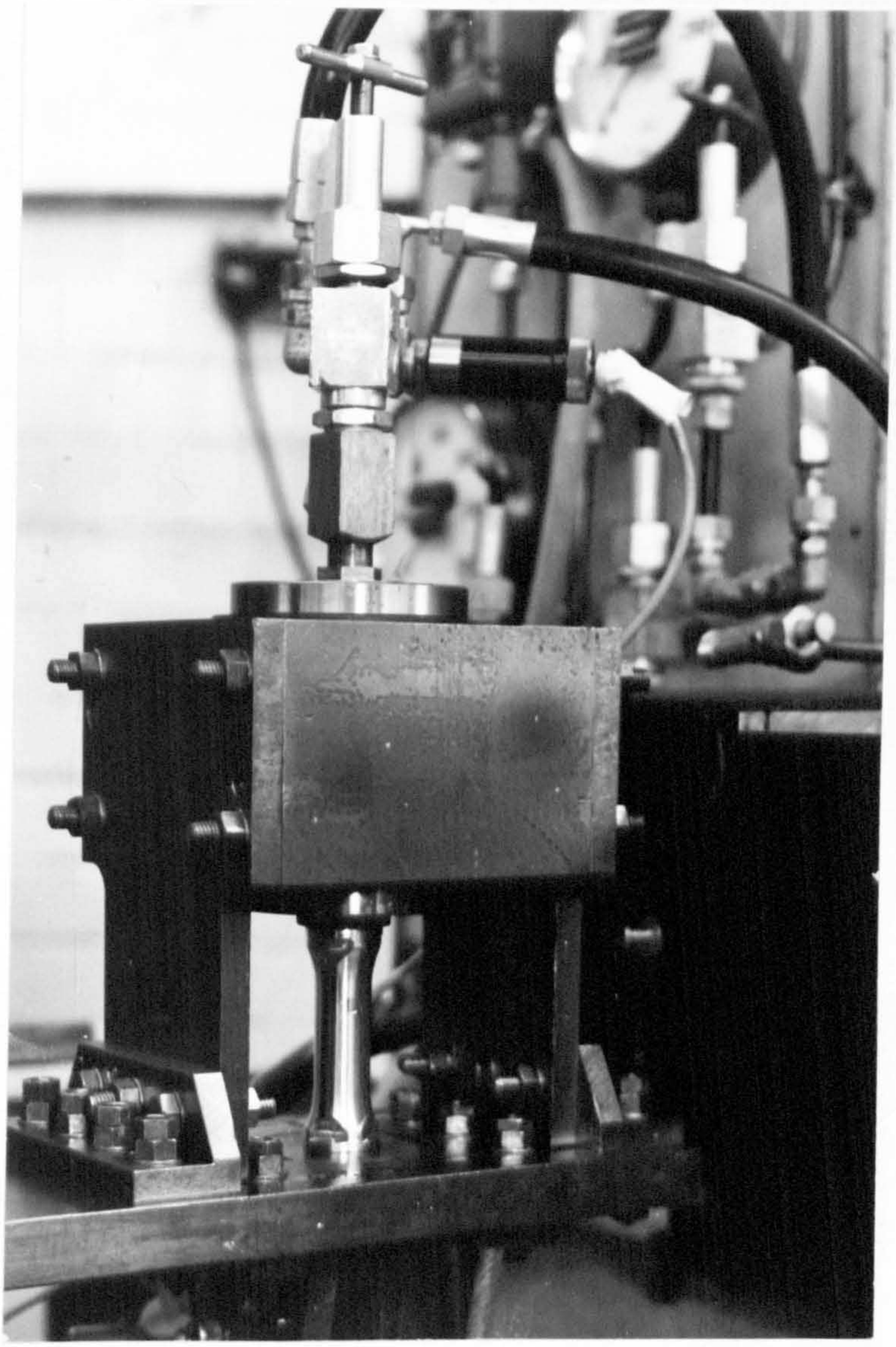

PLATE 2. MECHANICAL PART OF TEST SYSTEM.

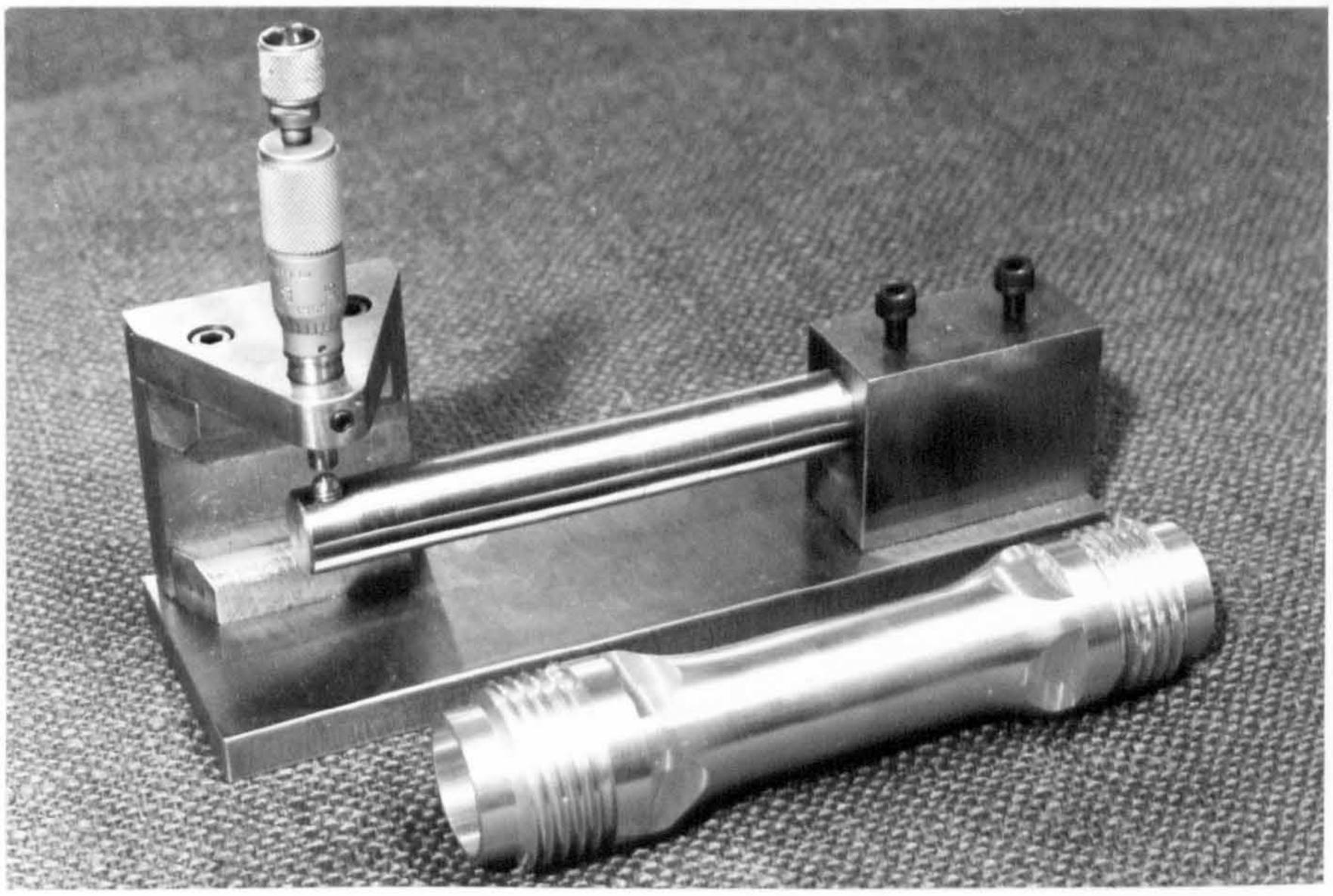

PLATE 3. SPECIMEN WALL THICKNESS MEASURING RIG.

Large longitudinal crack.

PLATE 4. FATIGUE FRACTURES.

Small longitudinal crack.

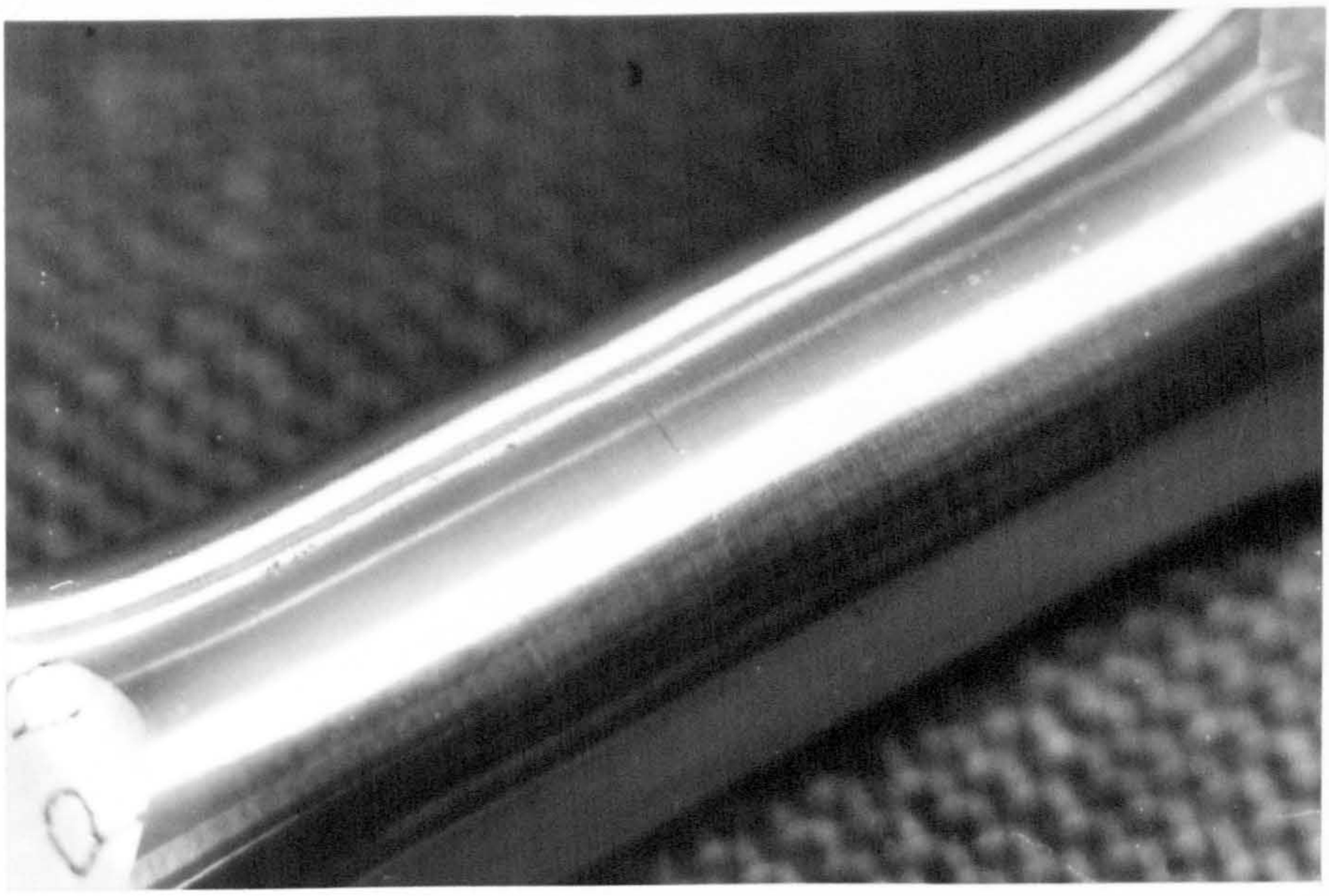

Small transverse crack.

PLATE 4. (CONT) FATIGUE FRACTURES.

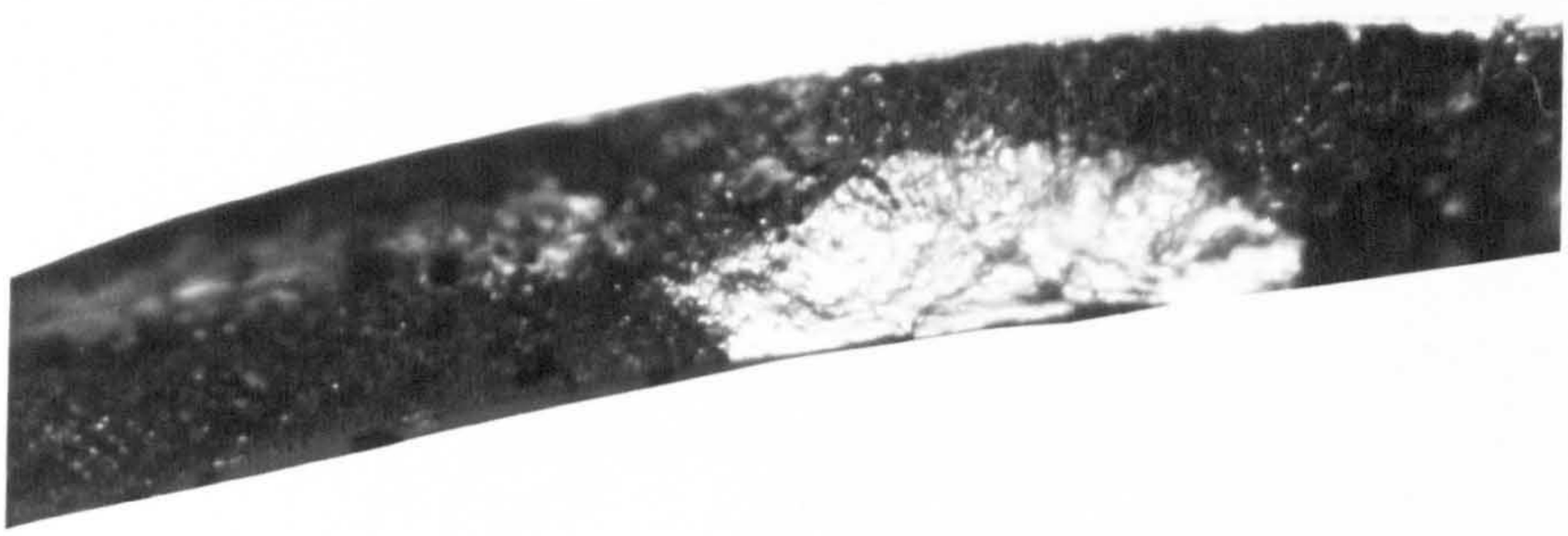

Fatigue crack in transverse plane.

Fatigue crack in longitudinal plane.

PLATE 5. FATIGUE CRACK DETAILS.

Transverse section. X 100.

Longitudinal section. X 100.

PLATE 6. MATERIAL PHOTOMICROGRAPHS.

PLATE 7. TYPICAL BUCKLED SPECIMEN.

Material	Type of loading	No. of results obtained	No. of tests made for each result	Type of spectrum	Cumulative cycle ratio $\sum\frac{n}{N}$	Ref.
			Plain testpieces			
24S–T4 (Al–Cu)	R.B.	14	10	Sinusoidal	0·43–1·41	242
		13	10	Exponential	0·33–1·00	
75S–T (Al–Zn)	R.B.	4	12	Various, in random sequence	0·37–1·25	243
24S–T Alclad sheet	Fluct. tension	8	2–5	Aircraft gust load	0·69–1·35	244
75S–T Alclad sheet	Fluct. tension	4	2	Aircraft gust load	0·79–0·98	
75S–T Alclad sheet	Fluct. tension	4	2–3	Aircraft manoeuvre load	0·82–1·64	
			Notched testpieces			
24S–T	R.B.	2	7–8	Random*	0·29–0·34	245
24S–T Alclad sheet	Fluct. tension	4	3	Aircraft gust load	0·9–3·0	241
DTD 363A (Al–Zn)	Fluct. tension	3	6	Aircraft gust load	1·06–2·04	246
			Components and structures			
Riveted joint 24S–T Alclad	Fluct. tension	5	2–4	Gust load	0·64–2·3	244
Riveted joint 24S–T Alclad	Fluct. tension	3	2	Manoeuvre load	1·2–2·3	
Riveted joint 75S–T Alclad	Fluct. tension	5	2–4	Gust load	1·3–4·7	
Riveted joint 75S–T Alclad	Fluct. tension	3	2	Manoeuvre load	1·4–2·6	
Aircraft wing panel	Fluct. tension	4	1	3 stress levels	1·28–1·61	247
Automobile components—steel	R.B.	3		Log. binomial	0·3–0·6	239
	R.B.	3		Log. binomial	0·1–0·12	
	R.B.	2		Log. binomial	0·003–0·018	

* It was assumed that each stress peak was equivalent to a half cycle of a sine wave of the same peak amplitude about zero mean load.

TABLE 1. CUMULATIVE CYCLE RATIOS DETERMINED FROM PROGRAMME OR SPECTRUM TESTS.

REPRODUCED FROM FORREST (84).

TABLE 2

SHELL TELLUS 27 OIL - SPECIFICATION

Shell Tellus 27 Oil is made up of a paraffinic, high viscosity index oil combined with additives to impart anti-wear, anti-oxidant and anti-corrosion properties. The additives used are zinc dialkyl dithiophosphate and a modified alkylated succinate. The mineral oil content of the final oil is approximately 99%.

Like other lubricating oils Tellus 27 is comprised of a very complex mixture of hydrocarbons and is particularly rich in paraffinic as opposed to napthenic or aromatic hydrocarbons.

Tellus 27 has no harmful corrosive effects on Duralumin alloys so long as the oil temperature is kept below 150°C.

The acidity of the base oil used to make up Tellus 27 is less than 0.05 mg KOH/g of oil. However, the additives present in the oil produce an apparent acidity of approximately 0.65 mg KOH/g by interacting with the KOH during the titration.

Other data:

Average molecular weight is approximately 360.

Surface tension is approximately 30 dynes/cm.

Autogeneous ignition temperature is approximate 400°C.

Specific gravity at atmospheric pressure and at 20°C. is 0.870.

Kinematic viscosity at atmospheric pressure and at 20°C is approximately 85 centistokes.

The above information was obtained from Shell International Petroleum Co. Ltd. and from their publication "Technical data on Shell Tellus oils", second edition.

TABLE 3

FAIREY HYDRAULIC POWER UNIT TYPE 6-3000

Dry weight	750 LBF
Fluid type	Shell Tellus 27
Fluid capacity	15 gallons
Maximum delivery	6 g.p.m.
Maximum pressure	3000 LBF/in^2
Filtration	5 microns
Accumulator	1 quart capacity charged with nitrogen or air at 1500 p.s.i.
Pump motor	380/420 V. 3 phase 50 c.p.s. 20 amps
Cooler motor	380/420 V. 3 phase 50 c.p.s. 1 amp
Maximum permissible oil temperature	75^{o}C

TABLE 4

B.S.S. 2L65

Element:	% Composition by Weight
Copper	3.8 - 4.8
Magnesium	0.55 - 0.85
Silicon	0.6 - 0.9
Iron	1.0
Manganese	0.4 - 1.2
Nickel	0.2
Zinc	0.2
Aluminium	Remainder

Mechanical Properties:	
0.1% Proof stress	26 Tonf/in^2
Ultimate tensile stress	30 Tonf/in^2
Elongation (2 inch gauge length)	8%

TABLE 5

STATIC TEST RESULTS

Specimen	No. of Specimens Tested	E, Tonf/in^2	0.1% Proof Stress, Tonf/in^2	U.T.S., Tonf/in^2	% Reduction in Area	% Elongation over 2 inch
1.128 inch diameter	1	4,750	30.1	33.4	24	
0.250 inch diameter cut from position shown in Fig. 15.	4	4,750	29.2	32.6	23	8
1.00 inch diameter compression specimen	2	4,730	31.3			
Hounsfield specimens cut from position shown in Fig.15) Long'l	4			29.9	24	
) Trans.	6			29.6	8	

TABLE 6

DETAILS OF FRACTURES

Comparison of Bar Strengths

All constant amplitude tests, except K = $-\frac{1}{2}$, -0

Bar	A	B	C	D	E	F	G	H	J	L
Number of Tests	11	9	8	8	13	11	11	9	11	7
Number Above Mean	5	1	5	7	4	6	6	5	6	4
Number Below Mean	6	8	3	1	9	5	5	4	5	3

Failure Position in Test Rig

All constant amplitude test results with positive $\sigma_{MAXIMUM} = \sigma_{HOOP}$

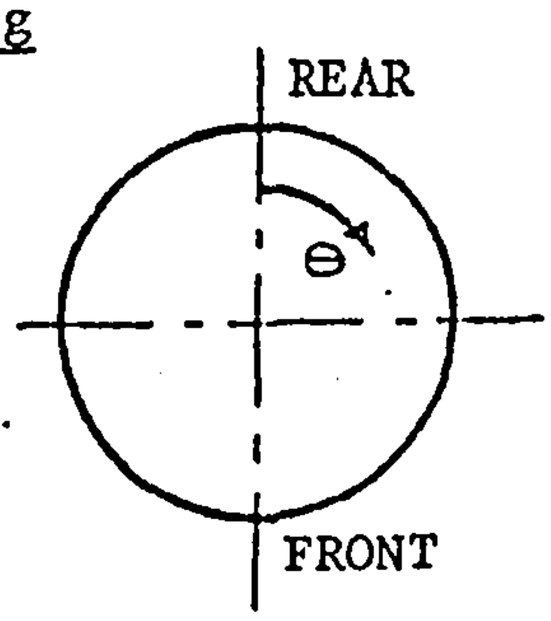

K	1	2	7.9	-2	-1	ALL
0°-90°	3	3½	7½	4½	2	20½
90°-180°	3	3½	½	3	4	14
180°-270°	1½	1	5½	6	3½	17½
270°-360°	4½	5	1½	3½	½	15
TOTAL	12	13	15	17	10	67

Failure Position in Specimen

All constant amplitude test results with positive $\sigma_{MAXIMUM} = \sigma_{HOOP}$

K	1	2	7.9	-2	-1	ALL
At $t_{MINIMUM}$	7	6	8	6	6	33
0-$^{6}/_{10}$ Thou. Difference	4	6	4	3	1	18
$^{6}/_{10}$ Thou. + Difference	2	3	4	8	3	20
TOTAL	13	15	16	17	10	71

TABLE 7a

ROTATING BENDING FATIGUE TESTS

LONGITUDINAL SPECIMENS - FULL SIZE

STRESS AMPLITUDE TONF/IN^2	CYCLES TO FAILURE, THOUSANDS	REMARKS
17.9	114	
16.7	176	
15.6	313	Retest
12.3	340	
15.6	375	
13.4	387	
13.4	885	
15.6	1,647	
8.9	2,889	
13.4	10,186	
11.2	12,907	Not broken Retested at 15.6 T/in^2
12.3	14,855	

TABLE 7b

ROTATING BENDING FATIGUE TESTS

LONGITUDINAL SPECIMENS - SHORT

STRESS AMPLITUDE TONF/IN^2	CYCLES TO FAILURE, THOUSANDS	REMARKS
17.9	84	
17.9	113	Retest
15.6	173	
14.5	192	
16.7	208	Retest
16.7	261	
13.4	278	
12.3	403	
11.2	1,057	Not broken Retested at 12.3 T/in^2
12.3	6,382	Retest
11.2	10,868	
12.3	17,854	Not broken Retested at 17.9 T/in^2
10.0	33,527	Not broken Retested at 16.7 T/in^2

TABLE 7c

ROTATING BENDING FATIGUE TESTS

TRANSVERSE SPECIMENS - SHORT

STRESS AMPLITUDE TONF/IN^2	CYCLES TO FAILURE, THOUSANDS	REMARKS
17.9	29	
16.7	38	
15.6	70	
15.6	98	
12.3	120	
13.4	125	Retest
12.3	181	
13.4	226	
11.2	818	Retest
11.2	923	
12.3	1,548	
8.9	11,355	Not broken Retested at 11.2 T/in^2
11.2	11,583	Not broken Retested at 13.4 T/in^2

TABLE 8

UNIAXIAL REPEATED TENSION FATIGUE TEST RESULTS

VIBROPHORE

STRESS AMPLITUDE TONF/IN^2	CYCLES TO FAILURE, THOUSANDS	REMARKS
POLISHED SPECIMENS:		
12	111	
12	161	
11	135	
11	135	
10	428	
10	426	
9.5	483	
9.5	4,290	
9	778	
9	3,600	
UNPOLISHED SPECIMENS:		
12	39	
12	39	
12	152	
11	47	Re-test
11	92	
10	145	
10	156	Failed at thread
10	363	Failed at thread
10	889	
10	915	
9.5	169	
9.5	1,961	
9.5	3,024	
9	165	
9	1,900	
9	7,600	
8	11,000	
7	16,000	

Material	Tensile strength tons/in²	Testing conditions	Fatigue strength, as percentage of maximum value (and in tons/in²)						Investigator	Ref.
			Highly polished	Polished	Ground	Smooth turned	Rough turned	Very rough turned		
0·02% C steel	19	R.B.		100 (±11·6, 00 emery)		92	88		Moore and Kommers	120
0·45% C steel		R.B.	100 (±14, superfinished)	100 (000 emery)		90	90		Horger and Neifert	325
0·49% C steel	43	R.B.	100 (±23, rouge)	94 (00 emery)	88	84	82		Moore and Kommers	120
0·6% C steel	47	R.B.		100 (±24)	92	84	72		Glaubitz	120
4 S 11 (3% Ni Cr steel)	54–59	R.B.	100 (±29, superfinished)	100 (0 emery)	96	97			Roberts and Grayshon	120
Cr Mo steel	62	R.B.		100 (±34)	93	74	65		Glaubitz	120
DTD 331 Ni Cr Mo W steel	80–90	R.B.	100 (±38, superfinished)		99				Roberts and Grayshon	120
Ni Cr steel	118	R.B. (10⁷)	100 (±52, 0000 emery longt.)	94 (00 emery)					Hankins, Becker and Mills	326
Ni Cr Mo steel	138	R.B. (10⁷)	100 (±65, 0000 emery longt.)	76 (00 emery)						
Brass, annealed		Ax (60–80 × 10³)		100 (±12)		93	86	81	Siebel and Gaier	327
Al Cu alloy, aged		Ax (60–80 × 10³)		100 (±11)		93	72			
Al Mg alloy, annealed		Ax (60–80 × 10³)		100 (±9·3)		100	77	68		
Mg alloy, annealed		Ax (60–80 × 10³)		100 (±7·6)			100			
DTD 683 Al Zn Mg alloy	35–37	R.B. (10⁷ cycles)	100 (±12, longt. polish)	94 (circumferential polish)		88	88		N. J. F. Gunn	328

† R.B. = rotating bending
Ax = axial

TABLE 9. THE EFFECT OF SURFACE ROUGHNESS ON FATIGUE STRENGTH
REPRODUCED FROM FORREST (84)

TABLE 10

BIAXIAL CONSTANT AMPLITUDE FATIGUE TESTS ON TUBULAR SPECIMENS - RESULTS - TEST SERIES 2

TABLE 10a

K = 0

SPECIMEN NUMBER	LONGITUDINAL STRESS AMPLITUDE TONF/IN^2	CYCLES TO FAILURE, THOUSANDS	CYCLING SPEED CYCLES/SEC.
B15	13.6	20.9	15
A 5	12.9	27.1	15
D 1	13.3	35.6	15
A12	9.4	37.5	15
C 1	11.6	40.3	15
D11	11.5	63.5	15
E 9	10.0	67.1	30
A18	10.5	75.0	30
E 8	9.1	91.9	30
C 3	9.5	94.8	15
D 9	11.5	134.8	15
E13	8.0	330	30
J 1	8.7	540	40
J 6	8.7	544	40
F14	8.1	1,000NR	30
D 5	9.8	1,003NR	15
E20	8.1	1,010NR	30
J 7	8.7	1,230NR	40

N = NOT BROKEN

R = RESTED OVERNIGHT

T = RETEST

TABLE 10b

K = 0.5

SPECIMEN NUMBER	LONGITUDINAL STRESS AMPLITUDE TONF/IN^2	CYCLES TO FAILURE, THOUSANDS	CYCLING SPEED CYCLES/SEC.
E 5	14.5	1.1	30
E 6	13.2	5.2	15
F14	13.4	12.2T	15
F 2	13.6	17.5	15
F11	13.1	18.5	15
F18	11.4	22.1	30
E18	11.7	33.5	30
E 3	10.9	59.3	30
F16	10.9	115	30
E 4	9.9	115	30
E14	11.4	141	30
F 6	9.9	200	30
D 6	9.5	317	30
F13	8.4	323+	30
F 5	8.4	616	30
F 9	8.4	735	40
F10	8.4	1,000NR	30

Specimen F13 is thought to have been overloaded and thus failed prematurely due to electronic interference from other equipment.

N = Not broken

R = Rested overnight

T = Retest

TABLE 10c

K = 1.0

SPECIMEN NUMBER	HOOP STRESS AMPLITUDE TONF/IN^2	CYCLES TO FAILURE, THOUSANDS	CYCLING SPEED CYCLES/SEC
E17	11.4	5.8	30
F10	12.7	8.0T	15
F12	11.7	14.6	15
F 1	11.8	16.2	30
G 2	10.0	41.3	30
G 3	10.1	51.8	30
G 4	10.0	55.0	30
H15	8.0	66.1	30
$H13_2$	8.1	144	30
H16	8.3	219	30
J11	7.0	419	30
J19	6.9	900R	50
J15	7.0	1,220R	30

R = Rested overnight

T = Retest

TABLE 10d

K = 2

SPECIMEN NUMBER	HOOP STRESS AMPLITUDE TONF/IN^2	CYCLES TO FAILURE, THOUSANDS	CYCLING SPEED CYCLES/SEC
F 3	14.2	3.7T	15
B 3	14.1	5.0T	15
B16	12.8	7.2	15
D 3	13.0	8.6	15
B 6	10.3	10.7	15
C 7	13.2	15.2	15
C10	10.1	18.1	15
B 8	10.0	31.0	15
B 5	8.2	68.6	15
H12	7.2	114	40
E15	6.5	159	30
A 9	8.2	197	15
H13	7.2	201	40
$H13_1$	7.2	202	30
D 4	8.4	350	15
B 3	6.4	1,030NR	30
F 3	6.5	1,040NR	30
H 7	6.8	1,360NR	40

N = Not broken

R = Rested overnight

T = Retest

TABLE 10e

K = 7.9

SPECIMEN NUMBER	HOOP STRESS AMPLITUDE TONF/IN^2	CYCLES TO FAILURE, THOUSANDS	CYCLING SPEED CYCLES/SEC
B10	12.0	3.9	15
B17	11.8	11.6T	15
C 5	11.9	19.5	15
A 8	13.0	23.3	15
A 6	10.0	30.5	15
A17	9.9	37.1	15
B 4	9.3	46.2	15
E 2	6.8	50.2	15
C13	10.0	67.0	15
A 4	9.9	67.0	15
C15	8.3	85.7	15
A11	12.0	94.5	15
A 3	7.2	120	15
C14	8.3	141	15
J14	7.5	208	40
J16	7.5	223	40
D 6	6.7	1,000NR	15
B17	5.6	1,000NR	15
J17	7.5	1,500NR	40
G14	6.9	2,240NR	50

N = Not broken

R = Rested overnight

TABLE 10f

K = -2

SPECIMEN NUMBER	HOOP STRESS AMPLITUDE TONF/IN^2	CYCLES TO FAILURE, THOUSANDS	CYCLING SPEED CYCLES/SEC
H 7_1	10.1	6.8	30
E16	10.1	7.9	30
H 5	10.2	25.7	15
G 5	7.6	47.2	35
G 6	8.5	60.2	35
H10	9.6	64.7	30
H 6	9.6	76.6	30
J 3	9.6	96.2	30
G11	8.6	141	35
G12	9.2	146	30
J12	9.1	155	30
G19	7.7	177	35
J 9	9.1	258	30
J20	6.7	466	35
J13	6.7	492	35
G 9	8.6	497	35
H20	7.7	683	35

TABLE 10g

K = -1

SPECIMEN NUMBER	HOOP STRESS AMPLITUDE TONF/IN^2	CYCLES TO FAILURE, THOUSANDS	CYCLING SPEED CYCLES/SEC
G 8	7.6	32.7	35
L10	9.1	46.6	40
J 4	7.6	103	35
L 7	6.7	118	40
L 3	6.8	120	40
C 4	7.6	138	35
L 4	6.7	309	40
L19	5.8	499	40
L14	5.8	826	40
L15	5.7	1,351	40

TABLE 10h

$K = -\frac{1}{2}$

SPECIMEN NUMBER	LONGITUDINAL STRESS AMPLITUDE TONF/IN^2	CYCLES TO FAILURE, THOUSANDS	CYCLING SPEED CYCLES/SEC
D 2	8.3	14.7	40
M 3	8.4	40.3	"
T15	7.7	311	"
E10	8.2	570	"
G13	7.7	607	"
G 1	8.2	618	"
D 7	6.1	943	"
G18	7.5	1,058NR	"

N = Not broken

R = Rested overnight

TABLE 10k

$K = -0$

SPECIMEN NUMBER	LONGITUDINAL STRESS AMPLITUDE TONF/IN^2	CYCLES TO FAILURE, THOUSANDS	CYCLING SPEED CYCLES/SEC
J17	10.8	194T	30
T20	10.8	196	30
T 9	9.9	449	40
T11	9.9	790	40
T10	9.3	950N	40

N = Not broken

T = Retest

TABLE 11

BIAXIAL PROGRAMME FATIGUE TESTS, AT CONSTANT PRINCIPAL STRESS RATIO K, RESULTS - SERIES 3

TABLE 11a

K = 0

Stress Levels - Tonf/in^2

$S_1 = 12.0$, $S_2 = 10.0$, $S_3 = 8.75$

Cycles to Failure, Thousands

$N_1 = 40$, $N_2 = 100$, $N_3 = 500$

SPECIMEN NUMBER	STRESS LEVELS, CYCLE BLOCKS	n_1	n_2	n_3	$\frac{n_1}{N_1}$	$\frac{n_2}{N_2}$	$\frac{n_3}{N_3}$	$\Sigma\frac{n}{N}$
		THOUSANDS						
M 6	S_1-S_2	25.5	20.0		0.64	0.20		0.84
T 8	10^4-10^4	12.8	10.0		0.33	0.10		0.43
T 1		13.5	0		0.45	0		0.45
K13	S_1-S_2	12.0	122.8		0.30	1.23		1.54
T13	10^3-10^4	12.0	122.1		0.30	1.22		1.52
T14		9.0	87.3		0.22	0.87		1.09
N 6	S_2-S_3		80.1	80.0		0.80	0.16	0.96
P 4	10^4-10^4		80.1	80.0		0.80	0.16	0.96
S14			117.7	110.0		1.18	0.22	1.40
P11	S_2-S_3		9.0	86.9		0.09	0.17	0.26
S16	10^3-10^4		15.0	145.8		0.15	0.29	0.44
P16			19.0	187.1		0.19	0.37	0.56
S12	S_2-S_3		19.8	100.0		0.20	0.20	0.40
S 1	10^4-10^5		20.0	166.2		0.20	0.33	0.53
P20			30.0	288.9		0.30	0.58	0.88
N15	S_1-S_3	17.7		12.8	0.44		0.03	0.47
T10	10^4-10^4	19.0		10.0	0.48		0.02	0.50
G14		22.2		20.0	0.54		0.04	0.58
S10	S_1-S_3	7.0		69.1	0.18		0.14	0.32
N 9	10^3-10^4	13.3		130.0	0.33		0.26	0.59
A13		17.0		164.6	0.43		0.33	0.76
P 7	S_1-S_3	10.0		39.1	0.25		0.08	0.33
S 7	10^4-10^5	10.0		47.1	0.25		0.12	0.37
N 3		15.2		100.0	0.38		0.20	0.58

TABLE 11b

K = 2

Stress Levels - Tonf/in^2 Cycles to Failure, Thousands

$S_1 = 9.5$, $S_2 = 8.5$, $S_2^1 = 8.0$, $S_3 = 7.0$ $N_1 = 30$, $N_2 = 60$, $N_2^1 = 100$, $N_3 = 5$

SPECIMEN NUMBER	STRESS LEVELS, CYCLE BLOCKS	n_1	n_2	n_3	$\frac{n_1}{N_1}$	$\frac{n_2}{N_2}$	$\frac{n_3}{N_3}$	$\Sigma \frac{n}{N}$
		THOUSANDS						
H 7	S_1-S_3	48.9		35.2	1.63		0.07	1.70
D12	10^4-10^4	33.6		25.2	1.12		0.05	1.17
J 8		65.2		67.0	2.17		0.13	2.30
H 2	S_1-S_2	58.0	52.2		1.93	0.87		2.80
H 9	10^4-10^4	18.6	10.0		0.62	0.17		0.79
H19		15.6	10.0		0.52	0.17		0.69
K 6	S_1-S_2^1	50.1	150.0		1.67	1.50		3.17
K 7	10^4-3×10^4	20.0	46.8		0.67	0.47		1.14
K16		23.5	60.0		0.78	0.60		1.38
A 2	S_1-S_3	36.8		300.0	1.23		0.60	1.83
B14	10^4-10^5	90.0		950.0	3.00		1.90	4.90
H18		10.6		84.0	0.35		0.17	0.52
C 2		30.0		284.3	1.00		0.57	1.57
H 1		30.0		231.7	1.00		0.46	1.46
H11	S_3-S_1	10.0		197.8	0.33		0.40	0.73
C11	10^5-10^4	25.7		300.0	0.86		0.60	1.46
G16		50.0		559.2	1.67		1.12	2.79
K19	S_2^1-S_3		40.0	322.3		0.40	0.64	1.04
K15	10^4-10^5		10.0	22.0		0.25	0.04	0.29
K11			10.0	70.5		0.10	0.14	0.24
K 8			11.6	62.1		0.12	0.12	0.24
K10	S_2^1-S_3		110.0	100.0		1.10	0.20	1.30
F15	10^4-10^4		53.9	50.0		0.54	0.10	0.64
M 4			3.2	-		0.03	-	0.03
L20			80.0	70.0		0.80	0.14	0.94

TABLE 11b (Continued)

K = 2

SPECIMEN NUMBER	STRESS LEVELS, CYCLE BLOCKS	n_1	n_2	n_3	$\frac{n_1}{N_1}$	$\frac{n_2}{N_2}$	$\frac{n_3}{N_3}$	$\Sigma \frac{n}{N}$
		THOUSANDS						
T 7	S_1-$S_2{}^1$	8.0	73.8		0.27	0.74		1.01
T19	10^3-10^4	4.4	40.0		0.15	0.40		0.55
M 8		4.0	20.2		0.13	0.20		0.33
T 3	S_1-S_3	6.0		51.6	0.20		0.10	0.30
M11	10^3-10^4	34.0		339.1	1.13		0.68	1.81
T17		6.0		57.9	0.20		0.12	0.32
M12	$S_2{}^1$-S_3		19.0	189.2		0.19	0.38	0.57
M13	10^3-10^4		18.0	178.9		0.18	0.36	0.54
T12			53.0	524.5		0.53	1.05	1.58

TABLE 11c

K = 7.9

Stress Levels - Tonf/in^2 | Cycles to Failure, Thousands

$S_1 = 9.5$, $S_2 = 8.0$, $S_3 = 7.0$ | $N_1 = 50$, $N_2 = 150$, $N_3 = 1{,}000$

SPECIMEN NUMBER	STRESS LEVELS, CYCLE BLOCKS	n_1	n_2	n_3	$\frac{n_1}{N_1}$	$\frac{n_2}{N_2}$	$\frac{n_3}{N_3}$	$\Sigma \frac{n}{N}$
		THOUSANDS						
L11	S_1-S_3	49.0		486.2	0.98		0.48	1.46
M 7	10^3-10^4	27.0		264.9	0.54		0.26	0.80
T 6		36.2		360.0	0.72		0.36	1.08
D10	S_1-S_2	54.2	50.0		1.08	0.33		1.41
K14	10^4-10^4	25.7	20.0		0.51	0.13		0.64
L 6		27.8	20.0		0.56	0.13		0.69
T 4	S_1-S_2	10.1	100.0		0.20	0.67		0.87
M 5	10^3-10^4	9.7	90.0		0.19	0.60		0.79
L17		4.0	34.2		0.08	0.23		0.31
K12	S_1-S_3	20.0		112.4	0.40		0.11	0.51
L 2	10^4-10^5	20.0		142.1	0.40		0.14	0.54
L 9		14.6		100.0	0.29		0.10	0.39
M 1	S_2-S_3		10.0	57.8		0.07	0.06	0.13
K17	10^4-10^5		10.0	73.6		0.07	0.07	0.14
L 5			10.0	73.1		0.07	0.07	0.14
D 8	S_2-S_3		53.8	50.0		0.36	0.05	0.41
K 9	10^4-10^4		50.0	48.8		0.33	0.05	0.38
L13			116.2	110.0		0.78	0.11	0.89
M10	S_2-S_3		12.9	100.0		0.09	0.10	0.19
T20	10^3-10^4		100.5	1005.8		0.67	1.00	1.67
E19			16.0	168.9		0.11	0.17	0.28
G18	S_1-S_3	60.6		50.0	1.21		0.05	1.26
N18	10^4-10^4	46.3		40.0	0.92		0.04	0.96
P 9		35.5		30.0	0.71		0.03	0.74

TABLE 11d

K = -1

Stress Levels - Tonf/in^2

$S_1 = 8.0$, $S_2 = 7.0$, $S_3 = 6.0$

Cycles to Failure, Thousands

$N_1 = 50$, $N_2 = 120$, $N_3 = 500$

SPECIMEN NUMBER	STRESS LEVELS, CYCLE BLOCKS	n_1	n_2	n_3	$\frac{n_1}{N_1}$	$\frac{n_2}{N_2}$	$\frac{n_3}{N_3}$	$\Sigma \frac{n}{N}$
		THOUSANDS						
O 13	S_2-S_3		90.0	83.3		0.75	0.17	0.92
S 17	10^4-10^4		50.0	43.1		0.42	0.09	0.51
N 12			143.1	140.0		1.20	0.28	1.48
P 1	S_2-S_3		10.0	97.2		0.08	0.19	0.27
P 8	10^3-10^4		16.0	155.4		0.13	0.31	0.44
S 18			25.0	248.2		0.21	0.50	0.71
N 5	S_2-S_3		40.0	345.3		0.33	0.69	1.02
N 8	10^4-10^5		30.0	238.0		0.25	0.48	0.73
S 19			20.0	160.0		0.17	0.32	0.49

TABLE 11e

OVERALL MEAN CYCLE RATIO SUMS

STRESS LEVELS	CYCLE BLOCKS	K			
		0	2	7.9	-1
S_1-S_2	10^4-10^4	0.63	0.74	0.91	
	10^3-10^4	1.38	0.63	0.66	
S_2-S_3	10^4-10^4	1.11	0.79	0.54	0.97
	10^3-10^4	0.42	0.90	0.23	0.47
	10^4-10^5	0.60	0.51	0.14	0.75
S_1-S_3	10^4-10^4	0.52	1.44	0.99	
	10^3-10^4	0.56	0.81	1.11	
	10^4-10^5	0.43	1.34	0.48	
MEAN		0.71	1.02	0.63	0.73
OVERALL MEAN		0.77			

TABLE 12

BIAXIAL PROGRAMME FATIGUE TESTS AT TWO PRINCIPAL STRESS RATIOS K, RESULTS - SERIES 4.

TABLE 12a

K = 0 and 7.9

All cycle blocks are 10^4 cycles.

SPECIMEN NUMBER	STRESS LEVELS TONF/IN^2 S_0-$S_{7.9}$	n_0	$n_{7.9}$	N_0	$N_{7.9}$
		THOUSANDS			
N2	12-9.5	22.4	20.0	40.0	50.0
P17	12-9.5	20.6	20.0	40.0	50.0
S13	10-8.5	100.0	94.0	100.0	100.0
N11	10-8.5	80.0	76.1	100.0	100.0
M2	9.5-9.5	20.1	17.1	170.0	48.0
S3	9.5-9.5	80.0	74.2	170.0	48.0
H4	9.5-9.5	40.0	40.0	170.0	48.0

TABLE 12b

K = -1 and 7.9

All cycle blocks are 10^4 cycles

SPECIMEN NUMBER	STRESS LEVELS TONF/IN^2 S_{-1}-$S_{7.9}$	n_{-1}	$n_{7.9}$	N_{-1}	$N_{7.9}$
		THOUSANDS			
P12	7 - 8	60.0	54.0	120.0	150.0
S2	7 - 8	30.0	21.6	120.0	150.0
P14	6 - 8	40.0	36.5	500.0	150.0
S8	6 - 8	80.0	71.6	500.0	150.0
N1	5 - 8	70.0	61.0	∞	150.0
P18	5 - 8	80.0	75.7	∞	150.0
N19	4 - 8	140.0	130.8	∞	150.0
N14	4 - 8	220.0	212.0	∞	150.0

TABLE 12c

K = -1 and 0

50,000 cycles at S_{-1}, then to failure at S_0

SPECIMEN NUMBER	STRESS LEVELS TONF/IN^2 S_{-1} - S_0	n_{-1}	n_0	N_{-1}	N_0
		THOUSANDS			
Y19	7 - 10	50.0	95.1	120.0	100.0
Y17	7 - 10	50.0	58.4	120.0	100.0

TABLE 12d

K = 0 and -1

20,000 cycles at S_0, then to failure at S_{-1}

SPECIMEN NUMBER	STRESS LEVELS TONF/IN^2 S_0 - S_{-1}	n_0	n_{-1}	N_0	N_{-1}
		THOUSANDS			
Y10	12 - 7	20.0	$\overrightarrow{100.0}$	40.0	120.0
Y 6	12 - 7	20.0	77.8	40.0	120.0

TABLE 13

GOUGH(12) MATERIAL AND TEST DATA

TEST SERIES	MATERIAL	U.T.S. Tonf/in^2	t Tonf/in^2	b Tonf/in^2	b/t
SOLID SPECIMENS (STEEL)					
GS 1	0.1% C.Steel (Normalised)	27.9	9.8	17.4	1.78
GS 2	0.4% C.Steel (Normalised)	42.0	13.4	21.5	1.60
GS 3	0.4% C.Steel (Spheroidised)	30.9	10.1	17.8	1.76
GS 4	0.9% C.Steel (Pearlitic)	54.9	15.6	22.8	1.46
GS 5	3% Ni.Steel (30/35 Tonf)	34.1	13.3	22.2	1.67
GS 6	3/3½% Ni.Steel (45/50 Tonf)	46.8	17.3	28.8	1.67
GS 7	Cr.Va.Steel (45/50 Tonf)	48.7	16.7	27.8	1.67
GS 8	3½% Ni.Cr.Steel (Normal Impact)	58.0	22.8	35.0	1.54
GS 9	3½% Ni.Cr.Steel (Low Impact)	58.1	21.0	33.0	1.57
GS10	Ni.Cr.Mo.Steel (75/80 Tonf)	80.5	22.2	42.8	1.93
GS11	Ni.Cr.Steel (95/105 Tonf)	108.0	29.3	50.0	1.71
HOLLOW SPECIMENS (STEEL)					
GH 1	0.1% C.Steel (Normalised)	27.9	9.1	17.5	1.93
GH 2	3½% Ni.Cr.Steel (Normal Impact)	58.0	20.5	33.6	1.64
SOLID SPECIMENS (CAST IRON)					
GS CI 1	Silac		14.2	15.6	1.10
GS CI 2	Nicrosilac		13.7	16.4	1.20
NOTCHED SPECIMENS (STEEL)					
GN 1	0.4% C.Steel (Normalised)	42.0	11.4	11.6	1.02
GN 2	3% Ni.Steel (30/35 Tonf)	34.1	9.8	13.6	1.39
GN 3	3/3½% Ni.Steel (45/50 Tonf)	46.8	11.9	19.6	1.65
GN 4	Cr.Va.Steel (45/40 Tonf)	48.7	10.4	14.0	1.35
GN 5	3½% Ni.Cr.Steel (Normal Impact)	58.0	15.3	17.4	1.38
GN 6	Ni.Cr.Mo.Steel (75/80 Tonf)	80.5	15.6	17.6	1.13

TABLE 14

GOUGH (12) DATA - STANDARD DEVIATION v. n (EQUATIONS 7.2 AND 7.5)

SERIES AND MATERIAL	θ	f	q	S	S_G	$S_{0.5}$	$S_{1.0}$	$S_{1.5}$	$S_{2.0}$	$S_{2.5}$	$P.D._G$	$P.D._{0.5}$	$P.D._{1.0}$	$P.D._{1.5}$	$P.D._{2.0}$	$P.D._{2.}$
	0	17.4	0	8.7	8.70	8.70	8.70	8.70	8.70	8.70	0	0	0	0	0	0
GS 1	15	17.0	2.3	8.8	8.75	8.71	8.73	8.74	8.75	8.76	-0.53	-0.99	-0.85	-0.71	-0.57	-0.43
0.1% C. Steel	30	15.7	4.5	9.1	8.92	8.76	8.81	8.86	8.90	8.95	-2.04	-3.79	-3.22	-2.67	-2.15	-1.66
(Normalised)	45	13.3	6.7	9.4	9.17	8.84	8.96	9.07	9.16	9.24	-2.41	-5.98	-4.69	-3.57	-2.58	-1.72
b = 17.4	60	9.5	8.3	9.5	9.49	8.99	9.20	9.36	9.47	9.56	-0.15	-5.40	-3.16	-1.51	-0.29	0.61
t = 9.8	75	5.1	9.5	9.9	9.71	9.20	9.48	9.63	9.71	9.75	-1.92	-7.03	-4.27	-2.77	-1.97	-1.53
$\frac{b}{t}$ = 1.78	90	0	9.8	9.8	9.80	9.80	9.80	9.80	9.80	9.80	0	0	0	0	0	0
	STANDARD DEVIATION, PER CENT										0.56	1.85	1.30	0.90	0.61	0.38
	0	21.5	0	10.75	10.75	10.75	10.75	10.75	10.75	10.75	0	0	0	0	0	0
GS 2	15	21.3	2.8	11.0	10.81	10.76	10.78	10.79	10.80	10.81	-1.77	-2.16	-2.05	-1.94	-1.83	-1.72
0.4% C. Steel	30	19.2	5.5	11.1	11.34	10.90	11.03	11.16	11.29	11.40	2.13	-1.84	-0.60	0.57	1.68	2.73
(Normalised)	45	16.4	8.2	11.6	11.93	11.09	11.38	11.64	11.86	12.05	2.84	-4.44	-1.91	0.30	2.23	3.91
b = 21.5	60	12.3	10.6	12.2	12.59	11.40	11.88	12.25	12.53	12.74	3.23	-6.59	-2.59	0.44	2.73	4.46
t = 13.4	75	6.6	12.2	12.7	13.17	11.93	12.59	12.95	13.15	13.26	3.73	-6.05	-0.89	1.96	3.55	4.42
$\frac{b}{t}$ = 1.60	90	0	13.4	13.4	13.40	13.40	13.40	13.40	13.40	13.40	0	0	0	0	0	0
	STANDARD DEVIATION, PER CENT										0.81	1.69	0.64	0.11	0.67	1.10

TABLE 14 CONTINUED

SERIES AND MATERIAL	θ	f	q	S	S_G	$S_{0.5}$	$S_{1.0}$	$S_{1.5}$	$S_{2.0}$	$S_{2.5}$	$P.D._G$	$P.D._{0.5}$	$P.D._{1.0}$	$P.D._{1.5}$	$P.D._{2.0}$	$P.D_{2.5}$
GS 3	0	17.8	0	8.9	8.90	8.90	8.90	8.90	8.90	8.90	0	0	0	0	0	0
0.4% C. Steel	15	17.8	2.4	9.2	8.90	8.90	8.90	8.90	8.90	8.90	-3.26	-3.26	-3.26	-3.26	-3.26	-3.26
(Spheroidised)	30	16.1	4.6	9.3	9.13	8.96	9.02	9.07	9.12	9.17	-1.83	-3.67	-3.07	-2.50	-1.95	-1.44
b = 17.8	45	13.5	6.8	9.6	9.43	9.06	9.19	9.31	9.41	9.50	-1.79	-5.68	-4.27	-3.05	-1.98	-1.05
t = 10.1	60	10.0	8.6	10.0	9.74	9.20	9.43	9.60	9.72	9.82	-2.63	-7.99	-5.74	-4.05	-2.79	-1.84
$\frac{b}{t}$ = 1.76	75	5.1	9.5	9.8	10.01	9.46	9.76	9.92	10.00	10.05	2.11	-3.49	-0.45	1.18	2.06	2.52
	90	0	10.1	10.1	10.10	10.10	10.10	10.10	10.10	10.10	0	0	0	0	0	0
	STANDARD DEVIATION, PER CENT										0.59	1.93	1.34	0.93	0.63	0.41
GS 4	0	22.8	0	11.4	11.40	11.40	11.40	11.40	11.40	11.40	0	0	0	0	0	0
0.9% C. Steel	15	22.8	3.0	11.8	11.40	11.40	11.40	11.40	11.40	11.40	-3.39	-3.39	-3.39	-3.39	-3.39	-3.39
(Pearlitic)	30	20.8	6.0	12.0	12.21	11.59	11.77	11.94	12.11	12.26	1.72	-3.43	-1.93	-0.50	0.87	2.18
b = 22.8	45	18.2	9.1	12.9	13.08	11.85	12.25	12.61	12.92	13.21	1.40	-8.16	-5.06	-2.29	0.18	2.40
t = 15.6	60	13.8	11.9	13.8	14.21	12.33	13.06	13.62	14.06	14.40	2.94	-10.63	-5.38	-1.29	1.89	4.37
$\frac{b}{t}$ = 1.46	75	7.3	13.5	14.0	15.22	13.22	14.26	14.84	15.17	15.36	8.74	-5.55	1.82	5.99	8.35	9.69
	90	0	15.6	15.6	15.60	15.60	15.60	15.60	15.60	15.60	0	0	0	0	0	0
	STANDARD DEVIATION, PER CENT										0.91	2.49	1.11	0.12	0.63	1.22

TABLE 14 CONTINUED

SERIES AND MATERIAL	θ	f	q	S	S_G	$S_{0.5}$	$S_{1.0}$	$S_{1.5}$	$S_{2.0}$	$S_{2.5}$	P.D.$_G$	P.D.$_{0.5}$	P.D.$_{1.0}$	P.D.$_{1.5}$	P.D.$_{2.0}$	P.D.$_{2.5}$
GS 5 3% Ni. Steel (30/35 Tonf) b = 22.2 t = 13.3 $\frac{b}{t}$ = 1.67	0	22.2	0	11.1	11.10	11.10	11.10	11.10	11.10	11.10	0	0	0	0	0	0
	15	21.2	2.8	11.0	11.31	11.15	11.20	11.25	11.29	11.34	2.83	1.37	1.81	2.25	2.67	3.09
	30	19.7	5.7	11.4	11.60	11.23	11.35	11.46	11.57	11.67	1.78	-1.51	-0.46	0.54	1.47	2.35
	45	17.2	8.6	12.2	12.03	11.36	11.60	11.80	11.98	12.14	-1.41	-6.86	-4.96	-3.28	-1.81	-0.51
	60	12.3	10.7	12.3	12.67	11.66	12.08	12.39	12.63	12.80	2.97	-5.18	-1.78	0.75	2.64	4.04
	75	6.7	12.6	13.0	13.12	12.09	12.64	12.94	13.10	13.19	0.88	-6.99	-2.80	-0.50	0.77	1.46
	90	0	13.3	13.3	13.30	13.30	13.30	13.30	13.30	13.30	0	0	0	0	0	0
	STANDARD DEVIATION, PER CENT										0.56	1.53	0.66	0.02	0.46	0.83
GS 6 3/3½% Ni.Steel (45/50 Tonf) b = 28.8 t = 17.3 $\frac{b}{t}$ = 1.67	0	28.8	0	14.4	14.40	14.40	14.40	14.40	14.40	14.40	0	0	0	0	0	0
	15	27.2	3.6	14.1	14.74	14.48	14.56	14.64	14.71	14.79	4.55	2.71	3.27	3.82	4.35	4.87
	30	25.4	7.3	14.7	15.09	14.58	14.74	14.90	15.04	15.18	2.67	-0.84	0.29	1.35	2.34	3.28
	45	21.5	10.8	15.2	15.75	14.79	15.14	15.43	15.68	15.90	3.62	-2.67	-0.43	1.51	3.18	4.63
	60	15.9	13.8	15.9	16.47	15.15	15.70	16.11	16.42	16.64	3.59	-4.75	-1.26	1.32	3.25	4.67
	75	8.6	16.0	16.6	17.06	15.72	16.43	16.83	17.04	17.16	2.78	-5.33	-1.00	1.37	2.66	3.37
	90	0	17.3	17.3	17.30	17.30	17.30	17.30	17.30	17.30	0	0	0	0	0	0
	STANDARD DEVIATION, PER CENT										1.38	0.87	0.07	0.75	1.26	1.67

TABLE 14 CONTINUED

SERIES AND MATERIAL	θ	f	q	S	S_G	$S_{0.5}$	$S_{1.0}$	$S_{1.5}$	$S_{2.0}$	$S_{2.5}$	$P.D._G$	$P.D._{0.5}$	$P.D._{1.0}$	$P.D._{1.5}$	$P.D._{2.0}$	$P.D._{2.5}$
GS 7	0	27.8	0	13.9	13.90	13.90	13.90	13.90	13.90	13.90	0	0	0	0	0	0
Cr.Va. Steel	15	26.6	3.6	13.7	14.16	13.96	14.02	14.08	14.14	14.19	3.34	1.91	2.34	2.77	3.19	3.06
(45/50 Tonf)	30	24.6	7.1	14.2	14.55	14.07	14.22	14.37	14.51	14.64	2.49	-0.94	0.16	1.19	2.17	3.08
b = 27.8	45	21.4	10.7	15.2	15.10	14.24	14.55	14.81	15.04	15.24	-0.63	-6.29	-4.31	-2.57	-1.05	0.29
t = 16.7	60	15.9	13.8	15.9	15.84	14.58	15.10	15.49	15.78	16.01	-0.39	-8.29	-5.04	-2.59	-0.73	0.68
$\frac{b}{t}$ = 1.67	75	8.6	15.9	16.5	16.45	15.14	15.83	16.22	16.43	16.55	-0.29	-8.23	-4.04	-1.71	-0.41	0.31
	90	0	16.7	16.7	16.70	16.70	16.70	16.70	16.70	16.70	0	0	0	0	0	0
	STANDARD DEVIATION, PER CENT										0.36	1.75	0.87	0.23	0.25	0.64
GS 8	0	35.0	0	17.5	17.50	17.50	17.50	17.50	17.50	17.50	0	0	0	0	0	0
3½% Ni.Cr.Steel	15	35.0	4.7	18.1	17.50	17.50	17.50	17.50	17.50	17.50	-3.32	-3.32	-3.32	-3.32	-3.32	-3.32
(Normal Impact)	30	31.8	9.2	18.4	18.53	17.75	17.99	18.21	18.43	18.63	0.73	-3.54	-2.26	-1.03	0.14	1.25
b = 35.0	45	26.5	13.3	18.8	19.94	18.19	18.79	19.31	19.76	20.16	6.04	-3.25	-0.07	2.70	5.12	7.21
t = 22.8	60	21.3	18.4	21.3	20.99	18.67	19.58	20.28	20.84	21.27	-1.44	-12.37	-8.10	-4.77	-2.17	-0.15
$\frac{b}{t}$ = 1.54	75	11.6	21.6	22.4	22.28	19.75	21.04	21.79	22.22	22.47	-0.54	-11.84	-6.06	-2.73	-0.81	0.29
	90	0	22.8	22.8	22.80	22.80	22.80	22.80	22.80	22.80	0	0	0	0	0	0
	STANDARD DEVIATION, PER CENT										0.12	2.75	1.58	0.73	0.08	0.42

TABLE 14 CONTINUED

SERIES AND MATERIAL	θ	f	q	S	S_G	$S_{0.5}$	$S_{1.0}$	$S_{1.5}$	$S_{2.0}$	$S_{2.5}$	$P.D._G$	$P.D._{0.5}$	$P.D._{1.0}$	$P.D._{1.5}$	$P.D._{2.0}$	$P.D._{2.5}$
GS 9	0	33.0	0	16.5	16.50	16.50	16.50	16.50	16.50	16.50	0	0	0	0	0	0
3½% Ni.Cr.Steel	15	33.4	4.5	17.3	16.38	16.47	16.45	16.42	16.39	16.36	-5.35	-4.78	-4.94	-5.10	-5.26	-5.42
(Low Impact)	30	30.5	8.8	17.6	17.23	16.67	16.84	17.00	17.16	17.30	-2.11	-5.26	-4.31	-3.40	-2.52	-1.68
b = 33.0	45	25.8	12.9	18.3	18.38	17.02	17.48	17.89	18.25	18.57	0.44	-6.99	-4.47	-2.25	-0.28	1.46
t = 21.0	60	20.4	17.7	20.4	19.40	17.46	18.22	18.81	19.28	19.65	-4.88	-14.40	-10.70	-7.78	-5.49	-3.68
$\frac{b}{t}$ = 1.57	75	10.9	20.2	21.0	20.56	18.42	19.51	20.15	20.51	20.72	-2.11	-12.32	-7.08	-4.07	-2.34	-1.34
	90	0	21.0	21.0	21.00	21.00	21.00	21.00	21.00	21.00	0	0	0	0	0	0
	STANDARD DEVIATION, PER CENT										1.12	3.50	2.52	1.81	1.27	0.85
GS 10	0	42.8	0	21.4	21.40	21.40	21.40	21.40	21.40	21.40	0	0	0	0	0	0
Ni.Cr.Mo.Steel	15	40.5	5.4	21.0	21.49	21.42	21.44	21.46	21.48	21.50	2.31	2.01	2.11	2.21	2.30	2.40
(75/80 Tonf)	30	35.4	10.2	20.4	21.66	21.47	21.54	21.60	21.65	21.70	6.16	5.26	5.58	5.87	6.14	6.38
b = 42.8	45	32.8	16.4	23.2	21.73	21.50	21.59	21.66	21.73	21.79	-6.32	-7.33	-6.95	-6.62	-6.34	-6.08
t = 22.2	60	23.0	19.9	23.0	21.97	21.61	21.77	21.89	21.97	22.03	-4.47	-6.03	-5.35	-4.85	-4.48	-4.22
$\frac{b}{t}$ = 1.93	75	11.9	22.2	23.0	22.14	21.78	21.98	22.08	22.14	22.17	-3.74	-5.31	-4.45	-3.99	-3.75	-3.62
	90	0	22.2	22.2	22.20	22.20	22.20	22.20	22.20	22.20	0	0	0	0	0	0
	STANDARD DEVIATION, PER CENT										0.49	0.91	0.72	0.59	0.49	0.41

TABLE 14 CONTINUED

SERIES AND MATERIAL	θ	f	q	S	S_G	$S_{0.5}$	$S_{1.0}$	$S_{1.5}$	$S_{2.0}$	$S_{2.5}$	$P.D._G$	$P.D._{0.5}$	$P.D._{1.0}$	$P.D._{1.5}$	$P.D._{2.0}$	$P.D._{2.5}$
GS 11	0	50.0	0	25.0	25.00	25.00	25.00	25.00	25.00	25.00	0	0	0	0	0	0
Ni.Cr.Steel	15	51.2	6.9	26.5	24.77	24.95	24.90	24.84	24.79	24.74	-6.52	-5.85	-6.05	-6.25	-6.45	-6.65
(95/105 Tonf)	30	47.6	13.7	27.5	25.43	25.10	25.21	25.31	25.40	25.50	-7.51	-8.71	-8.34	-7.98	-7.63	-7.28
b = 50.0	45	39.4	19.6	27.8	26.71	25.48	25.91	26.29	26.63	26.93	-3.92	-8.34	-6.79	-5.42	-4.21	-3.13
t = 29.3	60	27.8	24.1	27.8	28.04	26.09	26.91	27.52	27.97	28.31	0.87	-6.14	-3.20	-1.02	0.61	1.83
$\frac{b}{t}$ = 1.71	75	14.6	27.1	28.1	28.96	26.98	28.04	28.62	28.93	29.10	3.05	-4.00	-0.20	1.86	2.97	3.57
	90	0	29.3	29.3	29.30	29.30	29.30	29.30	29.30	29.30	0	0	0	0	0	0
	STANDARD DEVIATION, PER CENT										1.12	2.64	1.97	1.51	1.18	0.93
GH 1	0	17.5	0	8.75	8.75	8.75	8.75	8.75	8.75	8.75	0	0	0	0	0	0
0.1% C. Steel	15	16.8	2.2	8.7	8.78	8.76	8.76	8.77	8.78	8.78	0.90	0.66	0.74	0.81	0.89	0.97
(Normalised)	30	15.7	4.5	9.1	8.82	8.77	8.79	8.80	8.82	8.83	-3.08	-3.64	-3.45	-3.27	-3.10	-2.93
b = 17.5	45	13.2	6.6	9.3	8.90	8.80	8.84	8.87	8.90	8.93	-4.27	-5.42	-4.99	-4.62	-4.29	-4.01
t = 9.1	60	9.1	7.9	9.1	9.01	8.85	8.92	8.97	9.01	9.03	-1.03	-2.77	-2.00	-1.44	-1.04	-0.75
$\frac{b}{t}$ = 1.93	75	4.7	8.8	9.1	9.08	8.92	9.01	9.05	9.08	9.09	-0.27	-1.99	-1.03	-0.54	-0.28	-0.14
	90	0	9.1	9.1	9.10	9.10	9.10	9.10	9.10	9.10	0	0	0	0	0	0
	STANDARD DEVIATION, PER CENT										0.62	1.05	0.86	0.72	0.63	0.55

TABLE 14 CONTINUED

SERIES AND MATERIAL	θ	f	q	S	S_G	$S_{0.5}$	$S_{1.0}$	$S_{1.5}$	$S_{2.0}$	$S_{2.5}$	$P.D._G$	$P.D._{0.5}$	$P.D._{1.0}$	$P.D._{1.5}$	$P.D._{2.0}$	$P.D._{2.5}$
GH 2	0	33.6	0	16.8	16.80	16.80	16.80	16.80	16.80	16.80	0	0	0	0	0	0
3½% Ni.Cr. Steel	15	32.4	4.3	16.8	17.09	16.87	16.93	17.00	17.06	17.12	1.70	0.40	0.79	1.17	1.55	1.91
	30	29.5	8.5	17.0	17.72	17.03	17.25	17.46	17.65	17.83	4.21	0.20	1.48	2.68	3.81	4.87
(Normal Impact)	45	26.5	13.2	18.7	19.21	17.61	18.24	18.74	19.12	19.42	2.71	-5.83	-2.45	0.20	2.26	3.87
b = 33.6	60	19.3	16.7	19.3	19.36	17.70	18.38	18.89	19.28	19.58	0.30	-8.31	-4.79	-2.13	-0.11	1.42
t = 20.5	75	10.6	19.9	20.6	20.16	18.42	19.33	19.84	20.13	20.29	-2.13	-10.57	-6.15	-3.67	-2.27	-1.49
$\frac{b}{t}$ = 1.64	90	0	20.5	20.5	20.50	20.50	20.50	20.50	20.50	20.50	0	0	0	0	0	0
	STANDARD DEVIATION, PER CENT										0.54	1.93	0.89	0.14	0.42	0.85

TABLE 14 CONTINUED

SERIES AND MATERIAL	θ	f	q	S	S_G	$S_{0.5}$	$S_{1.0}$	$S_{1.5}$	$S_{2.0}$	$S_{2.5}$	$P.D._G$	$P.D._{0.5}$	$P.D._{1.0}$	$P.D._{1.5}$	$P.D._{2.0}$	$P.D._{2.5}$
GS CI 1	0	15.6	0	7.8	7.80	7.80	7.80	7.80	7.80	7.80	0	0	0	0	0	0
'Silal'	15	15.3	2.0	7.9	8.14	7.86	7.92	7.98	8.04	8.10	3.00	-0.48	0.29	1.06	1.82	2.57
Cast Iron	30	13.6	3.9	7.8	9.73	8.22	8.62	8.99	9.34	9.66	24.71	5.44	10.52	15.26	19.69	23.83
b = 15.6	45	12.6	6.3	8.9	10.48	8.45	9.03	9.55	10.03	10.45	17.73	-5.08	1.47	7.35	12.64	17.39
t = 14.2	60	9.9	8.6	9.9	12.04	9.10	10.14	10.96	11.62	12.15	21.61	-8.07	2.41	10.75	17.40	22.69
$\frac{b}{t}$ = 1.10	75	5.8	10.8	11.2	13.50	10.30	11.82	12.75	13.32	13.66	20.51	-8.06	5.54	13.83	18.89	21.97
	90	0	14.2	14.2	14.20	14.20	14.20	14.20	14.20	14.20	0	0	0	0	0	0
	STANDARD DEVIATION, PER CENT										7.00	1.30	1.62	3.86	5.64	7.08
GS CI 2	0	16.4	0	8.2	8.20	8.20	8.20	8.20	8.20	8.20	0	0	0	0	0	0
'Nicrosilal'	15	15.8	2.1	8.2	8.71	8.30	8.40	8.50	8.60	8.69	6.24	1.24	2.45	3.65	4.82	5.97
Cast Iron	30	14.9	4.3	8.6	9.40	8.46	8.70	8.94	9.16	9.37	9.24	-1.66	1.20	3.92	6.51	8.99
b = 16.4	45	12.4	6.2	8.8	10.90	8.92	9.54	10.08	10.56	10.97	23.87	1.34	8.43	14.59	19.95	24.61
t = 13.7	60	11.0	9.5	11.0	11.55	9.20	10.01	10.68	11.23	11.67	5.04	-16.40	-8.99	-2.92	2.05	6.12
$\frac{b}{t}$ = 1.20	75	5.9	11.1	11.5	13.12	10.40	11.72	12.51	12.99	13.27	14.08	-9.56	1.93	8.81	12.94	15.42
	90	0	13.7	13.7	13.70	13.70	13.70	13.70	13.70	13.70	0	0	0	0	0	0
	STANDARD DEVIATION, PER CENT										4.68	2.00	0.40	2.24	3.70	4.89

TABLE 14 CONTINUED

SERIES AND MATERIAL	θ	f	q	S	S_G	$S_{0.5}$	$S_{1.0}$	$S_{1.5}$	$S_{2.0}$	$S_{2.5}$	$P.D._G$	$P.D._{0.5}$	$P.D._{1.0}$	$P.D._{1.5}$	$P.D._{2.0}$	$P.D._{2.5}$
GN 1	0	11.6	0	5.8	5.80	5.80	5.80	5.80	5.80	5.80	0	0	0	0	0	0
0.4%	15	11.6	1.6	6.0	5.80	5.80	5.80	5.80	5.80	5.80	-3.33	-3.33	-3.33	-3.33	-3.33	-3.33
C. Steel	30	10.7	3.1	6.2	6.93	6.02	6.23	6.44	6.64	6.82	11.75	-2.88	0.56	3.85	7.02	10.06
(Normalised)	45	9.5	4.7	6.7	8.08	6.33	6.81	7.25	7.64	8.00	20.66	-5.49	1.70	8.20	14.09	19.42
b = 11.6	60	7.7	6.7	7.7	9.36	6.84	7.68	8.37	8.93	9.39	21.50	-11.20	-0.22	8.72	16.01	21.94
t = 11.4	75	4.7	8.8	9.1	10.68	7.84	9.13	9.96	10.48	10.82	17.41	-13.90	0.34	9.40	15.17	18.84
$\frac{b}{t}$ = 1.02	90	0	11.4	11.4	11.40	11.40	11.40	11.40	11.40	11.40	0	0	0	0	0	0
	STANDARD DEVIATION, PER CENT										5.44	2.94	0.08	2.15	3.92	5.36
GN 2	0	13.6	0	6.8	6.80	6.80	6.80	6.80	6.80	6.80	0	0	0	0	0	0
3% Ni.Steel	15	13.5	1.8	7.0	6.85	6.81	6.82	6.83	6.84	6.86	-2.09	-2.70	-2.54	-2.39	-2.23	-2.07
(30/35 Tonf)	30	12.6	3.7	7.3	7.30	6.91	7.02	7.13	7.23	7.32	0.00	-5.31	-3.83	-2.40	-1.03	0.29
	45	10.9	5.4	7.7	8.00	7.11	7.40	7.65	7.87	8.08	3.94	-7.61	-3.95	-0.68	2.25	4.87
b = 13.6	60	8.0	6.9	8.0	8.88	7.50	8.04	8.45	8.76	9.00	10.97	-6.26	0.44	5.58	9.52	12.55
t = 9.8	75	4.6	8.5	8.8	9.51	8.06	8.79	9.21	9.46	9.60	8.01	-8.47	-0.17	4.66	7.46	9.10
$\frac{b}{t}$ = 1.39	90	0	9.8	9.8	9.80	9.80	9.80	9.80	9.80	9.80	0	0	0	0	0	0
	STANDARD DEVIATION, PER CENT										1.67	2.43	0.80	0.40	1.28	1.98

TABLE 14 CONTINUED

SERIES AND MATERIAL	θ	f	q	S	S_G	$S_{0.5}$	$S_{1.0}$	$S_{1.5}$	$S_{2.0}$	$S_{2.5}$	$P.D._G$	$P.D._{0.5}$	$P.D._{1.0}$	$P.D._{1.5}$	$P.D._{2.0}$	$P.D._{2.5}$
GN 3	0	19.6	0	9.8	9.80	9.80	9.80	9.80	9.80	9.80	0	0	0	0	0	0
3/3½% Ni.Steel	15	18.5	2.5	9.6	10.05	9.86	9.92	9.97	10.03	10.08	4.69	2.71	3.31	3.90	4.47	5.03
(45/50 Tonf)	30	17.1	5.0	9.9	10.34	9.94	10.07	10.19	10.30	10.41	4.45	0.39	1.70	2.92	4.06	5.12
b = 19.6	45	13.8	6.9	9.8	10.91	10.14	10.42	10.66	10.86	11.03	1.32	3.45	6.34	8.77	10.81	12.52
t = 11.9	60	11.2	9.7	11.2	11.26	10.31	10.70	10.99	11.21	11.38	0.51	-7.92	-4.46	-1.85	0.13	1.62
$\frac{b}{t}$ = 1.65	75	6.0	11.1	11.5	11.72	10.74	11.26	11.54	11.70	11.79	1.91	-6.63	-2.11	0.39	1.77	2.53
	90	0	11.9	11.9	11.90	11.90	11.90	11.90	11.90	11.90	0	0	0	0	0	0
	STANDARD DEVIATION, PER CENT										1.83	0.64	0.38	1.13	1.70	2.15
GN 4	0	14.0	0	7.0	7.00	7.00	7.00	7.00	7.00	7.00	0	0	0	0	0	0
Cr.Va.Steel	15	13.5	1.8	7.0	7.29	7.06	7.12	7.18	7.24	7.30	4.15	0.88	1.74	2.58	3.41	4.22
(45/50 Tonf)	30	13.5	3.9	7.8	7.29	7.06	7.12	7.18	7.24	7.30	-6.53	-9.47	-8.70	-7.94	-7.20	-6.47
b = 14.0	45	11.1	5.6	7.9	8.42	7.37	7.70	8.00	8.26	8.50	6.64	-6.68	-2.48	1.26	4.59	7.56
t = 10.4	60	8.9	7.7	8.9	9.18	7.69	8.24	8.68	9.03	9.30	3.13	-13.61	-7.43	-2.51	1.42	4.54
$\frac{b}{t}$ = 1.35	75	5.1	9.5	9.8	10.02	8.35	9.16	9.65	9.95	10.13	2.20	-14.82	-6.52	-1.51	1.52	3.34
	90	0	10.4	10.4	10.40	10.40	10.40	10.40	10.40	10.40	0	0	0	0	0	0
	STANDARD DEVIATION, PER CENT										0.77	3.50	1.87	0.65	0.30	1.06

TABLE 14 CONTINUED

SERIES AND MATERIAL	θ	f	q	S	S_G	$S_{0.5}$	$S_{1.0}$	$S_{1.5}$	$S_{2.0}$	$S_{2.5}$	$P.D._G$	$P.D._{0.5}$	$P.D._{1.0}$	$P.D._{1.5}$	$P.D._{2.0}$	$P.D._{2.5}$
GN 5	0	17.4	0	8.7	8.70	8.70	8.70	8.70	8.70	8.70	0	0	0	0	0	0
3½% Ni.Cr. Steel	15	18.9	2.5	9.8	6.87	8.42	8.13	7.83	7.51	7.18	-29.9	-14.1	-17.0	-20.1	-20.1	-23.3
	30	17.0	4.9	9.8	9.10	8.78	8.85	8.93	9.00	9.07	-7.10	-10.4	-9.68	-8.16	-8.16	-7.42
(Normal Impact)	45	14.7	7.4	10.4	11.00	9.23	9.72	10.18	10.59	10.97	5.78	-11.2	-6.50	1.82	1.82	5.48
b = 17.4	60	10.9	9.4	10.9	13.11	10.08	11.17	12.03	12.71	13.25	20.3	-7.56	2.44	16.6	16.6	21.6
t = 15.3	75	6.7	12.1	12.5	14.56	11.27	12.83	13.79	14.38	14.74	16.5	-9.87	2.68	15.0	15.0	17.9
	90	0	15.3	15.3	15.30	15.30	15.30	15.30	15.30	15.30	0	0	0	0	0	0
$\frac{b}{t}$ = 1.38	STANDARD DEVIATION, PER CENT										0.45	4.25	2.25	0.84	0.16	0.87
GN 6	0	17.6	0	8.8	8.80	8.80	8.80	8.80	8.80	8.80	0	0	0	0	0	0
Ni.Cr.Mo. Steel (75/80 Tonf)	15	17.2	2.3	8.9	9.21	8.88	8.96	9.03	9.11	9.18	3.53	-0.25	0.61	1.47	2.31	3.14
	30	16.4	4.8	9.5	9.97	9.04	9.26	9.48	9.70	9.90	4.89	-4.89	-2.49	-0.17	2.06	4.22
	45	15.5	7.8	11.0	10.71	9.22	9.61	9.98	10.33	10.65	-2.65	-16.2	-12.6	-9.27	-6.13	-3.17
b = 17.6	60	11.0	9.5	11.0	13.36	10.22	11.35	12.24	12.94	13.50	21.47	7.05	3.18	11.3	17.7	22.7
t = 15.6	75	6.7	12.5	12.9	14.81	11.40	13.01	14.00	14.62	14.99	14.8	-11.6	0.86	8.55	13.3	16.2
$\frac{b}{t}$ = 1.13	90	0	15.6	15.6	15.60	15.60	15.60	15.60	15.60	15.60	0	0	0	0	0	0
	STANDARD DEVIATION, PER CENT										3.36	3.20	0.84	0.95	2.34	3.45

TABLE 14 CONTINUED

SERIES AND MATERIAL	θ	f q S S_G	$S_{3.0}$	$S_{3.5}$	$S_{4.0}$	$S_{4.5}$	$S_{5.0}$	$P.D._G$	$P.D._{3.0}$	$P.D._{3.5}$	$P.D._{4.0}$	$P.D._{4.5}$	$P.D._{5.0}$
GS 1	0		8.70	8.70	8.70	8.70	8.70		0	0	0	0	0
0.1% C.Steel	15		8.77	8.79	8.80	8.81	8.82		-0.29	-0.16	-0.03	0.11	0.24
(Normalised)	30		8.99	9.03	9.07	9.11	9.14		-1.19	-0.74	-0.32	0.08	0.46
b = 17.4	45		9.31	9.37	9.43	9.47	9.51		-0.97	-0.31	0.26	0.76	1.20
t = 9.8	60		9.62	9.67	9.70	9.73	9.75		1.27	1.77	2.13	2.40	2.60
$\frac{b}{t}$ = 1.78	75		9.77	9.79	9.79	9.80	9.80		-1.29	-1.16	-1.09	-1.05	-1.03
	90		9.80	9.80	9.80	9.80	9.80		0	0	0	0	0
	STANDARD DEVIATION, PER CENT								0.20	0.05	0.08	0.18	0.28
GS 3	0		8.90	8.90	8.90	8.90	8.90		0	0	0	0	0
0.4% C.Steel	15		8.90	8.90	8.90	8.90	8.90		-3.26	-3.26	-3.26	-3.26	-3.26
(Spheroidised)	30		9.21	9.26	9.30	9.34	9.37		-0.95	-0.48	-0.03	0.39	0.79
b = 17.8	45		9.58	9.64	9.70	9.75	9.80		-0.25	+0.45	1.07	1.61	2.07
t = 10.1	60		9.89	9.94	9.98	10.01	10.03		-1.13	-0.60	-0.20	0.10	0.33
$\frac{b}{t}$ = 1.76	75		10.07	10.09	10.09	10.10	10.10		2.77	2.90	2.98	3.02	3.04
	90		10.10	10.10	10.10	10.10	10.10		0	0	0	0	0
	STANDARD DEVIATION, PER CENT								0.22	0.08	0.05	0.15	0.24

TABLE 14 CONTINUED

SERIES AND MATERIAL	θ	f q S S_G	$S_{3.0}$	$S_{3.5}$	$S_{4.0}$	$S_{4.5}$	$S_{5.0}$	$P.D._G$	$P.D._{3.0}$	$P.D._{3.5}$	$P.D._{4.0}$	$P.D._{4.5}$	$P.D._{5.0}$
GS 9	0		16.50	16.50	16.50	16.50	16.50		0	0	0	0	0
3½% Ni.Cr. Steel	15		16.33	16.31	16.28	16.25	16.22		-5.58	-5.75	-5.91	-6.07	-6.24
(Low Impact)	30		17.45	17.58	17.72	17.84	17.97		-0.87	-0.09	0.66	1.38	2.08
b = 33.0	45		18.85	19.10	19.32	19.51	19.69		3.00	4.36	5.57	6.63	7.57
t = 21.0	60		19.94	20.16	20.34	20.48	20.59		-2.27	-1.16	-0.28	0.41	0.95
$\frac{b}{t}$ = 1.57	75		20.84	20.91	20.95	20.97	20.98		-0.77	-0.44	-0.26	-0.15	-0.08
	90		21.00	21.00	21.00	21.00	21.00		0	0	0	0	0
	STANDARD DEVIATION, PER CENT								0.52	0.25	0.02	0.18	0.34
GS 10	0		21.40	21.40	21.40	21.40	21.40		0	0	0	0	0
Ni.Cr.Mo.Steel	15		21.52	21.54	21.56	21.58	21.59		2.49	2.57	2.66	2.74	2.82
(75/80 Tonf)	30		21.75	21.79	21.83	21.86	21.89		6.61	6.81	6.99	7.15	7.31
b = 42.8	45		21.84	21.89	21.92	21.96	21.99		-5.86	-5.67	-5.50	-5.35	-5.22
t = 22.2	60		22.08	22.11	22.13	22.15	22.16		-4.02	-3.87	-3.77	-3.69	-3.63
$\frac{b}{t}$ = 1.93	75		22.18	22.19	22.20	22.20	22.20		-3.55	-3.52	-3.50	-3.49	-3.48
	90		22.20	22.20	22.20	22.20	22.20		0	0	0	0	0
	STANDARD DEVIATION, PER CENT								0.35	0.29	0.25	0.21	0.18

TABLE 14 CONTINUED

SERIES AND MATERIAL	θ	f q S S_G	$S_{3.0}$	$S_{3.5}$	$S_{4.0}$	$S_{4.5}$	$S_{5.0}$	$P.D._G$	$P.D._{3.0}$	$P.D._{3.5}$	$P.D._{4.0}$	$P.D._{4.5}$	$P.D._{5.0}$
GS 11	0		25.00	25.00	25.00	25.00	25.00		0	0	0	0	0
Ni.Cr.Steel	15		24.68	24.63	24.57	24.52	24.46		-6.86	-7.07	-7.28	-7.49	-7.70
(95/105 Tonf)	30		25.59	25.68	25.77	25.85	25.94		-6.95	-6.62	-6.30	-5.99	-5.68
b = 50.0	45		27.20	27.43	27.64	27.83	27.99		-2.17	-1.32	-0.57	0.10	0.70
t = 29.3	60		28.56	28.75	28.89	28.99	29.07		2.74	3.41	3.92	4.29	4.57
$\frac{b}{t}$ = 1.71	75		29.19	29.24	29.27	29.28	29.29		3.89	4.07	4.16	4.21	4.24
	90		29.30	29.30	29.30	29.30	29.30		0	0	0	0	0
	STANDARD DEVIATION, PER CENT								0.75	0.60	0.49	0.39	0.31
GH 1	0		8.75	8.75	8.75	8.75	8.75		0	0	0	0	0
0.1% C.Steel	15		8.79	8.80	8.80	8.81	8.82		1.04	1.11	1.18	1.25	1.32
(Normalised)	30		8.85	8.86	8.87	8.89	8.90		-2.78	-2.63	-2.49	-2.36	-2.24
b = 17.5	45		8.95	8.97	8.99	9.00	9.02		-3.77	-3.55	-3.37	-3.21	-3.07
t = 9.1	60		9.05	9.07	9.07	9.08	9.09		-0.54	-0.39	-0.28	-0.20	-0.15
$\frac{b}{t}$ = 1.93	75		9.09	9.10	9.10	9.10	9.10		-0.08	-0.04	-0.02	-0.01	-0.01
	90		9.10	9.10	9.10	9.10	9.10		0	0	0	0	0
	STANDARD DEVIATION, PER CENT								0.44	0.39	0.35	0.32	0.29

TABLE 14a

GOUGH(12) DATA - MEAN STANDARD DEVIATION v. n (EQUATIONS 7.2 & 7.5)

MAT'L (SOLID)	GOUGH	n				
		0.5	0.6	0.7	0.8	0.9
GS 2	0.813	1.686	1.447	1.225	1.017	0.824
GS 4	0.912	2.493	2.178	1.884	1.610	1.354
GS 5	0.564	1.534	1.333	1.145	0.970	0.807
GS 6	1.376	0.870	0.655	0.455	0.268	0.094
GS 7	0.362	1.748	1.548	1.361	1.187	1.024
GS 8	0.118	2.745	2.481	2.235	2.004	1.787
GH 2	0.543	1.930	1.692	1.471	1.264	1.071
Σ	3.688	13.006	11.334	9.776	8.320	6.961
MEAN	0.527	1.858	1.619	1.396	1.188	0.994

MAT'L (SOLID)	GOUGH	n				
		1.0	1.1	1.2	1.3	1.4
GS 2		0.643	0.474	0.315	0.166	0.026
GS 4		1.115	0.890	0.679	0.481	0.294
GS 5		0.655	0.512	0.377	0.251	0.132
GS 6		0.069	0.222	0.366	0.501	0.629
GS 7		0.871	0.728	0.593	0.466	0.346
GS 8		1.584	1.393	1.213	1.043	0.883
GH 2		0.890	0.721	0.562	0.412	0.272
Σ		5.827	4.940	4.105	3.320	2.572
MEAN		0.832	0.706	0.587	0.474	0.367

TABLE 14a CONTINUED

MAT'L (SOLID)	GOUGH	n				
		1.5	1.6	1.7	1.8	1.9
GS 2		0.107	0.232	0.350	0.461	0.568
GS 4		0.118	0.049	0.207	0.356	0.498
GS 5		0.020	0.086	0.187	0.282	0.373
GS 6		0.749	0.863	0.971	1.073	1.170
GS 7		0.232	0.125	0.023	0.073	0.165
GS 8		0.732	0.588	0.452	0.323	0.201
GH 2		0.140	0.015	0.103	0.214	0.319
$\sum$		2.098	1.958	2.293	2.782	3.294
MEAN		0.300	0.280	0.327	0.397	0.471

MAT'L (SOLID)	GOUGH	n				
		2.0	2.1	2.2	2.3	2.4
GS 2		0.668	0.764	0.855	0.942	1.025
GS 4		0.633	0.761	0.884	1.001	1.112
GS 5		0.459	0.541	0.619	0.694	0.766
GS 6		1.262	1.350	1.434	1.515	1.591
GS 7		0.253	0.337	0.416	0.493	0.566
GS 8		0.084	0.027	0.133	0.234	0.331
GH 2		0.419	0.513	0.603	0.689	0.770
$\sum$		3.778	4.293	4.944	5.568	6.161
MEAN		0.539	0.613	0.706	0.795	0.880

TABLE 14a CONTINUED

MAT'L (NOTCHED)	GOUGH	n				
		0.5	0.6	0.7	0.8	0.9
GN 1	5.439	2.944	2.307	1.705	1.134	0.592
GN 2	1.666	2.427	2.058	1.713	1.390	1.087
GN 3	1.831	0.640	0.408	0.190	0.013	0.203
GN 4	0.767	3.496	3.130	2.787	2.463	2.159
GN 5	0.445	4.253	3.791	3.363	2.964	2.593
GN 6	3.363	3.198	2.668	2.169	1.699	1.255
Σ	13.511	16.958	14.362	11.927	9.663	7.889
MEAN	2.252	2.826	2.394	1.988	1.610	1.315

MAT'L (NOTCHED)	GOUGH	n				
		1.0	1.1	1.2	1.3	1.4
GN 1		0.077	0.412	0.878	1.321	1.744
GN 2		0.804	0.538	0.287	0.051	0.171
GN 3		0.382	0.549	0.707	0.856	0.997
GN 4		1.871	1.600	1.343	1.099	0.869
GN 5		2.247	1.925	1.625	1.345	1.084
GN 6		0.836	0.440	0.066	0.290	0.627
Σ		6.417	5.464	4.906	4.962	5.492
MEAN		1.070	0.911	0.817	0.827	0.915

MAT'L (NOTCHED)	GOUGH	n				
		1.5	1.6	1.7	1.8	1.9
GN 1		2.148	2.533	2.902	3.255	3.593
GN 2		0.382	0.580	0.769	0.947	1.117
GN 3		1.130	1.255	1.375	1.488	1.596
GN 4		0.649	0.441	0.243	0.054	0.127
GN 5		0.841	0.613	0.401	0.202	0.017
GN 6		0.947	1.252	1.542	1.819	2.084
Σ		6.097	6.674	7.232	7.765	8.534
MEAN		1.016	1.112	1.205	1.294	1.422

TABLE 14a CONTINUED

MAT'L (NOTCHED)	GOUGH	n				
		2.0	2.1	2.2	2.3	2.4
GN 1		3.917	4.227	4.526	4.813	5.089
GN 2		1.278	1.432	1.578	1.718	1.851
GN 3		1.698	1.796	1.889	1.978	2.063
GN 4		0.299	0.463	0.621	0.772	0.917
GN 5		0.157	0.319	0.470	0.611	0.743
GN 6		2.336	2.578	2.810	3.032	3.245
Σ		9.685	10.815	11.894	12.924	13.908
MEAN		1.614	1.802	1.982	2.154	2.318

TABLE 15

GOUGH(12) DATA - VALUES OF CONSTANTS C_3 AND C_4 IN EQUATION 7.6

TEST SERIES	MATERIAL	C_3 (=t) TONF/IN^2	C_4
GS 1	0.1% C Steel	9.8	0.043
GS 2	0.4% C Steel (N)	13.4	0.075
GS 3	0.4% C Steel (S)	10.1	0.045
GS 4	0.9% C Steel	15.6	0.109
GS 5	3% Ni Steel	13.3	0.060
GS 6	3/3½% Ni Steel	17.3	0.055
GS 7	Cr. Va. Steel	16.7	0.054
GS 8	3½% Ni. Cr. Steel (H.I.)	22.8	0.073
GS 9	3½% Ni. Cr. Steel (L.I.)	21.0	0.067
GS10	Ni. Cr. Mo. Steel	22.2	0.008
GS11	Ni. Cr. Steel	29.3	0.029

TABLE 16

FRITH(88) MATERIAL AND TEST DATA

TEST SERIES	MATERIAL	U.T.S. TONF/IN^2	t TONF/IN^2	b TONF/IN^2	b/t
	SOLID SPECIMENS				
FS 1	Cr.Mo.Steel (Table 5.32A)	61.3	27.55	46.20	1.68
FS 2	" (" 5.32J)	61.8	19.88	32.97	1.66
FS 3	" (" 5.32K)	61.2	23.81	38.19	1.60
FS 4	" (" 5.32L)	61.2	22.72	38.43	1.69
FS 5	" (" 5.32M)	61.8	23.75	40.70	1.71
FS 6	Ni.Cr.Mo.Steel (Table 5.34D)	71.5	21.50	38.20	1.78
FS 7	Cr.Mo.Va.Steel (Table 5.37A)	90.5	25.28	43.26	1.71
FS 8	" (" 5.37D)	88.6	26.72	45.74	1.71
FS 9	" (" 5.37E)	88.6	28.98	47.79	1.65
FS 10	Ni.Cr.Steel (Table 5.38A)	90.0	23.95	43.19	1.80
	HOLLOW SPECIMENS				
FH 1	Cr.Mo.Steel (Table 5.32B)	61.3	26.74	43.33	1.62
FH 2	Cr.Mo.Va.Steel (Table 5.37B)	90.5	25.04	42.75	1.71
FH 3	Ni.Cr.Steel (Table 5.38B)	90.0	22.00	42.31	1.93
	NOTCHED HOLLOW (OIL HOLE) SPECIMENS				
FH OH 1	Cr.Mo.Steel (Table 5.32N)	61.2	10.50	14.47	1.38
FH OH 2	" (" 5.32P)	61.2	19.45	27.43	1.41
FH OH 3	" (" 5.32Q)	61.2	18.68	27.43	1.47
FH OH 4	Ni.Cr.Mo.Va.Steel (Table 5.36E)	80.5	13.70	18.70	1.37
FH OH 5	Cr.Mo.Va.Steel (Table 5.37C)	90.5	15.25	19.48	1.28
FH OH 6	" (" 5.37F)	88.6	14.31	19.29	1.35
FH OH 7	" (" 5.37G)	88.6	22.97	30.53	1.33
FH OH 8	" (" 5.37H)	88.6	22.99	29.03	1.27
FH OH 9	" (" 5.38C)	90.0	14.61	20.24	1.39

TABLE NUMBERS REFER TO DETAILS OF HEAT TREATMENT IN REFERENCE (88)

TABLE 17

FRITH (88) DATA - STANDARD DEVIATION v. n (EQUATIONS 7.2 AND 7.5)

SERIES AND MATERIAL	θ	f	q	S	S_G	$S_{0.5}$	$S_{1.0}$	$S_{1.5}$	$S_{2.0}$	$S_{2.5}$	$P.D._G$	$P.D._{0.5}$	$P.D._{1.0}$	$P.D._{1.5}$	$P.D._{2.0}$	$P.D._{2.}$
FS 1	0	46.2	0	23.10	23.10	23.10	23.10	23.10	23.11	23.10	0	0	0	0	0	0
5.32 A	15	44.26	5.93	22.91	23.50	23.19	23.29	23.38	23.47	23.55	2.57	1.24	1.65	2.04	2.43	2.81
Cr.Mo.Steel	20.6	43.34	8.15	23.15	23.68	23.24	23.38	23.51	23.63	23.76	2.28	0.39	0.97	1.54	2.09	2.62
b = 46.20	30	39.25	11.33	22.66	24.42	23.45	23.77	24.07	24.34	24.59	7.77	3.48	4.90	6.20	7.41	8.52
t = 27.55	45	34.38	17.18	24.31	25.18	23.71	24.24	24.70	25.09	25.42	3.59	-2.46	-0.29	1.58	3.19	4.58
$\frac{b}{t}$ = 1.68	60	25.99	22.50	25.99	26.22	24.21	25.05	25.67	26.14	26.49	0.90	-6.83	-3.63	-1.22	0.58	1.94
	75	14.03	26.18	27.10	27.17	25.10	26.20	26.81	27.14	27.32	0.26	-7.39	-3.63	-1.09	0.15	0.83
	90	0	27.55	27.55	27.55	27.55	27.55	27.55	27.55	27.55	0	0	0	0	0	0
	STANDARD DEVIATION, PER CENT										1.08	0.72	0.020	0.56	0.98	1.32
FS 2	0	32.97	0	16.48	16.48	16.48	16.48	16.48	16.48	16.48	0	0	0	0	0	0
5.32 J	15	31.74	4.25	16.43	16.76	16.55	16.61	16.67	16.73	16.79	1.99	0.72	1.11	1.48	1.85	2.21
Cr.Mo.Steel	20.6	31.01	5.83	16.56	16.91	16.59	16.69	16.78	16.88	16.97	2.12	0.17	0.77	1.35	1.91	2.46
b = 32.97	30	29.8	8.60	17.21	17.16	16.65	16.81	16.96	17.11	17.24	-0.31	-3.24	-2.32	-1.44	-0.60	0.19
t = 19.88	45	25.54	12.76	18.06	17.92	16.89	17.25	17.57	17.84	18.09	-0.78	-6.47	-4.49	-2.74	-1.20	0.15
$\frac{b}{t}$ = 1.66	60	18.45	15.97	18.45	18.88	17.34	17.98	18.46	18.82	19.09	2.35	-6.02	-2.55	0.05	1.99	3.44
	75	9.86	18.39	19.05	19.60	18.02	18.87	19.33	19.58	19.71	2.89	-5.39	-0.97	1.44	2.76	3.49
	90	0	19.88	19.88	19.88	19.88	19.88	19.88	19.88	19.88	0	0	0	0	0	0
	STANDARD DEVIATION, PER CENT										0.51	1.26	0.53	0.01	0.42	0.74

TABLE 17 CONTINUED

SERIES AND MATERIAL	θ	f	q	S	S_G	$S_{0.5}$	$S_{1.0}$	$S_{1.5}$	$S_{2.0}$	$S_{2.5}$	$P.D._G$	$P.D._{0.5}$	$P.D._{1.0}$	$P.D._{1.5}$	$P.D._{2.0}$	$P.D._{2.5}$
FS 3	0	38.19	0	19.10	19.10	19.10	19.10	19.10	19.10	19.10	0	0	0	0	0	0
5.32 K	30	33.89	9.78	19.56	20.19	19.37	19.63	19.87	20.10	20.31	3.22	-0.98	0.34	1.58	2.75	3.85
b = 38.19	45	28.87	14.43	20.41	21.24	19.71	20.25	20.71	21.12	21.47	4.09	-3.43	-0.81	1.48	3.46	5.18
t = 23.81	60	22.30	19.25	22.23	22.32	20.21	21.07	21.72	22.22	22.59	0.42	-9.08	-5.24	-2.32	-0.08	1.63
$\frac{b}{t}$ = 1.60	90	0	23.81	23.81	23.81	23.81	23.81	23.81	23.81	23.81	0	0	0	0	0	0
	STANDARD DEVIATION, PER CENT										1.21	2.12	0.90	0.12	0.96	1.67
FS 4	0	38.43	0	19.21	19.21	19.21	19.21	19.21	19.21	19.21	0	0	0	0	0	0
5.32 L	15	36.29	4.86	18.79	19.63	19.31	19.41	19.50	19.60	19.68	4.44	2.79	3.30	3.80	4.28	4.75
	20.6	35.57	6.68	19.00	19.76	19.35	19.48	19.60	19.72	19.83	3.98	1.83	2.50	3.15	3.78	4.38
b = 38.43	30	33.68	9.72	19.44	20.08	19.44	19.65	19.84	20.03	20.20	3.31	-0.01	1.07	2.08	3.02	3.91
t = 22.72	45	27.80	13.90	19.65	20.96	19.74	20.19	20.56	20.89	21.16	6.66	0.45	2.72	4.65	6.29	7.68
$\frac{b}{t}$ = 1.69	60	20.90	18.10	20.90	21.74	20.14	20.82	21.31	21.68	21.96	4.03	-3.66	-0.41	1.98	3.75	5.05
	75	11.26	20.99	21.75	22.44	20.82	21.69	22.16	22.42	22.56	3.18	-4.26	-0.26	1.90	3.08	3.71
	90	0	22.72	22.72	22.72	22.72	22.72	22.72	22.72	22.72	0	0	0	0	0	0
	STANDARD DEVIATION, PER CENT										1.59	0.18	0.55	1.09	1.50	1.83

TABLE 17 CONTINUED

SERIES AND MATERIAL	θ	f	q	S	S_G	$S_{0.5}$	$S_{1.0}$	$S_{1.5}$	$S_{2.0}$	$S_{2.5}$	$P.D._G$	$P.D._{0.5}$	$P.D._{1.0}$	$P.D._{1.5}$	$P.D._{2.0}$	$P.D._2$
FS 5	0	40.7	0	20.35	20.35	20.35	20.35	20.35	20.35	20.35	0	0	0	0	0	0
5.32 M	15	38.91	5.21	20.14	20.66	20.43	20.50	20.57	20.64	20.71	2.60	1.42	1.79	2.14	2.50	2.84
	20.6	38.33	7.20	20.47	20.76	20.45	20.55	20.64	20.73	20.82	1.43	-0.10	0.38	0.84	1.29	1.73
b = 40.70	30	36.32	10.49	20.97	21.09	20.54	20.72	20.88	21.04	21.19	0.56	-2.06	-1.21	-0.41	0.35	1.06
t = 23.75	45	30.17	15.09	21.33	21.95	20.82	21.23	21.58	21.88	22.14	2.89	-2.38	-0.47	1.17	2.59	3.80
$\frac{b}{t}$ = 1.71	60	23.01	19.91	23.01	22.72	21.19	21.83	22.31	22.66	22.93	-1.27	-7.89	-5.14	-3.07	-1.51	-0.34
	75	12.05	22.49	23.27	23.47	21.90	22.74	23.20	23.45	23.59	0.87	-5.89	-2.26	-0.29	0.78	1.34
	90	0	23.75	23.75	23.75	23.75	23.75	23.75	23.75	23.75	0	0	0	0	0	0
	STANDARD DEVIATION, PER CENT										0.44	1.05	0.43	0.02	0.37	0.65
FS 6	0	38.2	0	19.1	19.10	19.10	19.10	19.10	19.10	19.10	0	0	0	0	0	0
5.34 D	15	36.44	4.88	18.87	19.33	19.16	19.21	19.26	19.32	19.37	2.43	1.52	1.81	2.09	2.36	2.63
	20.6	34.84	6.55	18.61	19.52	19.21	19.31	19.41	19.50	19.59	4.91	3.21	3.77	4.30	4.80	5.29
b = 38.20	30	32.34	9.34	18.67	19.81	19.29	19.47	19.63	19.78	19.92	6.10	3.33	4.28	5.15	5.95	6.68
t = 21.50	45	27.77	13.88	19.63	20.27	19.45	19.76	20.01	20.23	20.42	3.24	-0.90	0.64	1.95	3.07	4.02
$\frac{b}{t}$ = 1.78	60	19.87	17.18	19.87	20.88	19.77	20.25	20.60	20.85	21.03	5.07	-0.51	1.92	3.67	4.94	5.85
	75	10.84	20.23	20.94	21.32	20.22	20.82	21.14	21.31	21.40	1.80	-3.43	-0.58	0.94	1.75	2.18
	90	0	21.5	21.50	21.50	21.50	21.50	21.50	21.50	21.50	0	0	0	0	0	0
	STANDARD DEVIATION, PER CENT										1.46	0.20	0.74	1.12	1.42	1.6

TABLE 17 CONTINUED

SERIES AND MATERIAL	θ	f	q	S	S_G	$S_{0.5}$	$S_{1.0}$	$S_{1.5}$	$S_{2.0}$	$S_{2.5}$	P.D.$_G$	P.D.$_{0.5}$	P.D.$_{1.0}$	P.D.$_{1.5}$	P.D.$_{2.0}$	P.D.$_{2.5}$
ES 7	0	43.26	0	21.63	21.63	21.63	21.63	21.63	21.63	21.63	0	0	0	0	0	0
5.37 A	15	41.79	5.60	21.63	21.89	21.69	21.75	21.81	21.87	21.93	1.22	0.27	0.57	0.85	1.13	1.40
	20.6	40.02	7.52	21.38	22.19	21.77	21.90	22.03	22.16	22.28	3.80	1.82	2.45	3.05	3.63	4.19
b = 43.26	30	38.32	11.06	22.13	22.47	21.85	22.05	22.24	22.42	22.58	1.52	-1.29	-0.38	0.48	1.29	2.05
t = 25.28	45	32.35	16.17	22.87	23.31	22.12	22.55	22.92	23.24	23.52	1.92	-3.26	-1.40	0.22	1.61	2.82
$\frac{b}{t}$ = 1.71	60	24.30	21.03	24.30	24.19	22.54	23.23	23.74	24.13	24.42	-0.46	-7.23	-4.40	-2.29	-0.71	0.48
	75	12.96	24.17	25.04	24.97	23.28	24.19	24.68	24.95	25.10	-0.26	-7.02	-3.41	-1.43	-0.35	0.24
	90	0	25.28	25.28	25.28	25.28	25.28	25.28	25.28	25.28	0	0	0	0	0	0
	STANDARD DEVIATION, PER CENT										0.48	1.04	0.41	0.06	0.41	0.70
FS 8	0	45.74	0	22.87	22.87	22.87	22.87	22.87	22.87	22.87	0	0	0	0	0	0
5.37 D	30	40.59	11.71	22.87	23.74	23.09	23.30	23.50	23.69	23.86	1.37	-1.40	-0.50	0.35	1.15	1.90
b = 45.74	45	36.00	18.00	23.42	24.41	23.30	23.69	24.03	24.34	24.60	-4.14	-8.47	-6.95	-5.61	-4.42	-3.36
t = 26.72	60	26.83	23.26	25.46	25.46	23.77	24.46	24.99	25.40	25.71	-5.10	-11.40	-8.83	-6.86	-5.35	-4.19
$\frac{b}{t}$ = 1.71	90	0	26.72	26.72	26.72	26.72	26.72	26.72	26.72	26.72	0	0	0	0	0	0
	STANDARD DEVIATION, PER CENT										1.24	3.34	2.56	1.90	1.36	0.89

TABLE 17 CONTINUED

SERIES AND MATERIAL	θ	f	q	S	S_G	$S_{0.5}$	$S_{1.0}$	$S_{1.5}$	$S_{2.0}$	$S_{2.5}$	$P.D._G$	$P.D._{0.5}$	$P.D._{1.0}$	$P.D._{1.5}$	$P.D._{2.0}$	$P.D._{2.}$
FS 9	0	47.79	0	23.90	23.90	23.90	23.90	23.90	23.90	23.90	0	0	0	0	0	0
5.37 E	15	47.07	6.30	24.37	24.06	23.93	23.97	24.01	24.05	24.08	-1.26	-1.79	-1.64	-1.48	-1.33	-1.17
	20.6	45.60	8.57	24.36	24.39	24.01	24.13	24.24	24.35	24.46	0.14	-1.43	-0.95	-0.49	-0.04	0.40
b = 47.79	30	43.98	12.70	25.39	24.74	24.10	24.30	24.49	24.67	24.85	-2.56	-5.07	-4.29	-3.54	-2.82	-2.13
t = 28.98	45	37.28	18.64	26.35	26.00	24.49	25.01	25.48	25.89	26.25	-1.31	-7.06	-5.07	-3.52	-1.76	-0.39
$\frac{b}{t}$ = 1.65	60	27.65	23.94	27.65	27.38	25.11	26.04	26.74	27.28	27.69	-0.97	-9.18	-5.83	-3.28	-1.35	0.13
	75	14.89	27.77	28.77	28.53	26.14	27.40	28.10	28.49	28.70	-0.85	-9.14	-4.78	-2.34	-0.99	-0.23
	90	0	28.98	29.98	28.98	28.98	28.98	28.98	28.98	28.98	0	0	0	0	0	0
	STANDARD DEVIATION, PER CENT										0.42	2.09	1.40	0.90	0.51	0.21
FS 10	0	43.19	0	21.60	21.60	21.60	21.60	21.60	21.60	21.60	0	0	0	0	0	0
5.38 A	15	42.10	5.64	21.79	21.72	21.63	21.65	21.68	21.71	21.74	-0.33	-0.76	-0.62	-0.49	-0.36	-0.23
	20.6	39.89	7.49	21.31	21.96	21.69	21.78	21.86	21.94	22.02	3.04	1.77	2.18	2.58	2.96	3.33
b = 43.19	30	38.01	10.97	21.94	22.15	21.74	21.88	22.01	22.13	22.24	0.95	-0.91	-0.29	0.30	0.85	1.36
t = 23.95	45	31.36	15.68	22.17	22.74	21.94	22.24	22.49	22.71	22.89	2.57	-1.02	0.32	1.46	2.43	3.26
$\frac{b}{t}$ = 1.80	60	22.22	19.23	22.22	23.35	22.26	22.74	23.08	23.33	23.50	5.09	0.18	2.33	3.88	4.98	5.77
	75	12.28	22.91	23.72	23.77	22.69	23.28	23.59	23.76	23.85	0.20	-4.32	-1.85	-0.54	0.17	0.54
	90	0	23.95	23.95	23.95	23.95	23.95	23.95	23.95	23.95	0	0	0	0	0	0
	STANDARD DEVIATION, PER CENT										0.72	0.31	0.13	0.45	0.69	0.87

TABLE 17 CONTINUED

SERIES AND MATERIAL	θ	f	q	S	S_G	$S_{0.5}$	$S_{1.0}$	$S_{1.5}$	$S_{2.0}$	$S_{2.5}$	$P.D._G$	$P.D._{0.5}$	$P.D._{1.0}$	$P.D._{1.5}$	$P.D._{2.0}$	$P.D._2$
FH 1	0	43.33	0	21.66	21.66	21.66	21.66	21.66	21.66	21.66	0	0	0	0	0	0
5.32 B	15	39.99	5.36	20.70	22.49	21.87	22.06	22.24	22.42	22.59	8.65	5.63	6.55	7.44	8.30	9.12
	20.6	39.31	7.38	21.00	22.65	21.91	22.14	22.36	22.56	22.76	7.84	4.32	5.41	6.45	7.44	8.39
b = 43.33	30	37.24	10.74	21.50	23.10	22.04	22.38	22.70	22.99	23.27	7.44	2.49	4.09	5.57	6.94	8.21
t = 26.74	45	31.14	15.57	22.02	24.25	22.44	23.10	23.65	24.12	24.52	10.14	1.90	4.87	7.39	9.53	11.34
$\frac{b}{t}$ = 1.62	60	24.20	20.96	24.20	25.27	22.95	23.91	24.62	25.16	25.56	4.41	-5.18	-1.22	1.74	3.95	5.61
	75	13.45	25.10	25.98	26.29	23.91	25.17	25.86	26.25	26.47	1.21	-7.96	-3.14	-0.45	1.04	1.88
	90	0	26.74	26.74	26.74	26.74	26.74	26.74	26.74	26.74	0	0	0	0	0	0
	STANDARD DEVIATION, PER CENT										2.46	0.07	1.03	1.75	2.31	2.77
FH 2	0	42.75	0	21.37	21.37	21.37	21.37	21.37	21.37	21.37	0	0	0	0	0	0
5.37 B	15	41.20	5.52	21.33	21.66	21.44	21.51	21.57	21.64	21.70	1.53	0.53	0.83	1.14	1.43	1.73
	20.6	39.43	7.41	21.06	21.96	21.52	21.66	21.79	21.92	22.05	4.28	2.19	2.85	3.48	4.09	4.68
b = 42.75	30	37.39	10.79	21.58	22.29	21.61	21.84	22.04	22.24	22.42	3.29	0.15	1.18	2.14	3.04	3.88
t = 25.04	45	32.68	16.34	23.11	22.97	21.84	22.23	22.59	22.90	23.17	-0.61	-5.52	-3.77	-2.25	-0.92	0.25
$\frac{b}{t}$ = 1.71	60	24.12	20.88	24.12	23.93	22.29	22.97	23.49	23.87	24.16	-0.77	-7.60	-4.76	-2.63	-1.02	0.18
	75	12.73	23.76	24.60	24.74	23.04	23.95	24.44	24.72	24.86	0.56	-6.34	-2.65	-0.63	0.47	1.07
	90	0	25.04	25.04	25.04	25.04	25.04	25.04	25.04	25.04	0	0	0	0	0	0
	STANDARD DEVIATION, PER CENT										0.51	1.03	0.39	0.08	0.44	0.73

TABLE 17 CONTINUED

SERIES AND MATERIAL	θ	f	q	S	S_G	$S_{0.5}$	$S_{1.0}$	$S_{1.5}$	$S_{2.0}$	$S_{2.5}$	$P.D._G$	$P.D._{0.5}$	$P.D._{1.0}$	$P.D._{1.5}$	$P.D._{2.0}$	$P.D._{2.5}$
FH 3	0	42.31	0	21.15	21.15	21.15	21.15	21.15	21.15	21.15	0	0	0	0	0	0
5.38 B	15	39.46	5.28	20.43	21.27	21.18	21.21	21.24	21.27	21.29	4.10	3.69	3.83	3.96	4.09	4.21
	20.6	37.53	7.05	20.04	21.34	21.20	21.25	21.29	21.34	21.37	6.48	5.81	6.04	6.26	6.46	6.66
b = 42.31	30	35.14	10.14	20.29	21.42	21.23	21.30	21.36	21.42	21.47	5.57	4.63	4.97	5.28	5.56	5.81
t = 22.00	45	30.53	15.25	21.58	21.56	21.28	21.39	21.48	21.56	21.63	-0.07	-1.38	-0.88	-0.45	-0.09	0.21
$\frac{b}{t}$ = 1.93	60	21.82	18.88	21.82	21.78	21.39	21.56	21.69	21.78	21.84	-0.19	-1.96	-1.17	-0.61	-0.29	0.09
	75	11.30	21.02	21.80	21.94	21.56	21.77	21.88	21.94	21.97	0.65	-1.09	-0.12	0.38	0.64	0.78
	90	0	22.0	22.0	22.00	22.00	22.00	22.00	22.00	22.00	0	0	0	0	0	0
	STANDARD DEVIATION, PER CENT										1.03	0.60	0.79	0.92	1.02	1.10

TABLE 17 CONTINUED

SERIES AND MATERIAL	θ	f	q	S	S_G	$S_{0.5}$	$S_{1.0}$	$S_{1.5}$	$S_{2.0}$	$S_{2.5}$	$P.D._G$	$P.D._{0.5}$	$P.D._{1.0}$	$P.D._{1.5}$	$P.D._{2.0}$	$P.D._{2.5}$
FHOH 1	0	14.47	0	7.23	7.23	7.24	7.24	7.24	7.24	7.24	0	0	0	0	0	0
5.32 N	15	14.24	1.91	7.37	7.36	7.26	7.29	7.31	7.34	7.36	-0.13	-1.48	-1.13	-0.78	-0.44	-0.09
	20.6	14.04	2.64	7.50	7.47	7.28	7.33	7.38	7.43	7.47	-0.46	-2.88	-2.24	-1.61	-0.98	-0.37
b = 14.47	30	13.64	3.94	7.87	7.67	7.33	7.42	7.51	7.60	7.68	-2.57	-6.86	-5.69	-4.55	-3.45	-2.37
t = 10.50	45	11.51	5.75	8.14	8.58	7.59	7.90	8.18	8.43	8.66	5.40	-6.78	-2.91	0.54	3.61	6.36
$\frac{b}{t}$ = 1.38	60	8.82	7.64	8.82	9.42	7.95	8.51	8.95	9.29	9.55	6.80	-9.85	-3.52	1.43	5.29	8.31
	75	4.81	8.98	9.29	10.19	8.62	9.42	9.87	10.14	10.29	9.70	-7.24	1.34	6.29	9.14	10.79
	90	0	10.50	10.50	10.50	10.50	10.50	10.50	10.50	10.50	0	0	0	0	0	0
	STANDARD DEVIATION, PER CENT										1.16	2.18	0.88	0.08	0.82	1.41

TABLE 17 CONTINUED

SERIES AND MATERIAL	θ	f	q	S	S_G	$S_{0.5}$	$S_{1.0}$	$S_{1.5}$	$S_{2.0}$	$S_{2.5}$	$P.D._G$	$P.D._{0.5}$	$P.D._{1.0}$	$P.D._{1.5}$	$P.D._{2.0}$	$P.D._{2.5}$
FHOH 2	0	27.43	0	13.72	13.72	13.72	13.72	13.72	13.72	13.72	0	0	0	0	0	0
5.32 P	15	25.77	3.45	13.34	14.51	13.89	14.06	14.23	14.39	14.54	8.74	4.13	5.41	6.65	7.86	9.02
	20.6	25.23	4.74	13.47	14.74	13.95	14.18	14.39	14.60	14.80	9.46	3.56	5.23	6.84	8.38	9.85
b = 27.43	30	24.01	6.93	13.86	15.25	14.08	14.43	14.75	15.06	15.34	10.03	1.62	4.11	6.45	8.63	10.67
t = 19.45	45	20.78	10.39	14.70	16.41	14.46	15.11	15.67	16.16	16.59	11.60	-1.64	2.76	6.59	9.92	12.83
$\frac{b}{t}$ = 1.41	60	16.03	13.89	16.03	17.70	15.07	16.10	16.89	17.49	17.95	10.43	-6.02	0.43	5.35	9.12	12.00
	75	9.18	17.13	17.73	18.89	16.13	17.53	18.34	18.81	19.08	6.57	-9.01	-1.12	3.44	6.08	7.61
	90	0	19.45	19.45	19.45	19.45	19.45	19.45	19.45	19.45	0	0	0	0	0	0
	STANDARD DEVIATION, PER CENT										3.53	0.46	1.05	2.19	3.10	3.85
FHOH 3	0	27.43	0	13.72	13.72	13.72	13.72	13.72	13.72	13.72	0	0	0	0	0	0
5.32 Q	15	25.29	3.39	13.09	14.57	13.91	14.10	14.29	14.46	14.63	11.29	6.28	7.73	9.13	10.46	11.75
	20.6	24.74	4.65	13.21	14.77	13.97	14.20	14.43	14.64	14.84	11.80	5.71	7.51	9.21	10.83	12.37
b = 27.43	30	22.90	6.61	13.22	15.39	14.14	14.54	14.89	15.22	15.52	16.41	6.99	9.95	12.65	15.13	17.38
t = 18.68	45	19.79	9.89	14.00	16.29	14.46	15.10	15.64	16.10	16.49	16.33	3.31	7.84	11.70	14.97	17.75
$\frac{b}{t}$ = 1.47	60	15.80	13.68	15.80	17.19	14.91	15.82	16.51	17.03	17.43	8.81	-5.62	0.13	4.49	7.80	10.32
	75	9.12	17.01	17.62	18.20	15.82	17.03	17.73	18.13	18.36	3.28	-10.23	-3.35	0.61	2.90	4.22
	90	0	18.68	18.68	18.68	18.68	18.68	18.68	18.68	18.68	0	0	0	0	0	0
	STANDARD DEVIATION, PER CENT										4.22	0.40	1.85	2.97	3.86	4.58

TABLE 17 CONTINUED

SERIES AND MATERIAL	θ	f	q	S	S_G	$S_{0.5}$	$S_{1.0}$	$S_{1.5}$	$S_{2.0}$	$S_{2.5}$	P.D.$_G$	P.D.$_{0.5}$	P.D.$_{1.0}$	P.D.$_{1.5}$	P.D.$_{2.0}$	P.D.$_{2.}$
FH OH 4	0	18.7	0	9.35	9.35	9.35	9.35	9.35	9.35	9.35	0	0	0	0	0	0
5.36 E	30	17.2	4.9	9.9	10.14	9.53	9.70	9.86	10.02	10.17	2.45	-3.76	-2.03	-0.38	1.21	2.73
b = 18.70	53	12.87	8.56	10.7	11.84	10.09	10.71	11.22	11.64	11.99	10.66	-5.69	-0.06	4.83	8.78	12.06
t = 13.70	76	6.21	12.32	12.7	13.29	11.19	12.26	12.87	13.22	13.43	4.65	-11.86	-3.50	1.32	4.10	5.70
$\frac{b}{t}$ = 1.37	90	0	13.7	13.7	13.70	13.70	13.70	13.70	13.70	13.70	0	0	0	0	0	0
	STANDARD DEVIATION, PER CENT										2.79	3.35	0.86	0.91	2.21	3.22
FH OH 5	0	19.48	0	9.74	9.74	9.74	9.74	9.74	9.74	9.74	0	0	0	0	0	0
5.37 C	15	19.29	2.58	9.99	9.88	9.77	9.79	9.82	9.85	9.87	-1.14	-2.23	-1.97	-1.70	-1.43	-1.17
	20.6	18.67	3.51	9.98	10.30	9.86	9.97	10.08	10.19	10.30	3.20	-1.25	-0.11	+1.00	2.09	3.16
b = 19.48	30	18.15	5.24	10.48	10.63	9.93	10.12	10.30	10.47	10.63	1.45	-5.24	-3.47	-1.77	-0.13	1.46
t = 15.25	45	16.26	8.13	11.50	11.69	10.22	10.65	11.05	11.41	11.74	1.64	-11.17	-7.38	-3.93	-0.77	2.11
	60	12.00	10.39	12.00	13.43	10.93	11.86	12.59	13.16	13.61	11.90	-8.96	-1.20	4.88	9.66	13.41
$\frac{b}{t}$ = 1.28	75	7.24	13.51	13.98	14.61	11.89	13.20	14.00	14.49	14.79	4.53	-14.94	-5.56	0.15	3.64	5.77
	90	0	15.25	15.25	15.25	15.25	15.25	15.25	15.25	15.25	0	0	0	0	0	0
	STANDARD DEVIATION, PER CENT										1.34	2.72	1.22	0.08	0.81	1.54

TABLE 17 CONTINUED

SERIES AND MATERIAL	θ	f	q	S	S_{G}	$S_{0.5}$	$S_{1.0}$	$S_{1.5}$	$S_{2.0}$	$S_{2.5}$	P.D.$_{G}$	P.D.$_{0.5}$	P.D.$_{1.0}$	P.D.$_{1.5}$	P.D.$_{2.0}$	P.D.$_{2.5}$
FH OH 6	0	19.29	0	9.64	9.64	9.64	9.64	9.64	9.64	9.64	0	0	0	0	0	0
5.37 F	15	18.62	2.49	9.64	10.03	9.73	9.81	9.89	9.96	10.04	4.07	0.90	1.73	2.55	3.36	4.14
	20.6	17.75	3.34	9.48	10.50	9.84	10.02	10.19	10.36	10.52	10.71	3.75	5.67	7.51	9.28	10.98
b = 19.29	30	16.83	4.86	9.70	10.94	9.95	10.24	10.51	10.76	10.99	12.80	2.60	5.57	8.33	10.92	13.33
t = 14.31	45	15.31	7.65	10.83	11.59	10.15	10.61	11.01	11.37	11.69	7.04	-6.24	-2.05	1.68	5.00	7.96
$\frac{b}{t}$ = 1.35	60	11.32	9.81	11.32	12.89	10.74	11.57	12.21	12.70	13.08	13.92	-5.16	2.23	7.89	12.22	15.54
	75	6.73	12.56	13.01	13.83	11.56	12.68	13.35	13.74	13.98	6.28	-11.19	-2.52	2.60	5.63	7.41
	90	0	14.31	14.31	14.31	14.31	14.31	14.31	14.31	14.31	0	0	0	0	0	0
	STANDARD DEVIATION, PER CENT										3.41	0.95	0.66	1.89	2.88	3.69
FH OH 7	0	30.53	0	15.26	15.26	15.26	15.26	15.26	15.26	15.26	0	0	0	0	0	0
5.37 G	30	26.55	7.67	15.33	15.33	15.79	16.27	16.72	17.14	17.54	13.89	2.97	6.13	9.10	11.83	14.39
	45	24.10	12.04	17.02	17.46	16.13	16.90	17.58	18.18	18.72	9.05	-5.24	-0.73	3.27	6.82	9.97
b = 30.53	60	18.01	15.60	18.01	18.56	17.05	18.43	19.48	20.29	20.91	14.48	-5.32	2.30	8.16	12.65	16.11
t = 22.97	90	0	22.97	22.97	22.97	22.97	22.97	22.97	22.97	22.97	0	0	0	0	0	0
$\frac{b}{t}$ = 1.33	STANDARD DEVIATION, PER CENT										5.88	1.19	1.21	3.22	4.92	6.36

TABLE 17 CONTINUED

SERIES AND MATERIAL	θ	f	q	S	S_G	$S_{0.5}$	$S_{1.0}$	$S_{1.5}$	$S_{2.0}$	$S_{2.5}$	$P.D._G$	$P.D._{0.5}$	$P.D._{1.0}$	$P.D._{1.5}$	$P.D._{2.0}$	$P.D._{2.5}$
FH OH 8	0	29.03	0	14.51	14.51	14.51	14.51	14.51	14.51	14.51	0	0	0	0	0	0
5.37 H	15	27.05	3.62	14.00	15.89	14.81	15.09	15.37	15.63	15.89	13.52	5.78	7.81	9.77	11.66	13.48
	20.6	28.42	5.34	15.19	14.96	14.61	14.69	14.78	14.87	14.95	-1.49	-3.85	-3.27	-2.69	-2.12	-1.56
b = 29.03	30	26.55	7.66	15.33	16.21	14.89	15.24	15.58	15.90	16.21	5.72	-2.90	-0.59	1.61	3.73	5.75
t = 22.99	45	23.47	11.74	16.60	17.91	15.37	16.14	16.83	17.45	18.10	7.89	-7.41	-2.78	1.38	5.12	8.49
$\frac{b}{t}$ = 1.27	60	18.74	16.23	18.74	19.90	16.18	17.52	18.59	19.46	20.15	6.20	-13.66	-6.52	-0.78	3.83	7.54
	75	10.52	19.62	20.32	22.06	17.89	19.92	21.14	21.88	22.32	8.58	-11.97	-1.97	4.04	7.66	9.84
	90	0	22.99	22.99	22.99	22.99	22.99	22.99	22.99	22.99	0	0	0	0	0	0
	STANDARD DEVIATION, PER CENT										2.51	2.11	0.46	0.83	1.86	2.70
FH OH 9	0	20.24	0	10.12	10.12	10.12	10.12	10.12	10.12	10.12	0	0	0	0	0	0
5.38 C	15	19.35	2.60	10.02	10.58	10.22	10.32	10.41	10.51	10.60	5.60	1.99	2.97	3.92	4.85	5.76
	20.6	19.2	3.60	10.25	10.66	10.24	10.35	10.46	10.57	10.68	3.95	-0.13	0.98	2.06	3.12	4.14
b = 20.24	30	17.42	5.03	10.05	11.45	10.45	10.75	11.03	11.28	11.52	13.97	3.93	6.92	9.70	12.28	14.67
t = 14.61	45	15.26	7.63	10.79	12.26	10.71	11.23	11.67	12.06	12.39	13.63	-0.73	4.03	8.16	11.75	14.86
$\frac{b}{t}$ = 1.39	60	12.57	10.87	12.57	13.06	11.07	11.82	12.41	12.88	13.25	3.92	-11.92	-5.96	-1.25	2.45	5.37
	75	7.05	13.14	13.62	14.14	11.96	13.05	13.69	14.07	14.29	3.83	-12.19	-4.21	0.49	3.27	4.91
	90	0	14.61	14.61	14.61	14.61	14.61	14.61	14.61	14.61	0	0	0	0	0	0
	STANDARD DEVIATION, PER CENT										2.79	1.18	0.29	1.43	2.34	3.09

TABLE 18

NISHIHARA AND KAWAMOTO (15) MATERIAL AND TEST DATA

TEST SERIES	MATERIAL	U.T.S. TONF/IN^2	t TONF/IN^2	b TONF/IN^2	b/t
	SOLID SPECIMENS				
NK 1	Mild Steel	24.3	9.85	17.75	1.81
NK 2	Medium Steel	33.6	9.10	15.81	1.74
NK 3	Hard Steel	45.6	13.32	20.35	1.52
NK 4	Ni.Cr.Steel (Hot-Rolled)	46.8	17.15	26.00	1.52
NK 5	Ni.Cr.Steel (Heat Treated)	61.5	20.30	35.60	1.75
NK 6	Cast Iron	14.3	6.98	8.88	1.27
NK 7	Duralumin D 26	29.0	5.07	10.14	2.00
NK 8	Duralumin D 24	24.4	5.71	10.15	1.78
NK 9	Brass	26.8	4.13	8.45	2.04

TABLE 19

NISHIHARA AND KAWAMOTO (15) DATA - STANDARD DEVIATION v. n (EQUATIONS 7.2 AND 7.5)

SERIES AND MATERIAL	θ	f	q	S	S_G	$S_{0.5}$	$S_{1.0}$	$S_{1.5}$	$S_{2.0}$	$S_{2.5}$	P.D.$_G$	P.D.$_{0.5}$	P.D.$_{1.0}$	P.D.$_{1.5}$	P.D.$_{2.0}$	P.D.$_{2.5}$
NK 1	0	0	9.85	9.85	9.85	9.85	9.85	9.85	9.85	9.85	0	0	0	0	0	0
Mild Steel	45	13.0	6.54	9.20	9.34	9.02	9.14	9.24	9.33	9.40	1.52	-2.00	-0.70	0.42	1.38	2.20
b = 17.75	90	17.75	0	8.88	8.88	8.88	8.88	8.88	8.88	8.88	0	0	0	0	0	0
t = 9.85																
$\frac{b}{t}$ = 1.81																
NK 2	0	0	9.10	9.10	9.10	9.10	9.10	9.10	9.10	9.10	0	0	0	0	0	0
Medium Steel	15	4.60	8.60	8.90	9.01	8.46	8.75	8.91	9.00	9.05	1.18	-5.00	-1.66	0.14	1.11	1.63
	30	8.65	7.54	8.65	8.76	8.22	8.46	8.62	8.74	8.84	1.27	-5.02	-2.36	-0.39	1.07	2.14
b = 15.81	45	11.88	5.95	8.40	8.45	8.06	8.20	8.32	8.43	8.52	0.55	-4.00	-2.36	-0.93	0.30	1.37
t = 9.10	60	14.08	3.92	8.05	8.17	7.97	8.04	8.10	8.15	8.21	1.45	-0.97	-0.18	0.57	1.27	1.93
$\frac{b}{t}$ = 1.74	75	15.60	2.05	8.09	7.94	7.91	7.92	7.93	7.94	7.94	-1.87	-2.19	-2.09	-1.99	-1.90	-1.80
	90	15.81	0	7.91	7.91	7.91	7.91	7.91	7.91	7.91	0	0	0	0	0	0
	STANDARD DEVIATION, PER CENT										0.21	1.37	0.69	0.21	0.15	0.42

TABLE 19 CONTINUED

SERIES AND MATERIAL	θ	f	q	S	S_G	$S_{0.5}$	$S_{1.0}$	$S_{1.5}$	$S_{2.0}$	$S_{2.5}$	$P.D._G$	$P.D._{0.5}$	$P.D._{1.0}$	$P.D._{1.5}$	$P.D._{2.0}$	$P.D._{2.5}$
NK 3	0	0	13.32	13.32	13.32	13.32	13.32	13.32	13.32	13.32	0	0	0	0	0	0
Hard Steel	15	6.40	11.90	12.38	13.04	11.56	12.33	12.77	13.10	13.15	5.35	-6.65	-0.40	3.11	5.08	6.18
	30	11.60	10.00	11.60	12.39	10.95	11.53	11.97	12.30	12.55	6.78	-5.64	-0.63	3.16	6.02	8.18
b = 20.35	45	15.70	7.78	11.10	11.55	10.56	10.89	11.19	11.45	11.68	4.07	-4.89	-1.86	0.80	3.14	5.19
t = 13.32	60	18.70	5.40	10.80	10.73	10.31	10.43	10.55	10.66	10.77	-0.69	-4.58	-3.43	-2.32	-1.26	-0.24
$\frac{b}{t}$ = 1.52	75	19.60	2.45	10.15	10.43	10.23	10.29	10.35	10.40	10.46	2.80	0.82	1.39	1.94	2.49	3.02
	90	20.35	0	10.17	10.17	10.17	10.17	10.17	10.17	10.17	0	0	0	0	0	0
	STANDARD DEVIATION, PER CENT										1.47	1.68	0.39	0.54	1.24	1.79
NK 4	0	0	17.15	17.15	17.15	17.15	17.15	17.15	17.15	17.15	0	0	0	0	0	0
Hot Rolled	22.5	12.38	14.90	16.18	16.30	14.29	15.17	15.79	16.21	16.50	0.75	-11.70	-6.22	-2.43	0.18	1.98
Ni.Cr.Steel	45	19.70	9.90	13.98	14.91	13.54	14.01	14.41	14.77	15.08	6.65	-3.16	0.18	3.10	5.63	7.84
b = 26.0	67.5	25.20	5.30	13.65	13.29	13.06	13.13	13.19	13.25	13.31	-2.65	-4.29	-3.83	-3.37	-2.92	-2.48
t = 17.15	90	26.00	0	13.00	13.00	13.00	13.00	13.00	13.00	13.00	0	0	0	0	0	0
$\frac{b}{t}$ = 1.52	STANDARD DEVIATION, PER CENT										0.75	3.01	1.55	0.43	0.46	1.15

TABLE 19 CONTINUED

SERIES AND MATERIAL	θ	f	q	S	S_G	$S_{0.5}$	$S_{1.0}$	$S_{1.5}$	$S_{2.0}$	$S_{2.5}$
NK 5	0	0	20.30	20.3	20.30	20.30	20.30	20.30	20.30	20.30
Heat Treated	22.5	15.55	18.70	20.3	19.85	18.65	19.21	19.58	19.82	19.99
Ni.Cr. Steel	45	26.00	12.92	18.4	19.01	18.16	18.47	18.74	18.97	18.16
b = 35.6	67.5	32.80	6.86	17.78	18.20	17.90	18.00	18.09	18.18	18.26
t = 20.3	90	35.60	0	17.80	17.80	17.80	17.80	17.80	17.80	17.80
$\frac{b}{t}$ = 1.75				STANDARD DEVIATION, PER CENT						
NK 6	0	0	6.98	6.98	6.98	6.98	6.98	6.98	6.98	6.98
Cast Iron	22.5	4.12	4.99	5.40	6.52	5.25	5.80	6.18	6.43	6.61
b = 8.88	45	6.72	3.37	4.75	5.67	4.77	5.06	5.31	5.53	5.72
t = 6.98	67.5	8.45	1.70	4.56	4.74	4.50	4.56	4.62	4.68	4.74
$\frac{b}{t}$ = 1.27	90	8.90	0	4.45	4.45	4.45	4.43	4.43	4.43	4.43
				STANDARD DEVIATION, PER CENT						

θ	P.D.$_G$	P.D.$_{0.5}$	P.D.$_{1.0}$	P.D.$_{1.5}$	P.D.$_{2.0}$	P.D.$_{2.5}$
0	0	0	0	0	0	0
22.5	-2.23	-8.14	-5.38	-3.56	-2.35	-1.55
45	3.30	-1.29	0.40	1.85	3.08	4.13
67.5	2.36	0.68	1.22	1.74	2.24	2.72
90	0	0	0	0	0	0
	0.54	1.38	0.59	0.01	0.47	0.83
	0	0	0	0	0	0
	20.69	-2.78	7.44	14.39	19.13	22.36
	19.29	0.43	6.48	11.75	16.32	20.38
	3.92	-1.27	0.07	1.37	2.63	3.87
	0	0	0	0	0	0
	6.81	0.61	2.14	4.26	5.91	7.23

TABLE 19 CONTINUED

SERIES AND MATERIAL	θ	f	q	S	S_G	$S_{0.5}$	$S_{1.0}$	$S_{1.5}$	$S_{2.0}$	$S_{2.5}$	$P.D._G$	$P.D._{0.5}$	$P.D._{1.0}$	$P.D._{1.5}$	$P.D._{2.0}$	$P.D._{2.5}$
NK 7	0	0	5.07	5.07												
Duralumin	15	2.62	4.90	5.07												
D 26	30	5.08	4.37	5.07												
b = 10.14	45	7.20	3.55	5.07												
t = 5.07	60	8.80	2.50	5.07												
$\frac{b}{t}$ = 2.00	75	9.82	1.19	5.07												
	90	10.14	0	5.07												
NK 8	0	0	5.71	5.71	5.71	5.71	5.71	5.71	5.71	5.71	0	0	0	0	0	0
Duralumin	45	7.60	3.82	5.40	5.36	5.16	5.24	5.30	5.35	5.40	-0.68	-4.44	-3.06	-1.88	-0.85	0.04
D 24	90	10.15	0	5.08	5.08	5.08	5.08	5.08	5.08	5.08	0	0	0	0	0	0
b = 10.15																
t = 5.71																
$\frac{b}{t}$ = 1.78																

TABLE 19 CONTINUED

SERIES AND MATERIAL	θ	f	q	S	S_G	$S_{0.5}$	$S_{1.0}$	$S_{1.5}$	$S_{2.0}$	$S_{2.5}$	$P.D._G$	$P.D._{0.5}$	$P.D._{1.0}$	$P.D._{1.5}$	$P.D._{2.0}$	$P.D._{2.5}$
NK 9	0	0	4.13	4.13												
Brass	22.5	3.18	3.94	4.25												
b = 8.45	45	6.05	3.06	4.29												
t = 4.13	67.5	7.82	1.62	4.22												
$\frac{b}{t}$ = 2.04	90	8.45	0	4.22												

TABLE 19a

NISHIHARA AND KAWAMOTO (15) DATA -

MEAN STANDARD DEVIATION v n (EQUATIONS 7.2 AND 7.5)

MAT'L	GOUGH	n					
		1.0	1.1	1.2	1.3	1.4	1.5
NK 2	0.206	0.691	0.582	0.479	0.383	0.293	0.209
NK 3	1.465	0.394	0.184	0.012	0.197	0.371	0.536
NK 4	0.747	1.550	1.301	1.065	0.841	0.628	0.425
NK 5	0.539	0.590	0.458	0.333	0.215	0.102	0.005
Σ	2.957	3.225	2.525	1.889	1.636	1.394	1.175
MEAN	0.739	0.806	0.631	0.472	0.409	0.348	0.294

MAT'L	GOUGH	n			
		1.6	1.7	1.8	1.9
NK 2		0.129	0.054	0.017	0.084
NK 3		0.691	0.839	0.978	1.111
NK 4		0.232	0.048	0.127	0.295
NK 5		0.106	0.203	0.295	0.382
Σ		1.158	1.134	1.417	1.872
MEAN		0.289	0.283	0.354	0.468

TABLE 20

RANGE OF t/b RATIO FOR STRUCTURAL MATERIALS

Material	Range of Ratio t/b	No. of Results Considered	Average Value t/b
Wrought Steels	0.52 - 0.69	31	0.60
Wrought Aluminium Alloys	0.43 - 0.74	13	0.55
Wrought Copper and Copper Alloys	0.41 - 0.67	7	0.56
Wrought Magnesium Alloys	0.49 - 0.60	2	0.54
Titanium	0.37 - 0.57	3	0.48
Cast Iron	0.79 - 1.01	9	0.90
Cast Aluminium and Magnesium Alloys	0.71 - 0.91	5	0.85

Reproduced from Forrest (84)

TABLE 21

REDUCTION IN FATIGUE STRENGTH FROM THE LONGITUDINAL DIRECTION TO TRANSVERSE DIRECTION

Reproduced from Findley and Mathur (22)

Metal	Reduction Per Cent	Investigator
Ni-Steel	21.3	J. Pomey
Ni-Steel	45.0	"
Cr-Steel	13.1	"
Cr-Steel	16.7	"
Cr-Mo Steel	26.8	"
Ni-Cr Steel	40.0	"
Ni-Cr Steel	15.7	"
Ni-Cr Steel	37.3	Pomey and Ancella
Ni-Cr Steel	1.6	"
Steel	4.5	M. Perrin
Steel	14.5	"
Steel	17.5	"
Ni-Cr-Mo Steel	30.0	Von Rossing
Ni-Cr-Mo Steel	17.0	"
Cr-Mo-Steel	8.0	"
Cr-Mo-Steel	2.5	"
Ni-Cr-Mo Steel	17.7	M. Lioret
Steel	15.0	
Steel	7.0	Schmidt
Steel	11.4	"
Steel	28.5	"
Cr-Ni Steel	13.3	R. Mailander
Cr-Ni Steel	21.0	"
Cr-Ni Steel	22.0	"
Ni Steel	23.8	A. Junger
Duralumin	20.0	Berner and Kostron
SAE 4340 Steel	32.0	Ransom & Mehl
Guntube Steels	16.0	"
SAE 4340 Steel	48.0	Ransom
Steel Forging	30.0	"
14 S-T, 24 S-T Aluminium Alloys	30,35	Marin

TABLE 22

COMPARISON OF CORRELATION OF ROS AND EICHINGER (34)

TEST DATA WITH VARIOUS FAILURE CRITERIA

MATERIAL	σ_D kg/mm²	σ_{-D} kg/mm²	σ_{ULT} kg/mm²	σ_{PROOF} YIELD	$\frac{\sigma_D}{\sigma_U}$	$\frac{\sigma_D}{\sigma_Y}$	$\frac{\sigma_Y}{\sigma_U}$	σ_{-D}/σ_{+D}			
								Test	Equation 8.2	Equation 7.19	Equation 7.21
Rohrstahl (Tube Steel)	23.15	35.4	72.5	53.2	0.32	0.44	0.74	1.52	1.50	1.39	1.40
Stahlguss (Cast Steel)	14.25	21.8	42.2	30.7	0.34	0.47	0.73	1.53	1.50	1.39	1.40
Arcos Ductilend	13.0	25.0	50.2	41.1	0.26	0.32	0.82	1.92	1.30	1.25	1.21
Arcos Stabilend	11.55	24.0	49.0	41.5	0.24	0.28	0.85	2.08	1.30	1.25	1.20
Perumal	8.4	18.5	63.0	52.5	0.13	0.16	0.83	2.20	1.0	0.95	1.00
Reinaluminium	2.3	3.6	7.2	3.0	0.32	0.77	0.42	1.56	1.50	1.39	>2
Avional D	11.5	18.5	50.5	33.1	0.23	0.35	0.66	1.60	1.30	1.25	1.25

TABLE 23

RELATION OF INTERACTION THEORY TO TEST DATA

TABLE 23a

K = 0

		$^{n}/_{N}$		MEAN	$\frac{n}{N}$			MEAN	$\frac{n}{N}$			MEAN	OVER ALL MEAN
		S_1-S_2			S_2-S_3				S_1-S_3				
		10^4-10^4	10^3-10^4	$\frac{n}{N}$	10^4-10^4	10^3-10^4	10^4-10^5	$\frac{n}{N}$	10^4-10^4	10^3-10^4	10^4-10^5	$\frac{n}{N}$	$\frac{n}{N}$
MINER		0.63	1.38	1.08	1.11	0.42	0.60	0.71	0.52	0.56	0.43	0.50	0.76
% INCREASE	0	0.57	0.89	0.73	0.72	0.35	0.55	0.50	0.52	0.58	0.43	0.51	0.58
IN SLOPE OF LOGS-LOGN	24	0.59	1.09	0.84	1.01	0.60	0.81	0.81	0.53	0.73	0.53	0.60	0.75
	41	0.64	1.27	0.96	1.31	0.82	1.14	1.09	0.56	0.92	0.60	0.69	0.91
CURVE	61	0.67	1.40	1.04	1.48	0.95	1.31	1.25	0.57	1.03	0.65	0.75	1.01

TABLE 23b

K = 2

		$\frac{n}{N}$ $S_1 - S_2$		MEAN $\frac{n}{N}$	$\frac{n}{N}$ $S_2 - S_3$			MEAN $\frac{n}{N}$	$\frac{n}{N}$ $S_1 - S_3$				MEAN $\frac{n}{N}$	OVER ALL MEAN $\frac{n}{N}$
		$10^4-3\times10^4$	10^3-10^4		10^4-10^5	10^4-10^4	10^3-10^4		10^4-10^4	10^4-10^5	10^5-10^4	10^3-10^4		
MINER				0.88	0.51	0.79	0.90	0.72	1.44	1.34		0.81	1.46	1.08
% INCREASE IN SLOPE OF LOGS-LOGN CURVE	0	0.90	0.43	0.66	0.50	0.59	0.92	0.67	1.33	1.61	1.55	0.74	1.31	0.95
	12	0.97	0.49	0.73	0.64	0.73	1.18	0.85	1.36	1.37	1.82	0.85	1.35	1.05
	33	1.05	0.56	0.80	0.83	0.90	1.54	1.09	1.41	1.61	2.18	1.00	1.56	1.23

TABLE 23c

K = 7.9

		$\frac{n}{N}$ $S_1 - S_2$		MEAN $\frac{n}{N}$	$\frac{n}{N}$ $S_2 - S_3$			MEAN $\frac{n}{N}$	$\frac{n}{N}$ $S_1 - S_3$			MEAN $\frac{n}{N}$	OVER ALL MEAN $\frac{n}{N}$
		10^4-10^4	10^3-10^4		10^4-10^5	10^4-10^4	10^3-10^4		10^3-10^4	10^4-10^5	10^4-10^4		
MINER		0.91	0.66	0.78	0.14	0.54	0.23	0.30	1.11	0.48	0.99	0.86	0.63
% INCREASE IN SLOPE OF LOGS-LOGN CURVE	0	0.83	0.43	0.63	0.11	0.34	0.19	0.22	1.12	0.48	0.99	0.87	0.56
	25	0.88	0.57	0.73	0.19	0.55	0.13	0.29	1.45	0.59	1.03	1.02	0.67
	51	0.91	0.66	0.76	0.26	0.67	0.48	0.47	1.78	0.69	1.06	1.18	1.81
	81	0.97	0.78	0.87	0.32	0.88	0.64	0.61	2.17	0.82	1.10	1.33	0.84

TABLE 23d

K = -1

		$\frac{n}{N}$			MEAN $\frac{n}{N}$
		$S_2 - S_3$			
		10^4-10^4	10^3-10^4	10^4-10^5	
MINER		0.97	0.47	0.75	0.73
% INCREASE IN SLOPE OF LOGS-LOGN CURVE	0	0.93	0.41	0.66	0.69
	16	1.16	0.58	0.92	0.89
	46	1.54	0.88	1.37	1.26

TABLE 24

THE STRENGTH OF THICK CYLINDERS SUBJECTED TO REPEATED INTERNAL PRESSURE

MORRISON AND OTHERS (48)

Reproduced from Forrest (84)

Material	Tensile Strength tons/in^2	Torsion fatigue strength on solid specimens (shear) tons/in^2	Range of pulsating fatigue strength (10^7 cycles) of thick cylinders (shear) tons/in^2					
			k = 1.2	1.4	1.6	1.8	2.0	3.0
Vibrac Ni Cr Mo steel	56.2	± 19.5	18.5	18.0	18.5	18.0	17.5	19.0
Vibrac autofrettaged	56.2				20.5		23.5	
Vibrac	66.4	± 23.6		23.5		23.5		
Hykro Cr Mo steel	53.8	± 18.6		18.5			19.0	
Hykro nitrided bore					29.0			
0.15% C steel	25.5	± 8.8		8.0			8.5	
18% Cr 8% Ni Ti stainless steel	38.3	± 11.9 to ± 14.2		10.5			16.5	
Aluminium-copper alloy DTD 364	32.6	± 6.2					9.0	
Titanium, commercially pure	26.8	± 10.2		11.0			13.0	

$$k = \frac{\text{Outer Diameter}}{\text{Inner Diameter}}$$

TABLE 25

SHEAR FATIGUE STRENGTH OF THICK CYLINDERS
TEST DATA COMPARED WITH PREDICTIONS OF
EQUATIONS 8.9 AND 8.11

Material	k	Pulsating Shear Fatigue Strength Tonf/in^2			Ratio $\frac{2}{1}$	Ratio $\frac{3}{1}$
		1	2	3		
		Test	Equation 8.9 Prediction	Equation 8.11 Prediction		
MORRISON ET AL (48)						
En 25 Steel - Soft	1.2	18.5	19.2	22.6	1.03	1.22
"	1.4	18.0	19.4	26.0	1.08	1.45
"	1.6	18.5	19.4	28.2	1.04	1.52
"	1.8	18.0	19.5	30.3	1.08	1.68
"	2.0	17.5	19.5	31.6	1.11	1.80
"	3.0	19.0	19.4	35.9	1.02	1.89
En 25 Steel - Hard	1.4	23.5	23.2	31.0	0.99	1.32
"	1.8	23.5	23.5	36.0	1.00	1.53
Hykro Cr Mo Steel	1.4	18.5	18.5	24.5	1.00	1.32
"	2.0	19.0	18.6	30.0	0.97	1.56
0.15% C. Steel	1.4	8.0	8.6	11.9	1.07	1.50
"	2.0	8.5	8.7	13.7	1.02	1.58
18% Cr Stainless Steel	1.4	10.5	13.1	17.4	1.25	1.66
"	2.0	16.5	13.0	20.0	0.78	1.20
DTD 364 Aluminium Alloy	2.0	9.0	7.7	11.3	0.86	1.26
Titanium	1.4	11.0	9.8	13.4	0.89	1.22
"	2.0	13.0	10.1	16.6	0.79	1.30
En 25 Steel - Soft*	1.4	24.0		25.6		1.07
HASLAM (54)						
En 26 Steel*	1.2	21.6		17.4		0.81
En 26 Steel	1.2	16.0	14.7	17.4	0.92	1.09

* Protected Bore

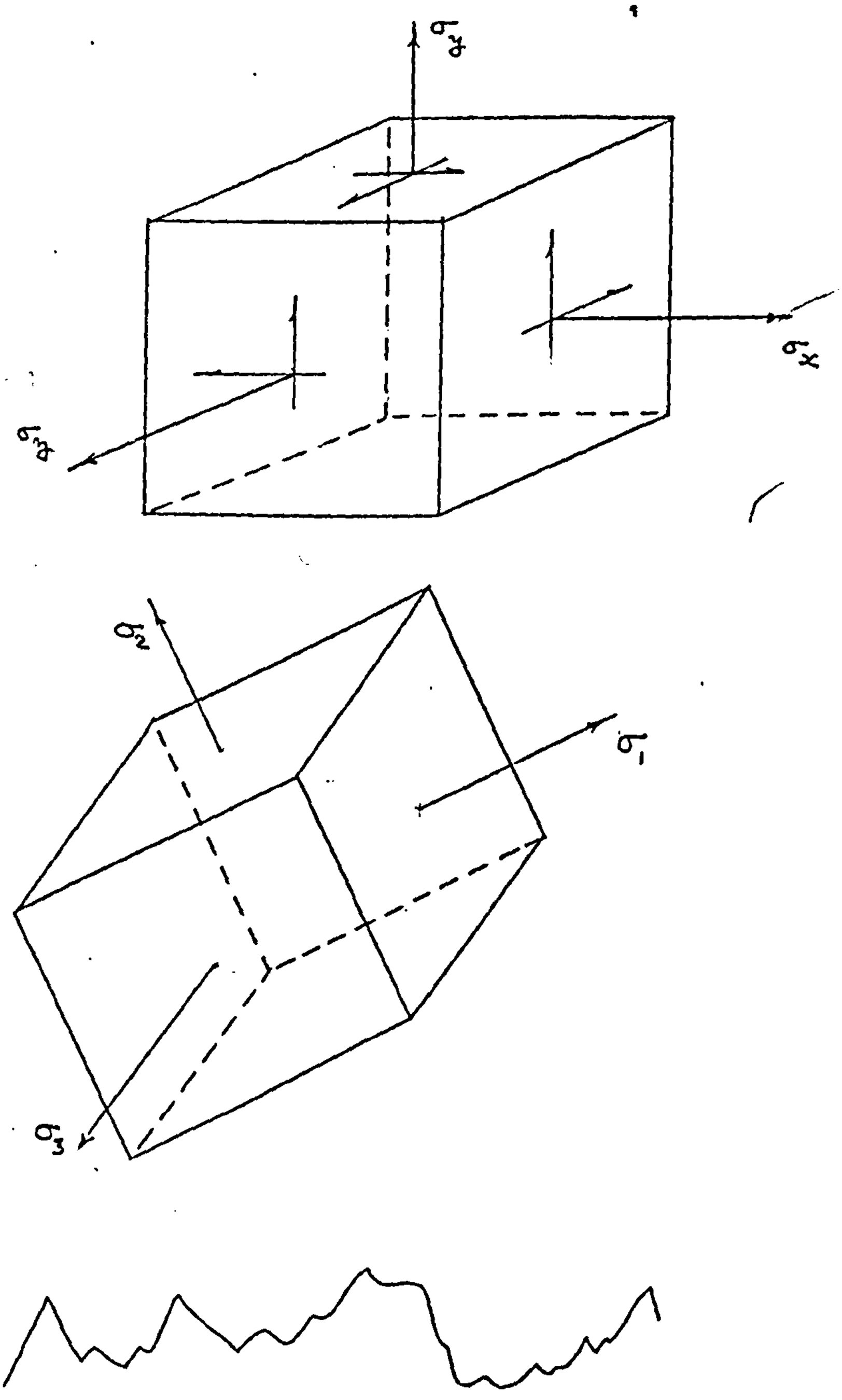

FIGURE 1. THE GENERAL STATE OF FATIGUE STRESS

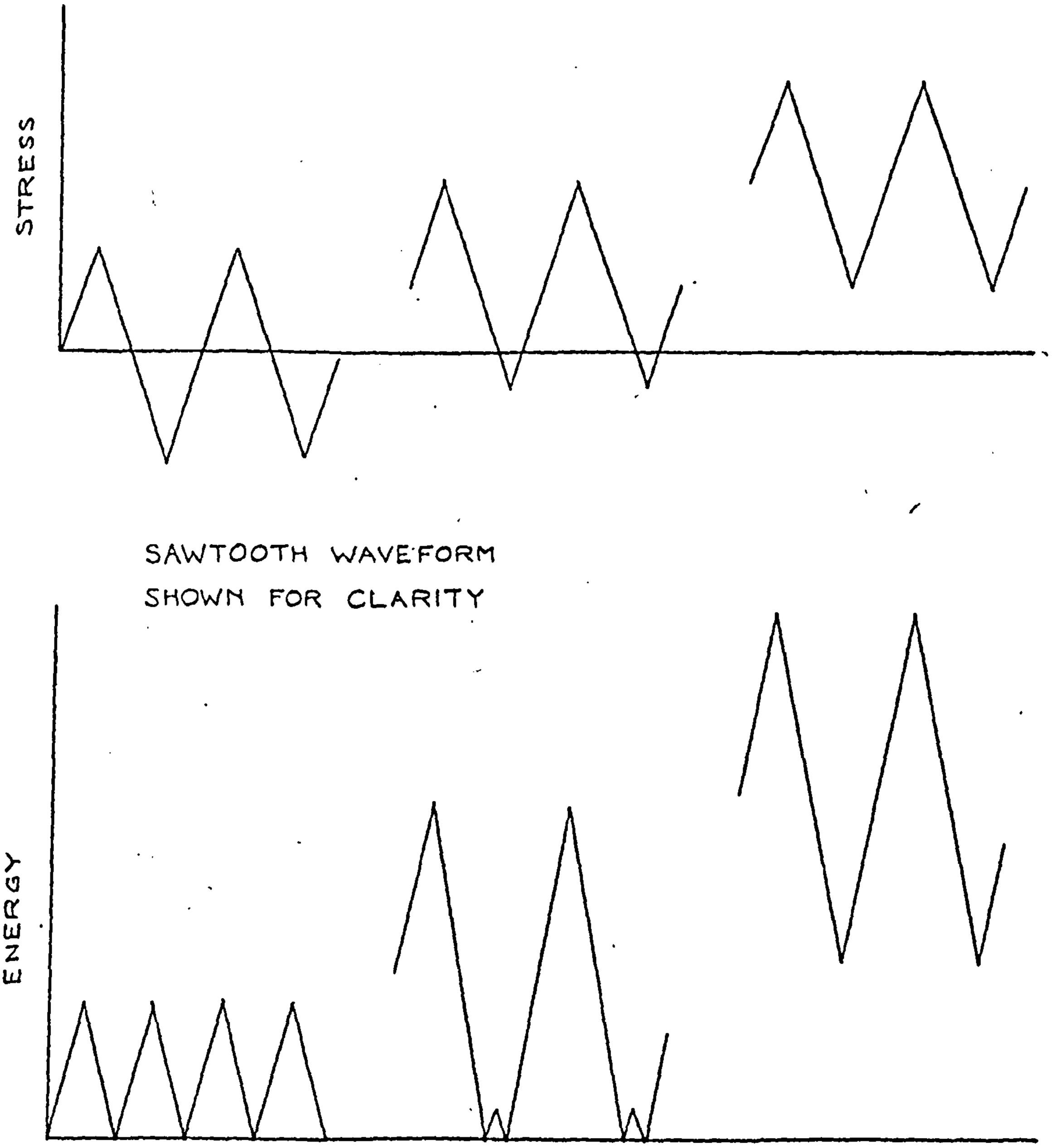

FIGURE 2. THE EFFECT OF MEAN STRESS ON ENERGY.

STRESS COMBINATION STATIC STRESS σ_m ALTERNATING STRESS AMPLITUDE σ_a	STATIC STRESS ON PLANES OF MAX. ALTERNATION OF SHEAR STRESS	PERMISSIBLE ALTERNATING STRESS FOR SAME FATIGUE LIFE $\sigma_a = F(\sigma_m)$
(1) 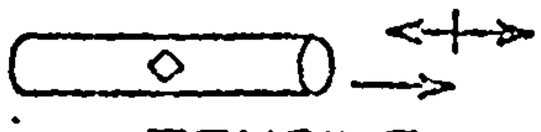 σ_m TENSILE σ_a AXIAL	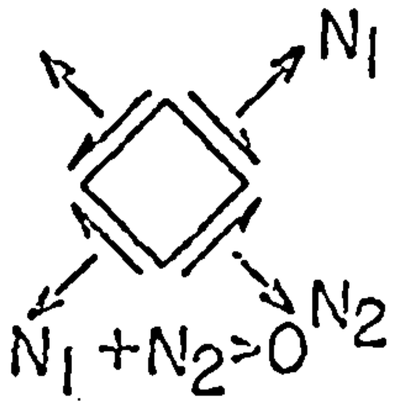	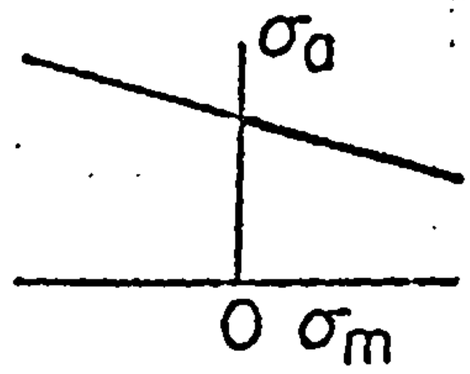
(2)  σ_m COMPRESSIVE σ_a AXIAL	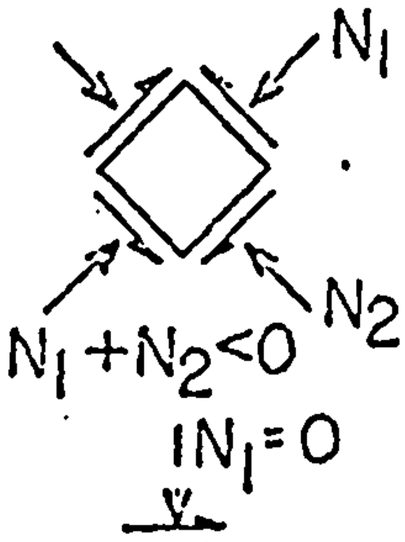	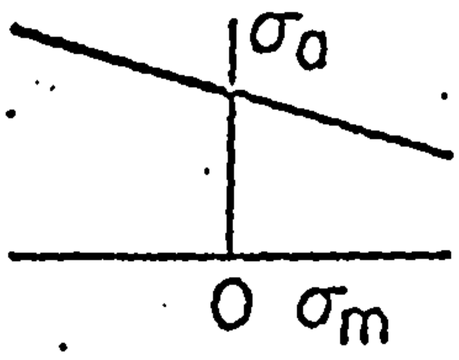
(3) 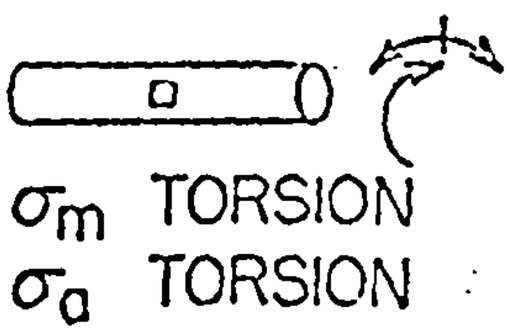 σ_m TORSION σ_a TORSION	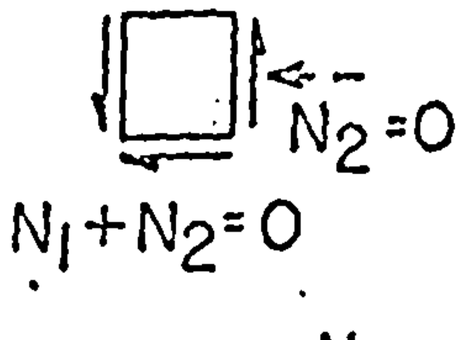	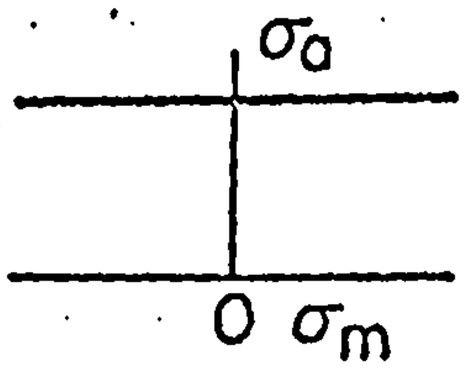
(4) 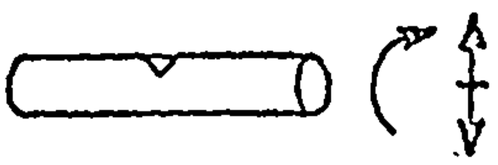 σ_m TORSION σ_a BENDING	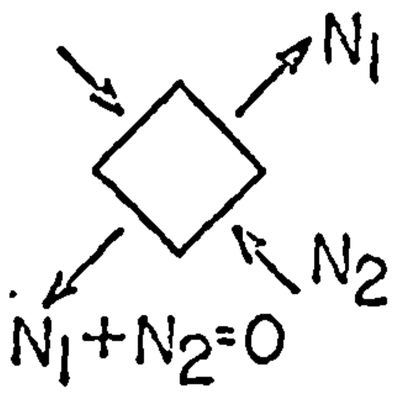	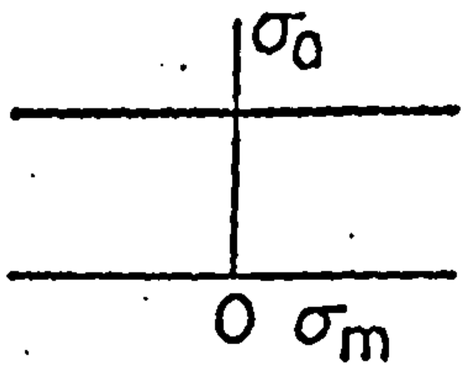
(5) 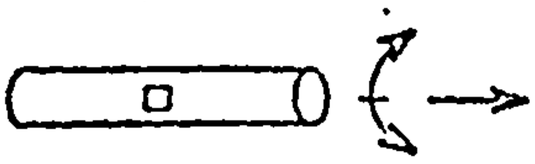 σ_m TENSION σ_a TORSION	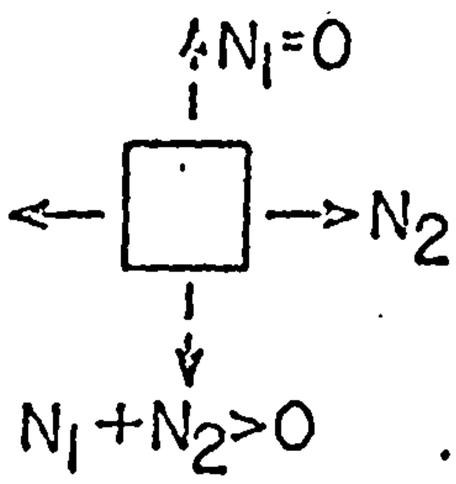	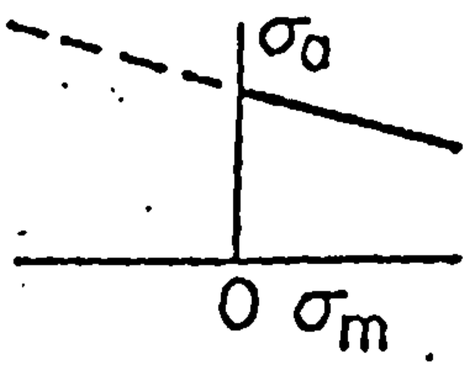

REPRODUCED FROM SINES (6)

FIGURE 3. SUMMARY OF EFFECT OF DIFFERENT COMBINATIONS OF STATIC AND ALTERNATING STRESSES ON FATIGUE LIFE.

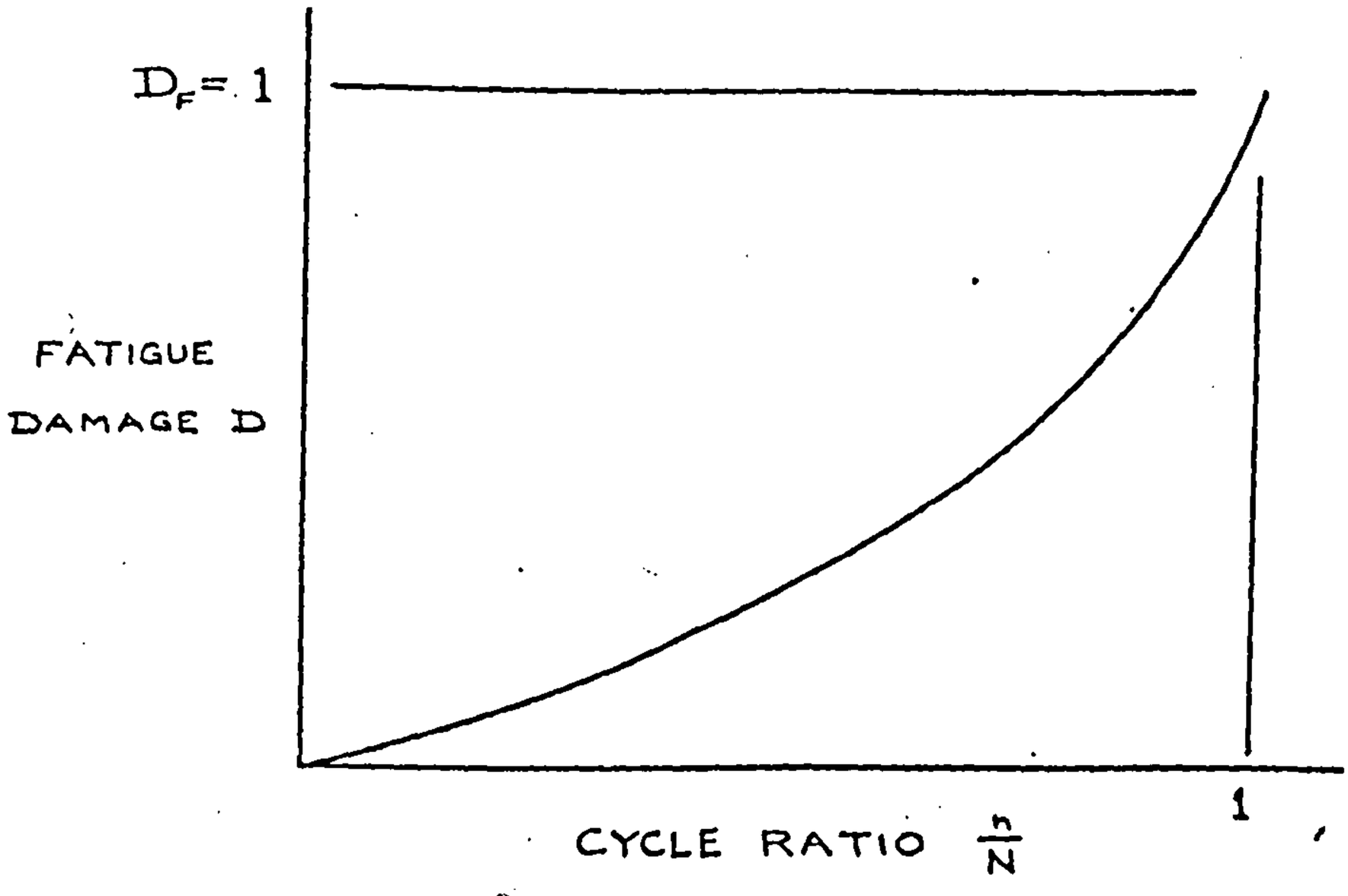

FIGURE 4. STRESS INDEPENDENT DAMAGE REPRESENTATION.

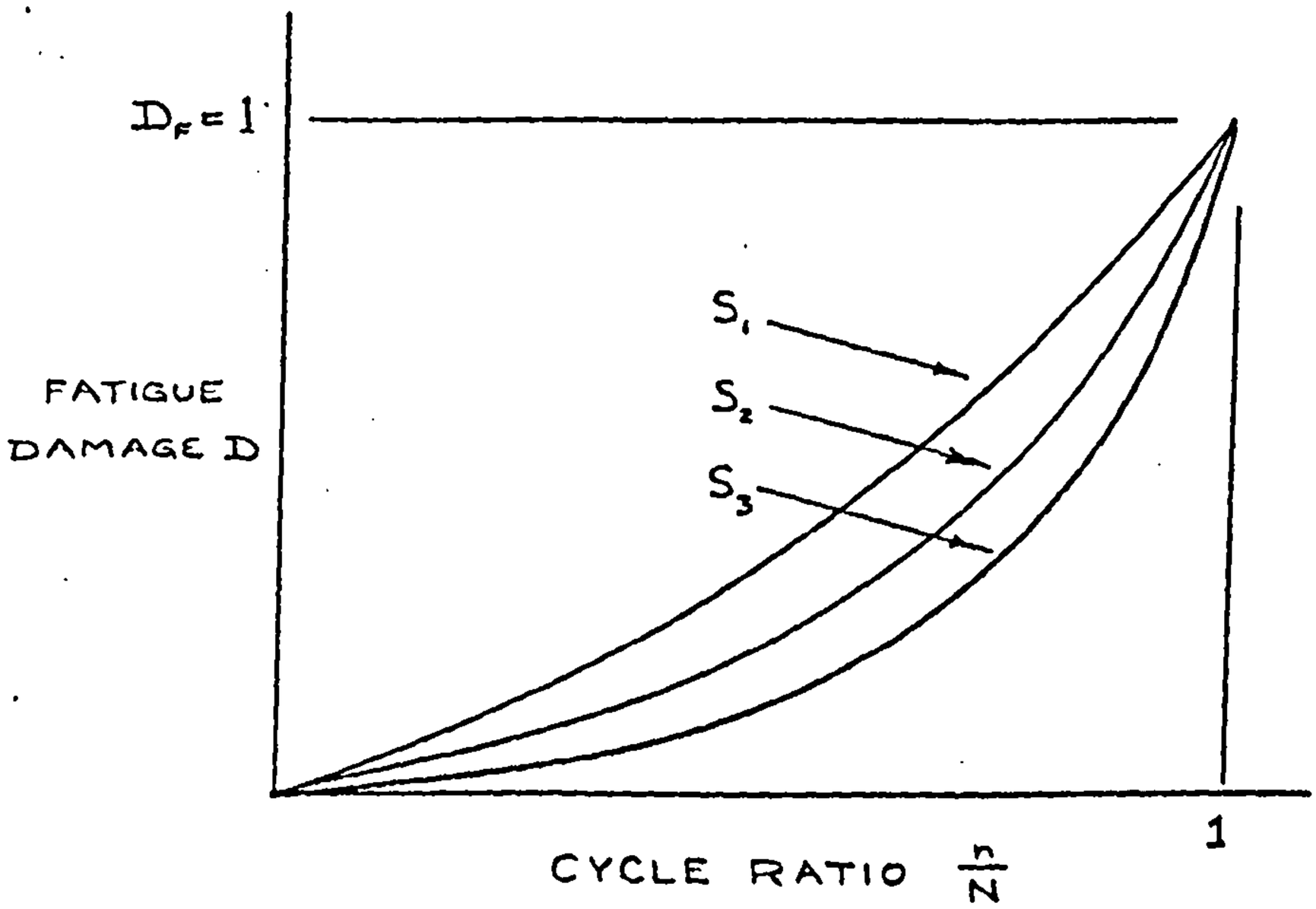

FIGURE 5. STRESS DEPENDENT DAMAGE REPRESENTATION.

CYCLE RATIO VERSUS DAMAGE CURVES FOR $D = \left[\frac{n}{N}\right]^{x_v}$

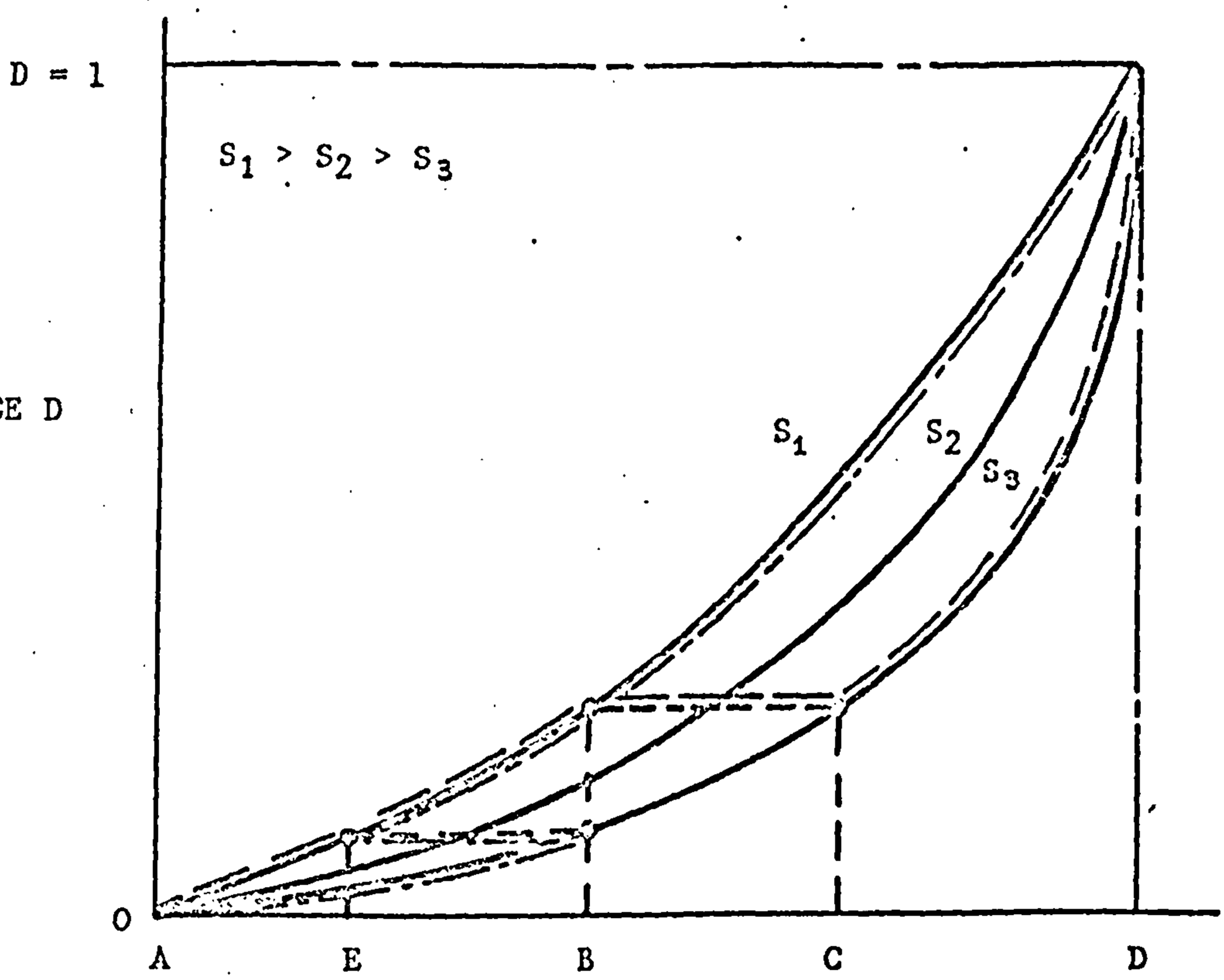

FOR OPERATION AT S_1 FOLLOWED BY OPERATION AT S_3

$$\sum \frac{n}{N} = (AB + CD) < 1 \qquad \text{— — — — — —}$$

FOR OPERATION AT S_3 FOLLOWED BY OPERATION AT S_1

$$\sum \frac{n}{N} = (AB + ED) > 1 \qquad \text{——— - ——— - ———}$$

FIGURE 6.

MARCO-STARKEY THEORY

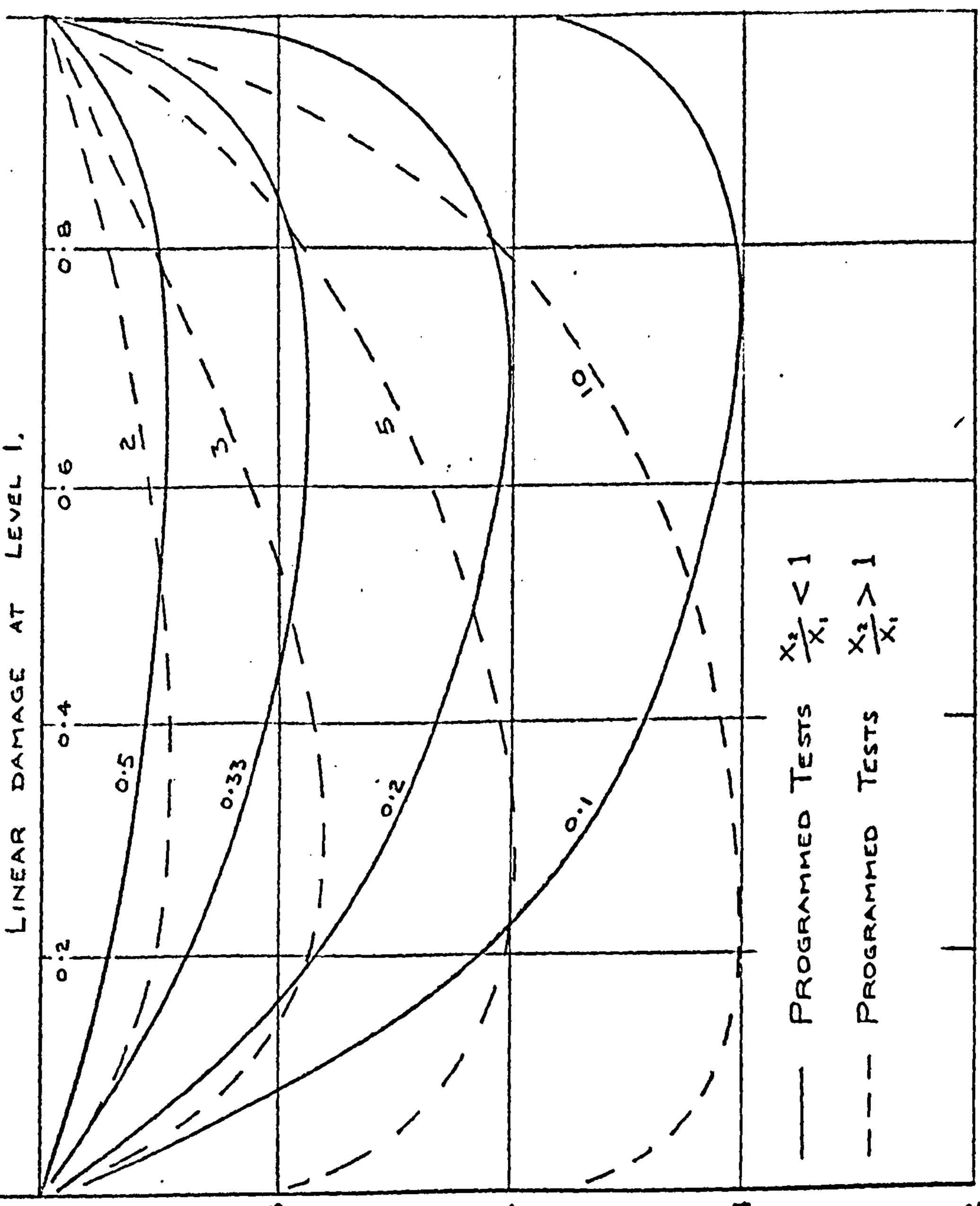

FIGURE 7. EXPECTED TWO LEVEL PROGRAMME TEST RESULTS - EDWARDS (78).

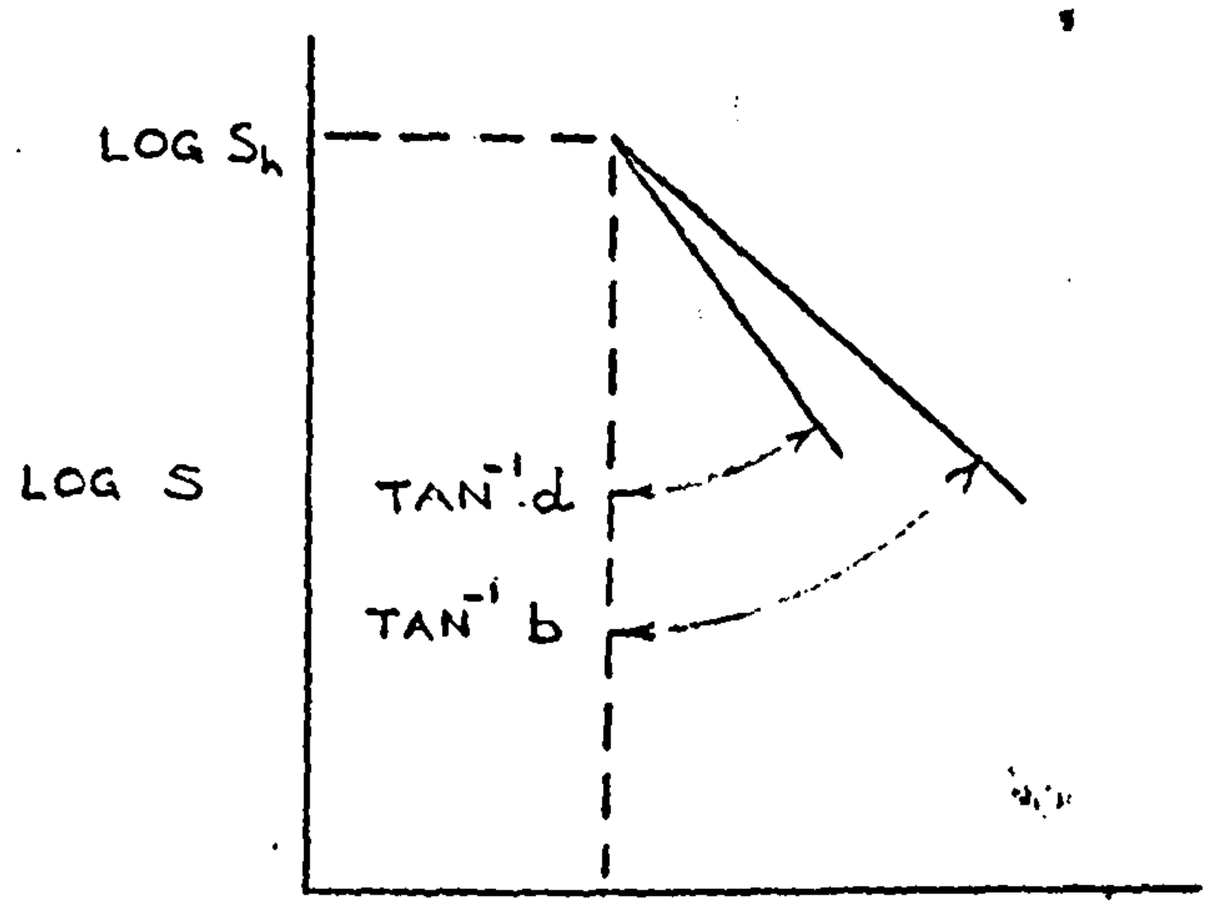

FIGURE 8a. MODIFIED S-N DIAGRAM FOR CORTEN-DOLAN THEORY.

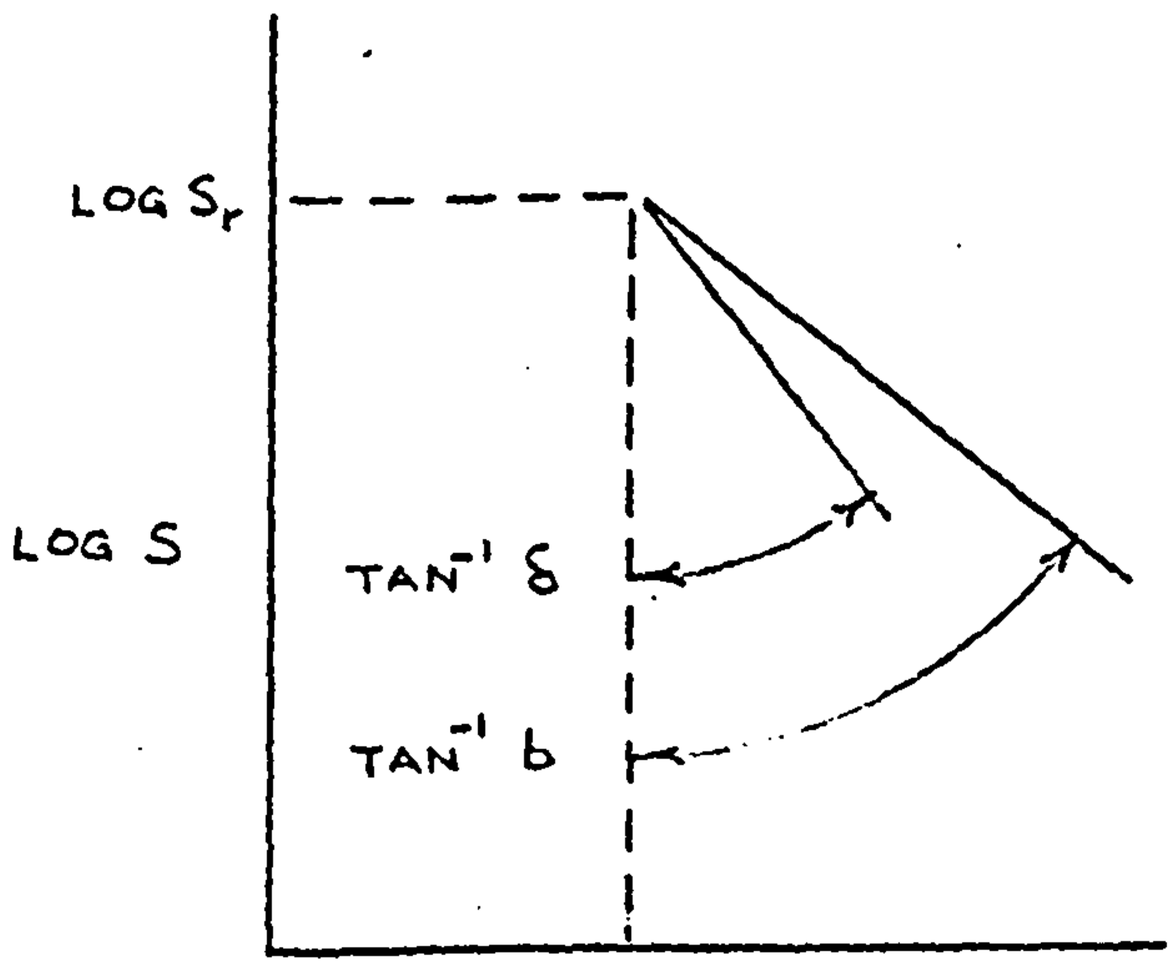

FIGURE 8b. MODIFIED S-N DIAGRAM FOR FREUDENTHAL-HELLER THEORY.

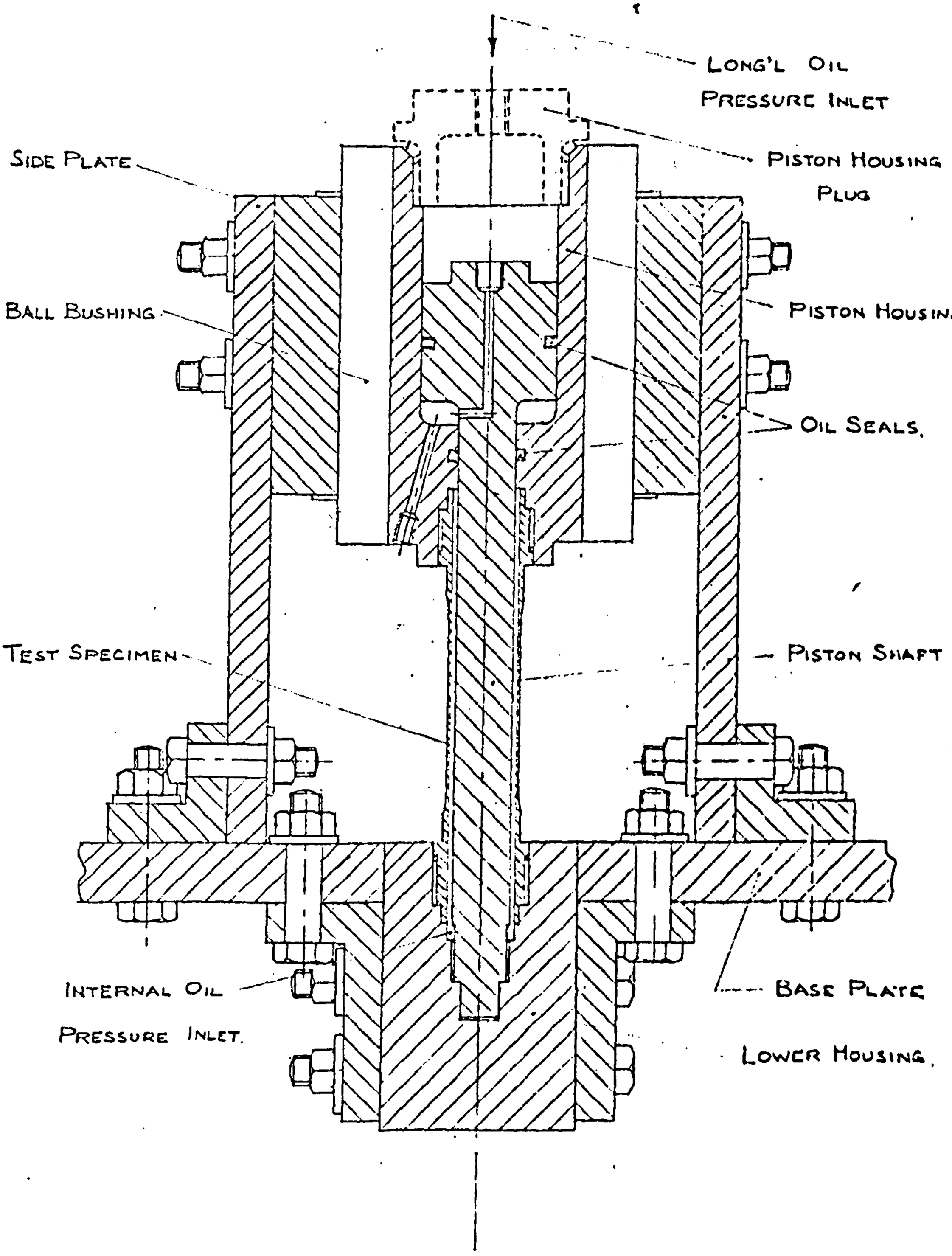

FIGURE 9. G.A. MECHANICAL SYSTEM.

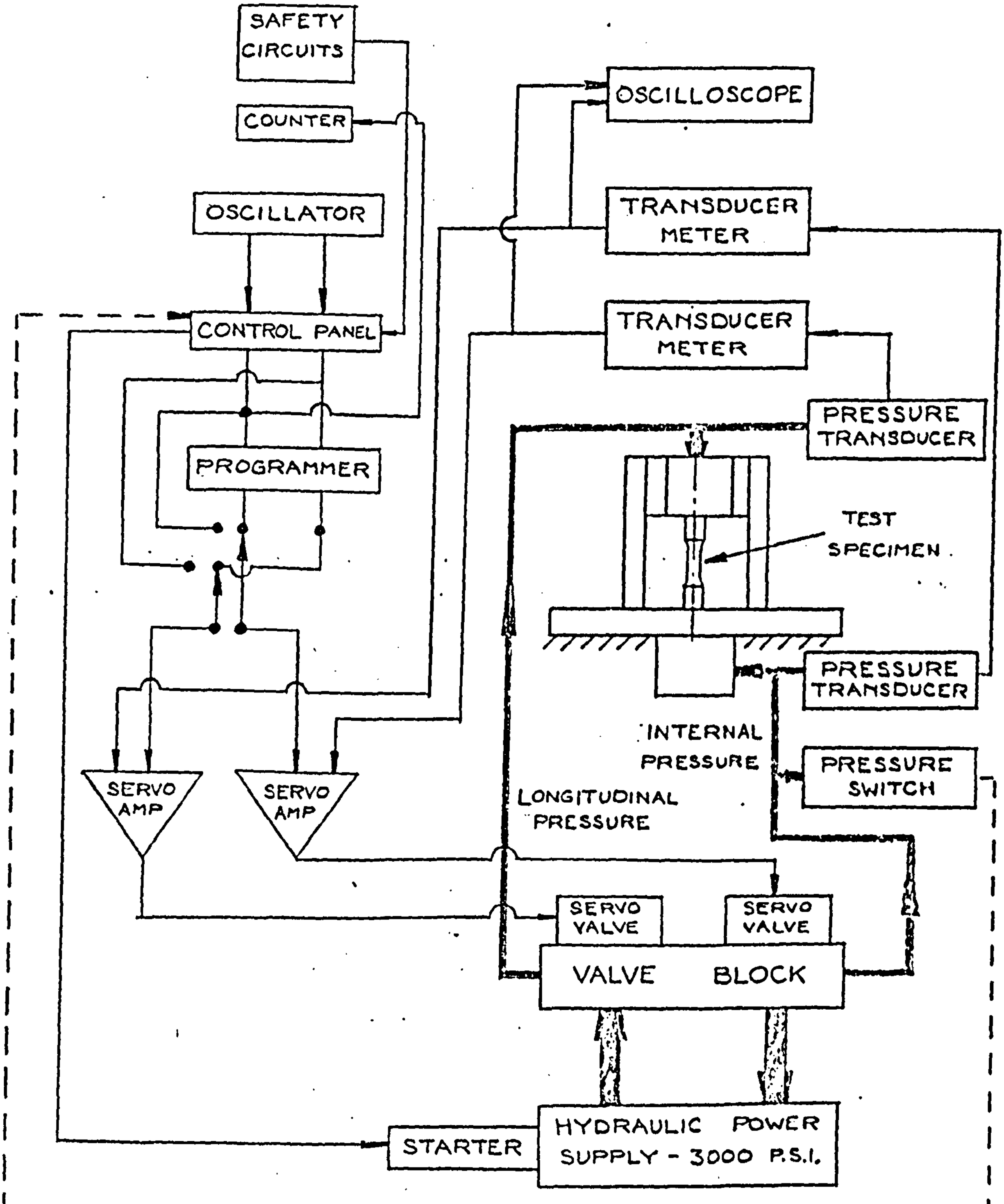

FIGURE 10. BIAXIAL STRESS FATIGUE TEST SYSTEM

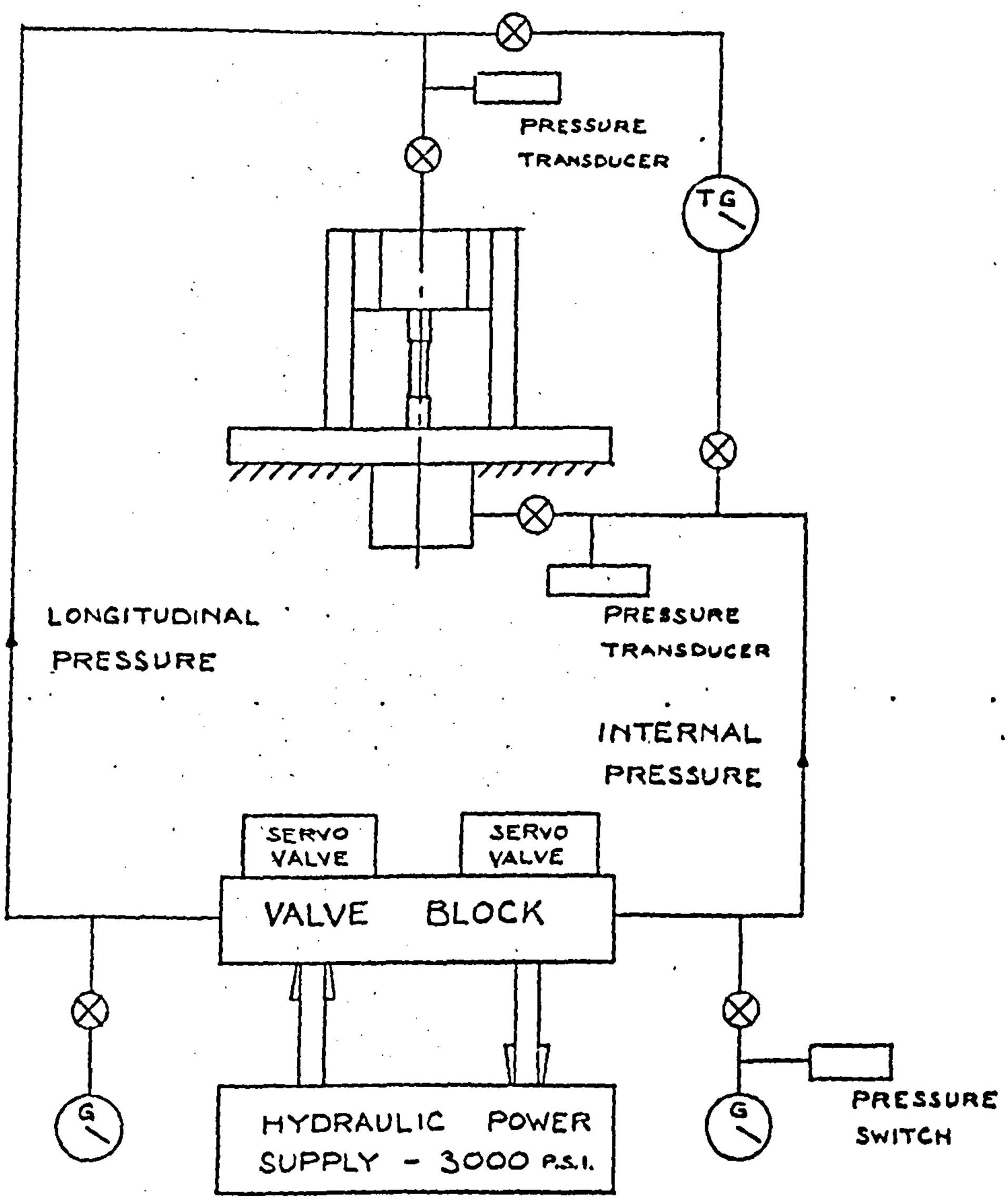

⊗ NEEDLE VALVE

G 0-3000 P.S.I. PRESSURE GAUGE

TG TEST PRESSURE GAUGE

FIGURE 11. HYDRAULIC CIRCUIT.

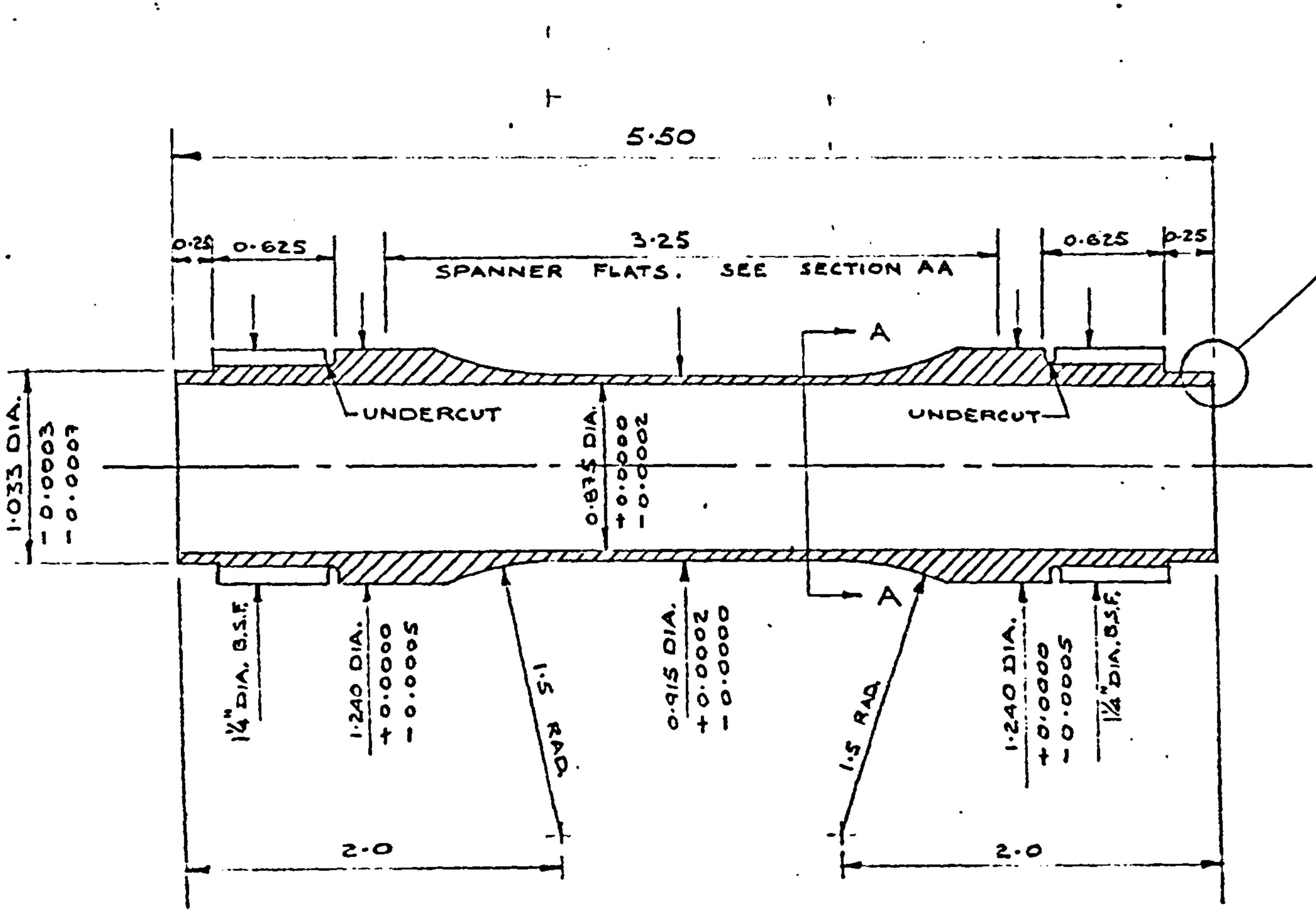

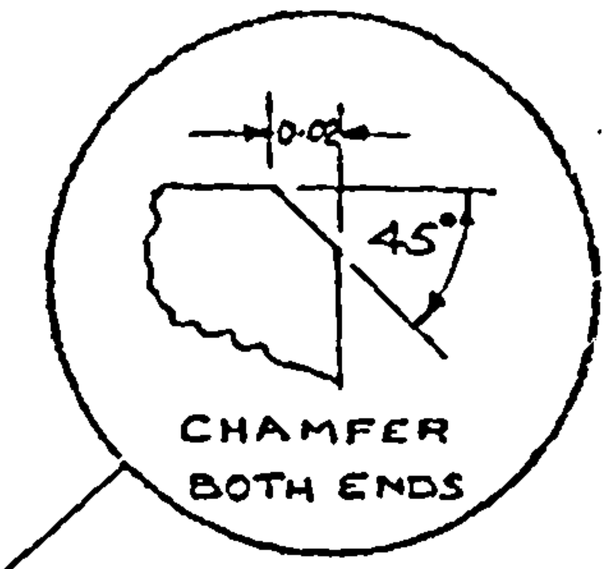

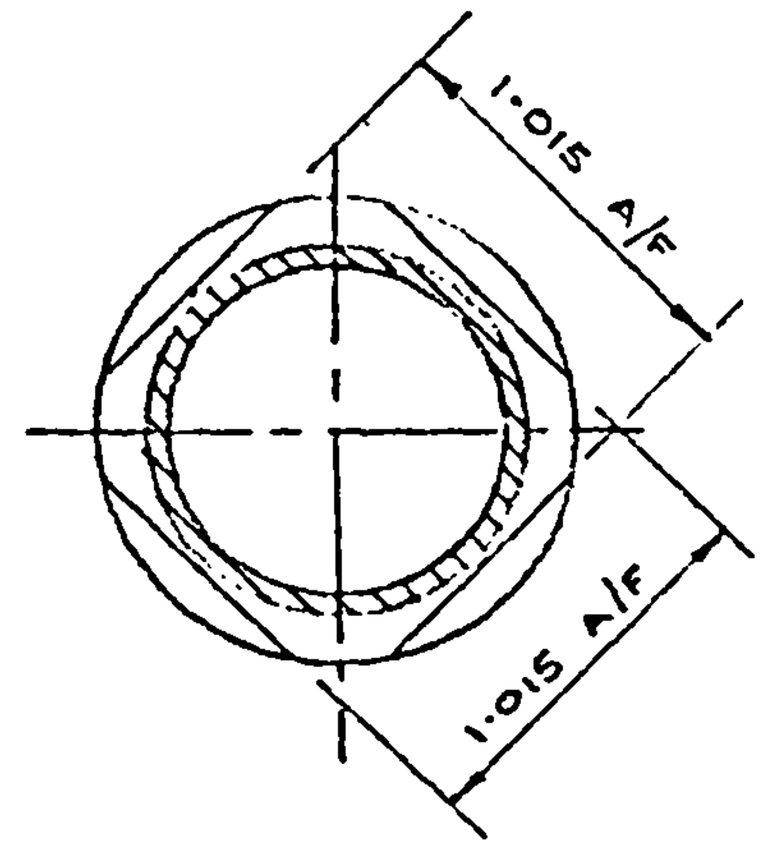

SECTION AA

SCALE: FULL SIZE

ALL DIMENSIONS IN INCHES

FIGURE 12 BIAXIAL FATIGUE TEST SPECIMEN

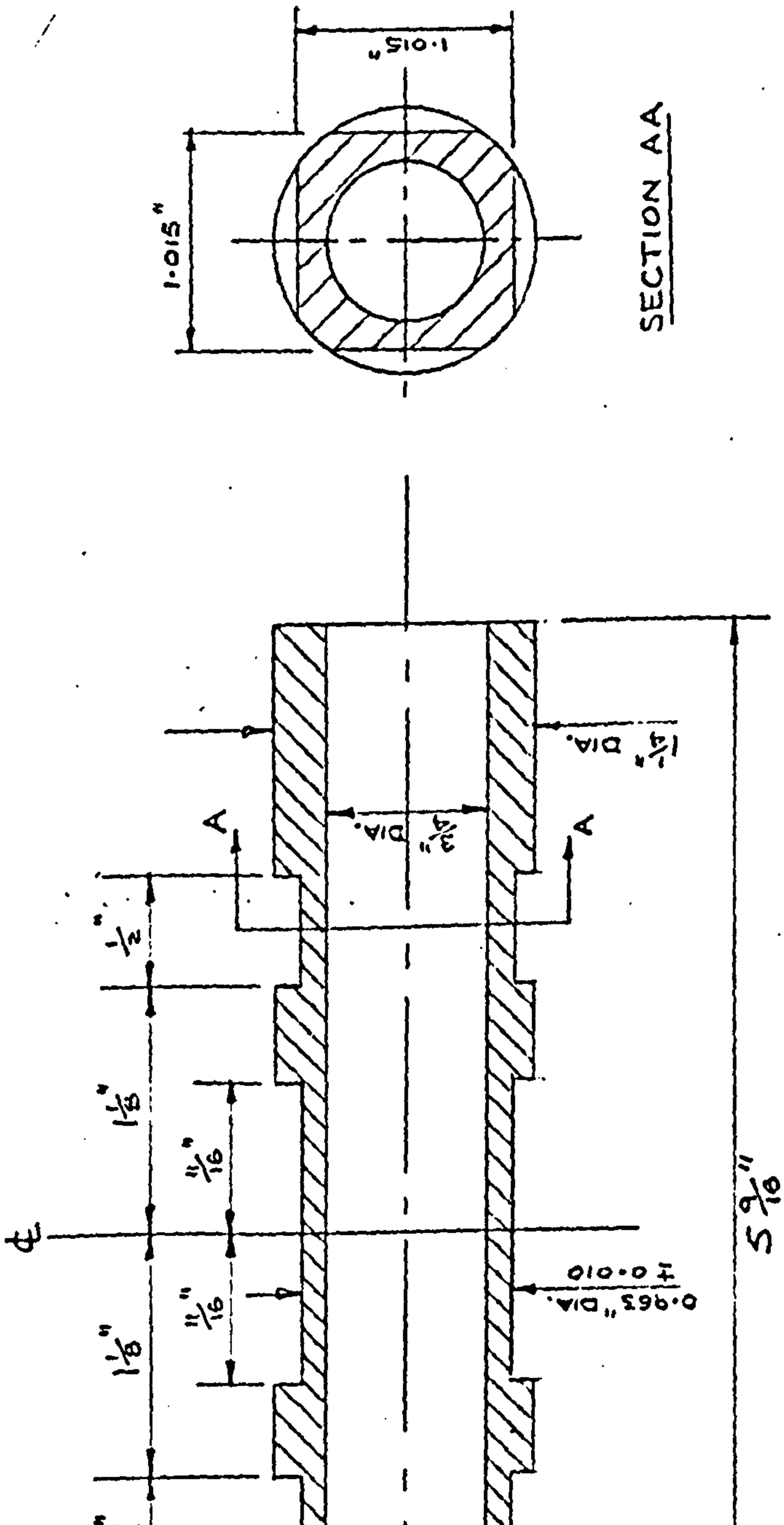

FIGURE 13 BIAXIAL FATIGUE TEST SPECIMEN
INITIAL MACHINING

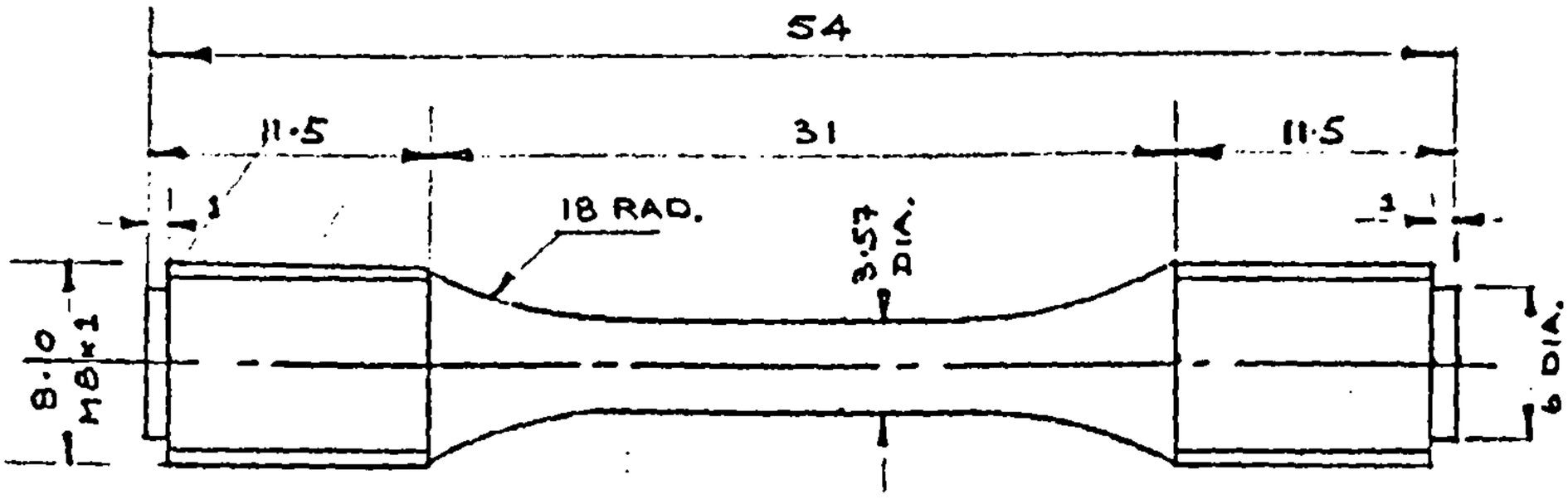

SCALE : 2 FULL SIZE

ALL DIMENSIONS IN mm.

FIGURE 14. VIBROPHORE FATIGUE TEST SPECIMEN

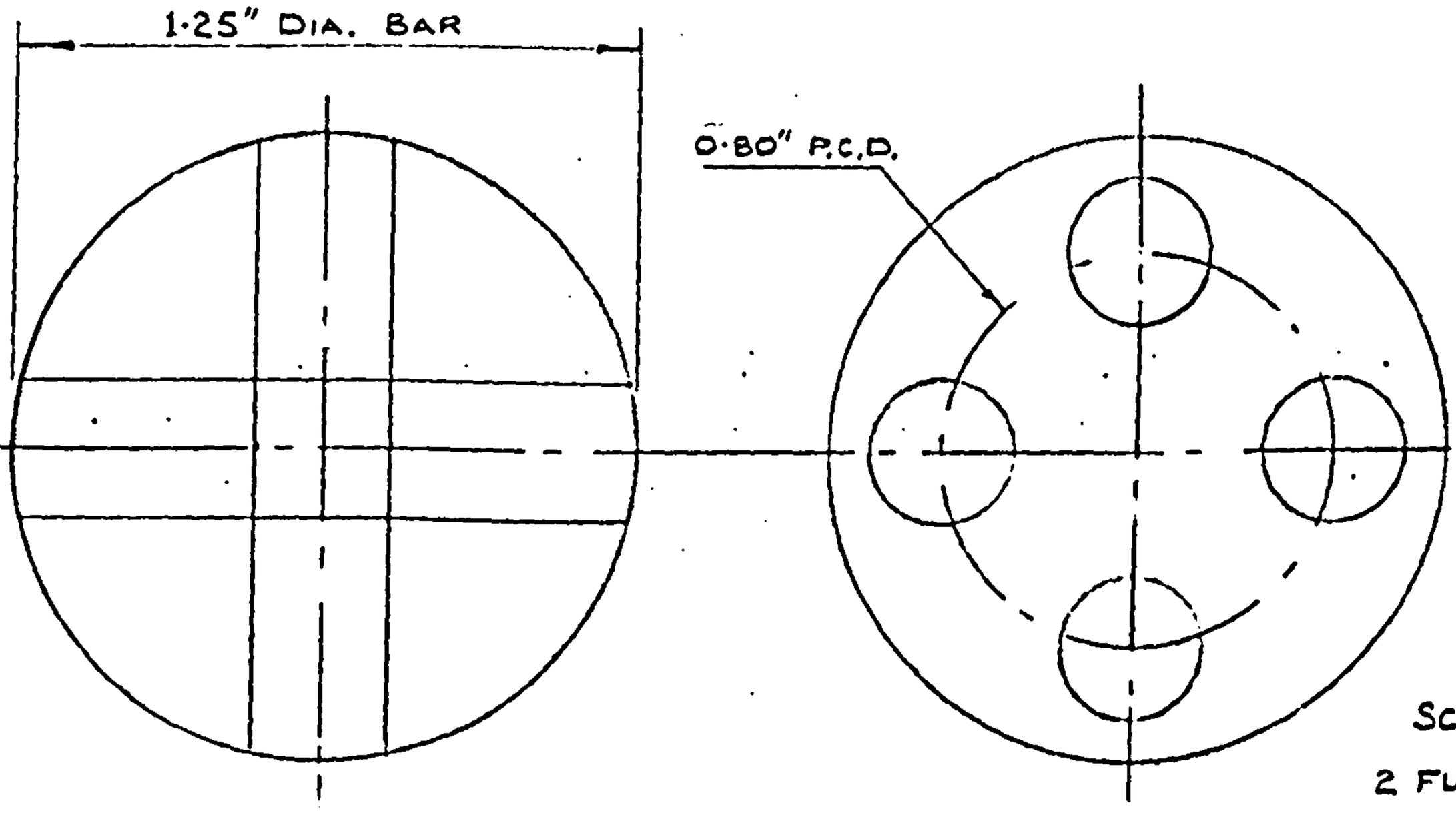

TRANSVERSE LONGITUDINAL

SCALE : 2 FULL SIZE

POSITION OF SPECIMENS

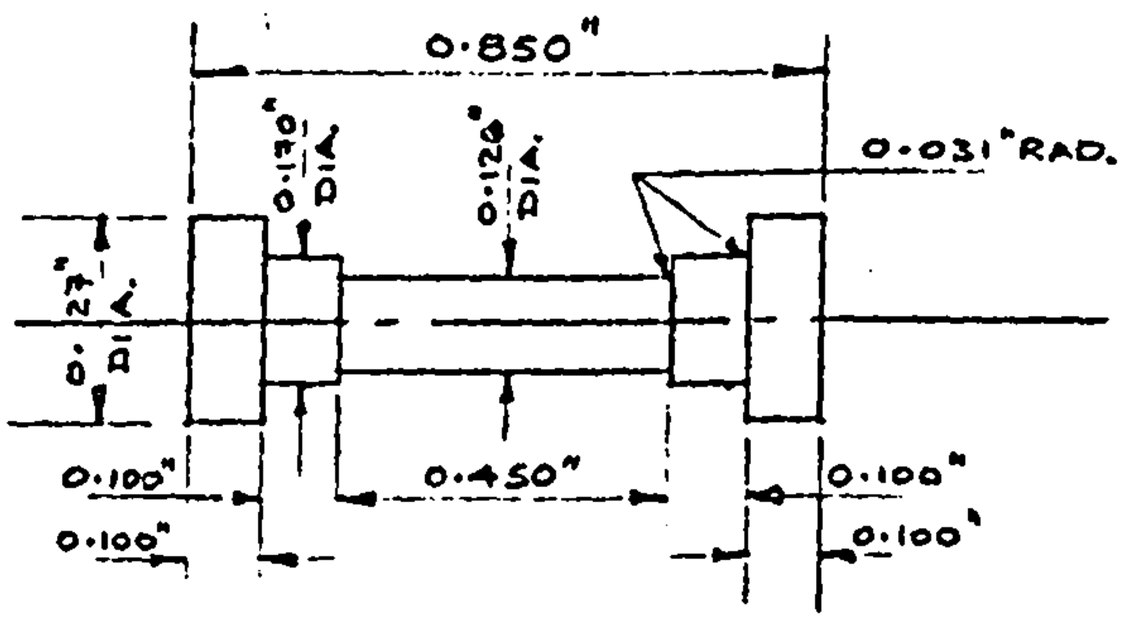

SCALE : 2 FULL SIZE

FIGURE 15 HOUNSFIELD TENSILE SPECIMEN.

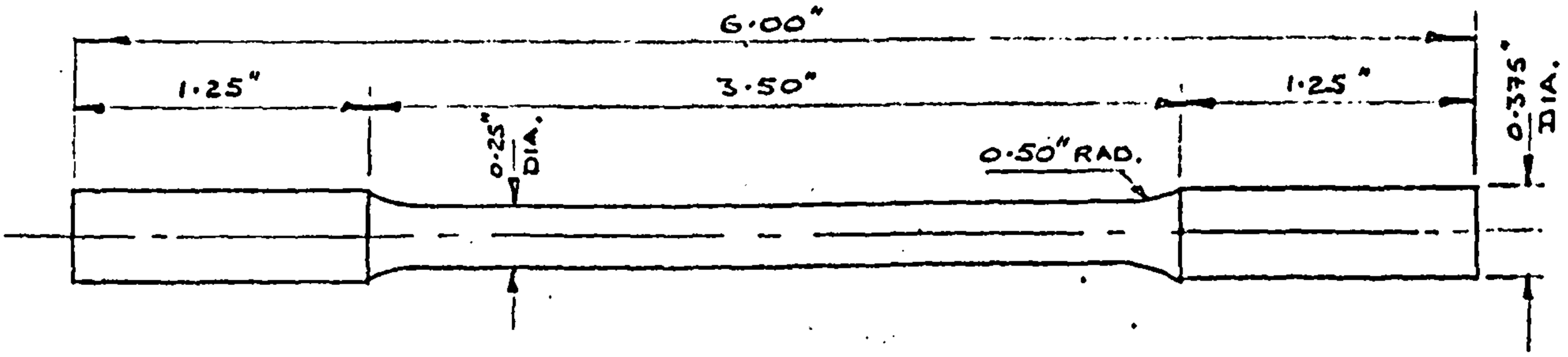

SCALE: FULL SIZE

FIGURE 16 TENSILE SPECIMEN

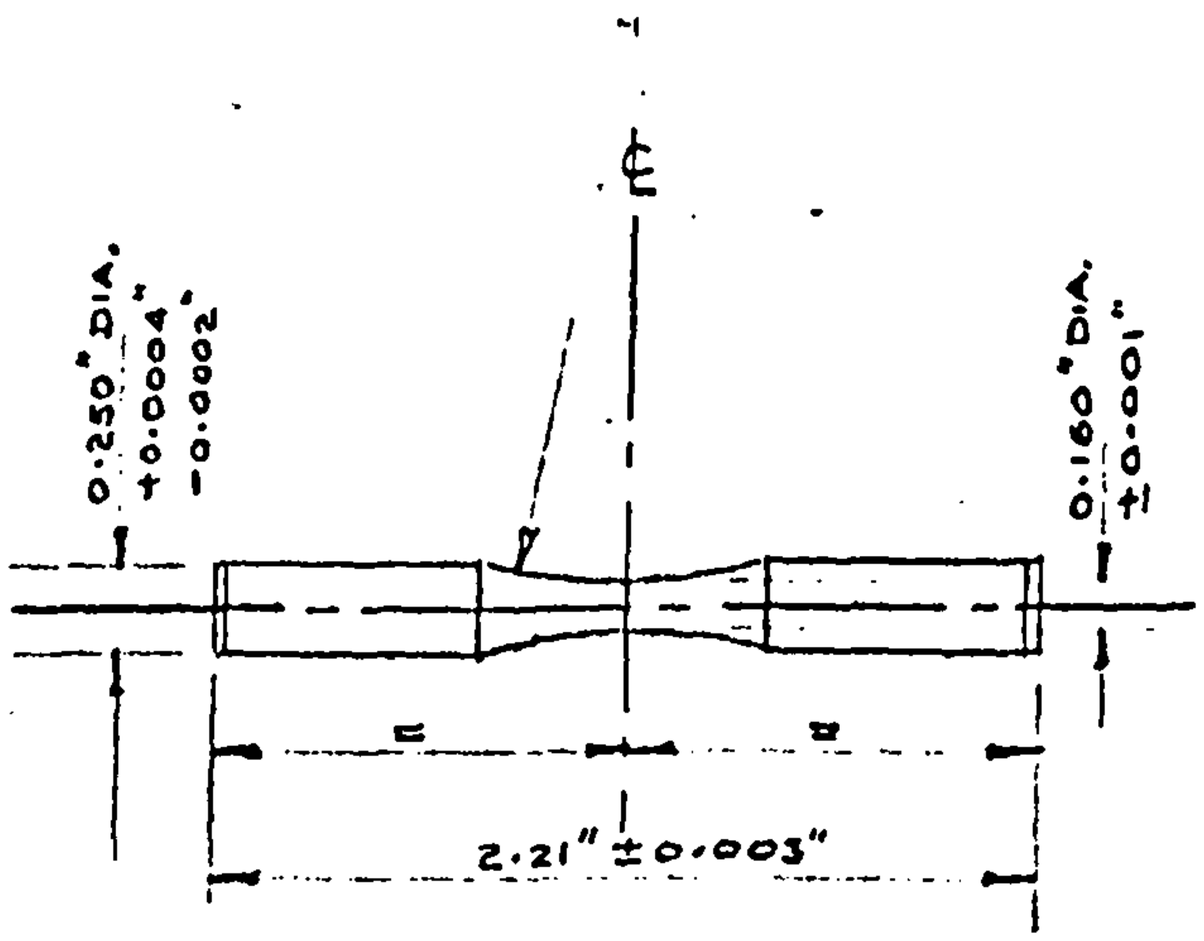

SCALE: FULL SIZE

FIGURE 17 ROTATING BENDING FATIGUE SPECIMEN

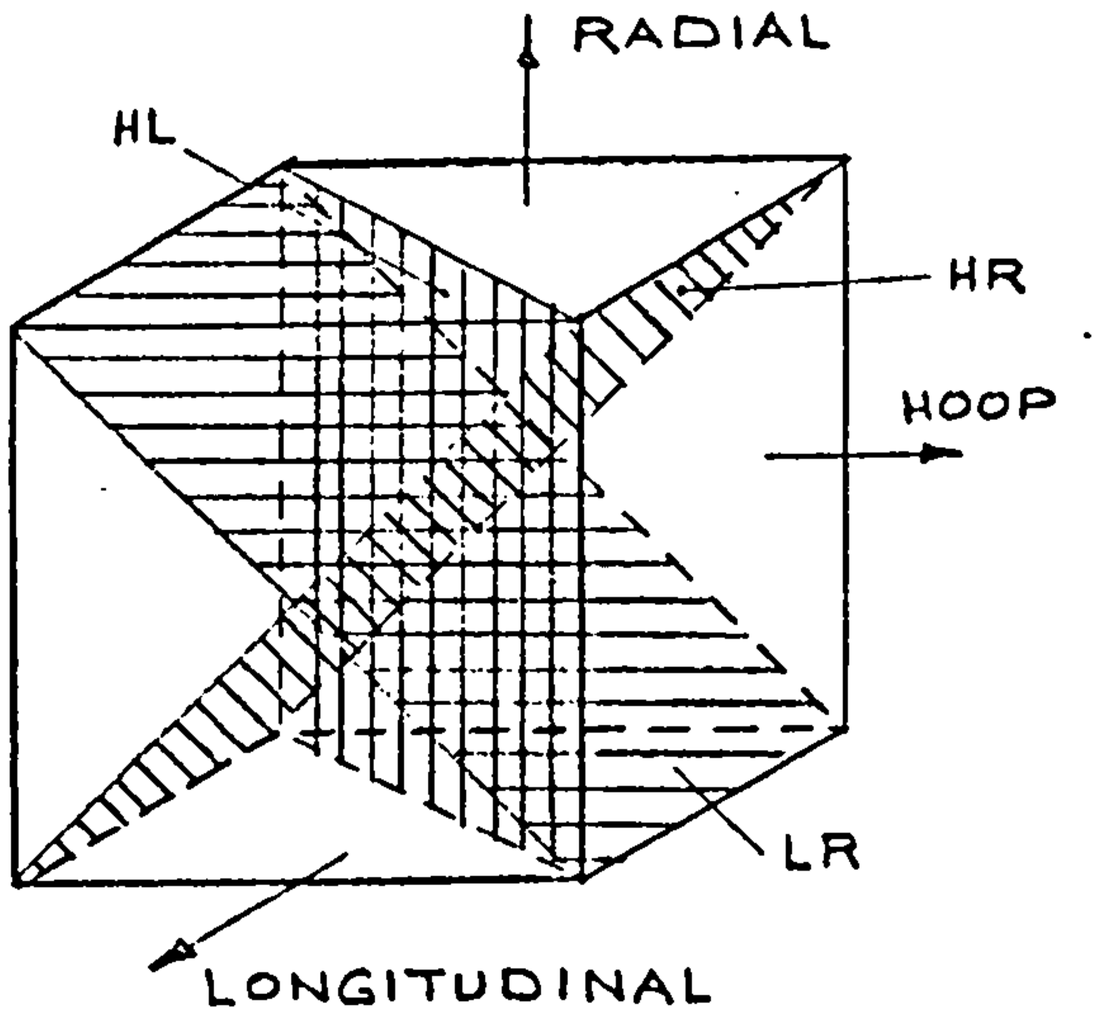

HL, LR, HR.

MAXIMUM SHEAR STRESS PLANES.

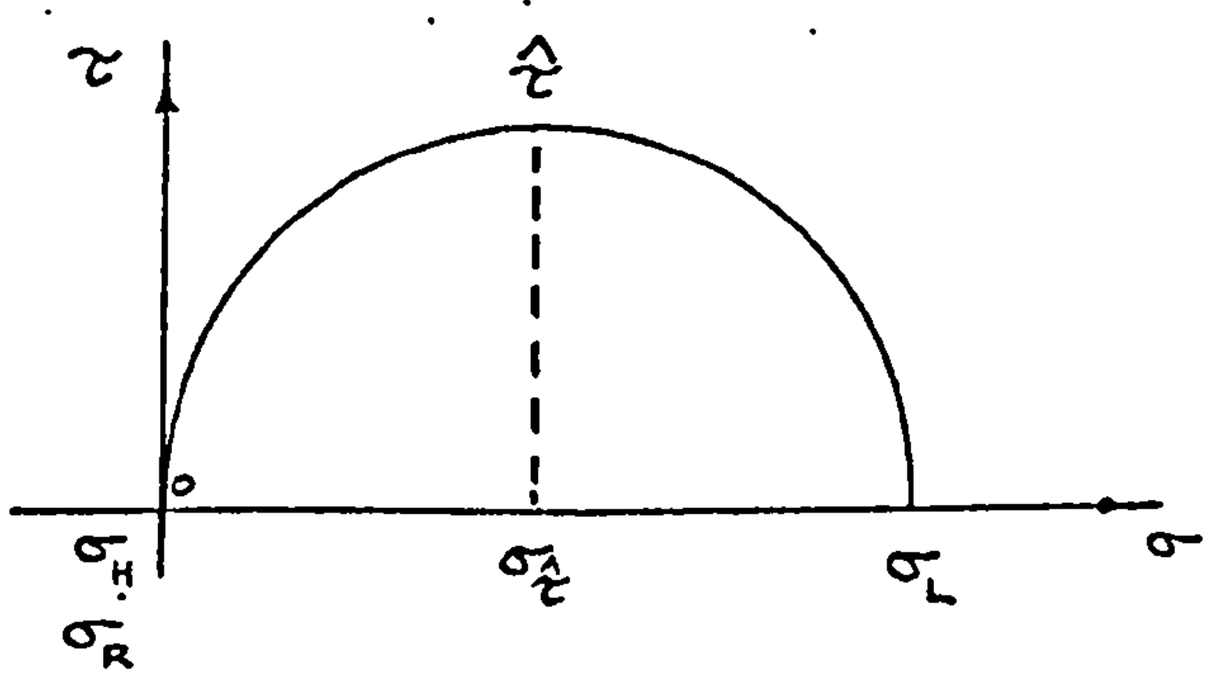

$K = 0$

$\hat{\tau} = \sigma_L/2.$

$\sigma_{\hat{\tau}} = \sigma_L/2.$

$\hat{\tau}$ PLANES : HL, RL.

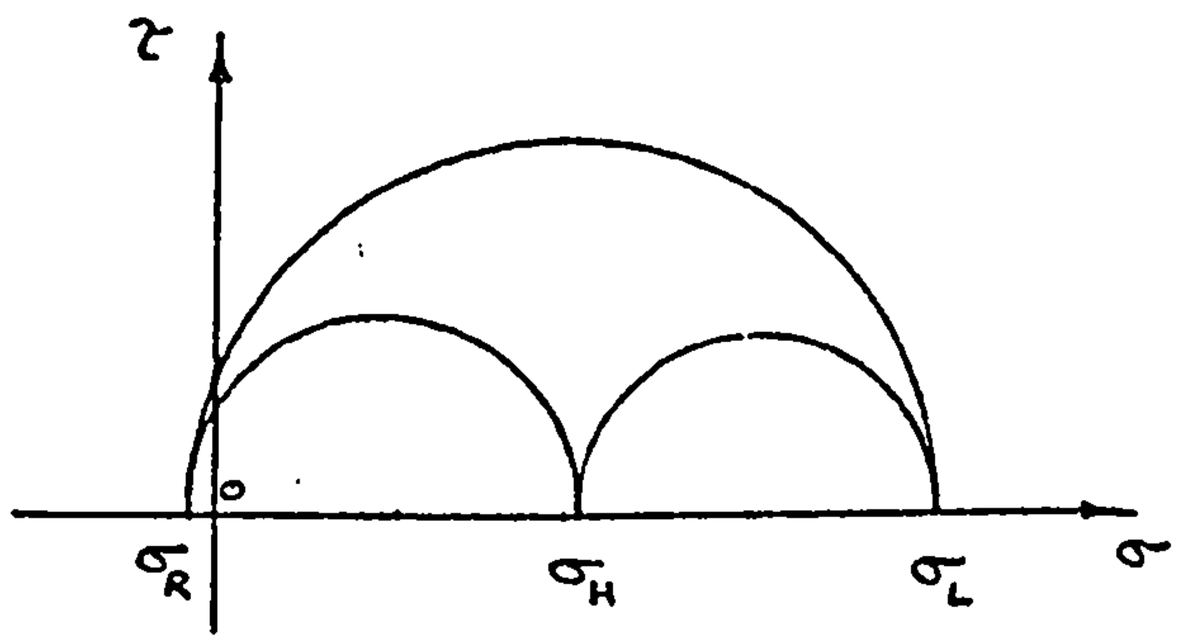

$K = 0.5$

$\hat{\tau} = \sigma_L/2$ [$\sigma_R/2$ SMALL]

$\sigma_{\hat{\tau}} = \sigma_L/2.$

$\hat{\tau}$ PLANE : LR.

FIGURE 18a. MOHR STRESS CIRCLES FOR RANGE OF K VALUES USED.

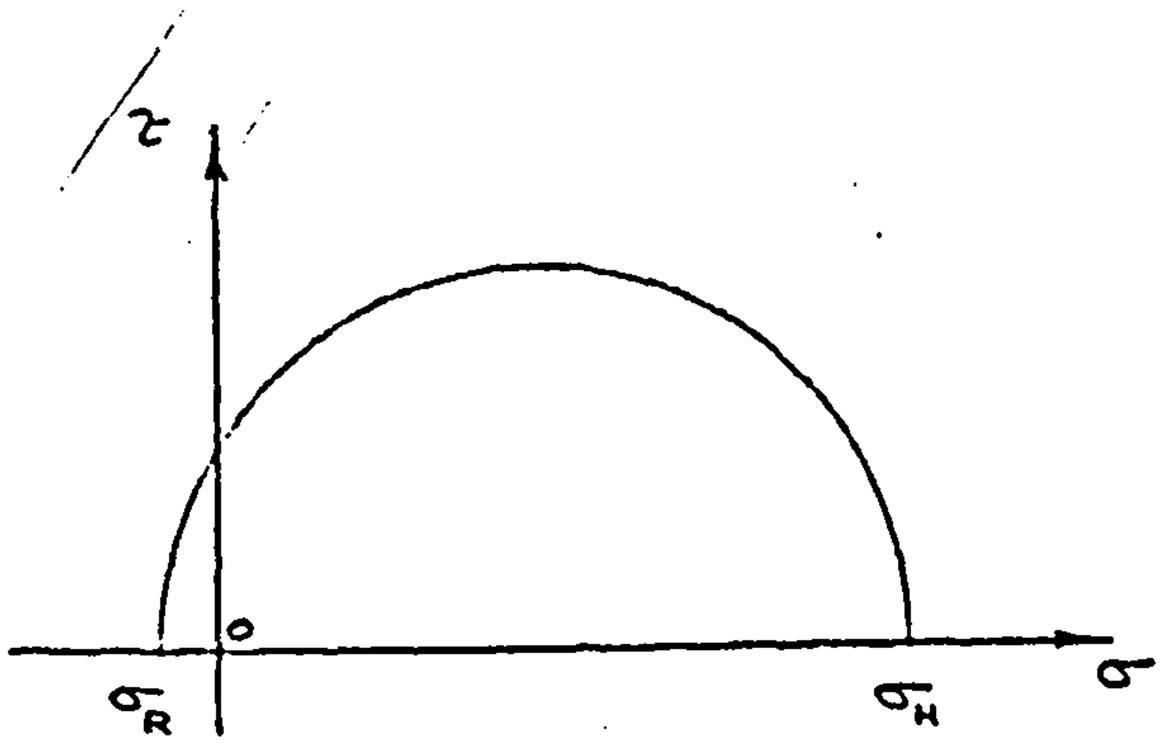

$K = 1$

$\hat{\tau} = \sigma_H/2 , \sigma_L/2.$

$\sigma_{\hat{\tau}} = \sigma_H/2 , \sigma_L/2.$

$\hat{\tau}$ PLANES : HR, LR

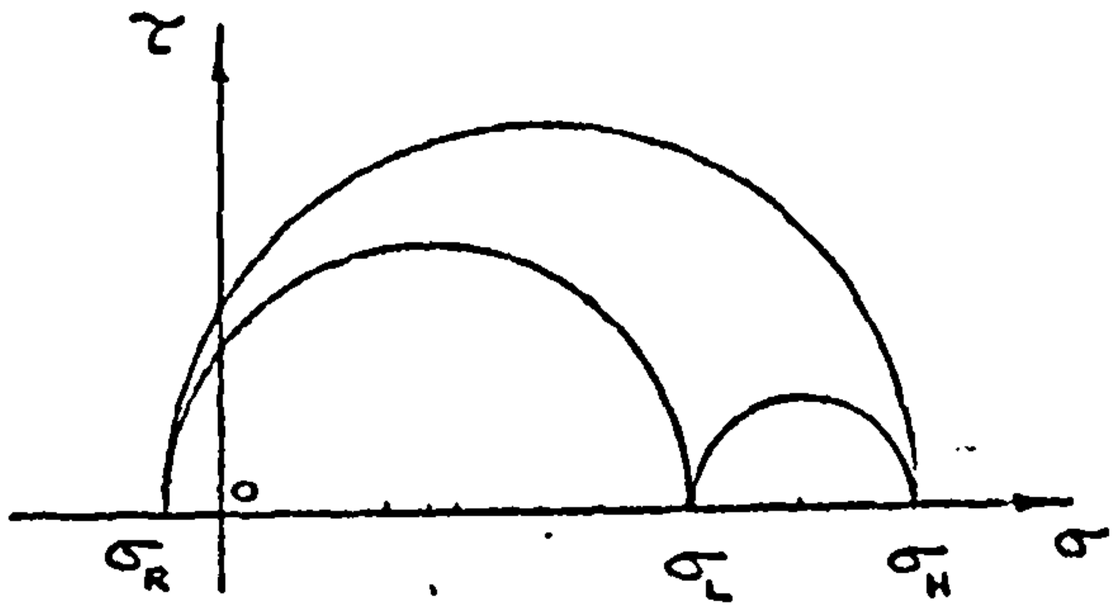

$K = 2$

$\hat{\tau} = \sigma_H/2.$

$\sigma_{\hat{\tau}} = \sigma_H/2.$

$\hat{\tau}$ PLANE : HR

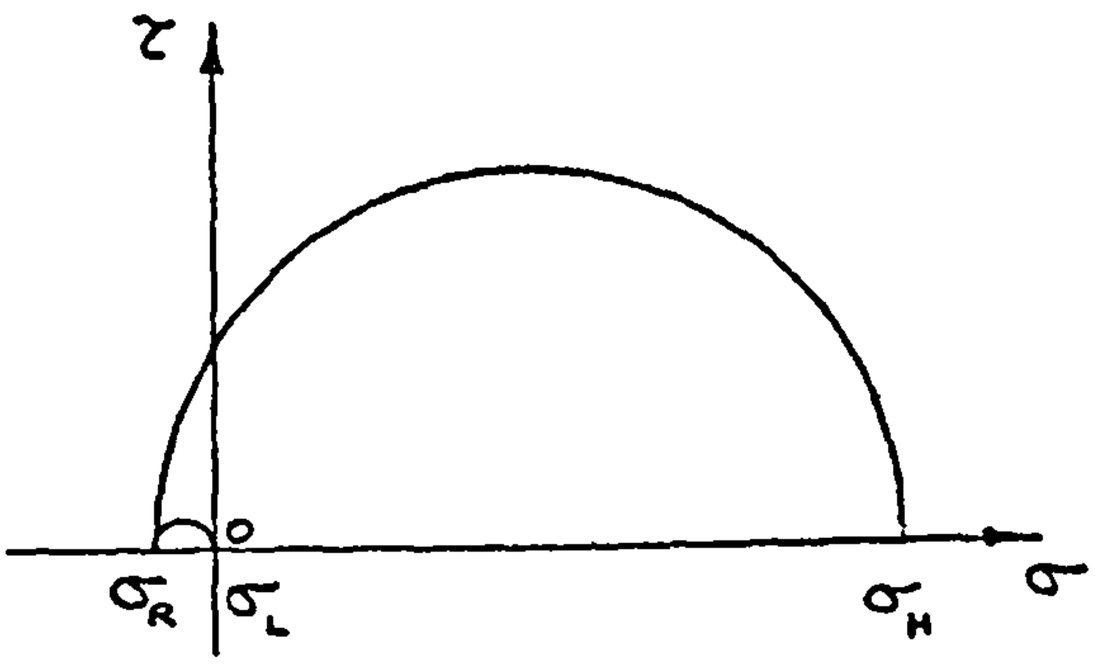

$K = \infty$

$\hat{\tau} = \sigma_H/2.$

$\sigma_{\hat{\tau}} = \sigma_H/2.$

$\hat{\tau}$ PLANES : HL, HR.

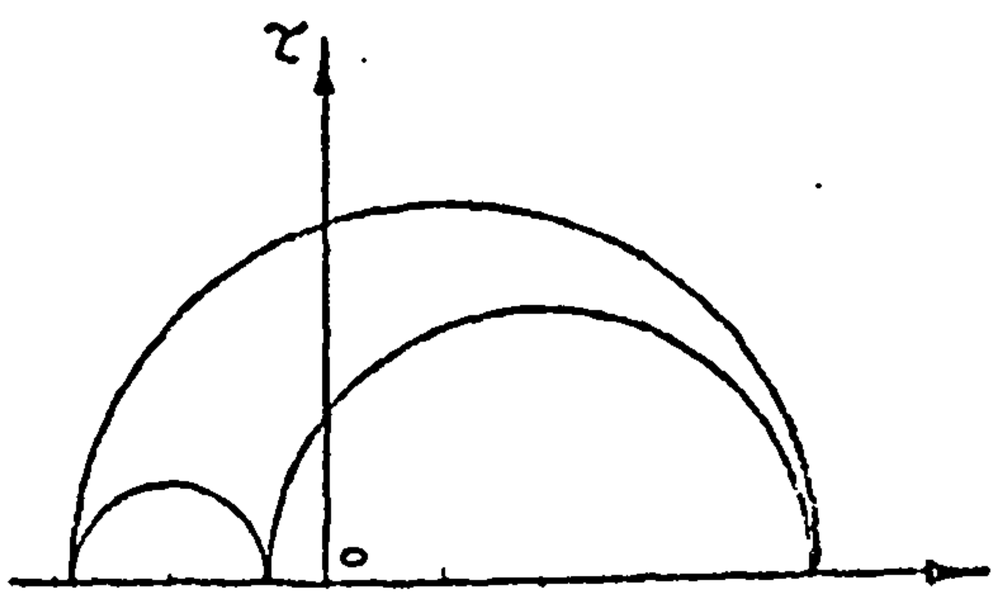

$K = -2.$

$\hat{\tau} = 3\sigma_H/4.$

$\sigma_{\hat{\tau}} = \sigma_H/4.$

$\hat{\tau}$ PLANE : HL

FIGURE 18b. MOHR STRESS CIRCLES FOR RANGE OF K VALUES USED.

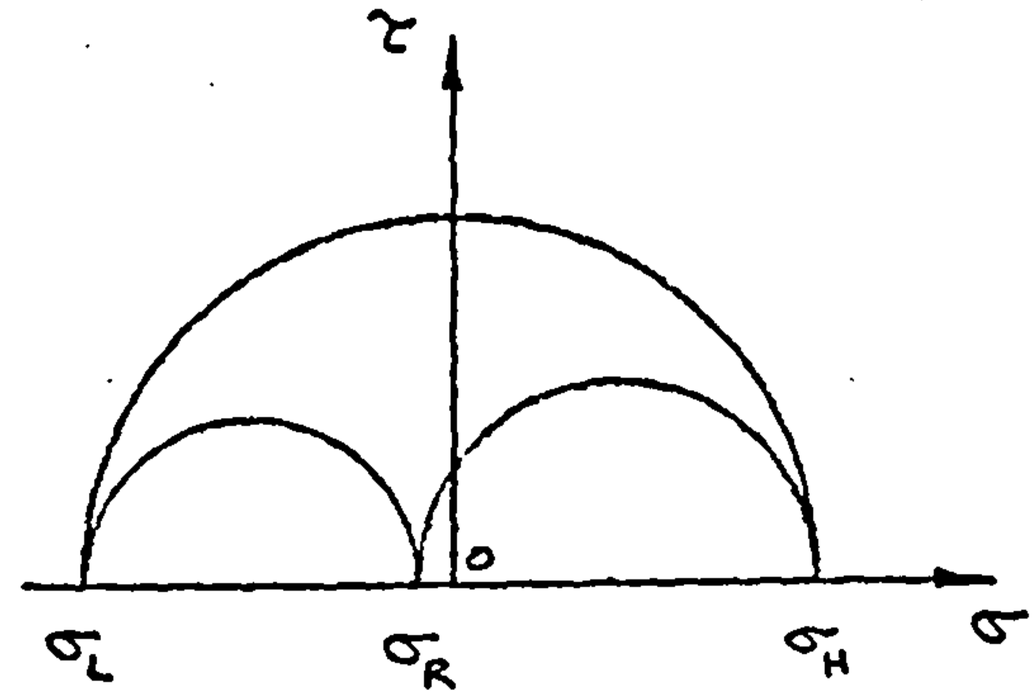

$K = -1$

$\hat{\tau} = \sigma_H$

$\sigma_{\hat{\tau}} = 0$

$\hat{\tau}$ PLANE : HL

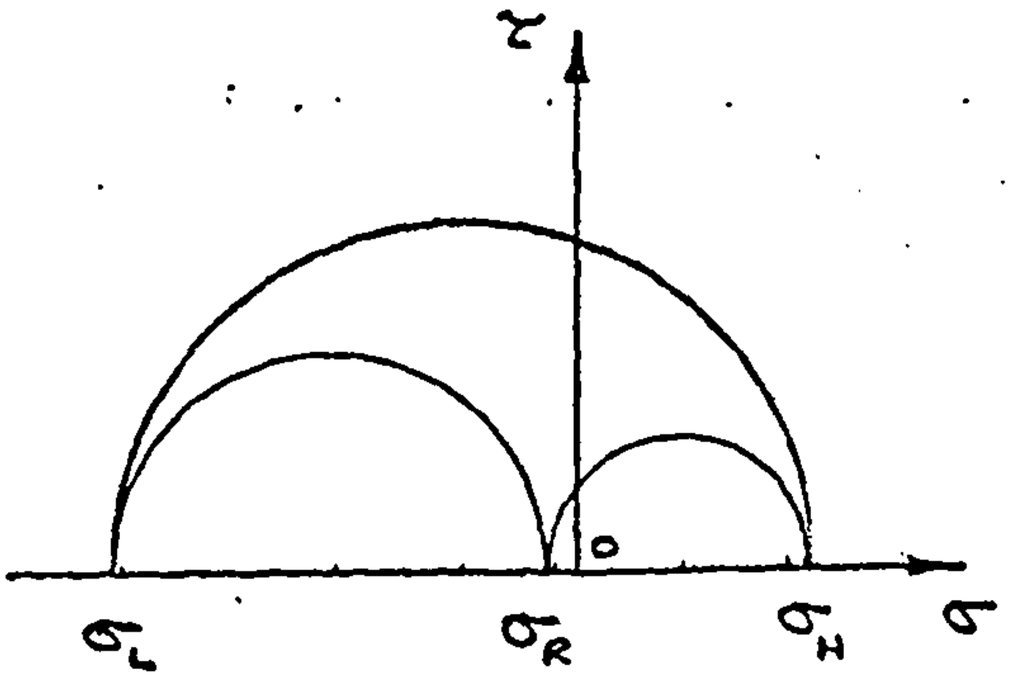

$K = -0.5$

$\hat{\tau} = 3\sigma_H/2$

$\sigma_{\hat{\tau}} = -\sigma_H/2.$

$\hat{\tau}$ PLANE : HL.

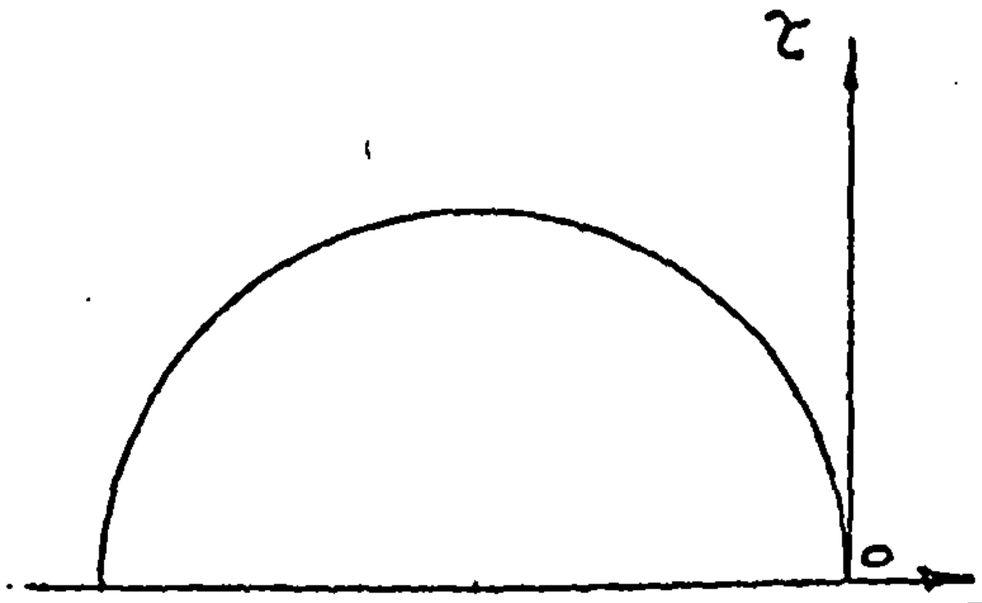

$K = -0$

$\hat{\tau} = \sigma_L/2.$

$\sigma_{\hat{\tau}} = -\sigma_L/2.$

$\hat{\tau}$ PLANES : HL, RL.

FIGURE 18c. MOHR STRESS CIRCLES FOR RANGE OF K VALUES USED.

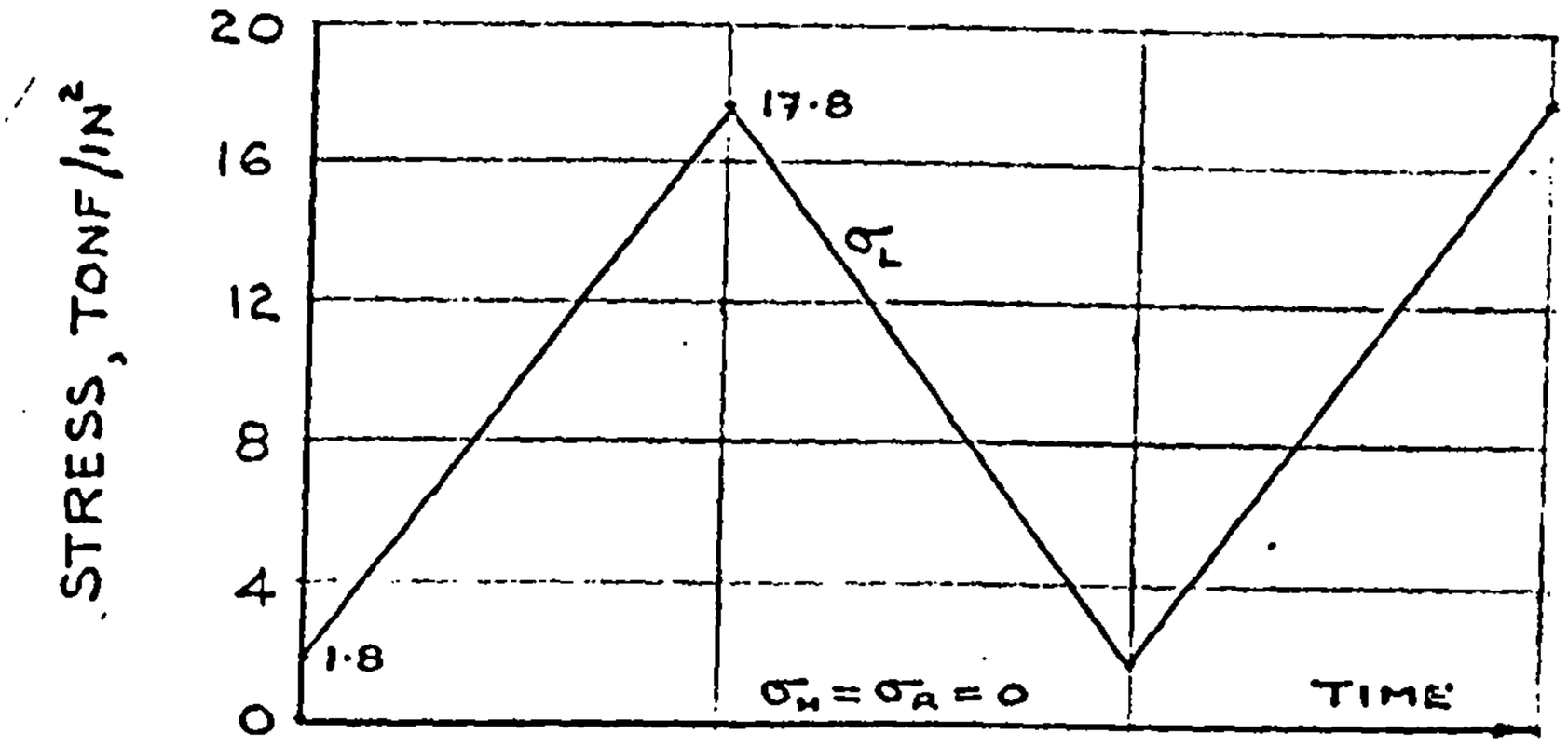

FLUCTUATION OF PRINCIPAL STRESSES

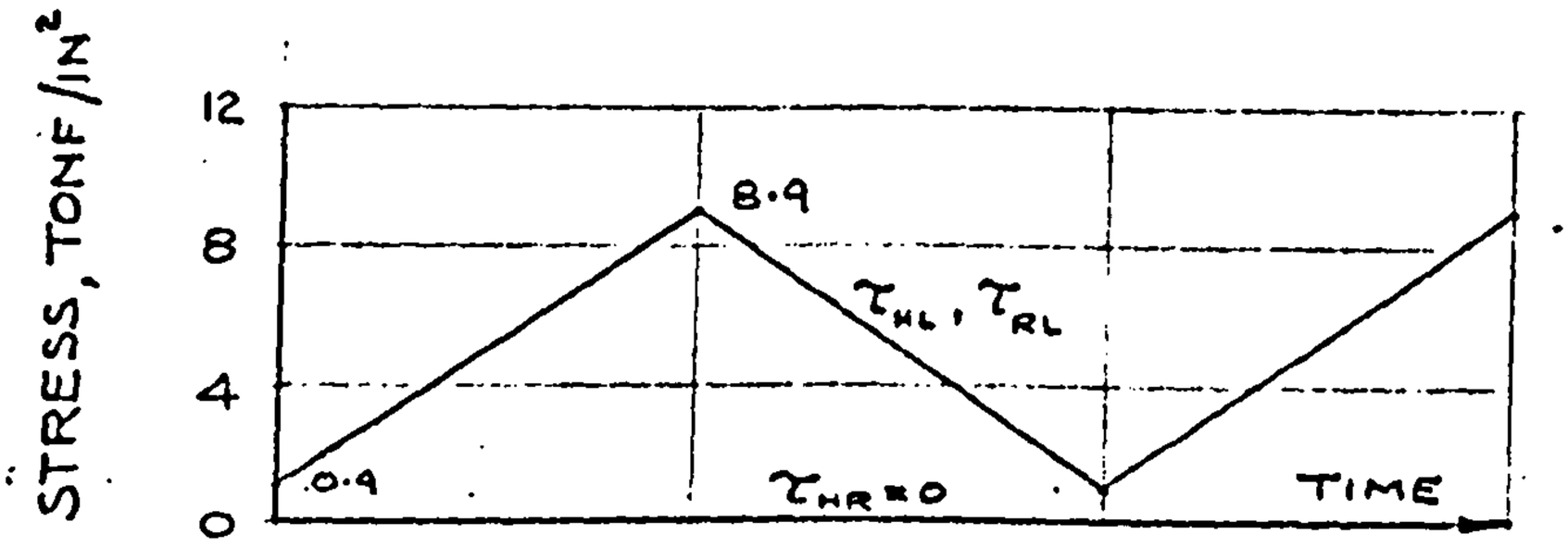

FLUCTUATION OF MAXIMUM SHEAR STRESSES

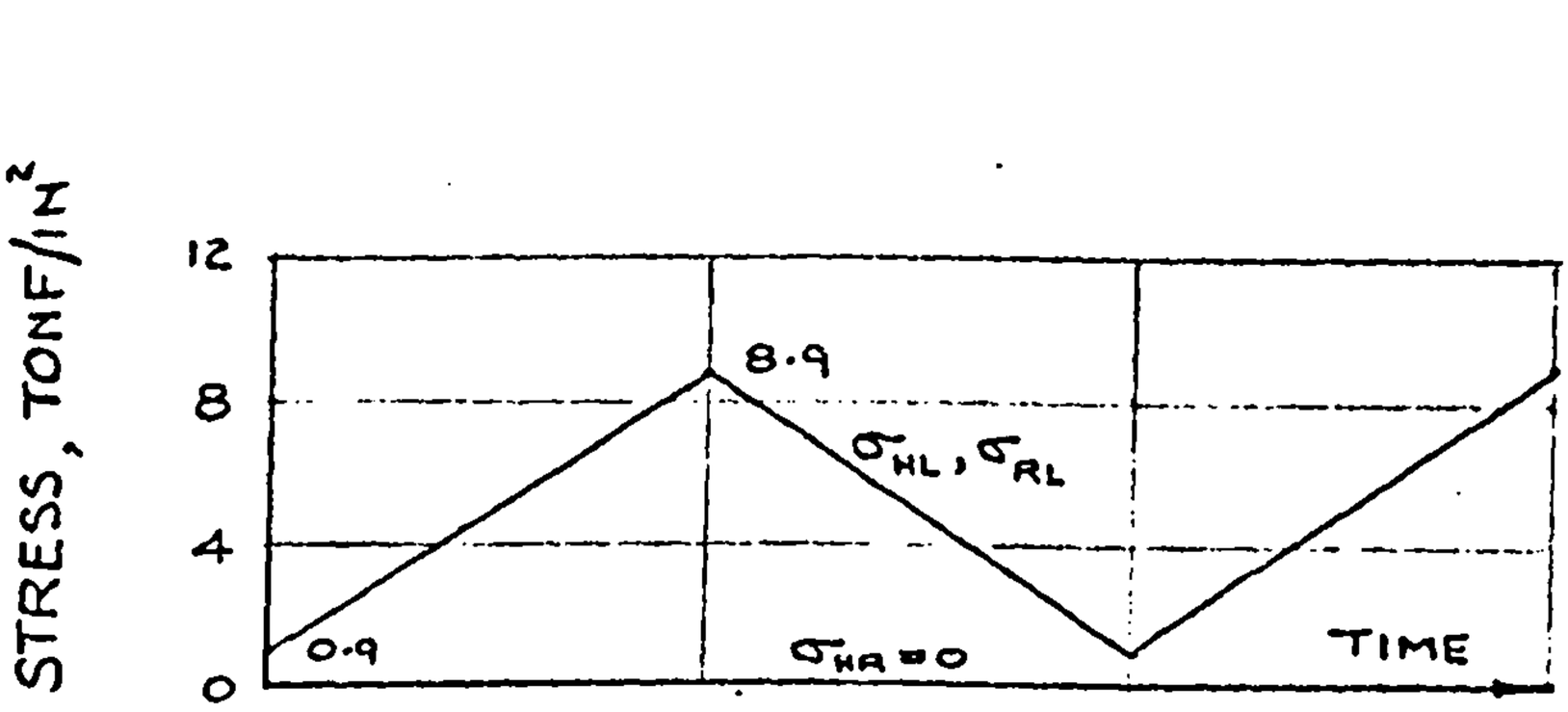

FLUCTUATION OF NORMAL STRESSES ON THE MAXIMUM SHEAR STRESS PLANES.

ALL STRESSES REFER TO INNER WALL OF SPECIMENS.
TRIANGULAR WAVEFORMS DEPICTED FOR SIMPLICITY.
σ_H, σ_L AND σ_R ARE PRINCIPAL STRESSES IN HOOP, LONGITUDINAL AND RADIAL DIRECTIONS.
SUBSCRIPTS HL, LR AND HR REFER TO MAXIMUM SHEAR STRESS PLANES BETWEEN PRINCIPAL STRESSES (σ_H, σ_L), (σ_L, σ_R) AND (σ_H, σ_R).

FIGURE 19a. STRESS-TIME RELATIONS FOR K=0

WITH LONGITUDINAL STRESS = 9·8 ± 8·0 TONF/IN²

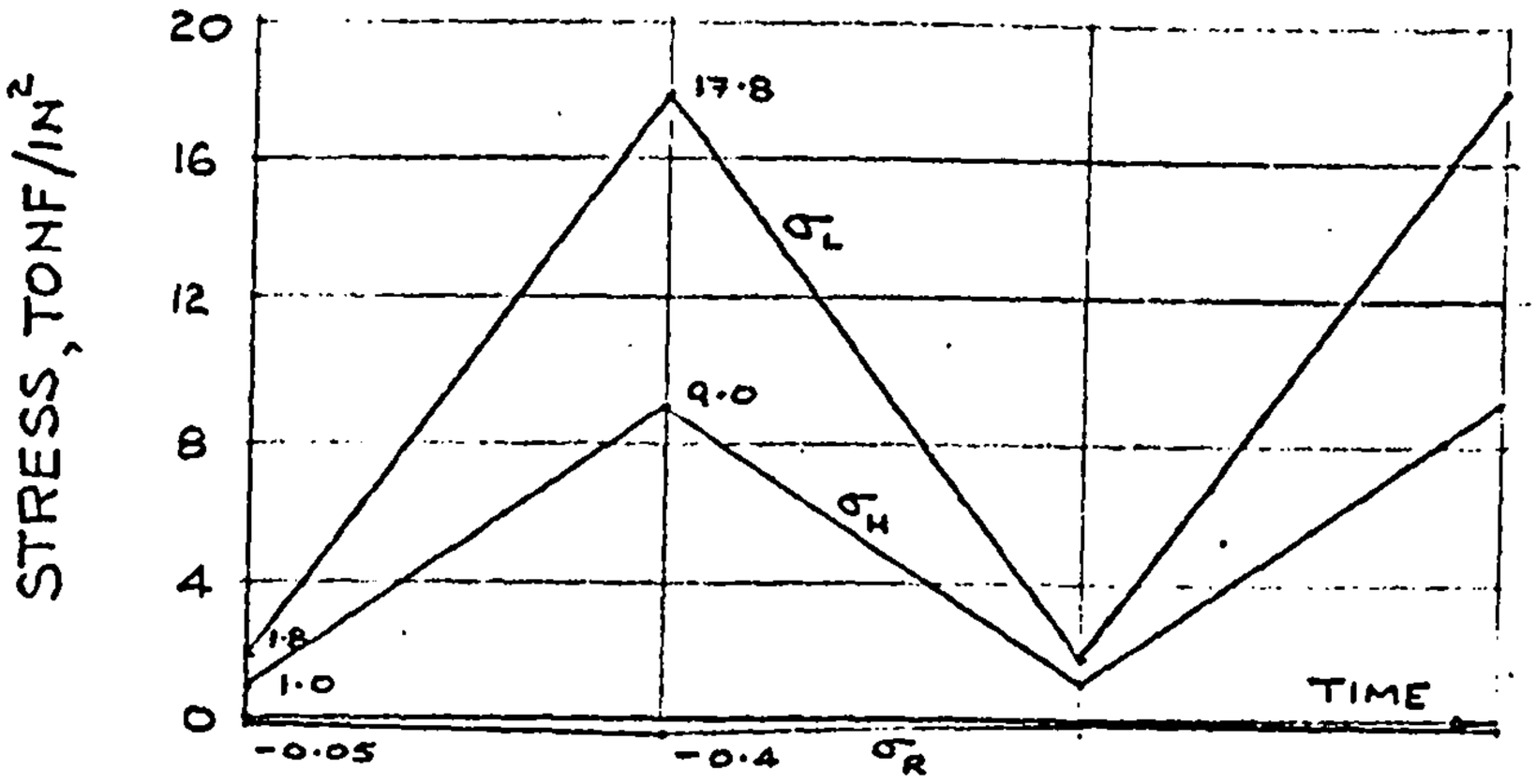

FLUCTUATION OF PRINCIPAL STRESSES

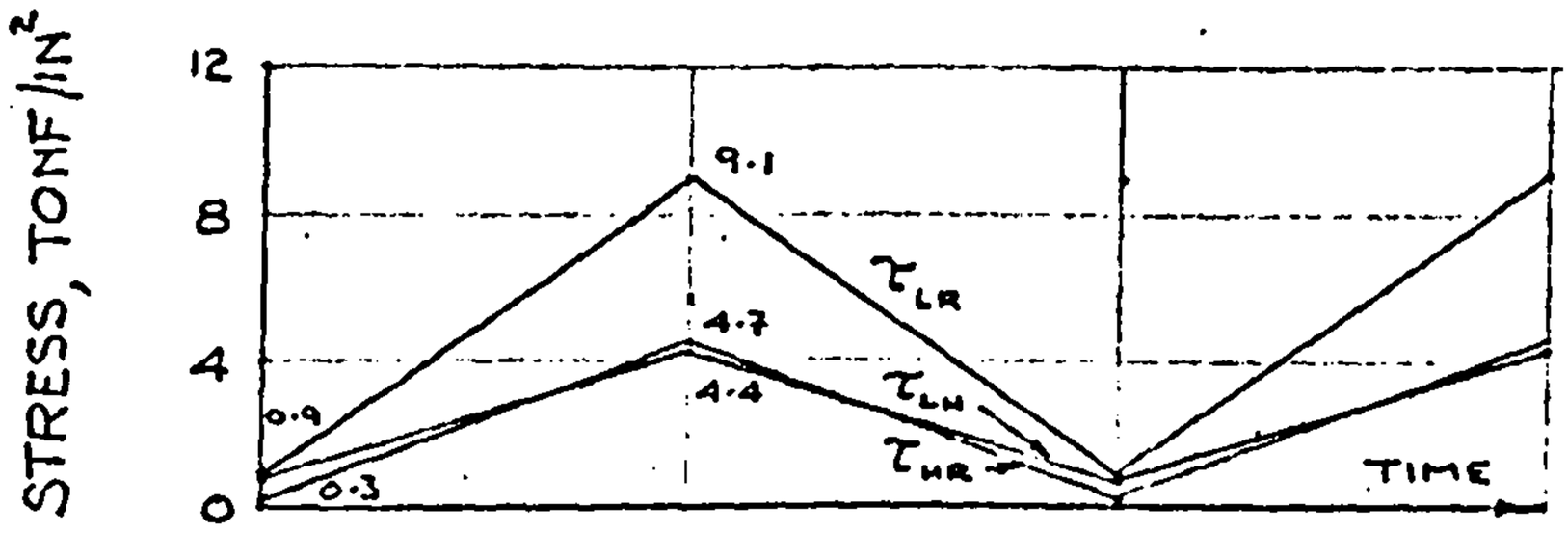

FLUCTUATION OF MAXIMUM SHEAR STRESSES

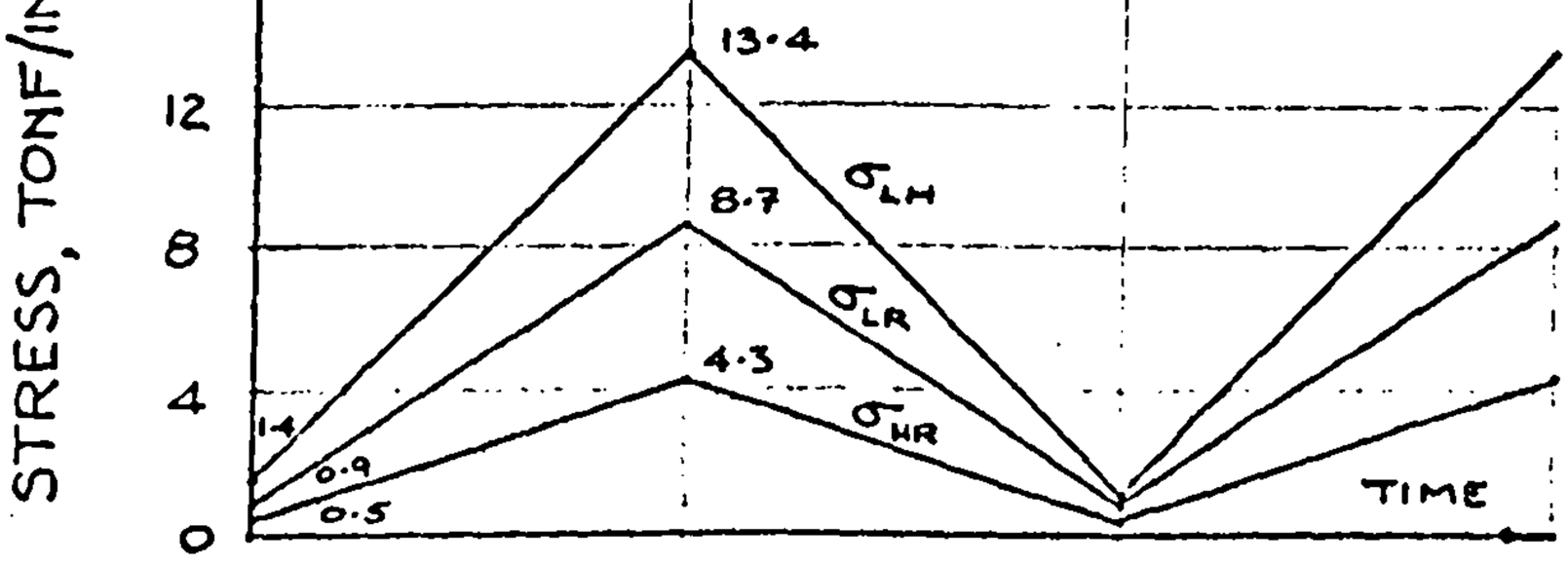

FLUCTUATION OF NORMAL STRESSES ON THE MAXIMUM SHEAR STRESS PLANES

FOR GENERAL NOTES SEE FIGURE 19a.

FIGURE 19b. STRESS-TIME RELATIONS FOR K=0·5 WITH LONGITUDINAL STRESS = 9·8±8·0 TONF/IN².

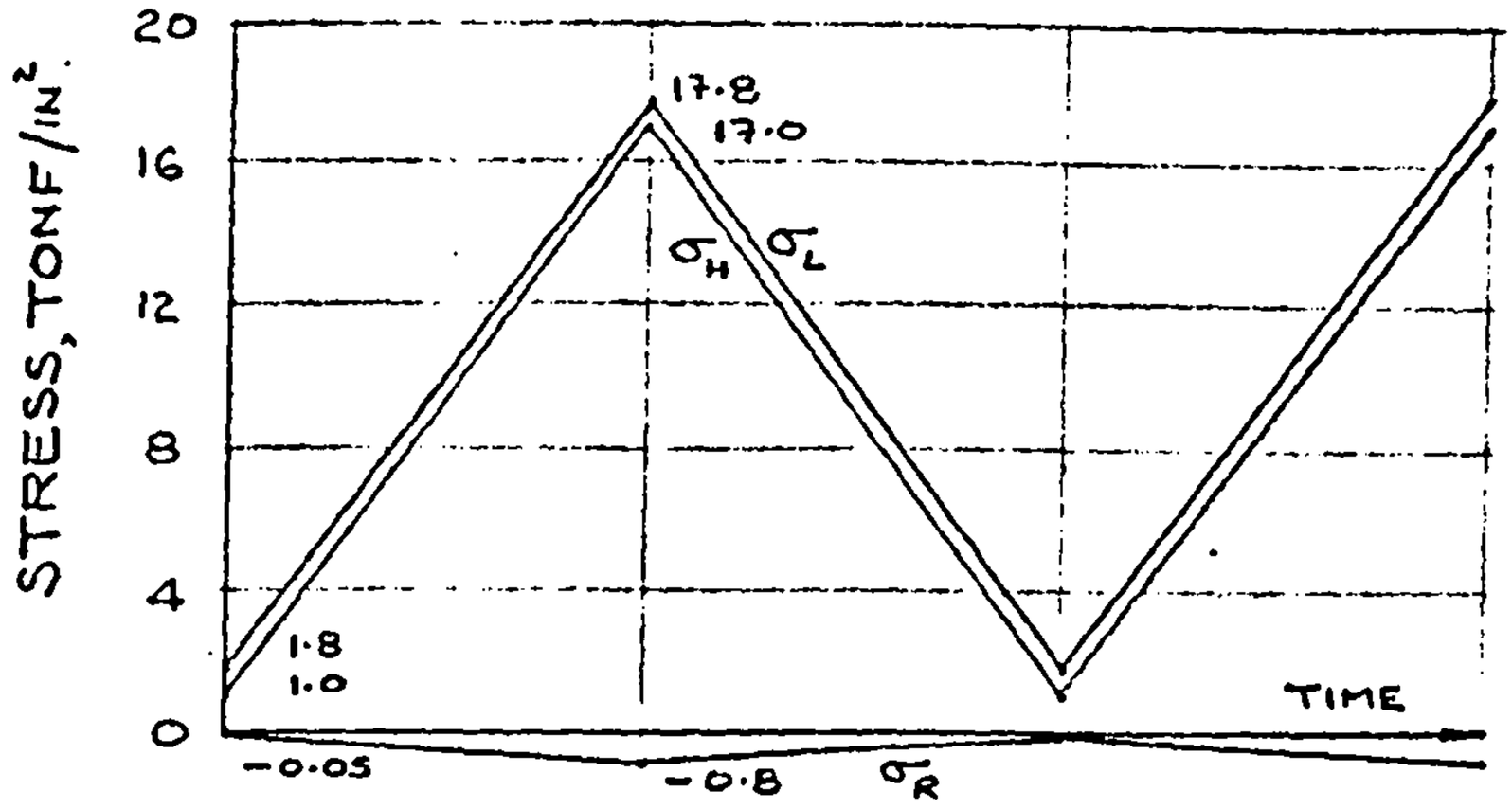

FLUCTUATION OF PRINCIPAL STRESSES

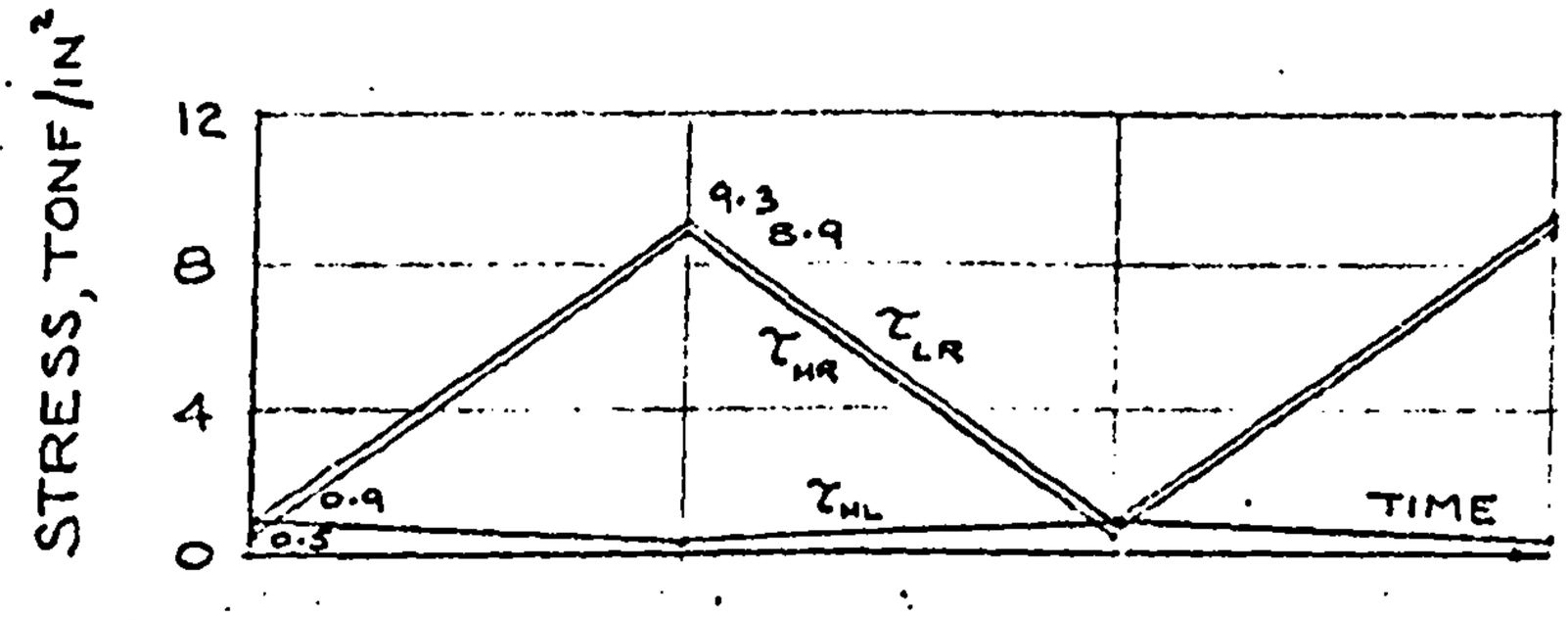

FLUCTUATION OF MAXIMUM SHEAR STRESSES

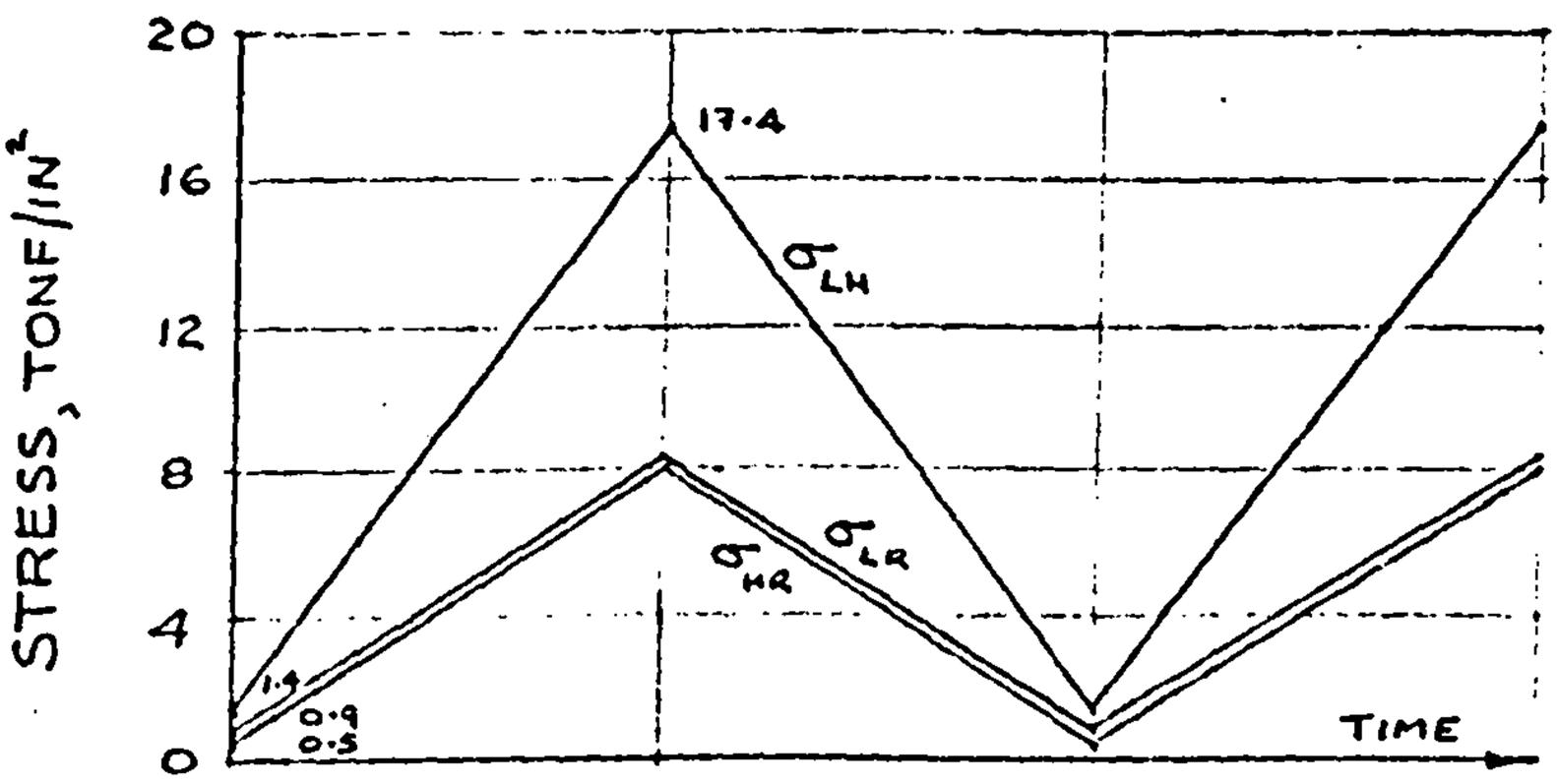

FLUCTUATION OF NORMAL STRESSES ON THE MAXIMUM SHEAR STRESS PLANES.

FOR GENERAL NOTES SEE FIGURE 19a.

FIGURE 19c. STRESS-TIME RELATIONS FOR K=1 WITH HOOP STRESS = 9·0 ± 8·0 TONF/IN².

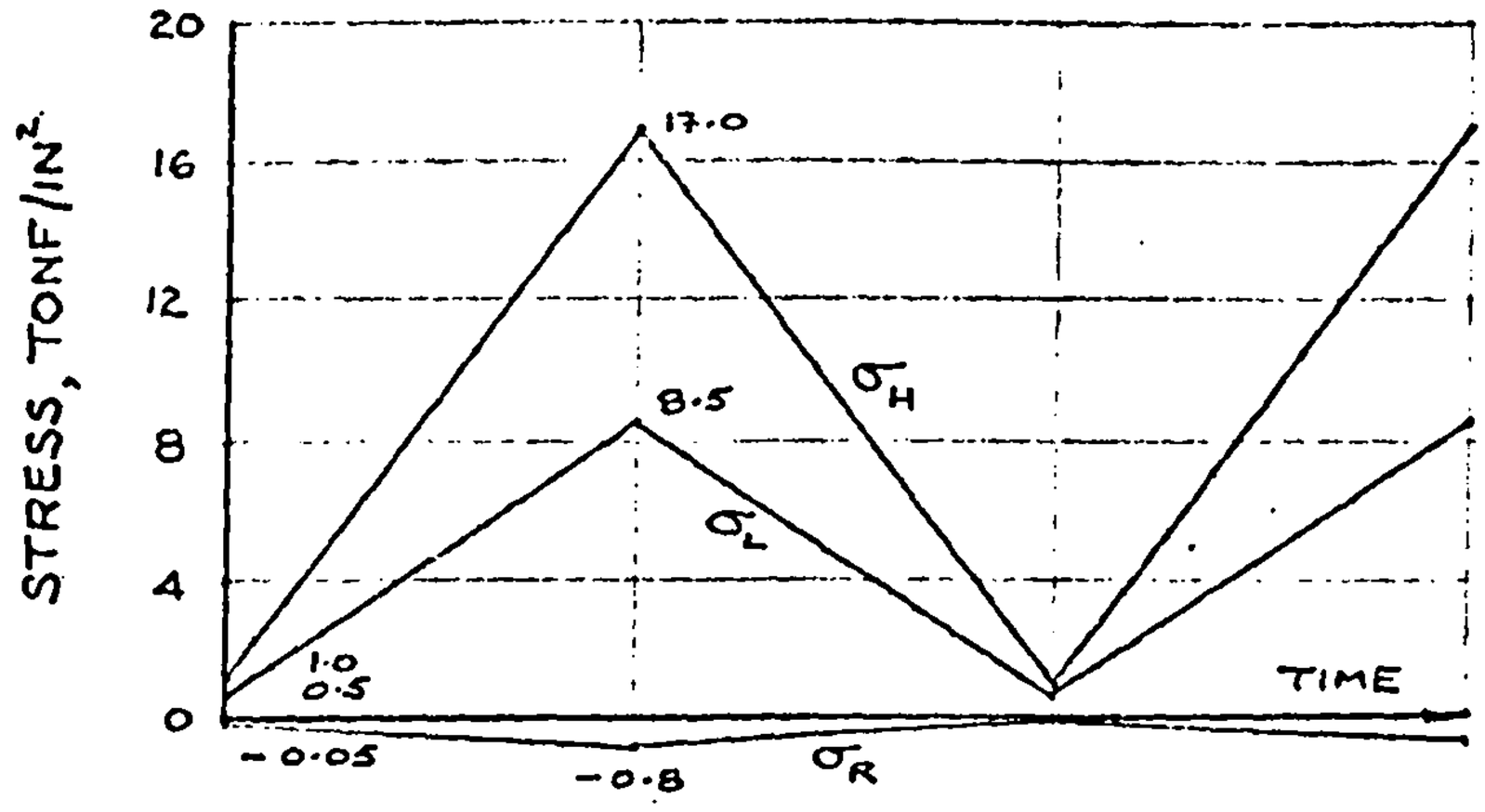

FLUCTUATION OF PRINCIPAL STRESSES

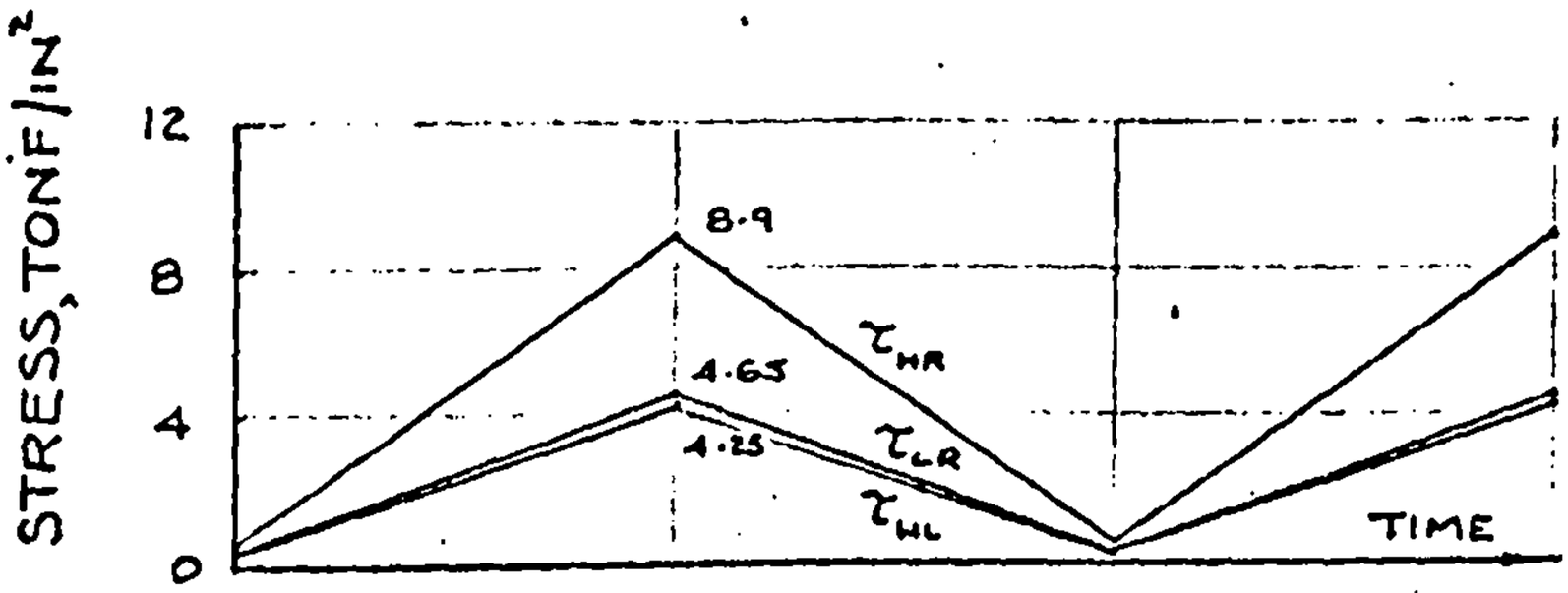

FLUCTUATION OF MAXIMUM SHEAR STRESSES

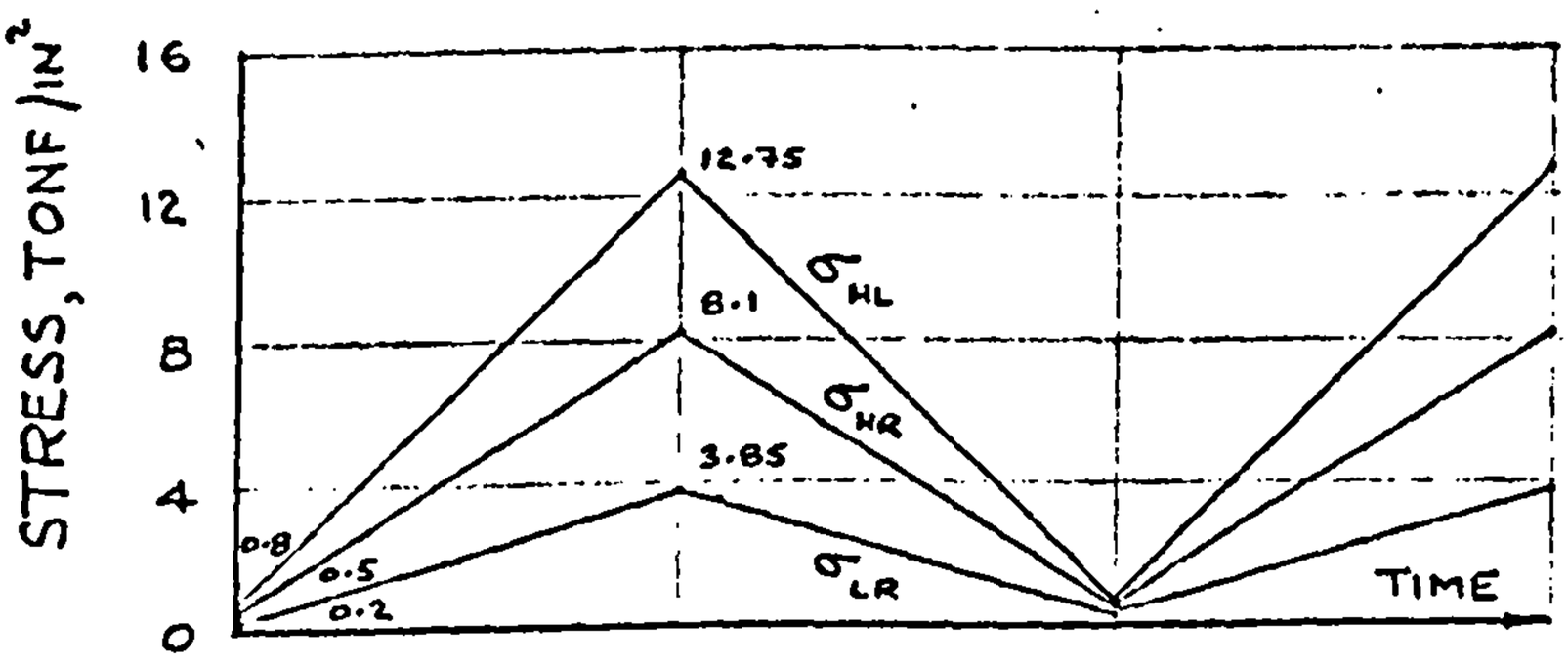

FLUCTUATION OF NORMAL STRESSES ON THE MAXIMUM SHEAR STRESS PLANES

FOR GENERAL NOTES SEE FIGURE 19a.

FIGURE 19d. STRESS-TIME RELATIONS FOR K=2 WITH HOOP STRESS = 9.0±8.0 TONF/IN².

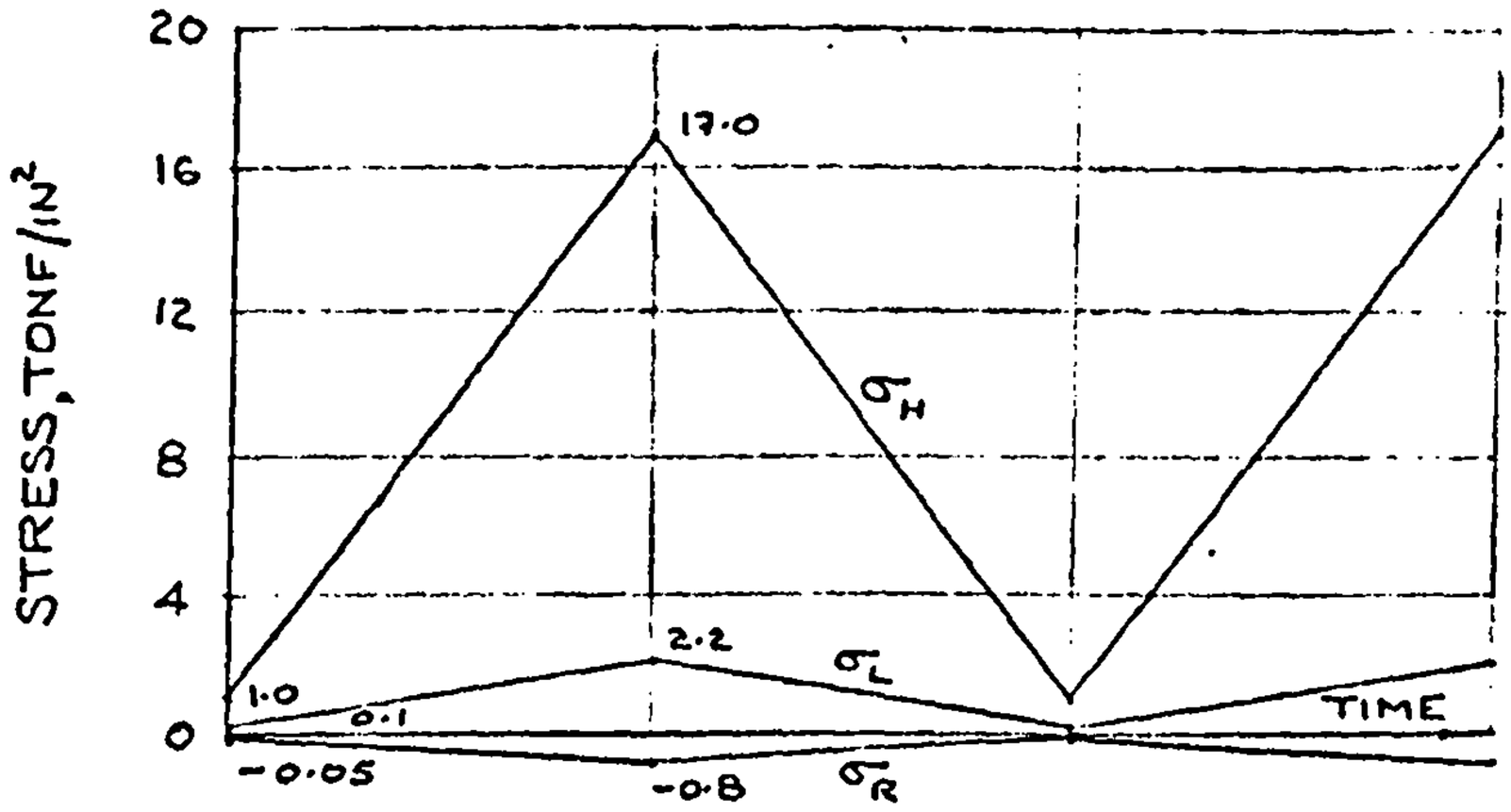

FLUCTUATION OF PRINCIPAL STRESSES

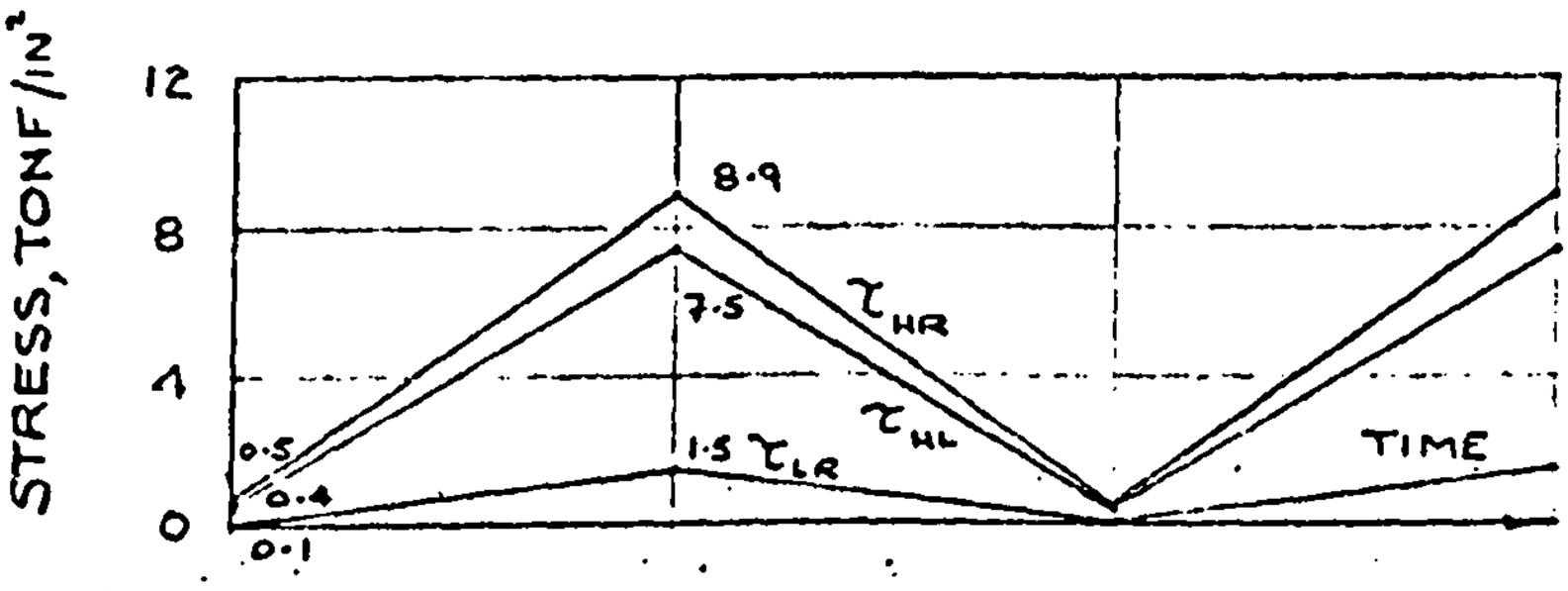

FLUCTUATION OF MAXIMUM SHEAR STRESSES

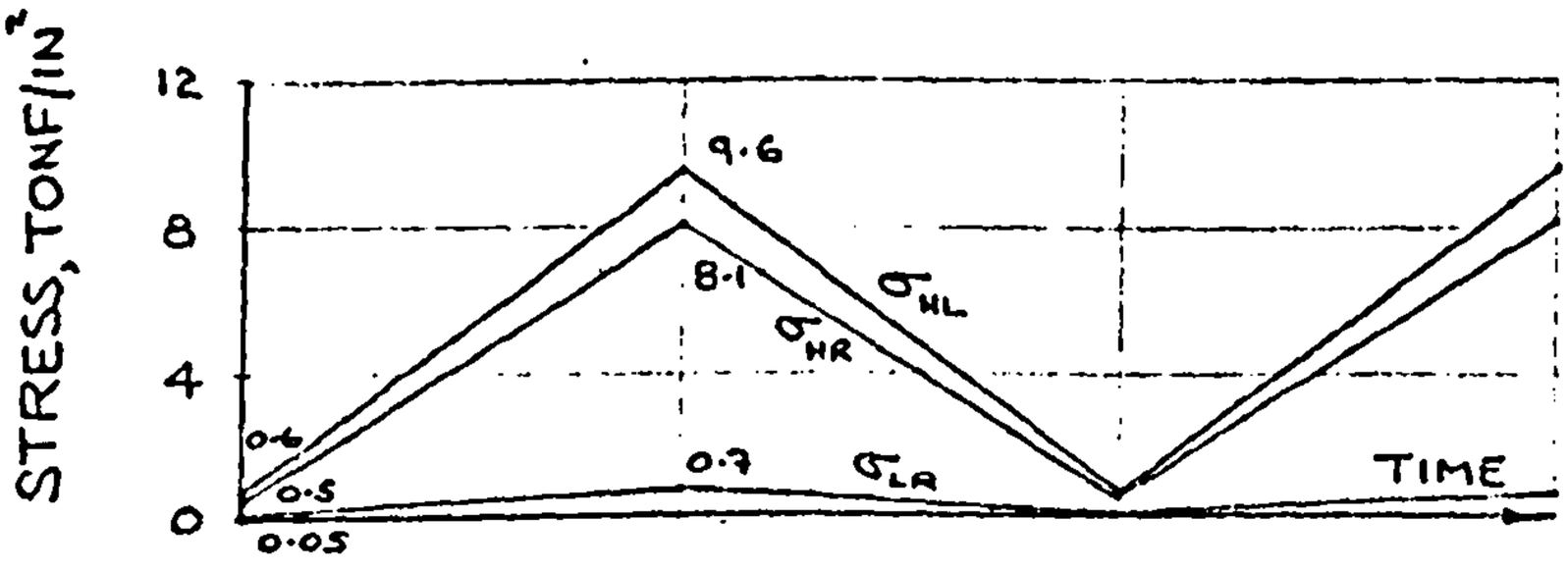

FLUCTUATION OF NORMAL STRESSES ON THE MAXIMUM SHEAR STRESS PLANES.

FOR GENERAL NOTES SEE FIGURE 19a.

FIGURE 19e. STRESS-TIME RELATIONS FOR K=7.9 WITH HOOP STRESS = 9.0 ± 8.0 TONF/IN².

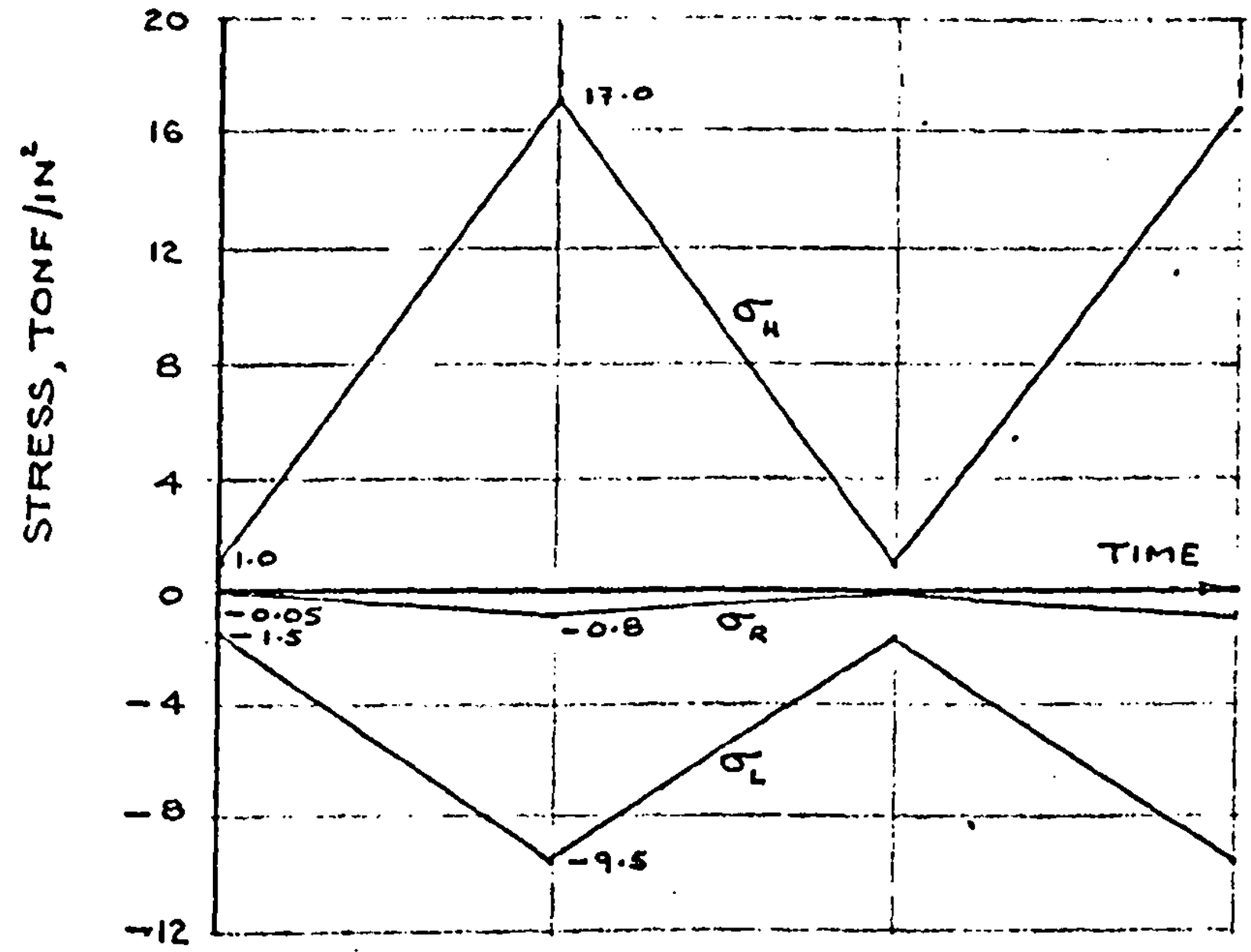

FLUCTUATION OF PRINCIPAL STRESSES

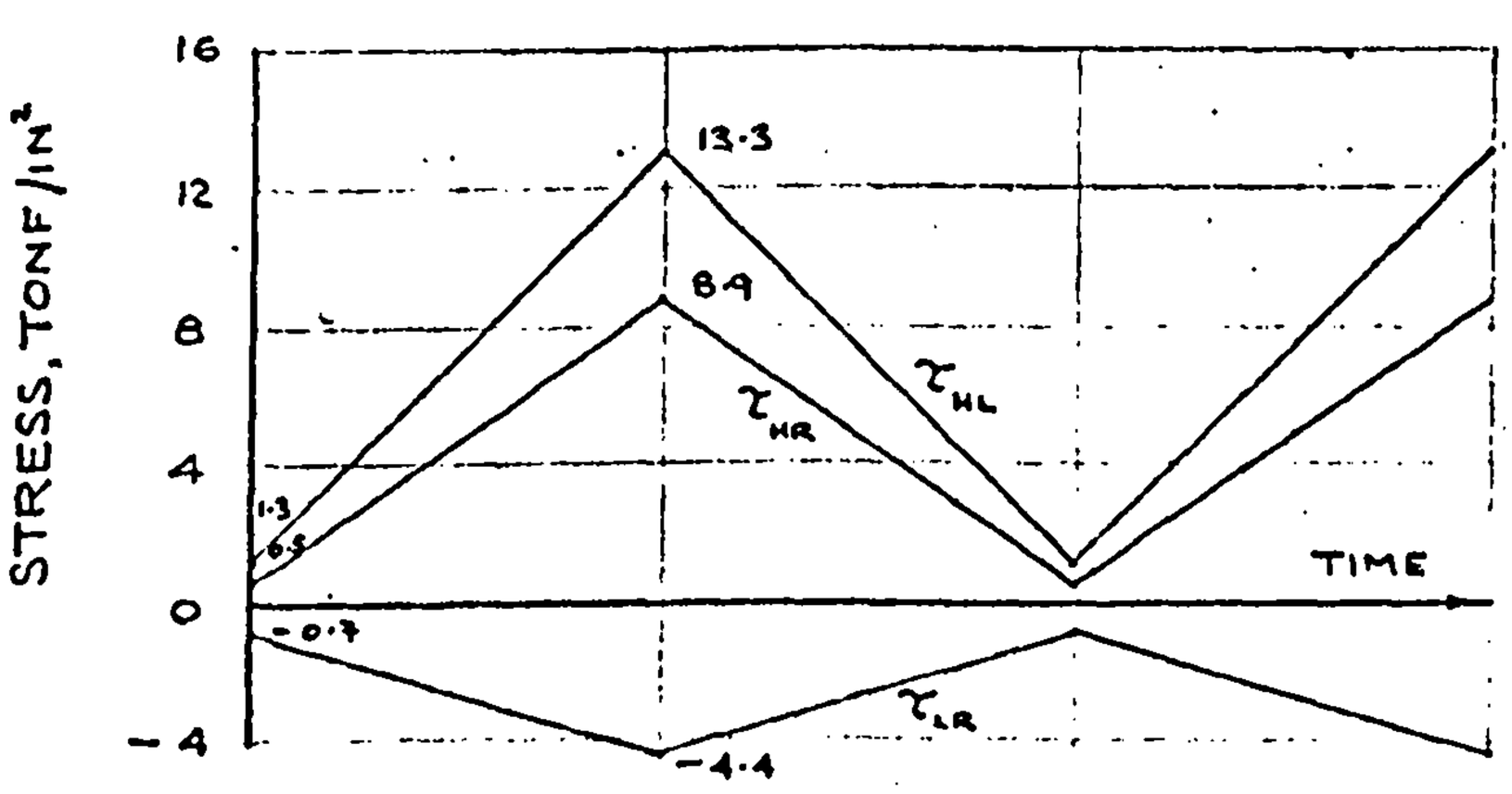

FLUCTUATION OF MAXIMUM SHEAR STRESSES

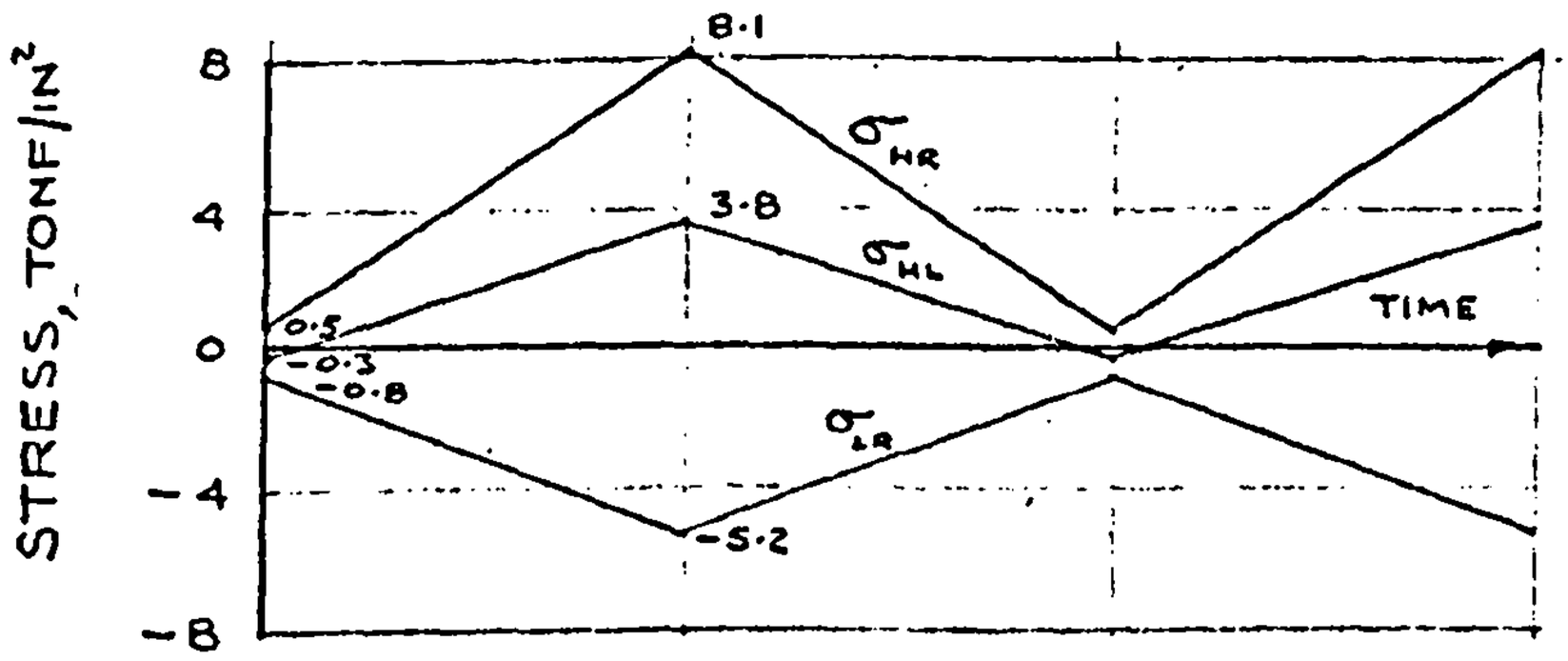

FLUCTUATION OF NORMAL STRESSES ON
THE MAXIMUM SHEAR STRESS PLANES

FOR GENERAL NOTES SEE FIGURE 19a.

FIGURE 19f. STRESS-TIME RELATIONS FOR K=-2
WITH HOOP STRESS = 9.0 ± 8.0 TONF/IN².

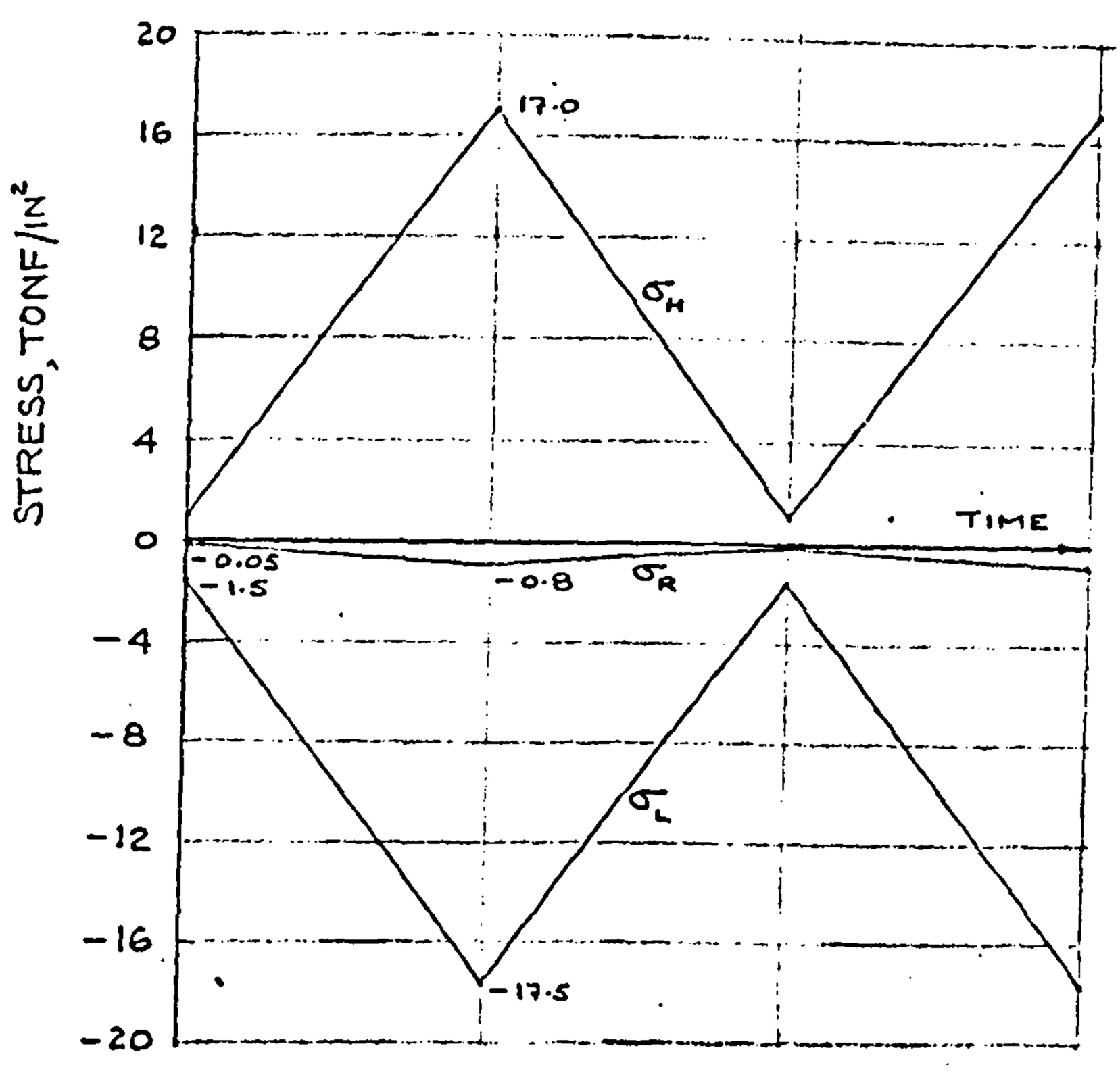

FLUCTUATION OF PRINCIPAL STRESSES

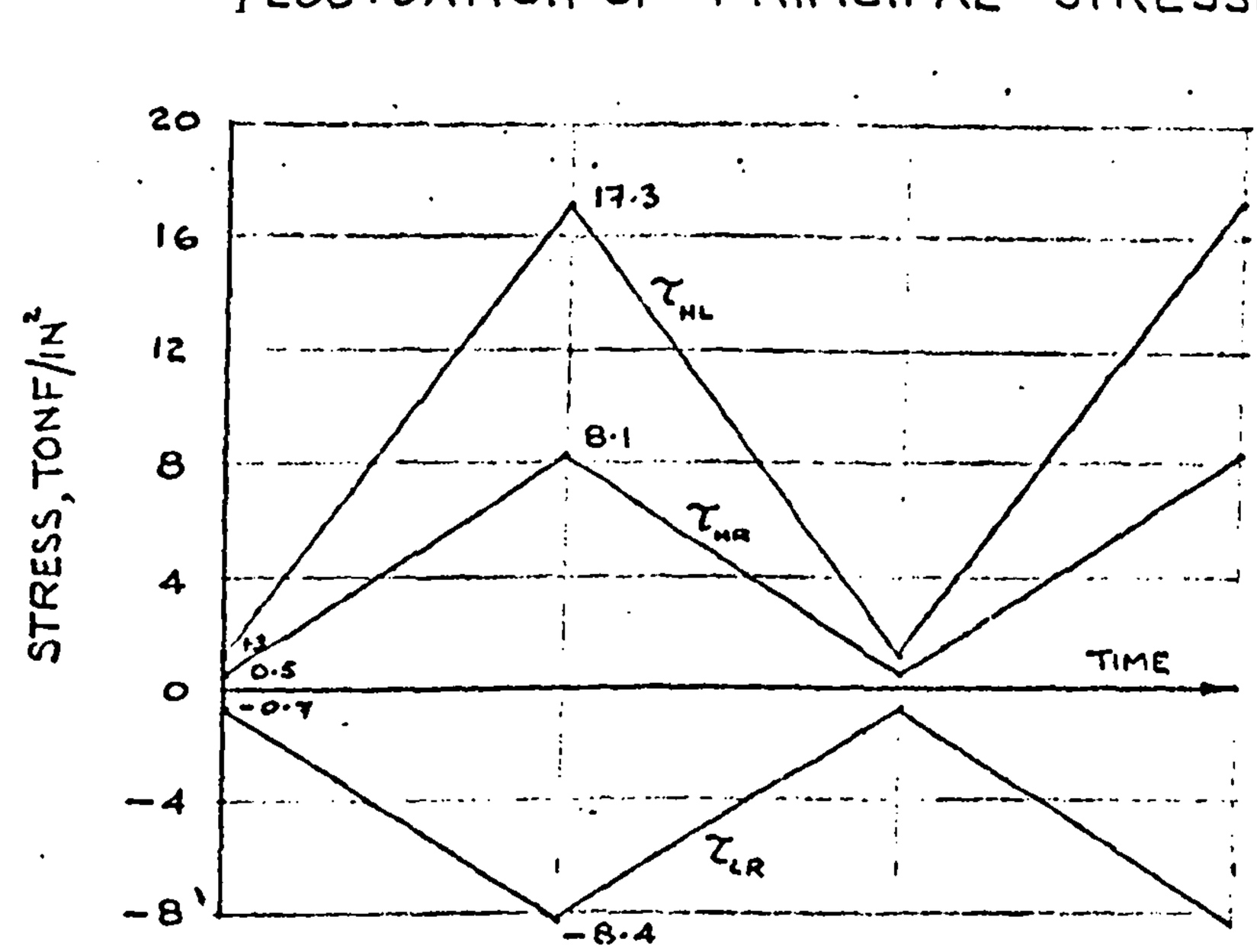

FLUCTUATION OF MAXIMUM SHEAR STRESSES

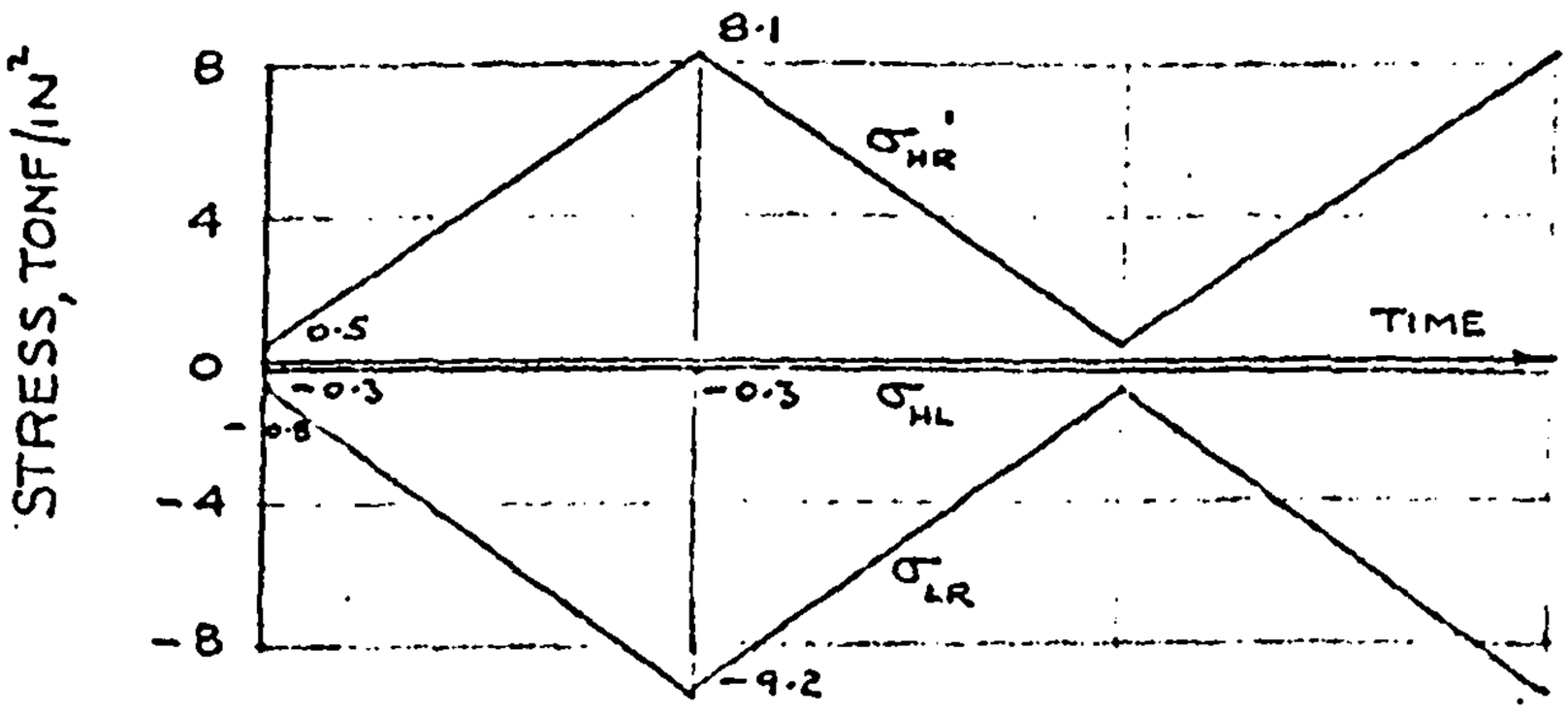

FLUCTUATION OF NORMAL STRESSES ON THE MAXIMUM SHEAR STRESS PLANES

FOR GENERAL NOTES SEE FIGURE 19a.

FIGURE 19g. STRESS-TIME RELATIONS FOR K=-1 WITH HOOP STRESS = 9.0 ± 8.0 TONF/IN²

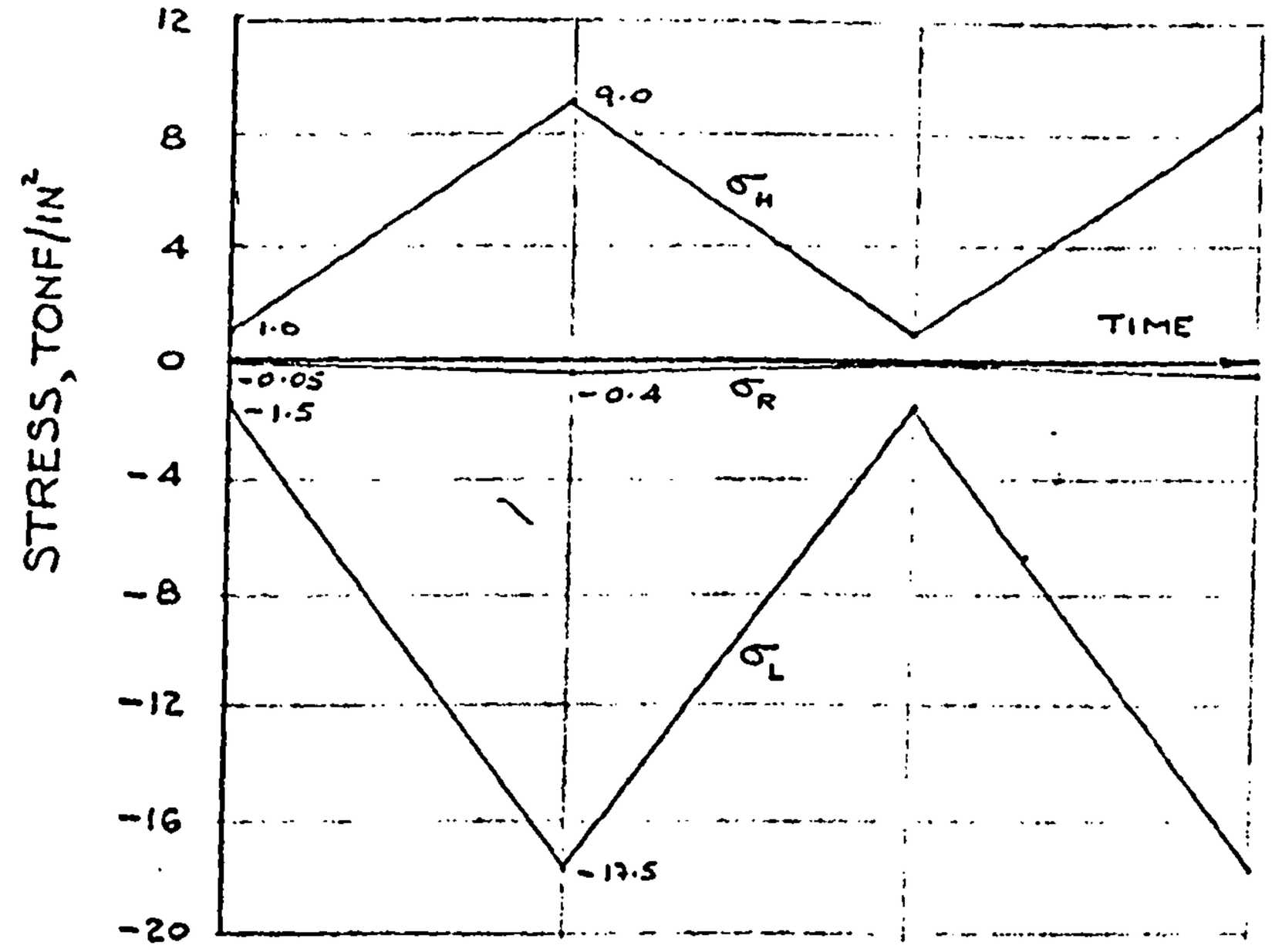

FLUCTUATION OF PRINCIPAL STRESSES

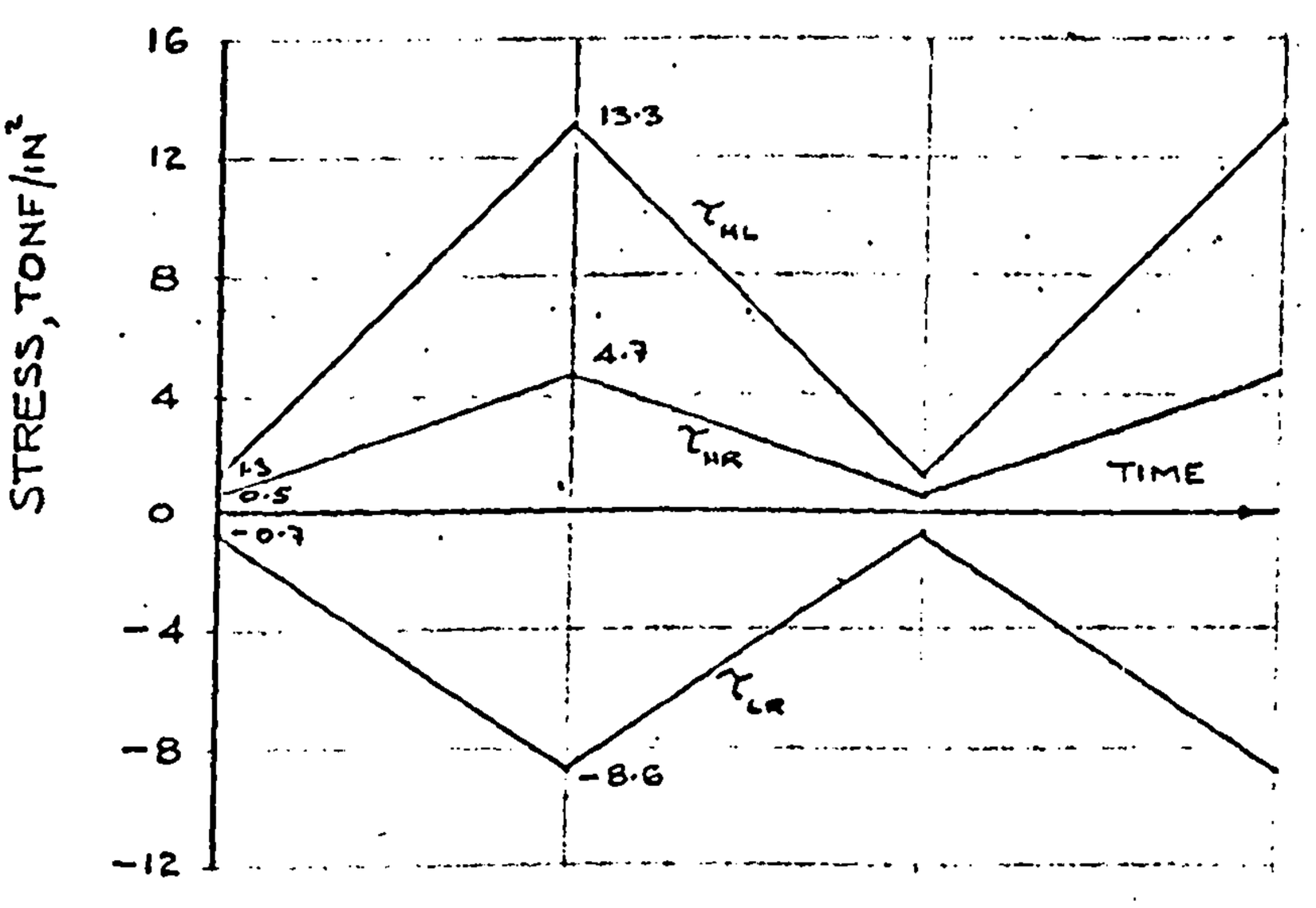

FLUCTUATION OF MAXIMUM SHEAR STRESSES

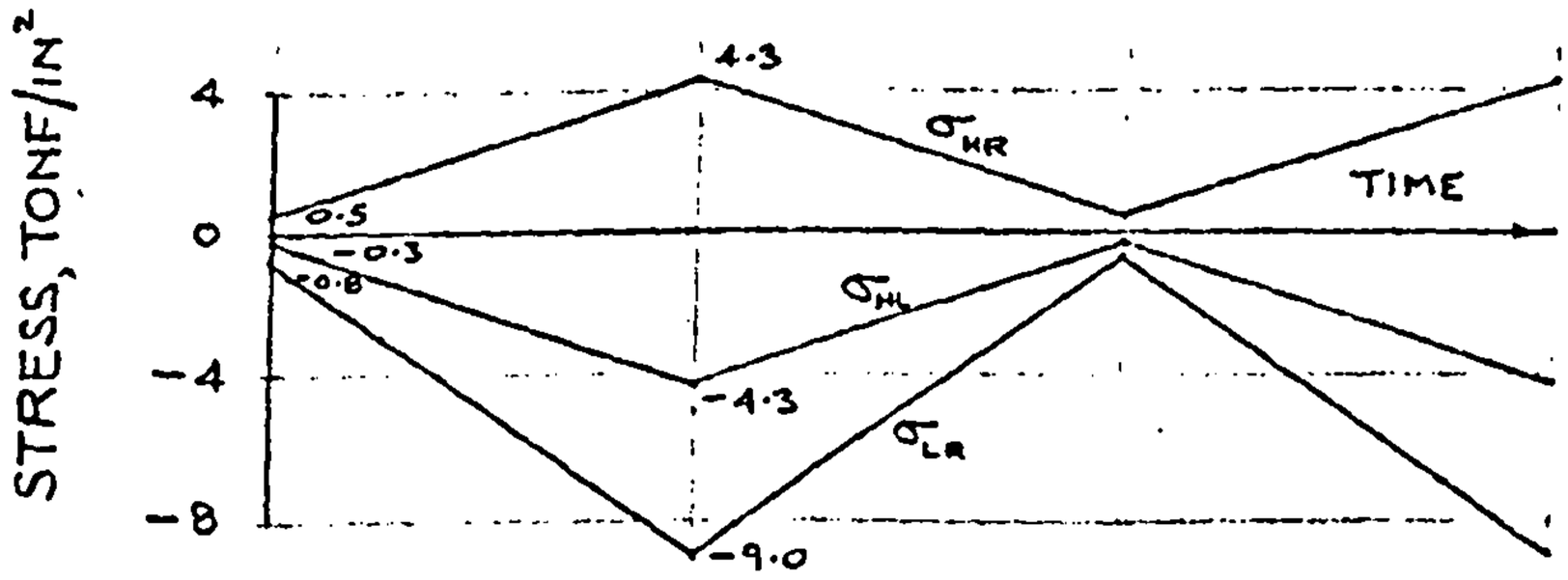

FLUCTUATION OF NORMAL STRESSES ON
THE MAXIMUM SHEAR STRESS PLANES

FOR GENERAL NOTES SEE FIGURE 19a.

FIGURE 19h. STRESS-TIME RELATIONS FOR K=-0.5

WITH LONGITUDINAL STRESS = -9.5 ± 8.0 TONF/IN².

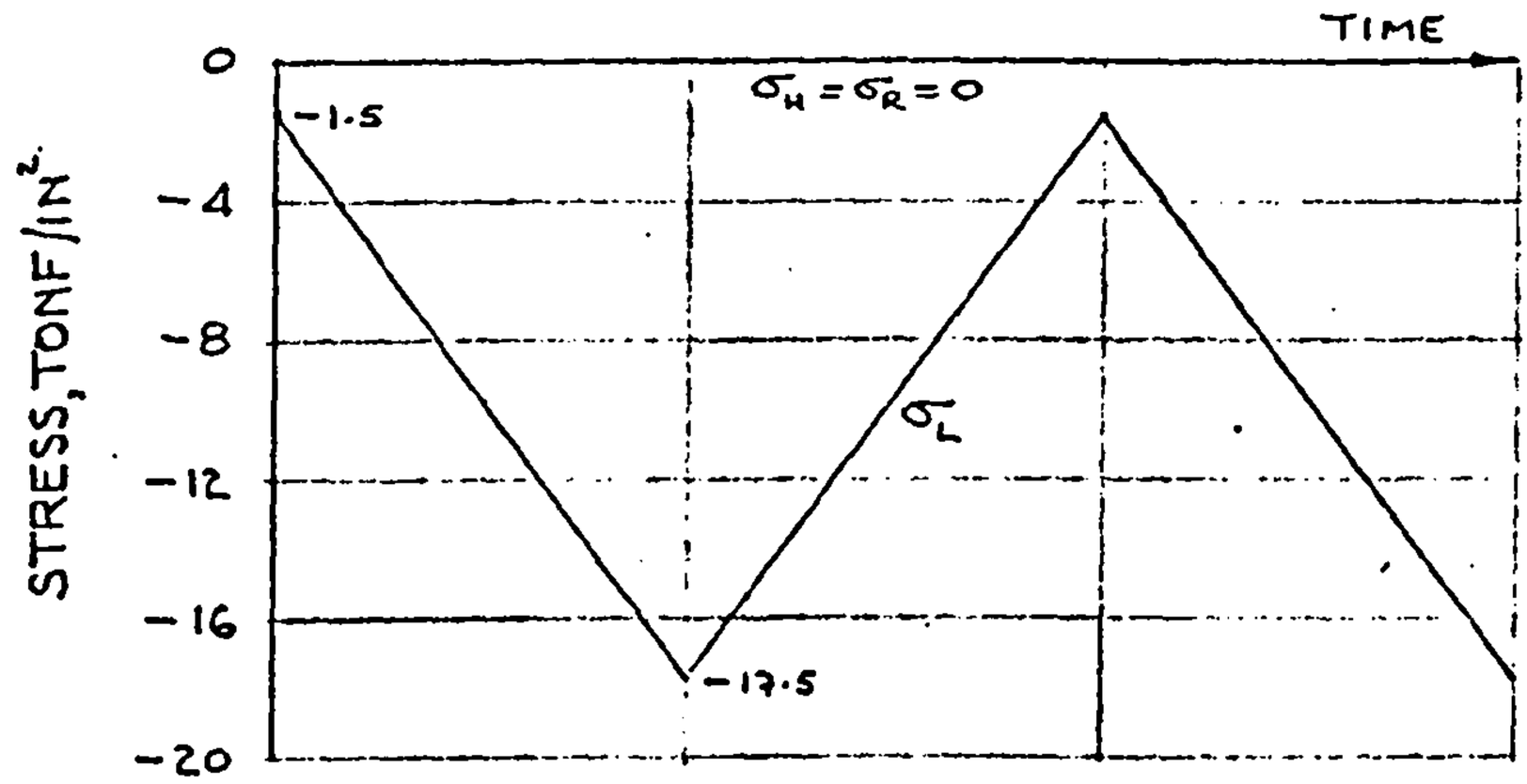

FLUCTUATION OF PRINCIPAL STRESSES

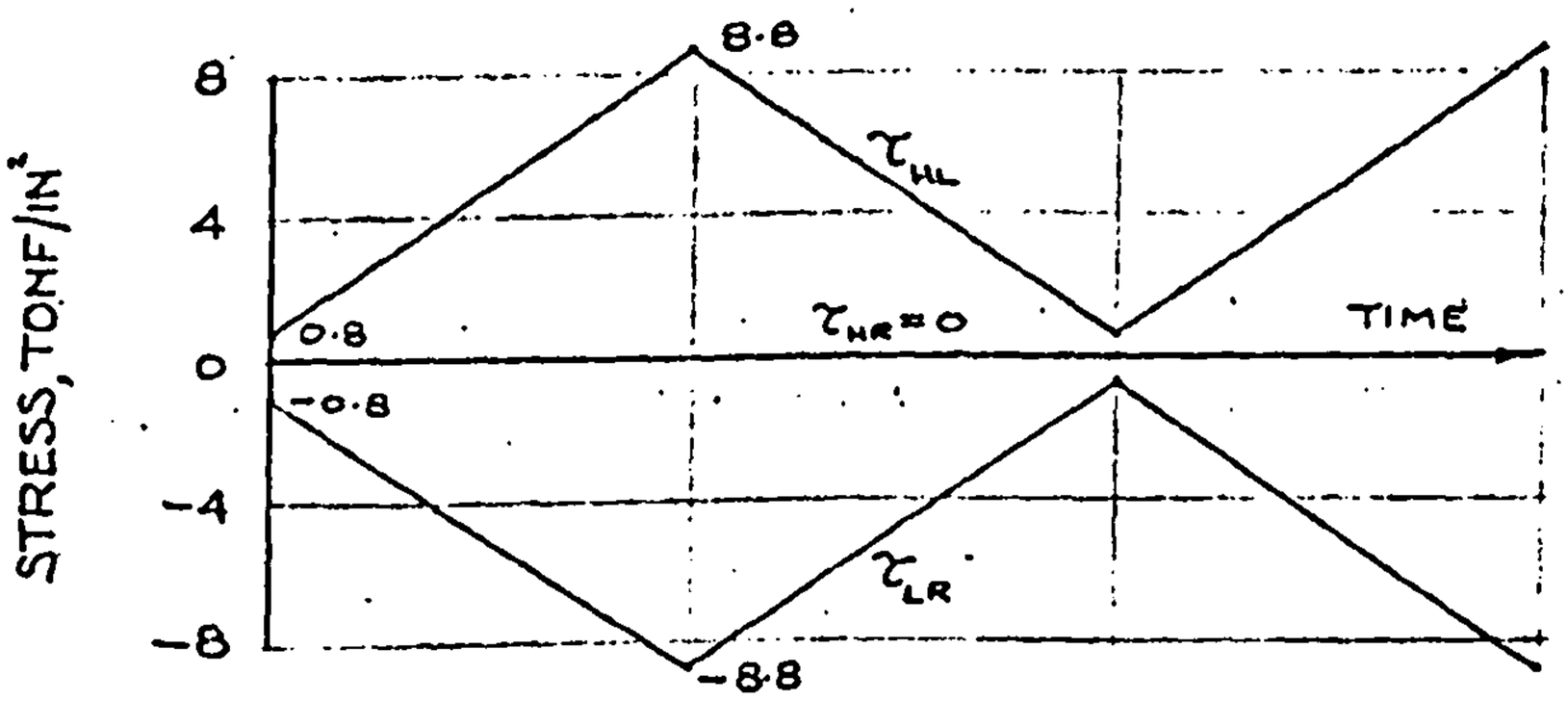

FLUCTUATION OF MAXIMUM SHEAR STRESSES

FLUCTUATION OF NORMAL STRESSES ON THE MAXIMUM SHEAR STRESS PLANES

FOR GENERAL NOTES SEE FIGURE 19a.

FIGURE 19j. STRESS-TIME RELATIONS FOR K=-0 WITH LONGITUDINAL STRESS = 9.5±8.0 TONF/IN²

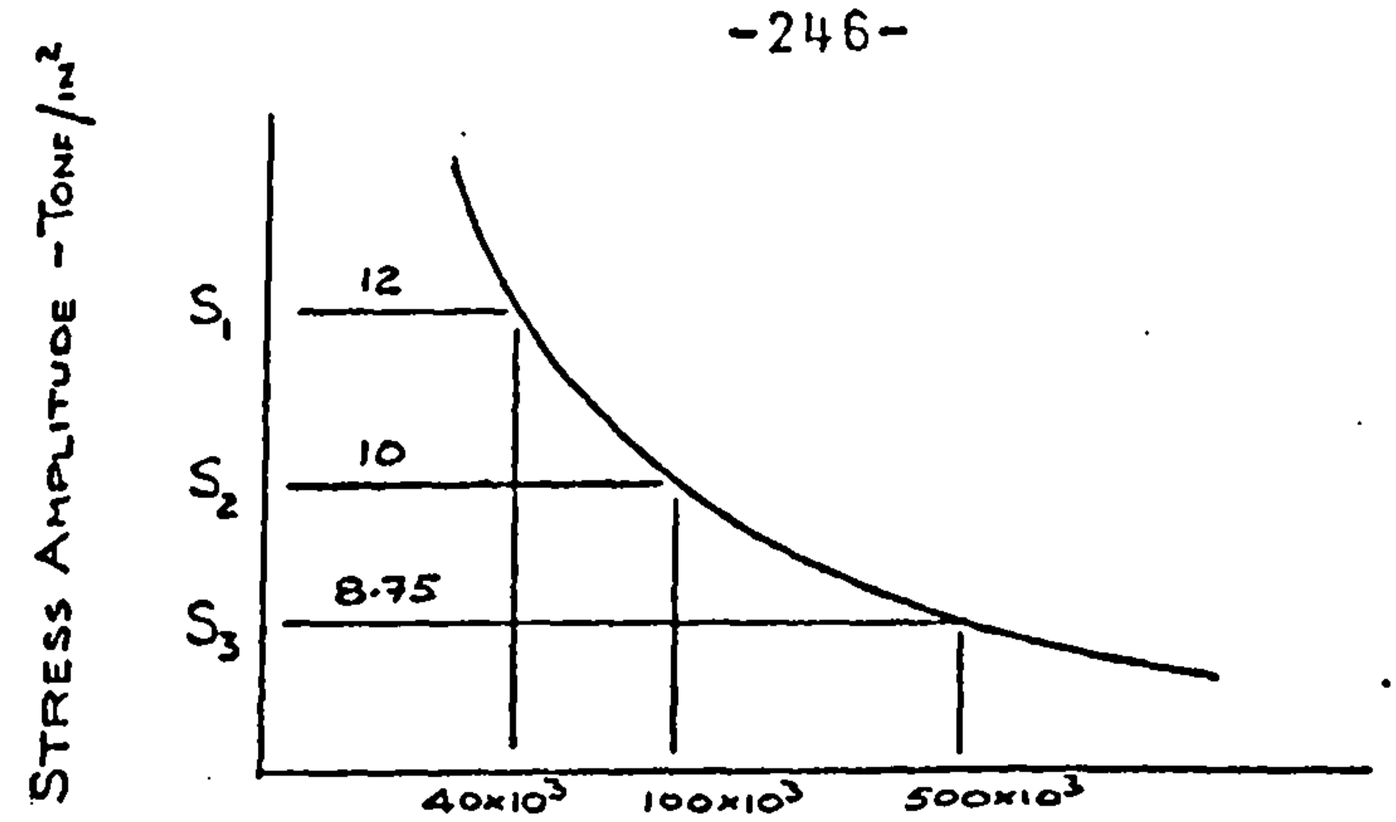

K = 0

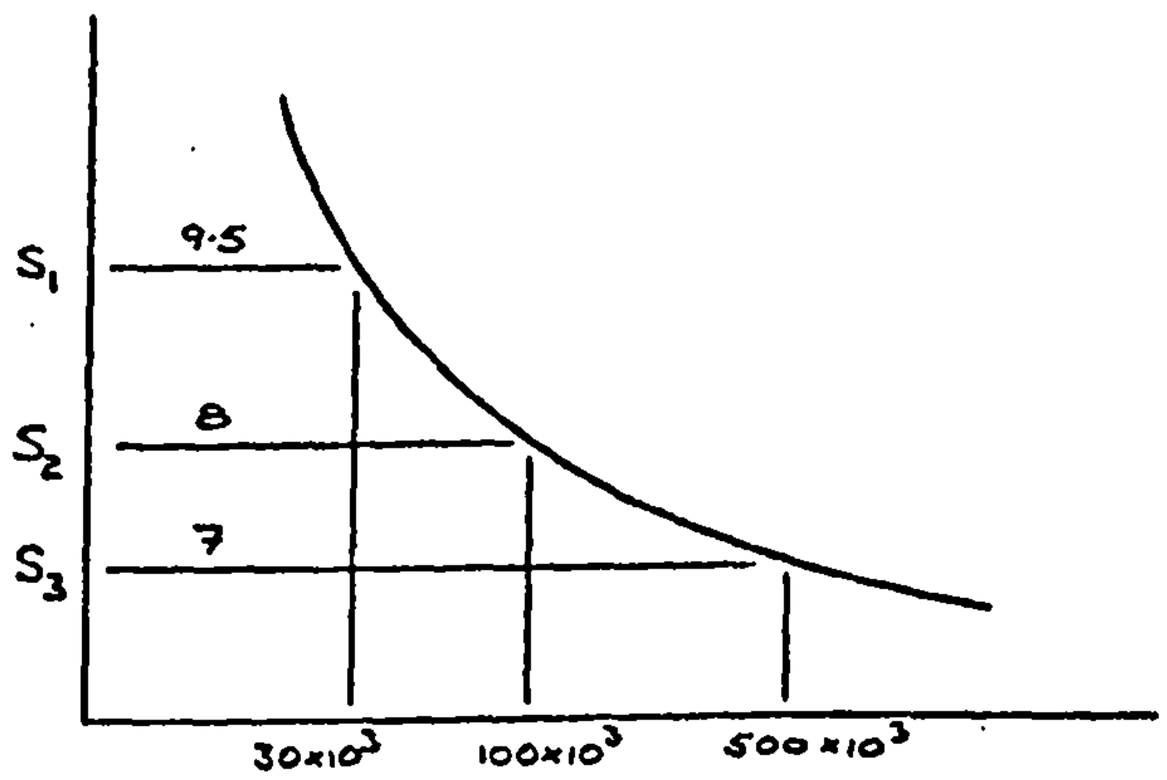

K = 2

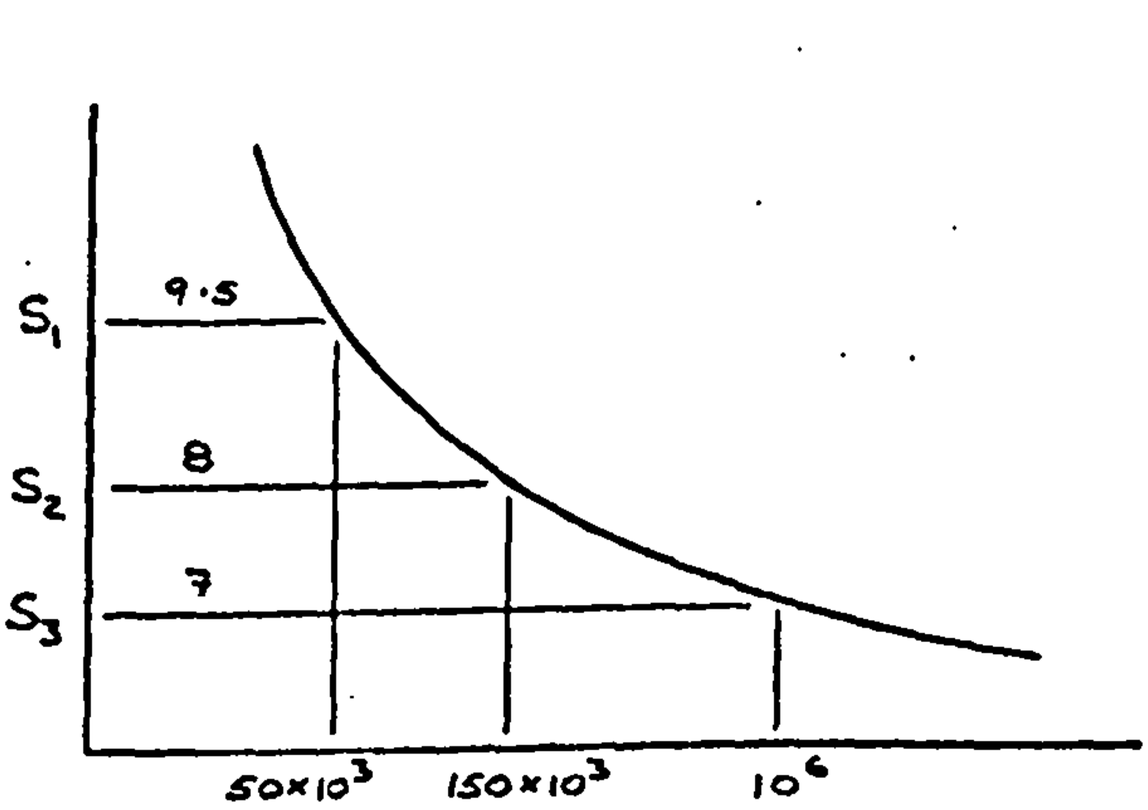

K = 7·9

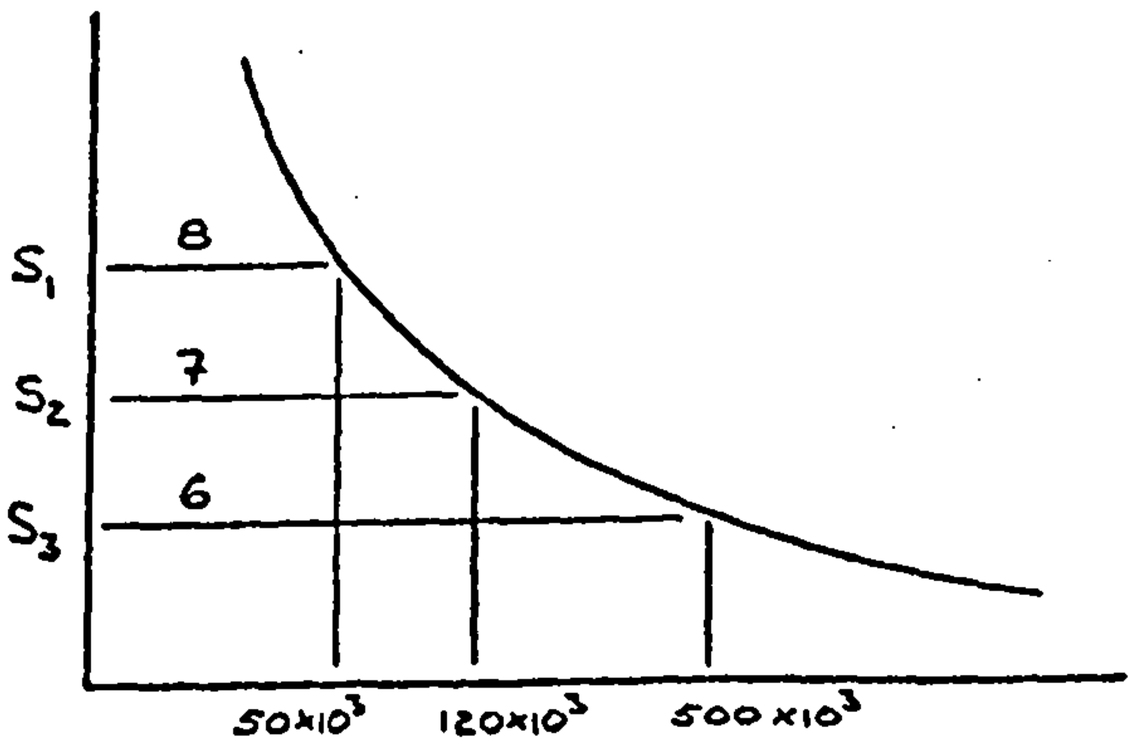

K = − 1.

FIGURE 20. STRESS LEVELS FOR CONSTANT K PROGRAMME TESTS.

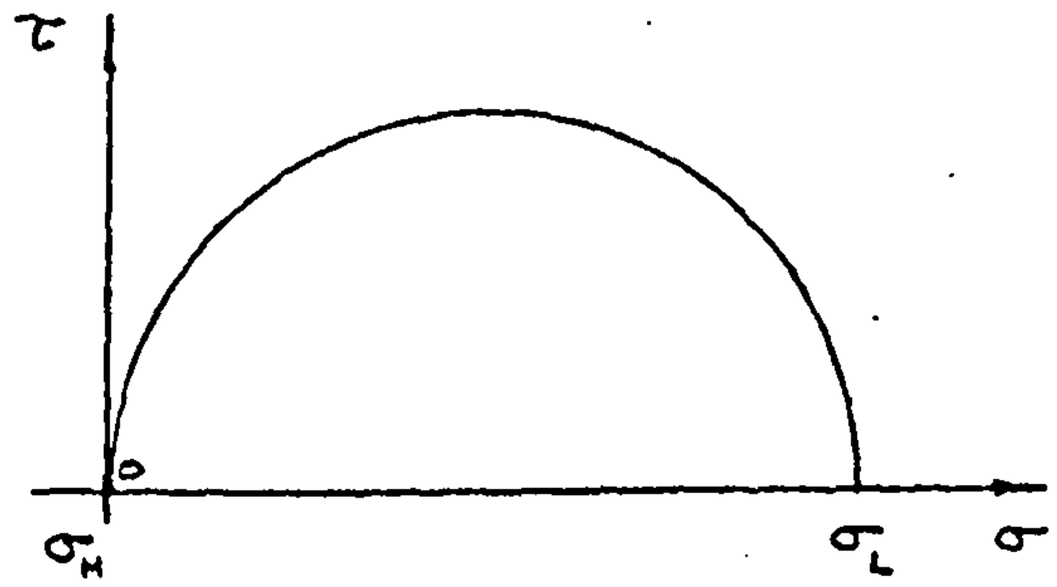

K = 0

$\hat{\tau}$ PLANES : LR, LH

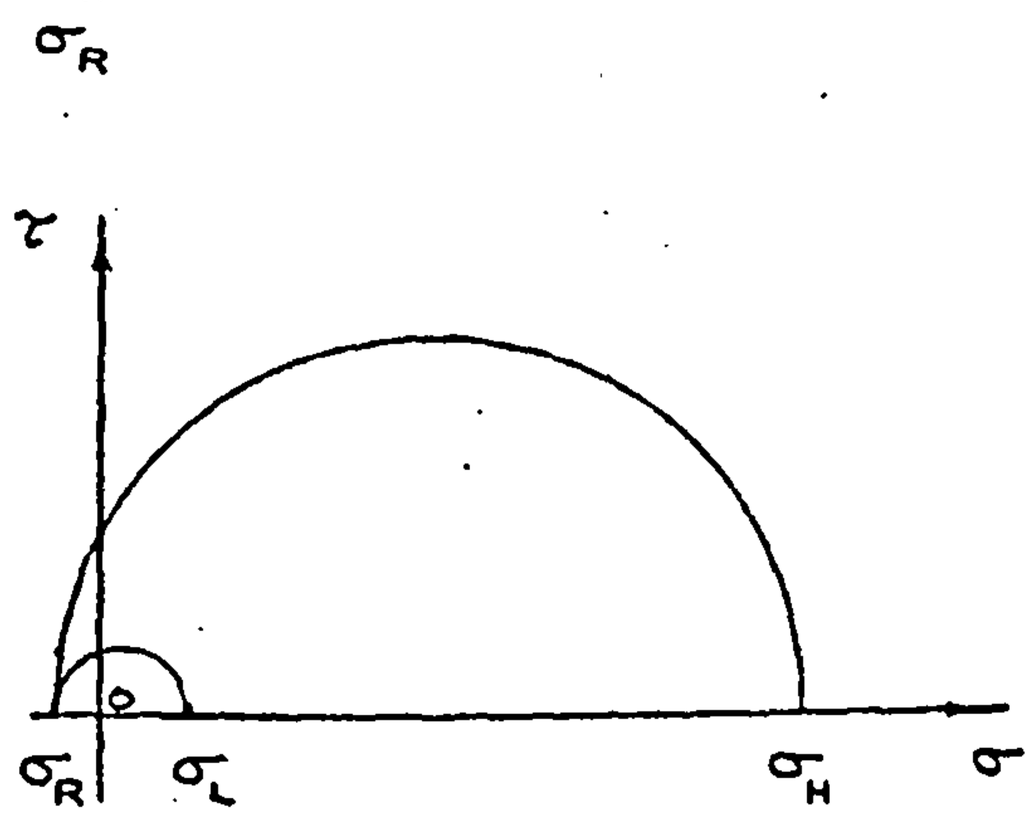

K = 7·9

$\hat{\tau}$ PLANE : HR

K = 0 AND 7·9

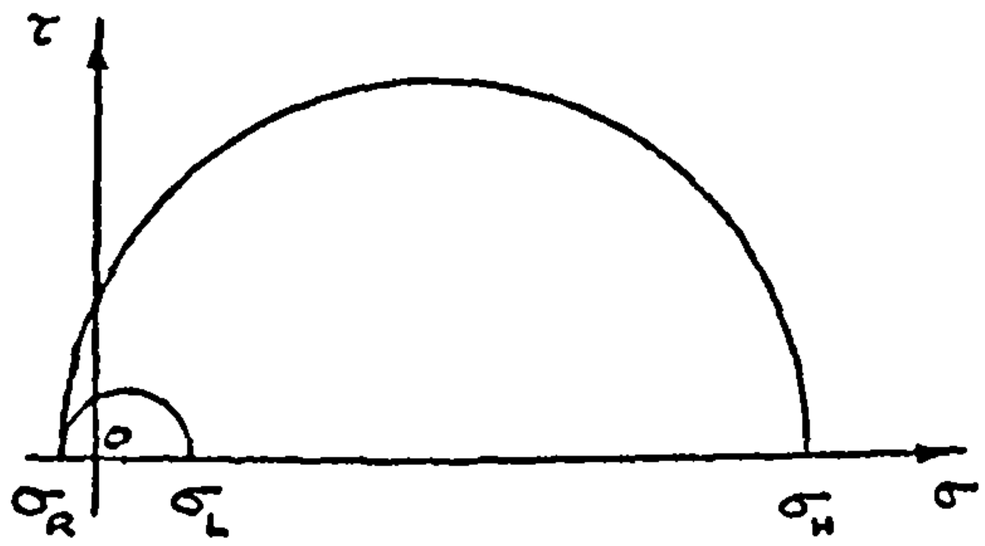

K = 7·9

$\hat{\tau}$ PLANE : HR

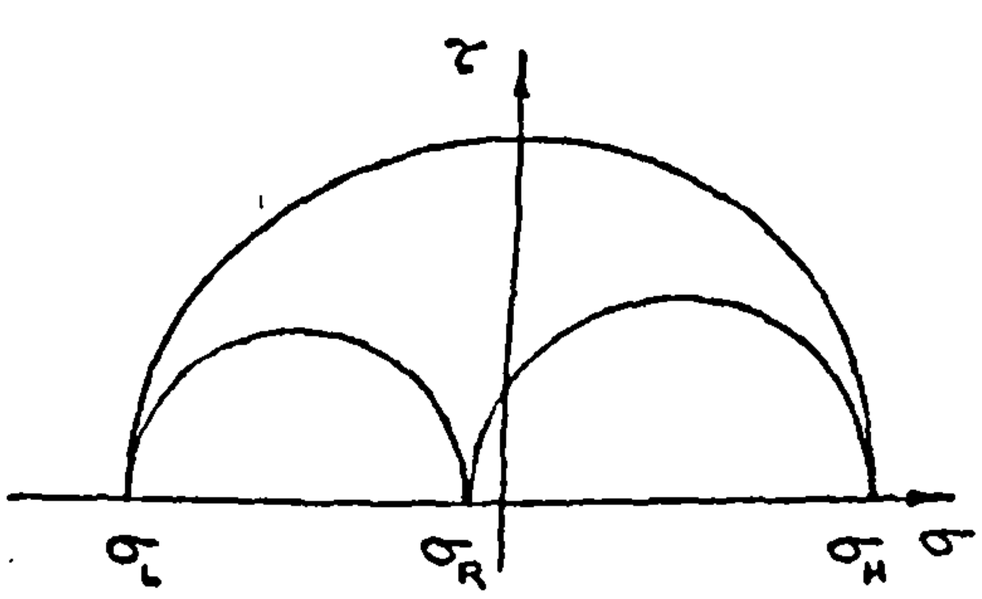

K = − 1

$\hat{\tau}$ PLANE : LH

K = 7·9 AND − 1

FIGURE 21. MOHR STRESS CIRCLES FOR VARIABLE K PROGRAMME TESTS.

σ_R

K = 0

$\hat{\tau}$ PLANES : LR, LH.

K = − 1

$\hat{\tau}$ PLANE : LH

K = 0 AND − 1

FIGURE 21 (CONT.) MOHR STRESS CIRCLES FOR VARIABLE K PROGRAMME TESTS.

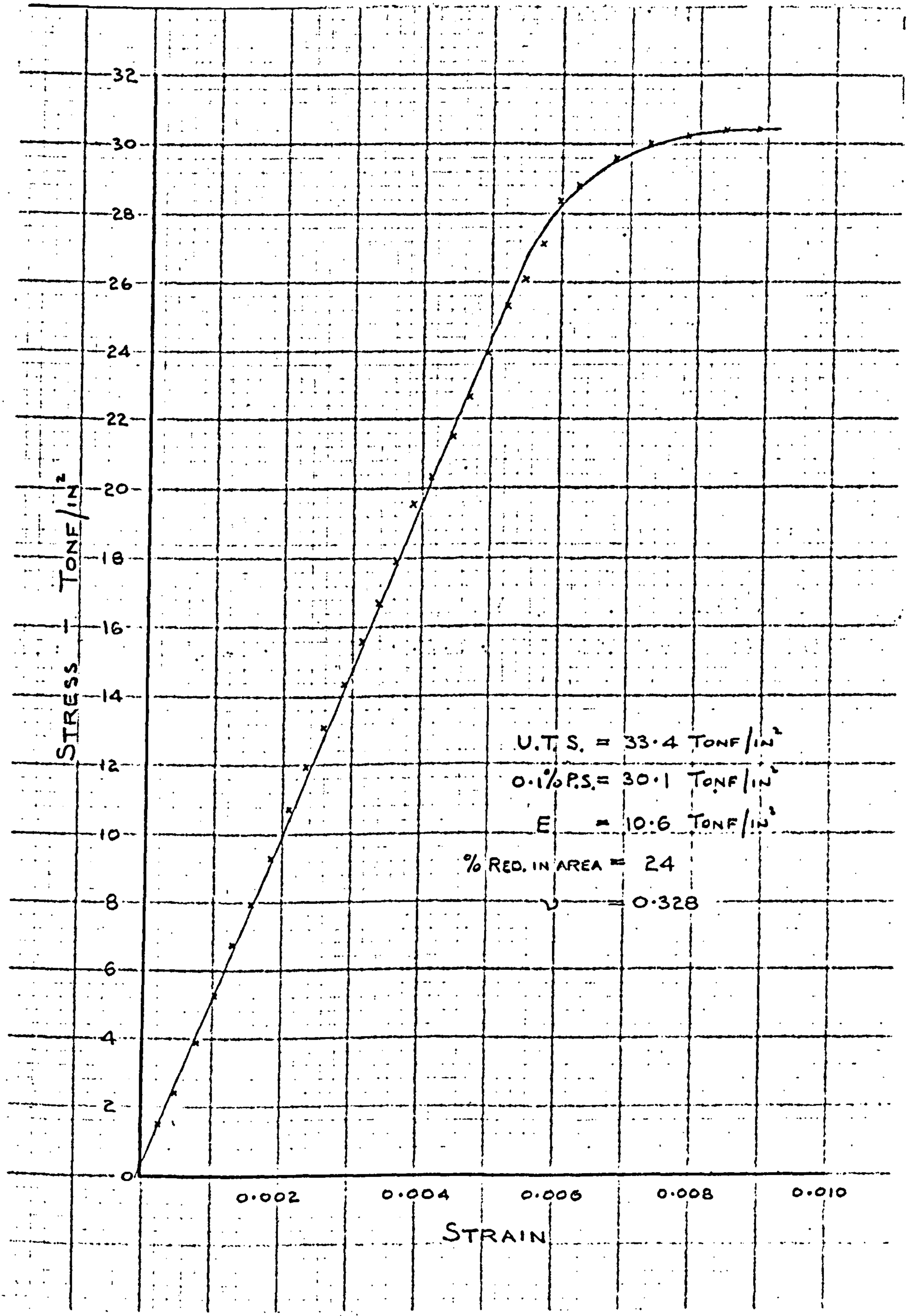

FIGURE 22. TENSILE TEST.

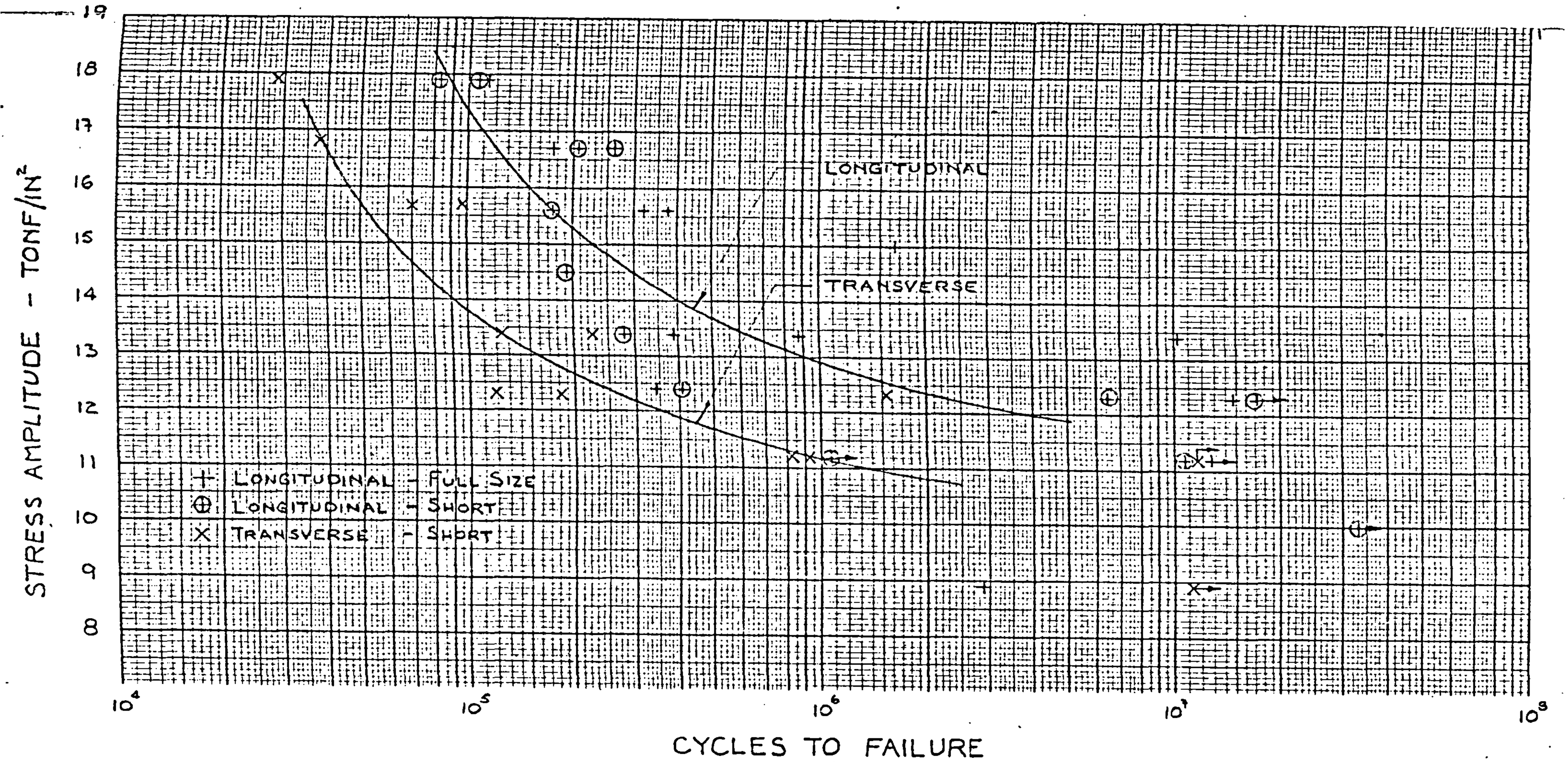

FIGURE 23. ROTATING BENDING FATIGUE TEST RESULTS.

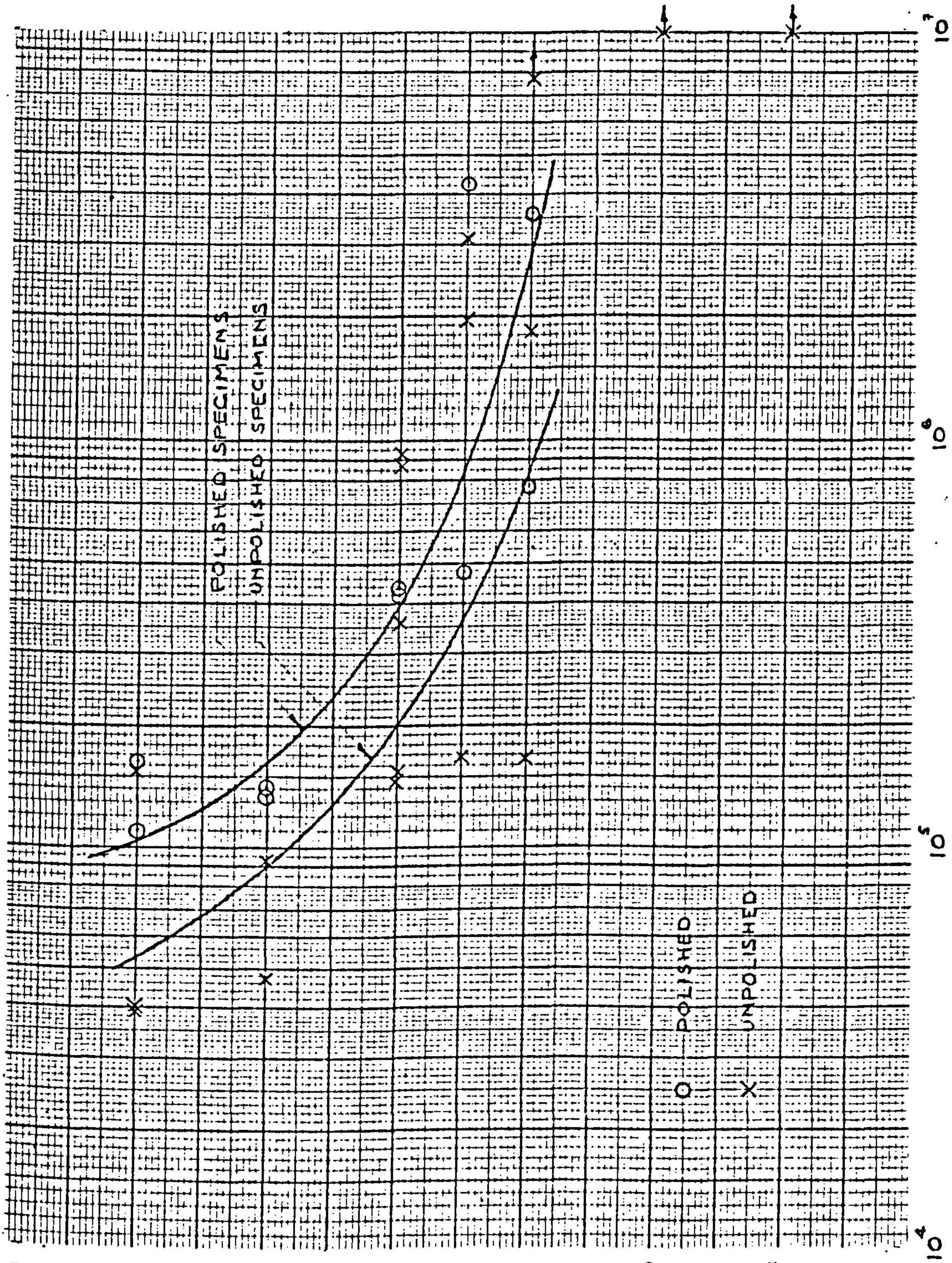

FIGURE 24. UNIAXIAL REPEATED TENSION FATIGUE RESULTS.

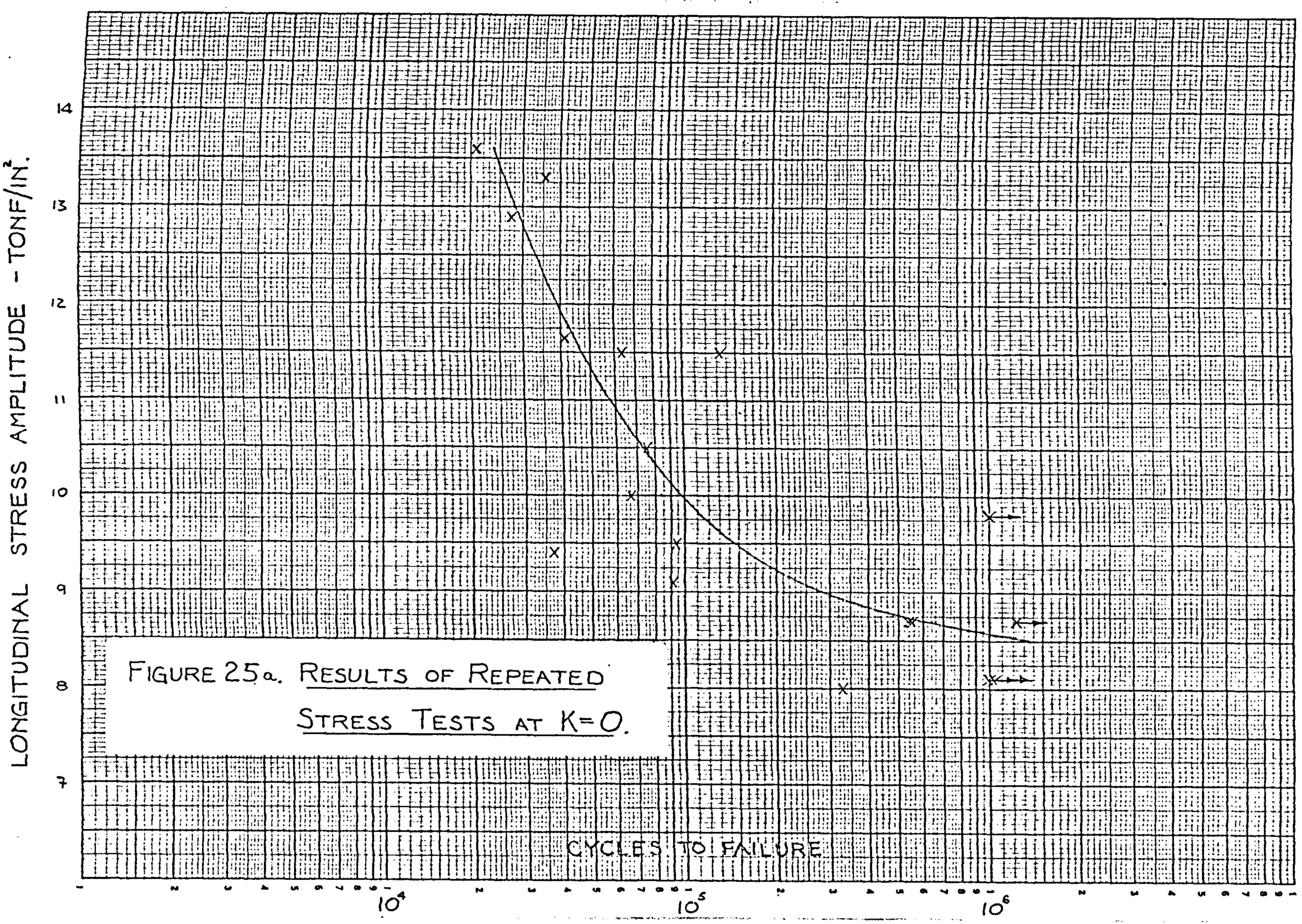

FIGURE 25a. RESULTS OF REPEATED STRESS TESTS AT K=0.

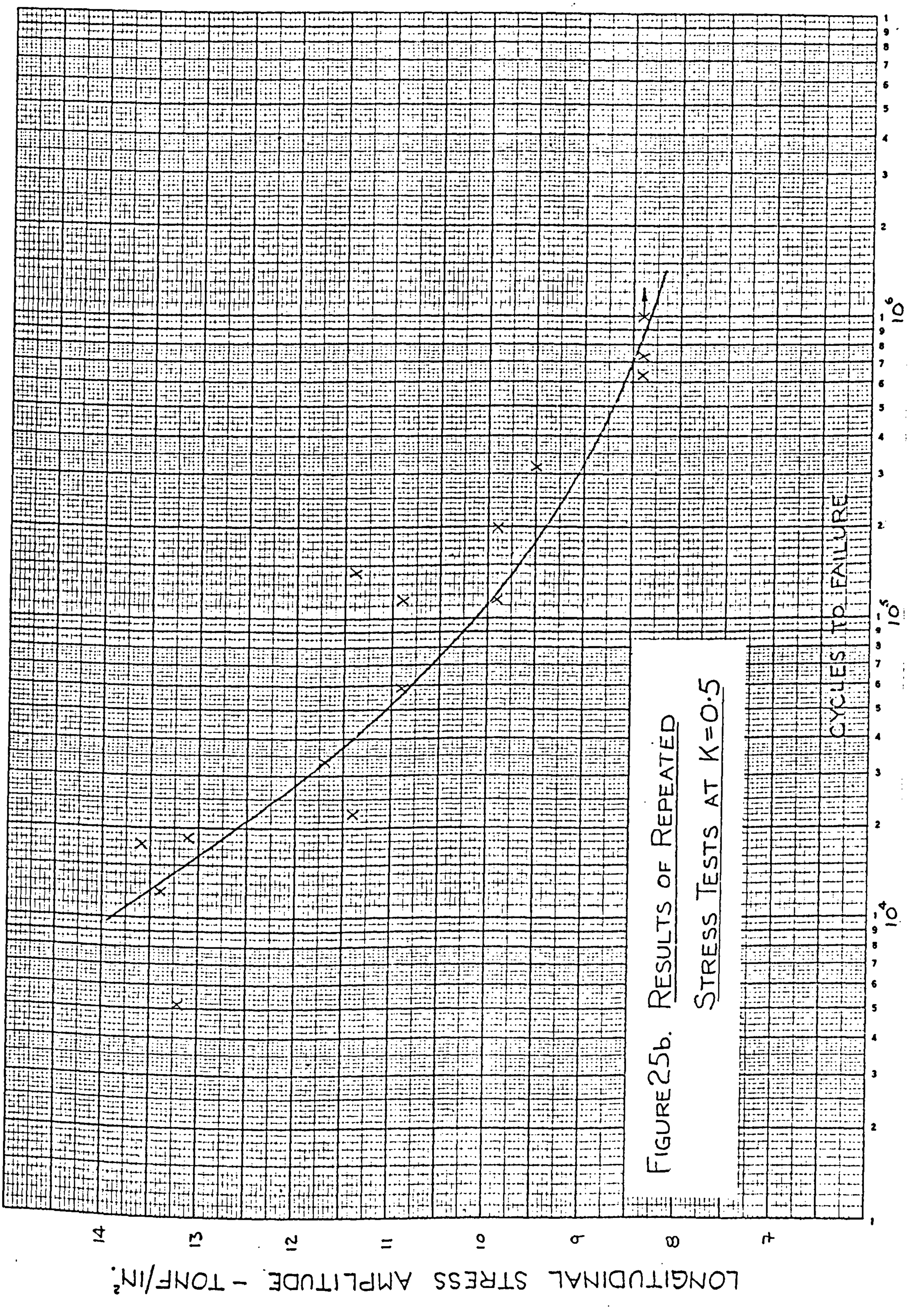

FIGURE 25b. RESULTS OF REPEATED STRESS TESTS AT K=0.5

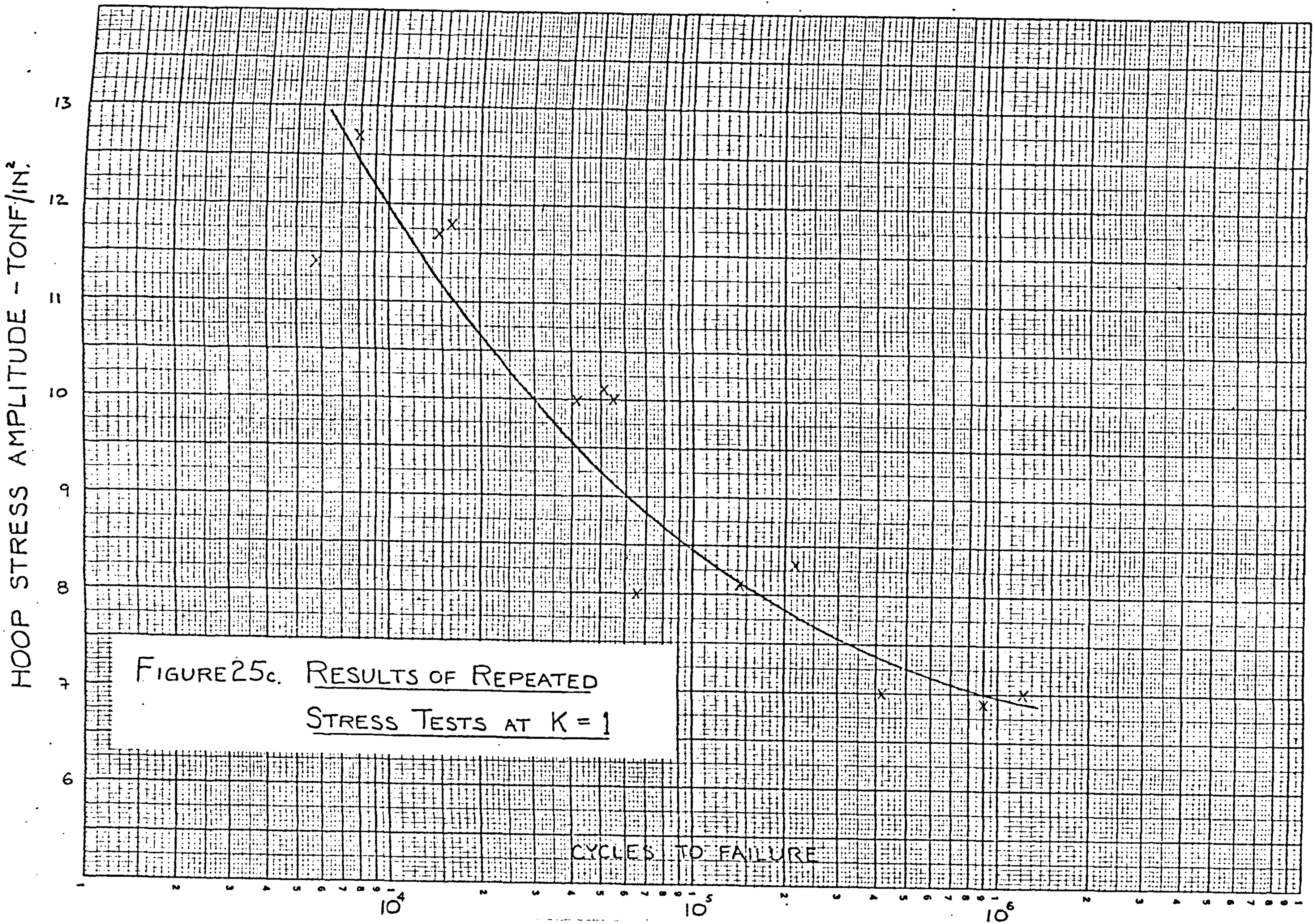

FIGURE 25c. RESULTS OF REPEATED STRESS TESTS AT K = 1

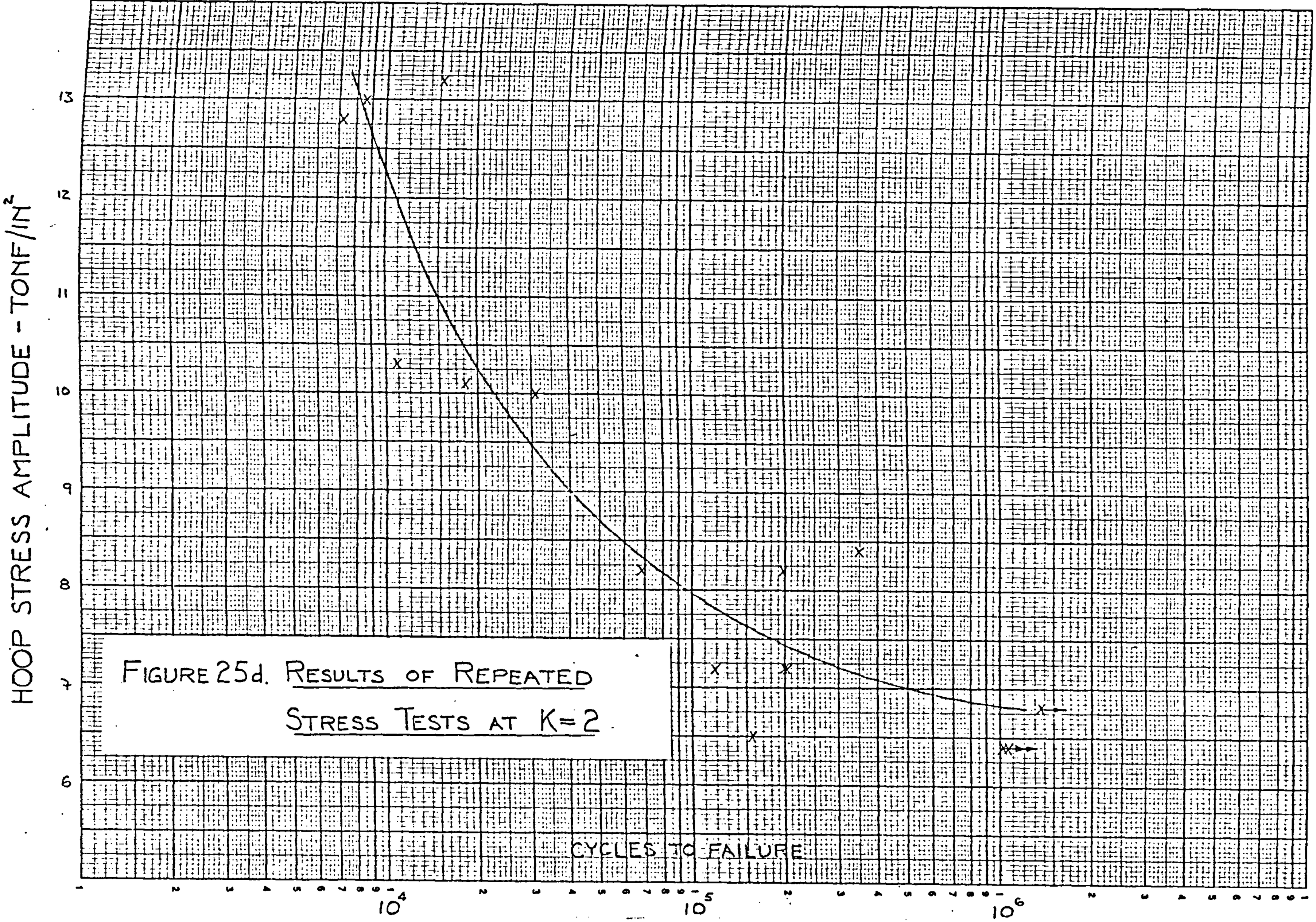

FIGURE 25d. RESULTS OF REPEATED STRESS TESTS AT K=2

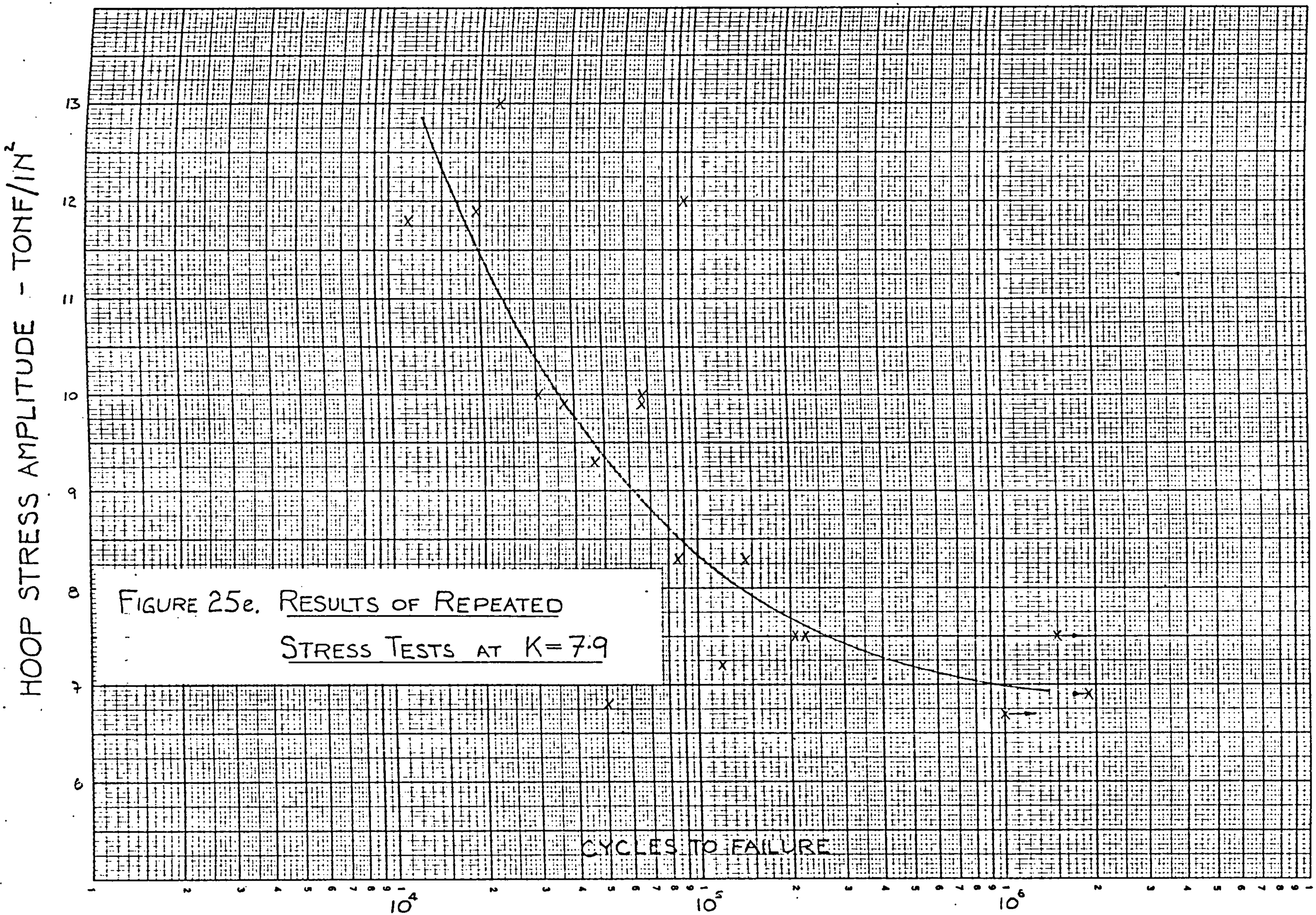

FIGURE 25e. RESULTS OF REPEATED STRESS TESTS AT K=7.9

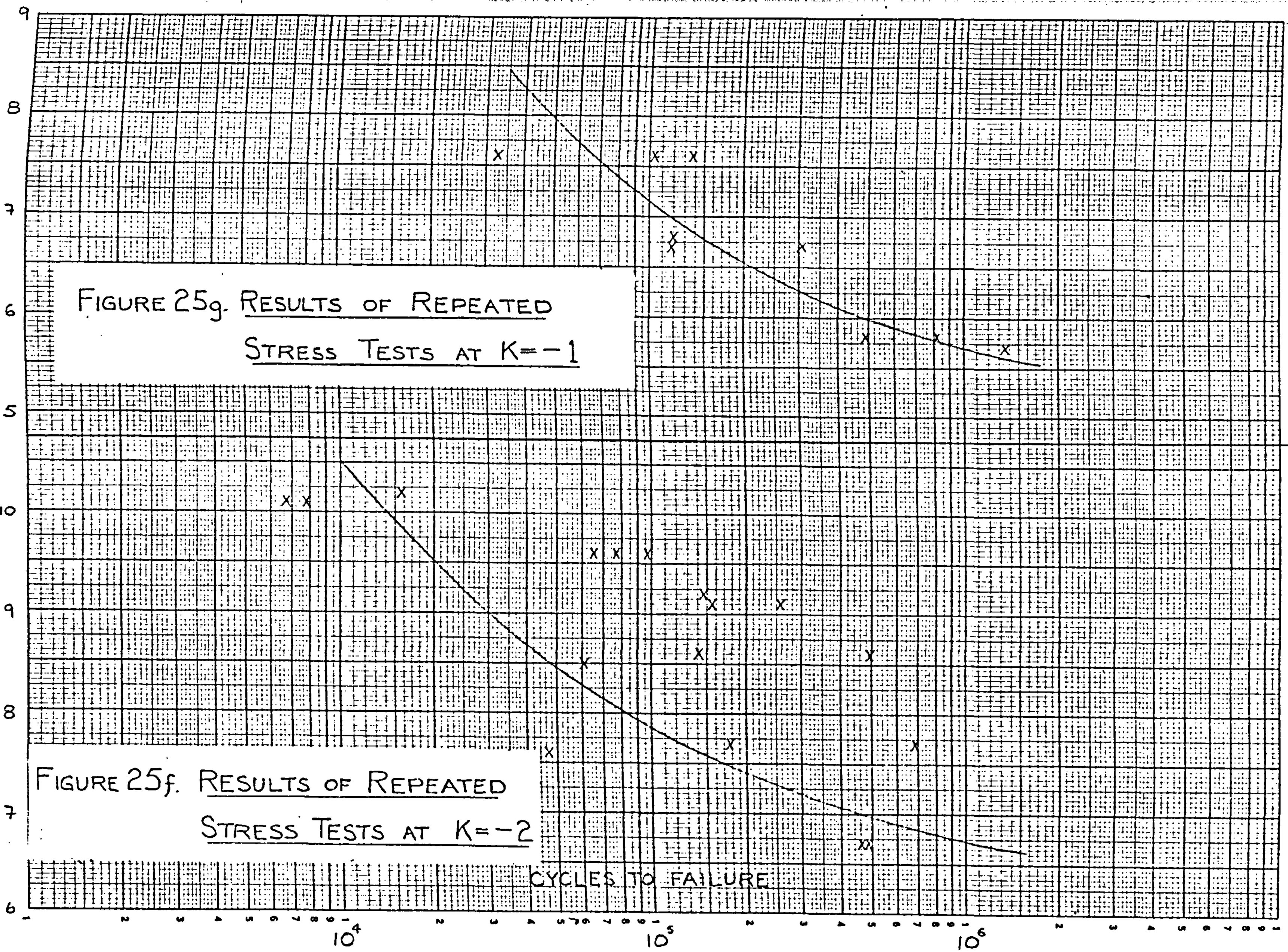

FIGURE 25g. RESULTS OF REPEATED STRESS TESTS AT K=-1

FIGURE 25f. RESULTS OF REPEATED STRESS TESTS AT K=-2

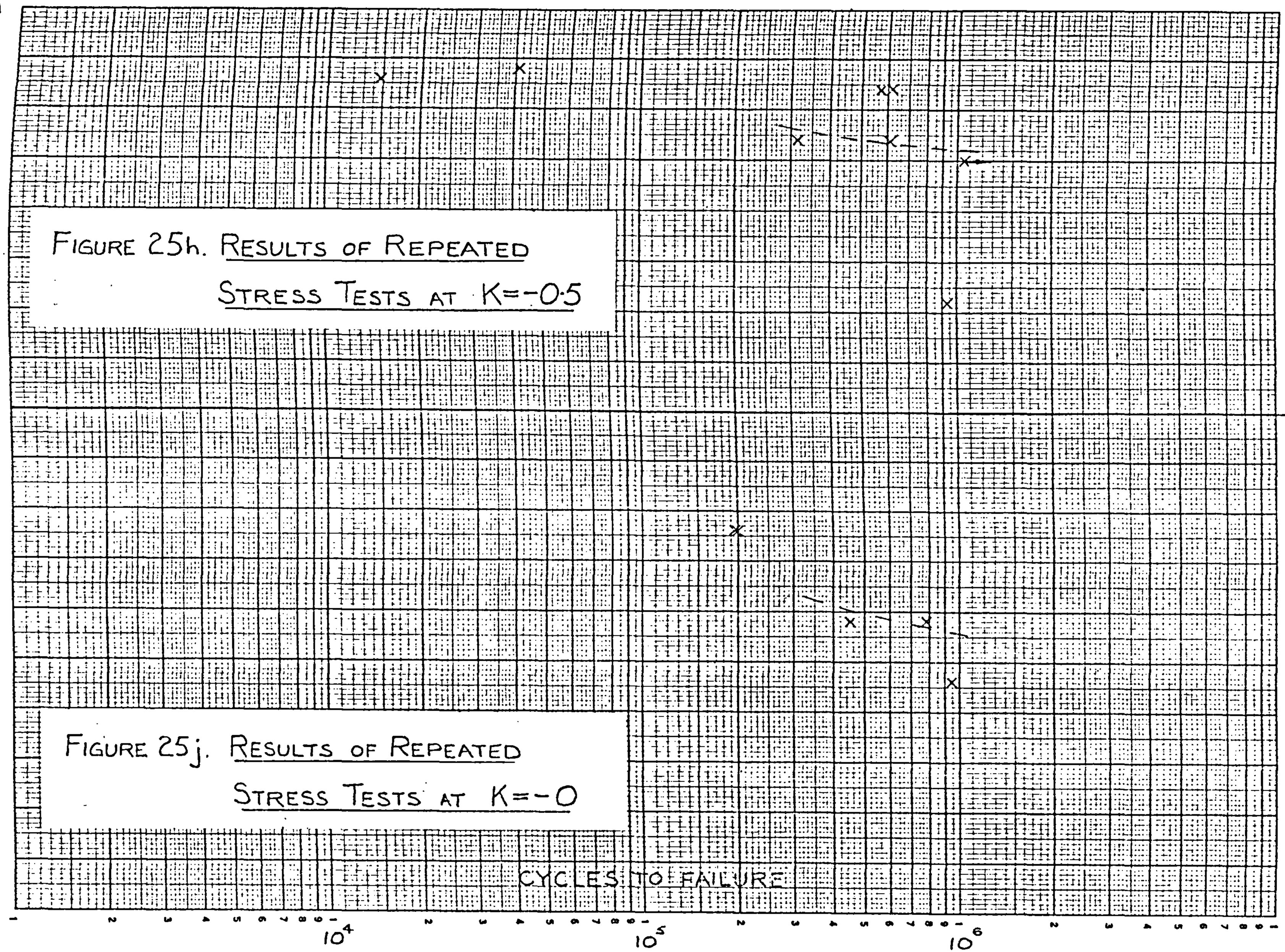

FIGURE 25h. RESULTS OF REPEATED STRESS TESTS AT K=-0·5

FIGURE 25j. RESULTS OF REPEATED STRESS TESTS AT K=-0

SHEAR STRESS AMPLITUDE - TONF/IN.^{2}

7·0
6·5
6·0
5·5
5·0
4·5
4·0
3·5

$K = -1$
$K = 0$
$K = 0.1$
$K = 0.2$
$K = 0.3$
$K = 0.4$
$K = 0.5$
$K = 0.6$
$K = 0.7$
$K = 0.8$
$K = 0.9$
$K = 1$

CYCLES TO FAILURE

10^4 10^5 10^6

FIGURE 25k. RESULTS OF ALL REPEATED STRESS TESTS ON SHEAR STRESS AMPLITUDE BASIS.

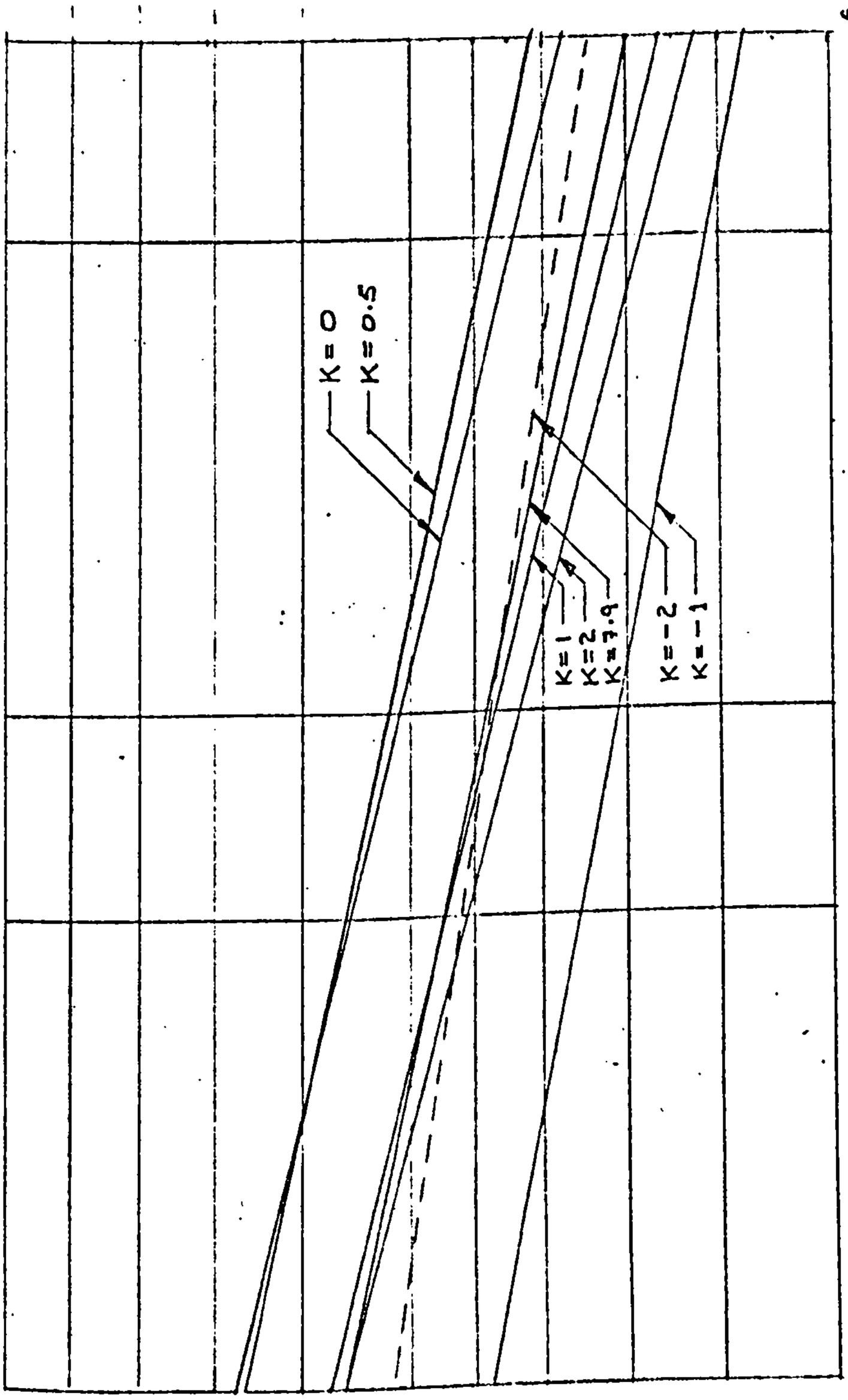

FIGURE 26. BIAXIAL CONSTANT AMPLITUDE FATIGUE TEST RESULTS

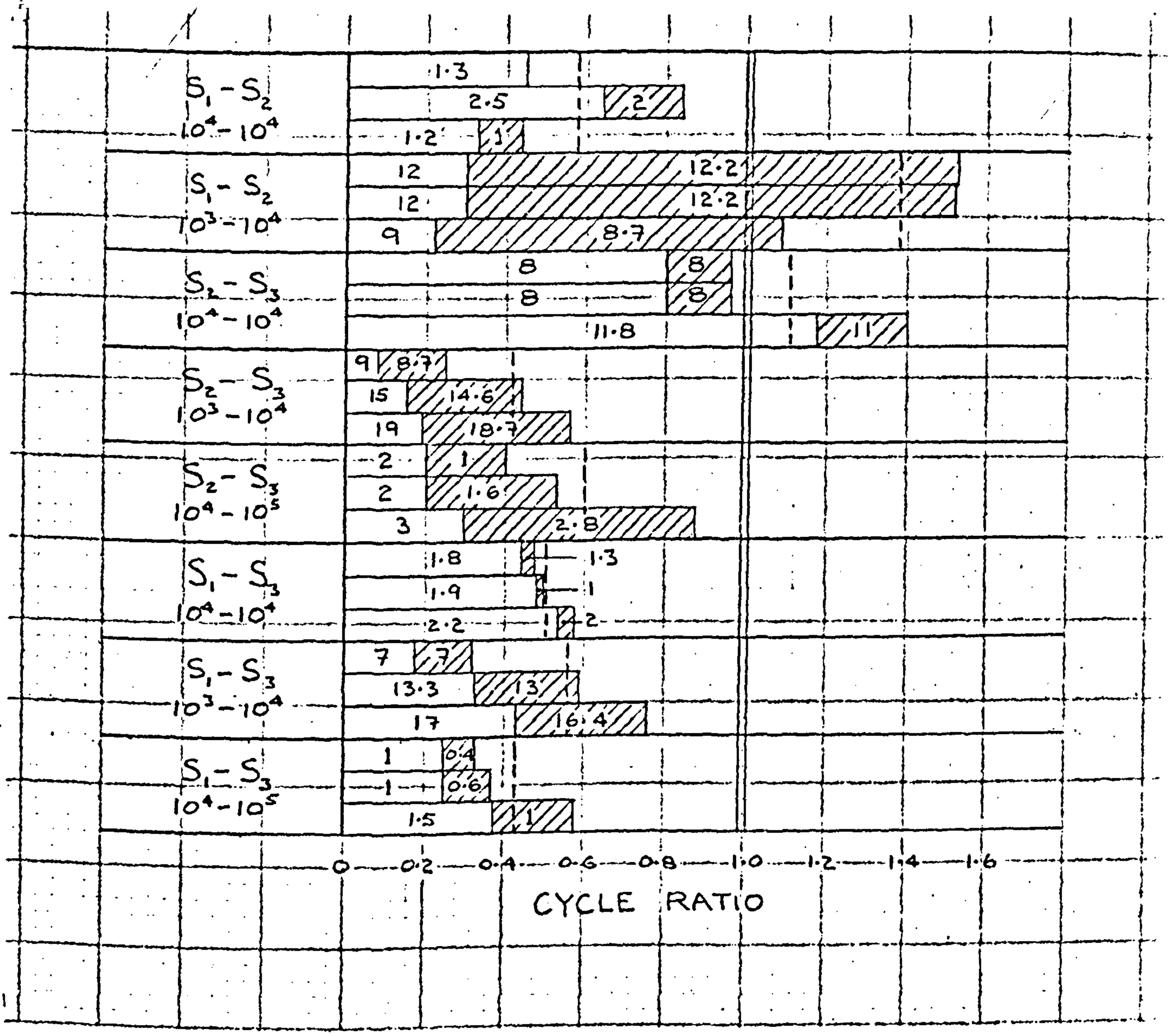

$S_1 = 12 \pm 12$ TONF/IN^2

$S_2 = 10 \pm 10$ TONF/IN^2

$S_3 = 8.75 \pm 8.75$ TONF/IN^2

▭ CYCLE RATIO AT HIGHER STRESS LEVEL

▨ CYCLE RATIO AT LOWER STRESS LEVEL

[17] NUMBER OF CYCLE BLOCKS.

¦ MEAN CYCLE RATIO SUM

‖ MINER PREDICTION

FIGURE 27a. CUMULATIVE DAMAGE TEST RESULTS, K=0

BLOCK DIAGRAM FOR INDIVIDUAL TESTS.

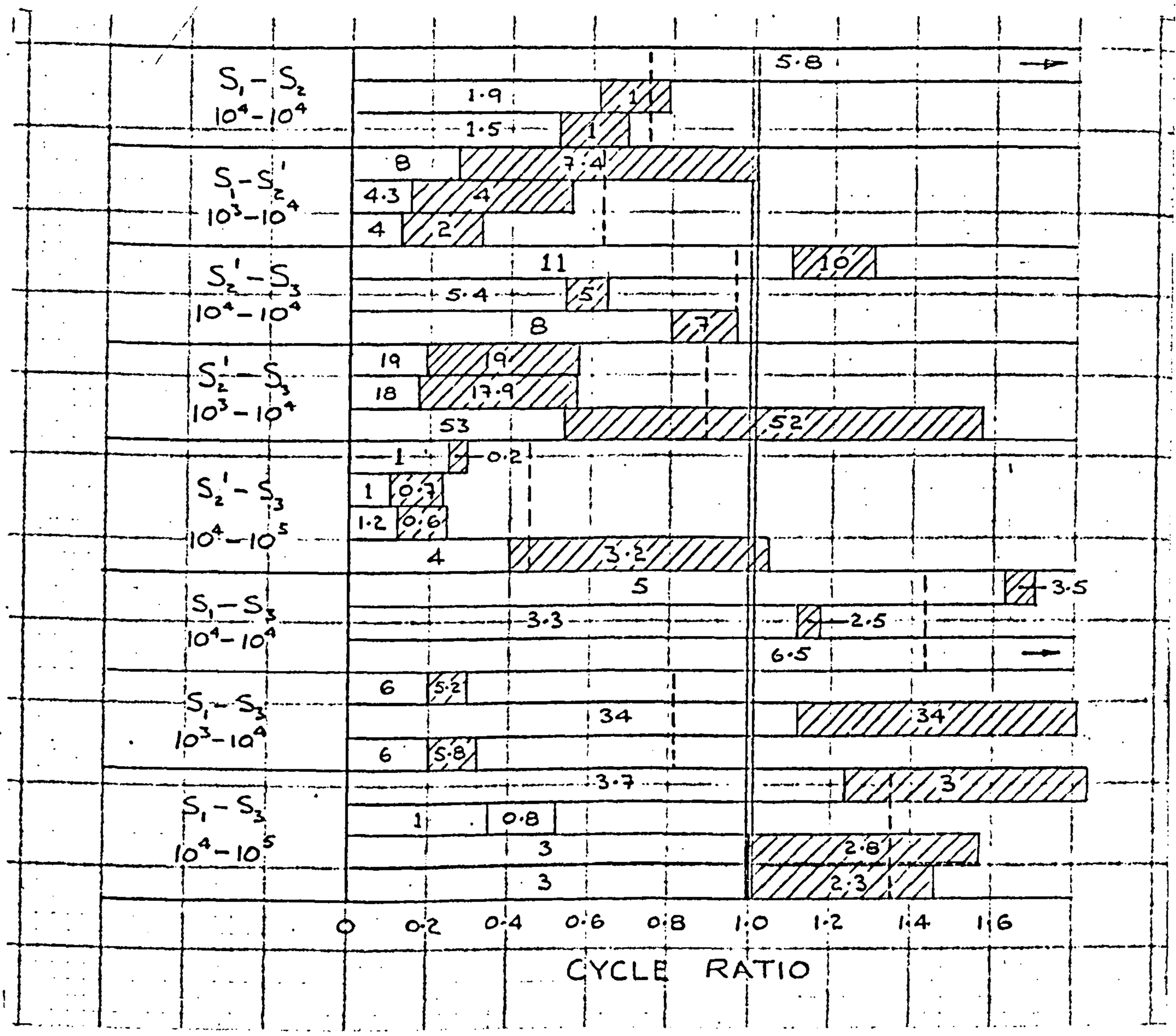

$S_1 = 9.5 \pm 9.5$ TONF/IN^2

$S_2 = 8 \pm 8$ TONF/IN^2

$S_3 = 7 \pm 7$ TONF/IN^2

▭ CYCLE RATIO AT HIGHER STRESS LEVEL

▨ CYCLE RATIO AT LOWER STRESS LEVEL

[17] NUMBER OF CYCLE BLOCKS

¦ MEAN CYCLE RATIO SUM.

‖ MINER PREDICTION

FIGURE 27b. CUMULATIVE DAMAGE TEST RESULTS, K=2

BLOCK DIAGRAM FOR INDIVIDUAL TESTS.

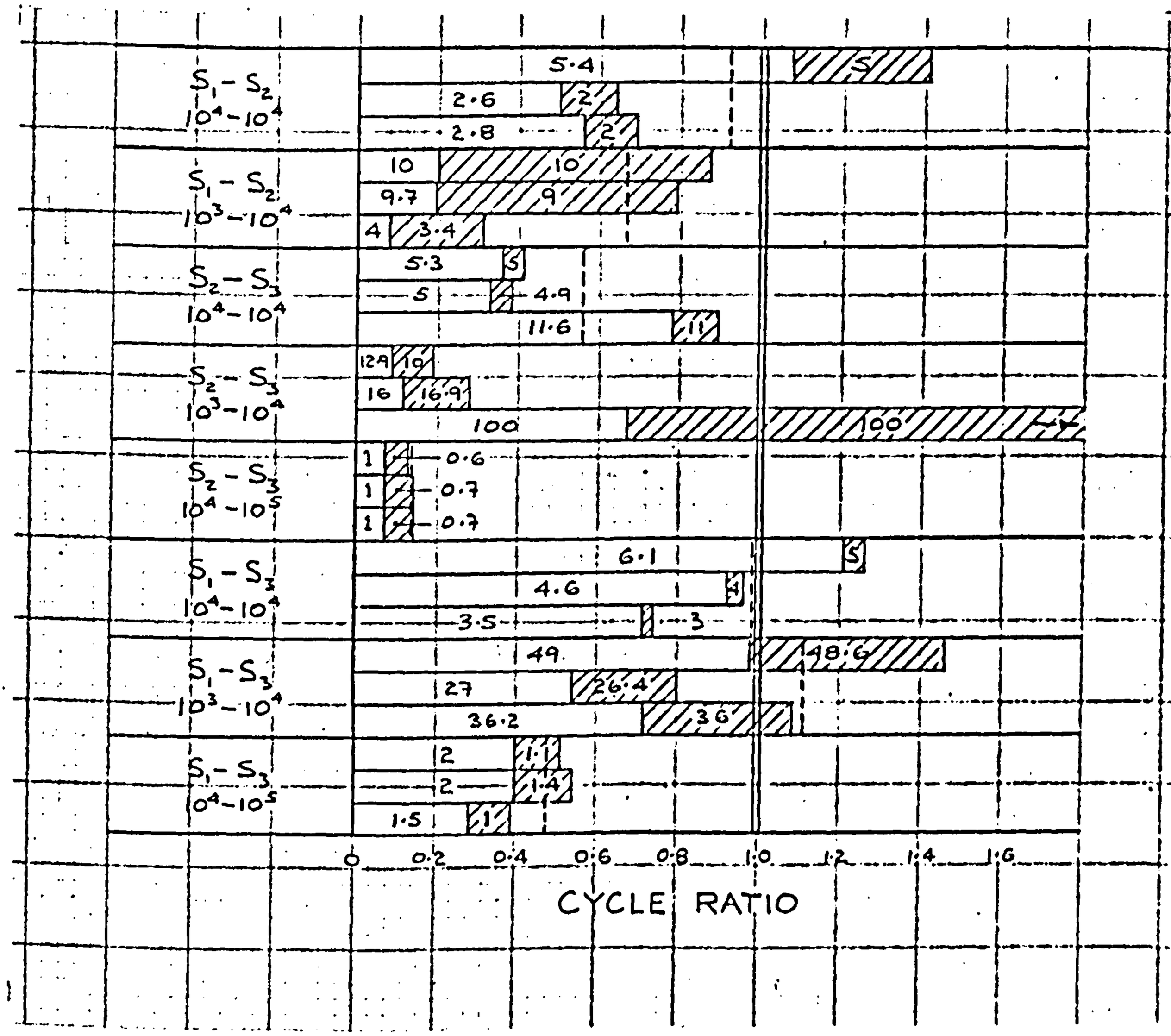

$S_1 = 9.5 \pm 9.5$ TONF/IN^2

$S_2 = 8 \pm 8$ TONF/IN^2

$S_3 = 7 \pm 7$ TONF/IN^2

▭ CYCLE RATIO AT HIGHER STRESS LEVEL

▨ CYCLE RATIO AT LOWER STRESS LEVEL

[17] NUMBER OF CYCLE BLOCKS

| MEAN CYCLE RATIO SUM

‖ MINER PREDICTION

FIGURE 27c. CUMULATIVE DAMAGE TEST RESULTS, K=7·9

BLOCK DIAGRAM FOR INDIVIDUAL TESTS.

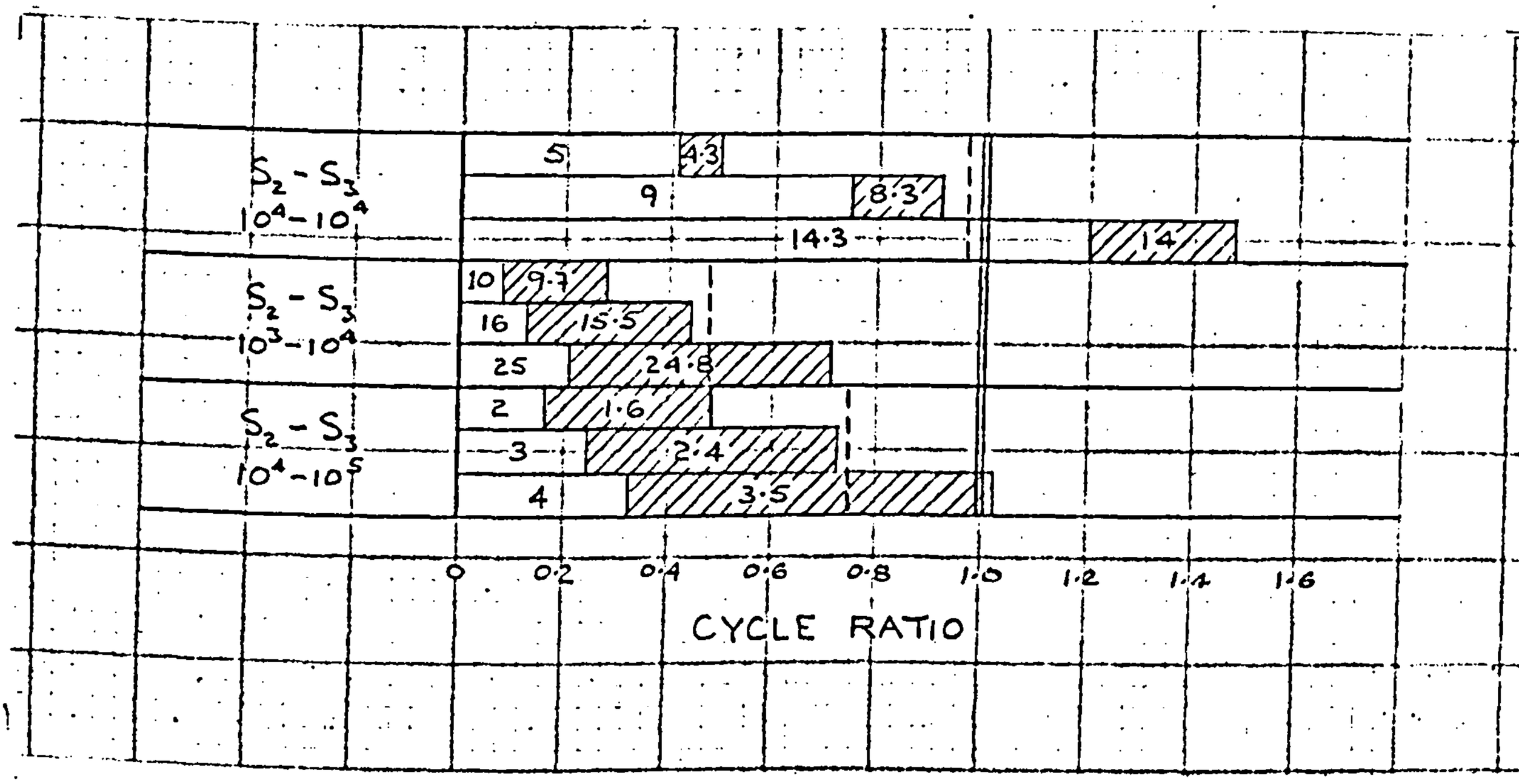

$S_1 = 8 \pm 8$ TONF/IN^2

$S_2 = 7 \pm 7$ TONF/IN^2

$S_3 = 6 \pm 6$ TONF/IN^2

▭ CYCLE RATIO AT HIGHER STRESS LEVEL

▨ CYCLE RATIO AT LOWER STRESS LEVEL

▭ NUMBER OF CYCLE BLOCKS.

| MEAN CYCLE RATIO SUM

‖ MINER PREDICTION

FIGURE 27d. CUMULATIVE DAMAGE TEST RESULTS, K=-1

BLOCK DIAGRAM FOR INDIVIDUAL TESTS.

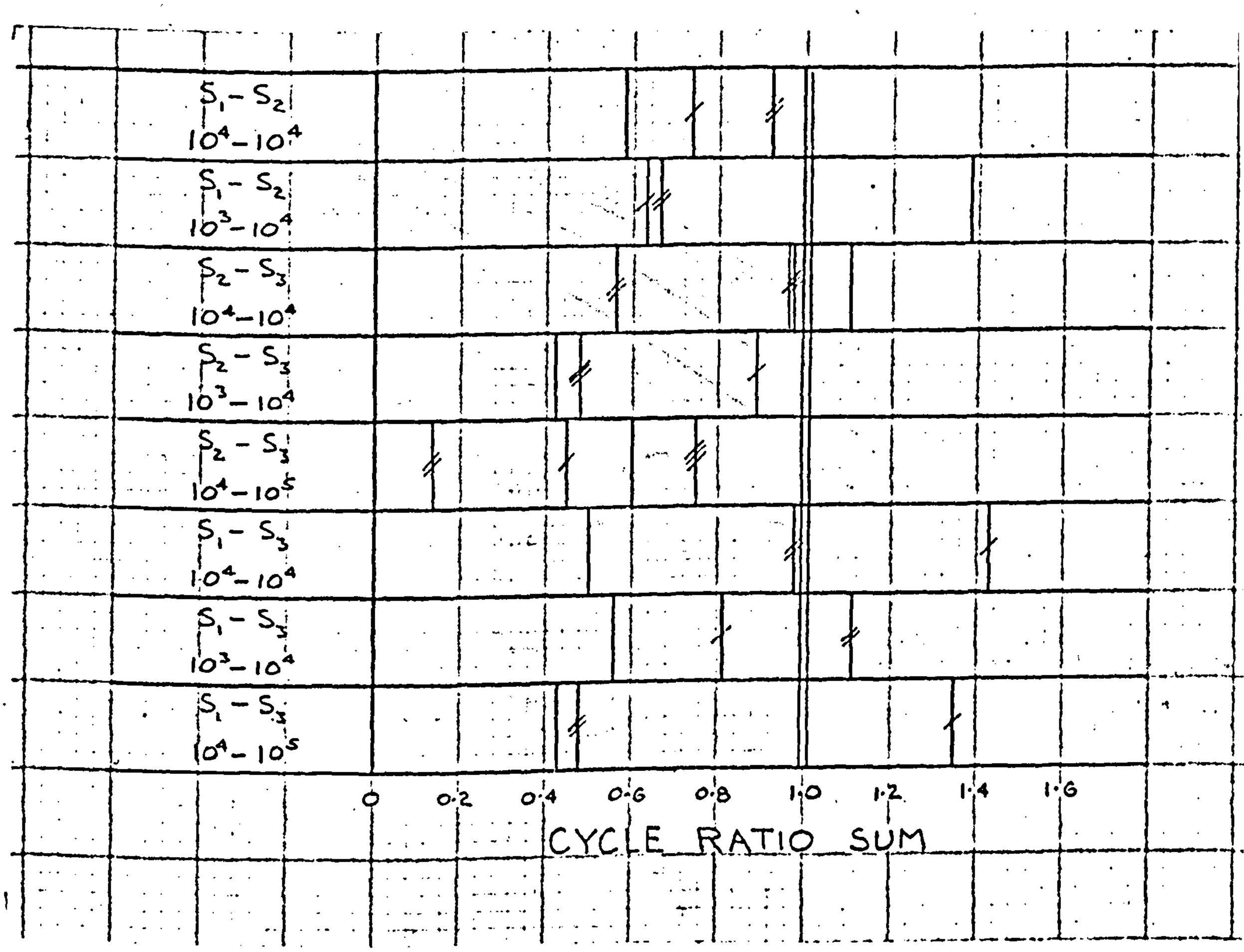

FIGURE 27e. CUMULATIVE DAMAGE TEST RESULTS.

SUMMARY OF MEAN CYCLE RATIO SUMS

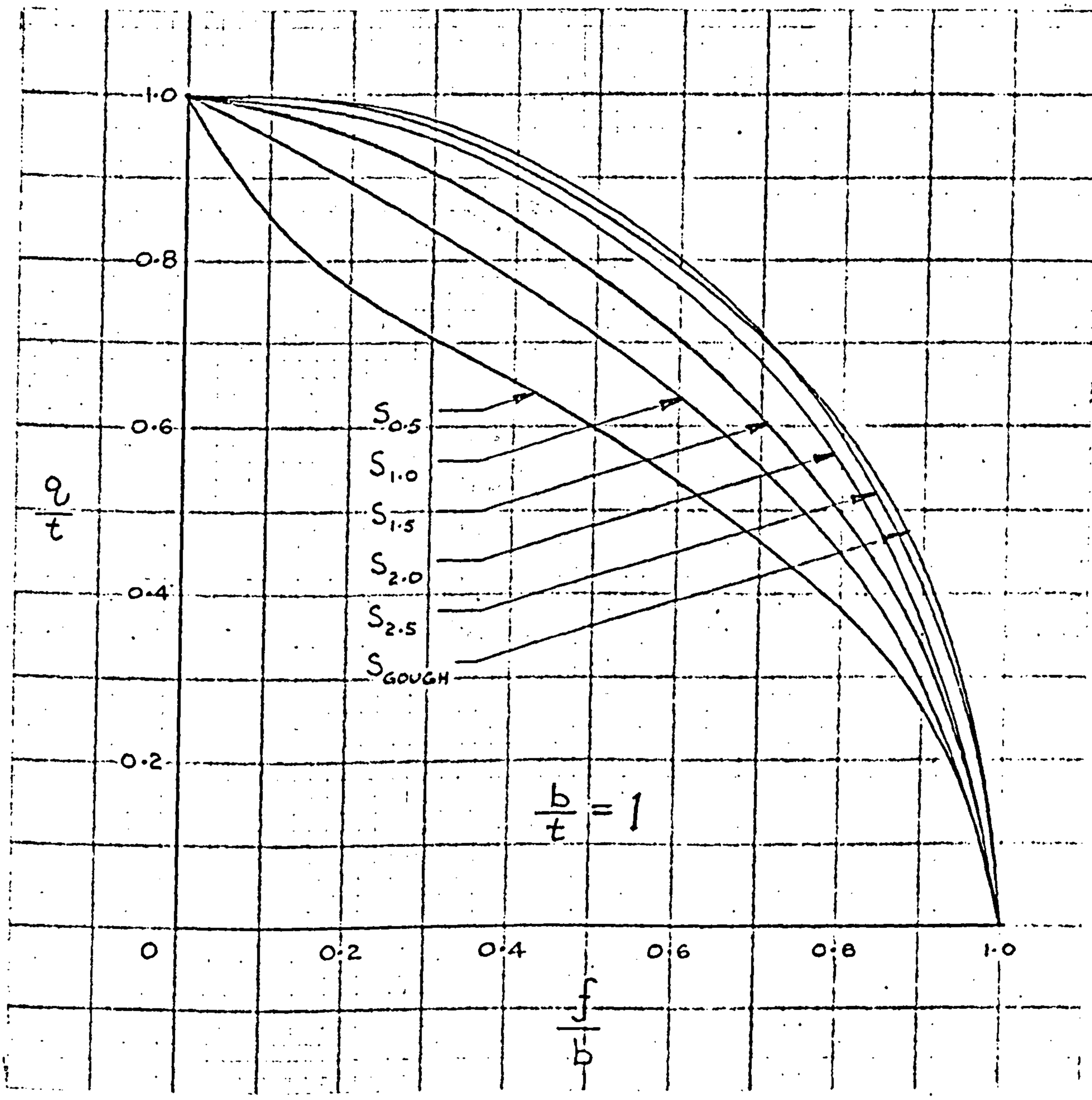

FIGURE 28a. ELLIPSE QUADRANTS

EQUATION 7.2.

FOR n = 0·5 TO 2·5 AND b/t = 1

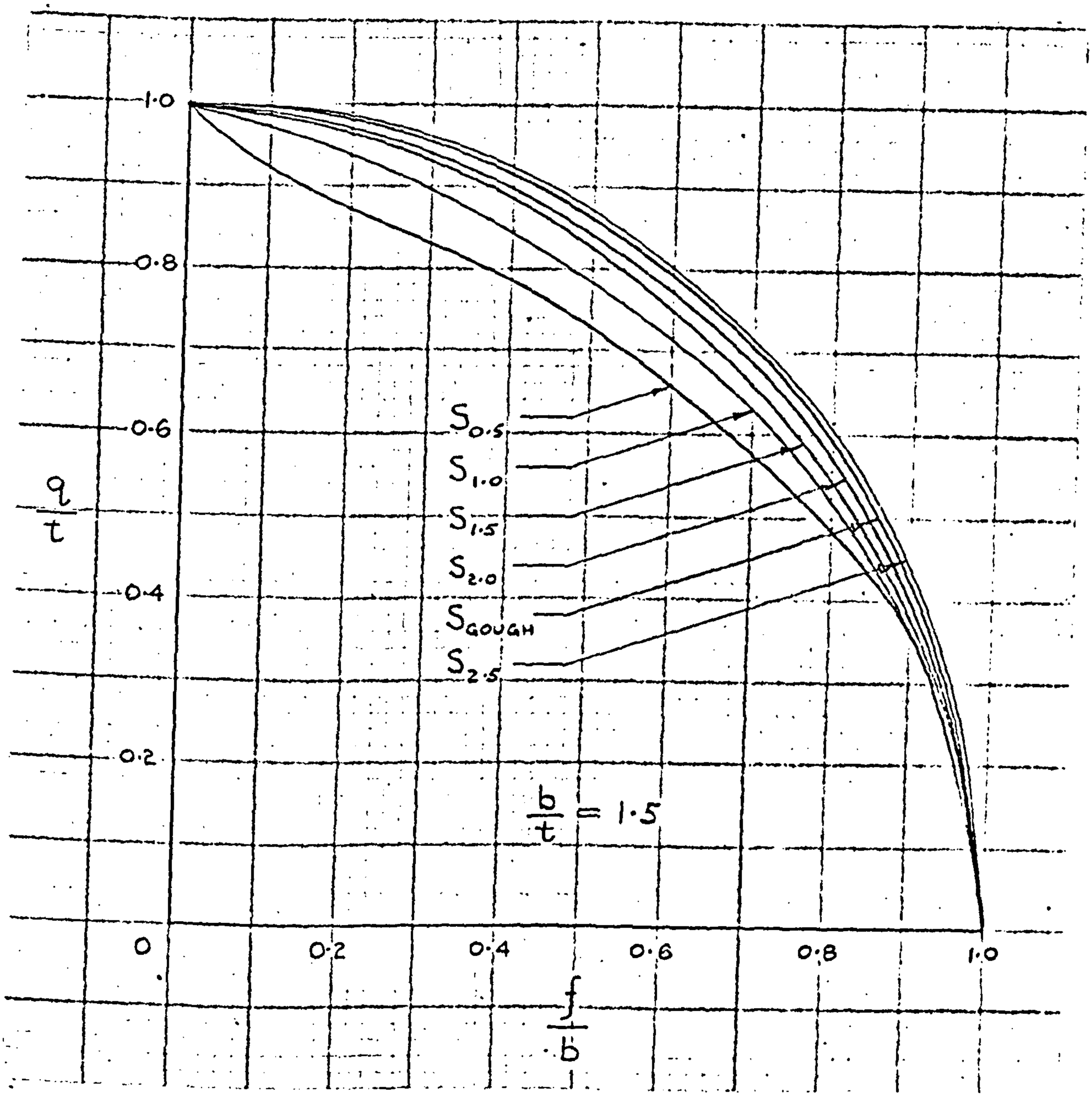

FIGURE 28b. ELLIPSE QUADRANTS

EQUATION 7.2.

FOR n = 0·5 TO 2·5 AND b/t = 1·5

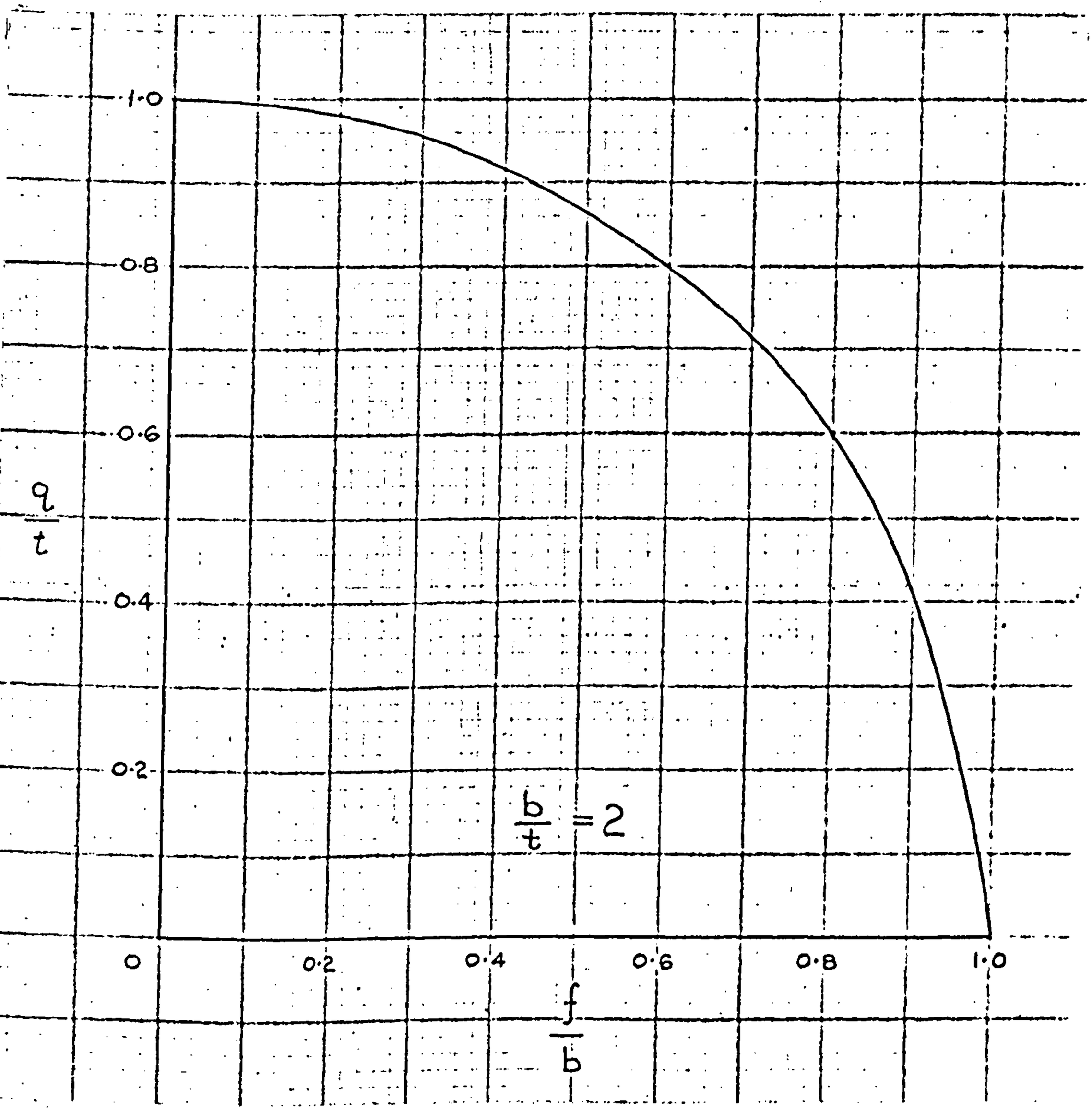

FIGURE 28c. ELLIPSE QUADRANT

EQUATION 7.2.

FOR n = 0·5 TO 2·5 AND b/t = 2

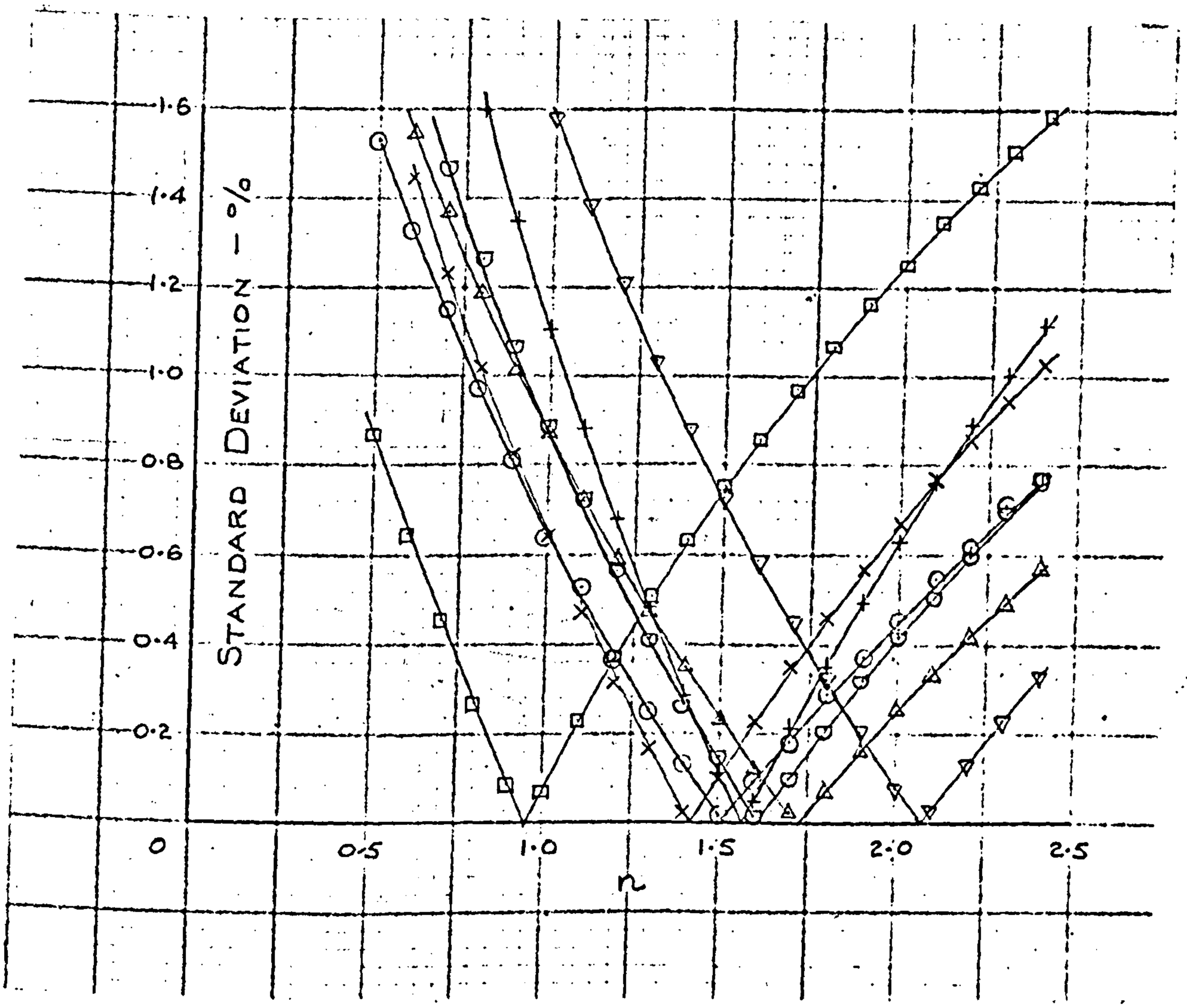

SYMBOL	b/t		MATERIAL
×	1·60	GS2.	0·4% C. STEEL (NORMALISED)
+	1·46	GS4	0·9% C. STEEL (PEARLITE).
⊙	1·67	GS5	3% Ni. STEEL (30/35 TONF)
⊡	1·67	GS6	3/3½% Ni. STEEL (45/50 TONF)
△	1·67	GS7	Cr. Va. STEEL (45/50 TONF).
▽	1·54	GS8	3½% Ni. Cr. STEEL (N.I.)
⊙	1·64	GH2	3½% Ni. Cr. STEEL (N.I.)

FIGURE 29a. GOUGH DATA - COMPARISON WITH EQUATION 7.2.

STANDARD DEVIATION v n.

GS AND GH SERIES - n = 0·5 TO 2·5

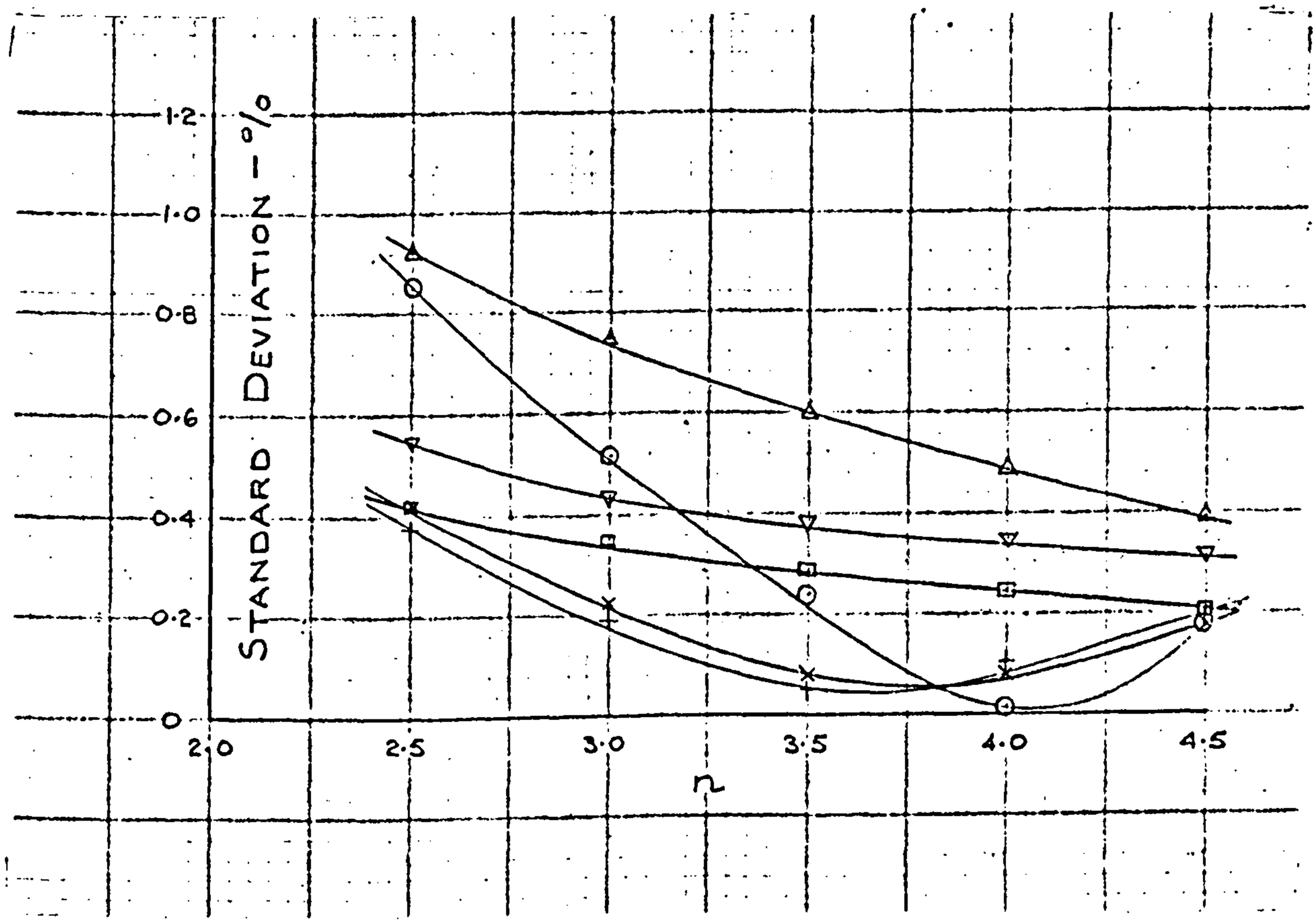

SYMBOL	b/t		MATERIAL
+	1·78	GS 1	0·1 % C. STEEL (NORMALISED).
×	1·76	GS 3	0·4 % C. STEEL (SPHEROIDISED).
⊙	1·57	GS 9	3½ % Ni. Cr. STEEL (LOW IMPACT).
⊡	1·93	GS 10	Ni. Cr. Mo. STEEL (75/80 TONF).
△	1·71	GS 11	Ni. Cr. STEEL (95/105 TONF).
▽	1·93	GH 1	0·1% C. STEEL (NORMALISED).

FIGURE 29b. GOUGH DATA - COMPARISON WITH EQUATION 7.2.

STANDARD DEVIATION v n.

GS AND GH SERIES - n = 2·5 TO 4·5

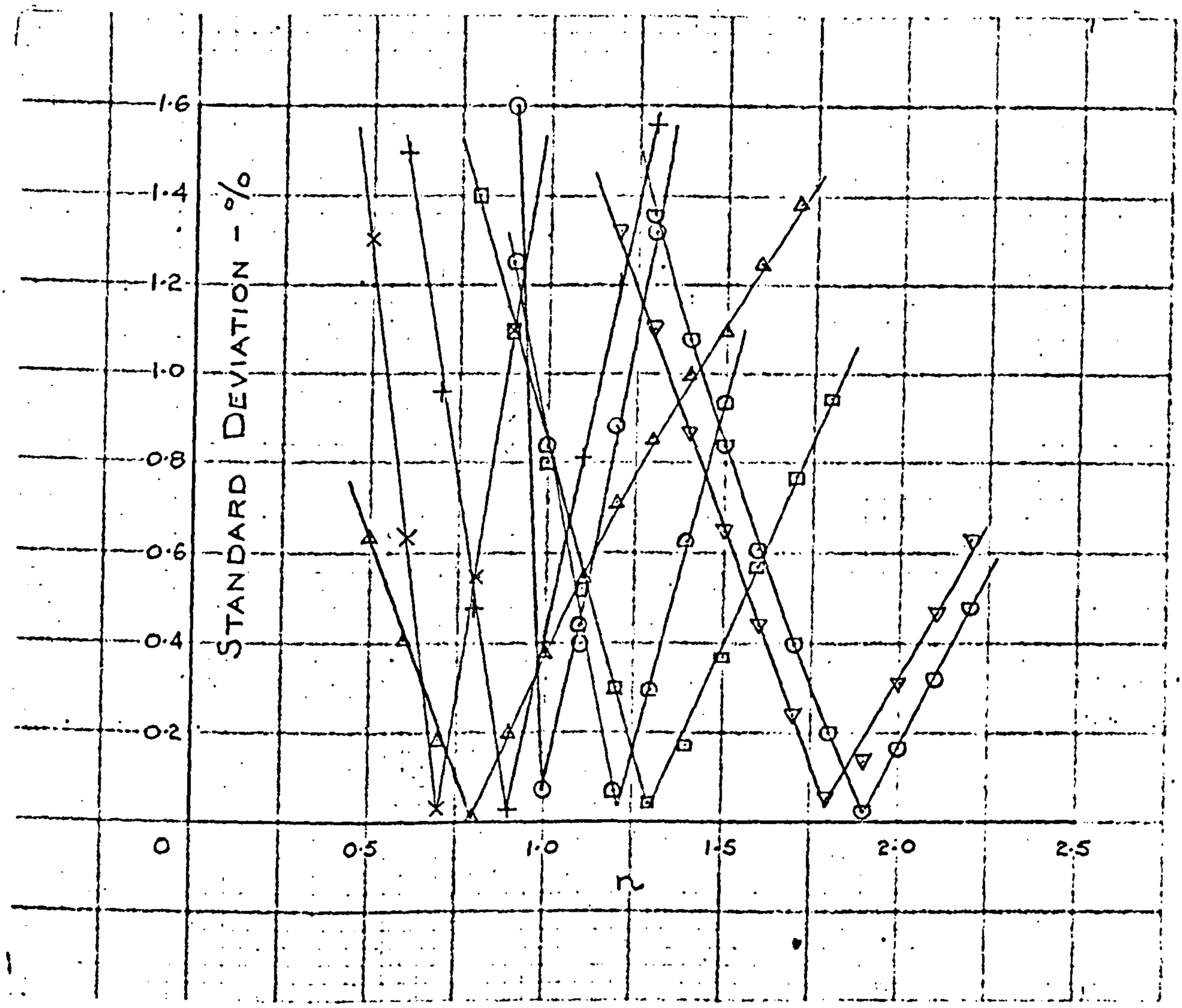

SYMBOL	b/t	MATERIAL	
×	1·10	GS CI 1	SILAL CAST IRON.
+	1·12	GS CI 2	NICROSILAL CAST IRON.
⊙	1·02	GN 1	0·4% C. STEEL (NORMALISED).
⊡	1·39	GN 2	3% Ni. STEEL (30/35 TONF).
△	1·65	GN 3	3/3½% Ni. STEEL (45/50 TONF).
▽	1·35	GN 4	Cr. Va. STEEL (45/50 TONF)
⊙	1·14	GN 5	3½% Ni. Cr. STEEL (N.I.)
⊙	1·13	GN 6	Ni. Cr. Mo. STEEL (75/80 TONF)

FIGURE 29c. GOUGH DATA – COMPARISON WITH EQUATION 7.2.

STANDARD DEVIATION v. n.

GS CI AND GN SERIES – n = 0·5 TO 2·5.

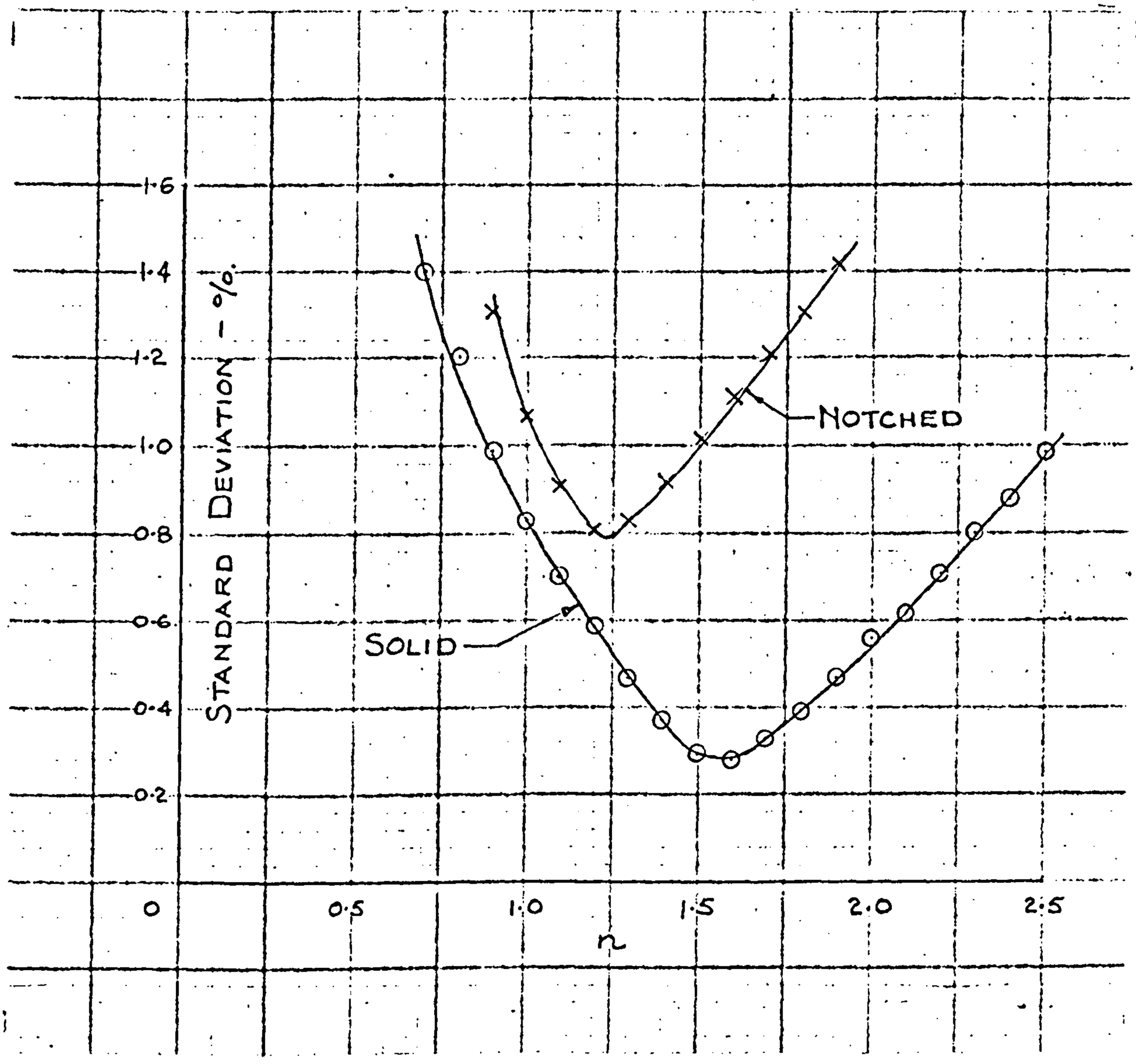

FIGURE 29d. GOUGH DATA - COMPARISON WITH EQUATION 7.2.

STANDARD DEVIATION v. n

MEAN VALUES FOR GS AND GN SERIES.

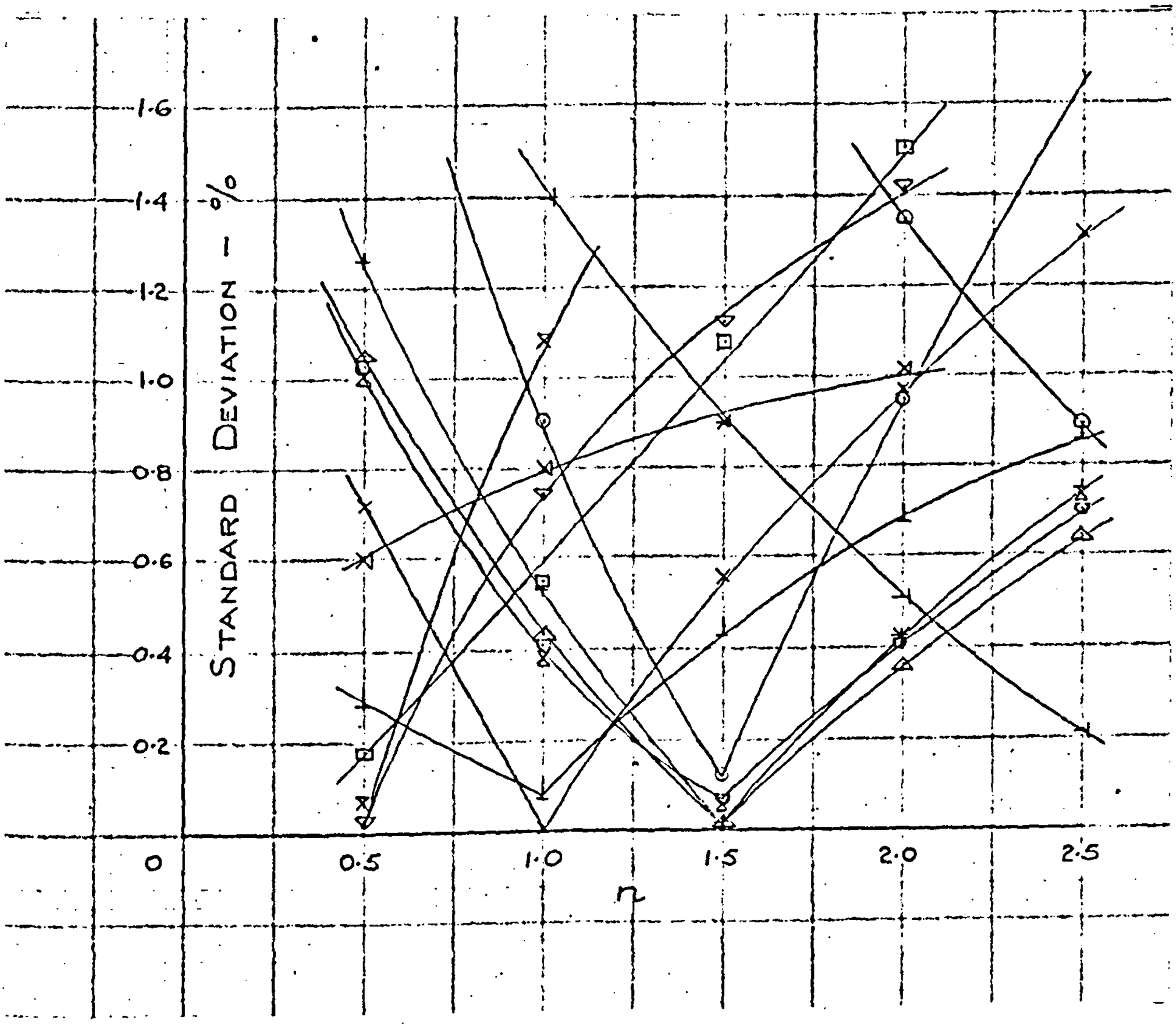

SYMBOL	b/t	MATERIAL		
×	1·68	FS 1	Cr. Mo. STEEL	TABLE 5.32A
+	1·66	FS 2	"	" 5.32 J
⊙	1·60	FS 3	"	" 5.32 K
⊡	1·69	FS 4	"	" 5.32 L
△	1·71	FS 5	"	" 5.32 M
▽	1·78	FS 6	Ni. Cr. Mo. STEEL	" 5.34 D
⊙	1·71	FS 7	Cr. Mo. Va. STEEL	" 5.37 A
⊡	1·71	FS 8	"	" 5.37 D
⊣	1·65	FS 9	"	" 5.37 E
⊥	1·80	FS 10	Ni. Cr. STEEL	" 5.38 A
x	1·62	FH 1	Cr. Mo. STEEL	" 5.32 B
⧖	1·71	FH 2	Cr. Mo. Va. STEEL	" 5.37 B
⧗	1·93	FH 3.	Ni. Cr. STEEL	" 5.38 B

FIGURE 30a. FRITH DATA - COMPARISON WITH EQUATION 7.2.

STANDARD DEVIATION v n.

FS AND FH SERIES - n = 0·5 TO 2·5.

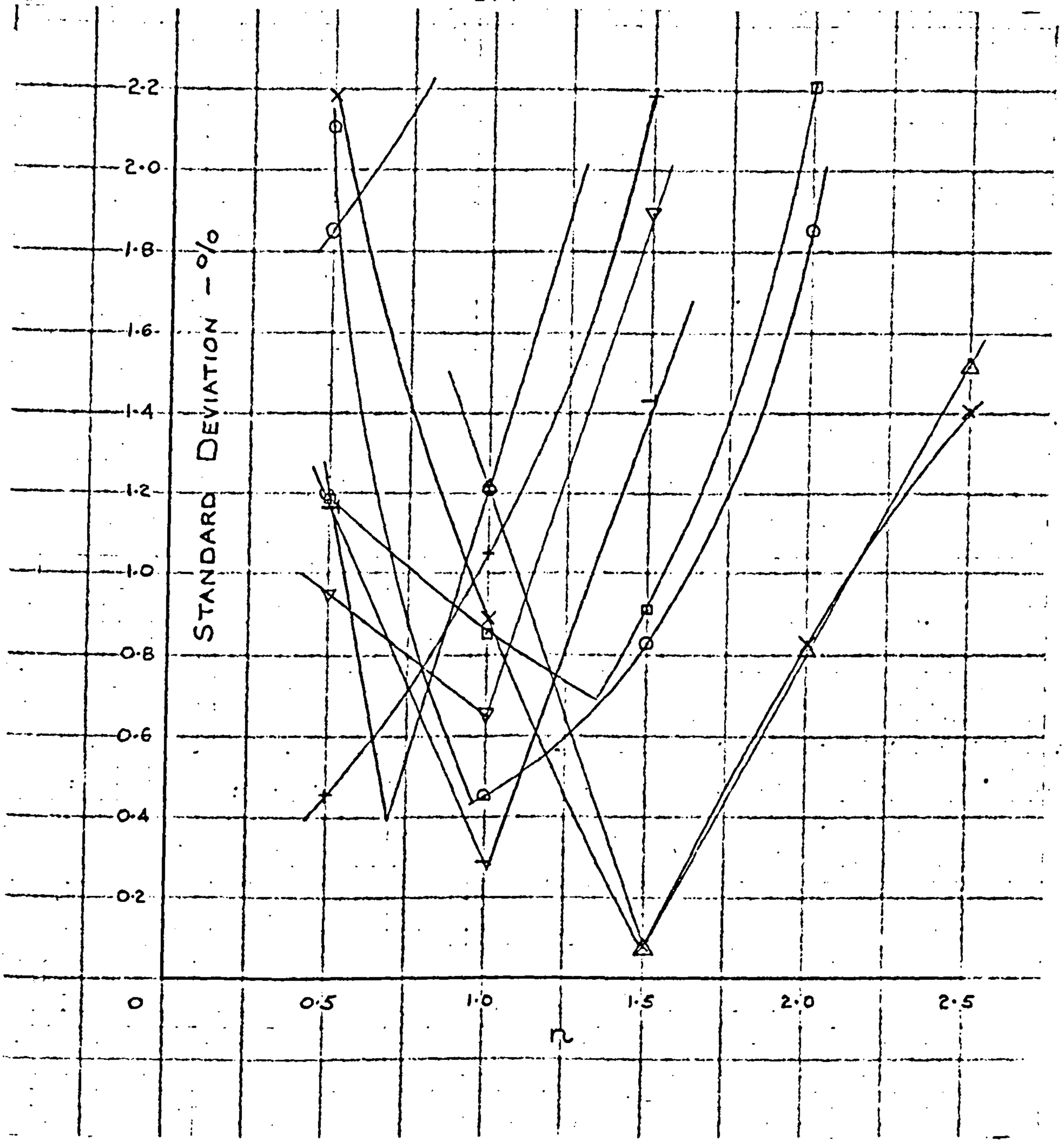

SYMBOL	b/t	MATERIAL		
×	1·38	FHOH 1	Cr.Mo. STEEL	TABLE 5.32 N
+	1·41	FHOH 2	"	" 5.32 P
⊙	1·47	FHOH 3	"	" 5.32 Q
⊡	1·37	FHOH 4	Ni.Cr.Va.Mo. STEEL	" 5.36 E
△	1·28	FHOH 5	Cr.Mo.Va. STEEL	" 5.37 C
▽	1·35	FHOH 6	"	" 5.37 F
⊙	1·33	FHOH 7	"	" 5.37 G
⊙	1·27	FHOH 8	"	" 5.37 H
⊣	1·39	FHOH 9	"	" 5.38 C

FIGURE 30b. FRITH DATA - COMPARISON WITH EQUATION 7.2.

STANDARD DEVIATION v n.

FHOH SERIES - n = 0·5 TO 2·5.

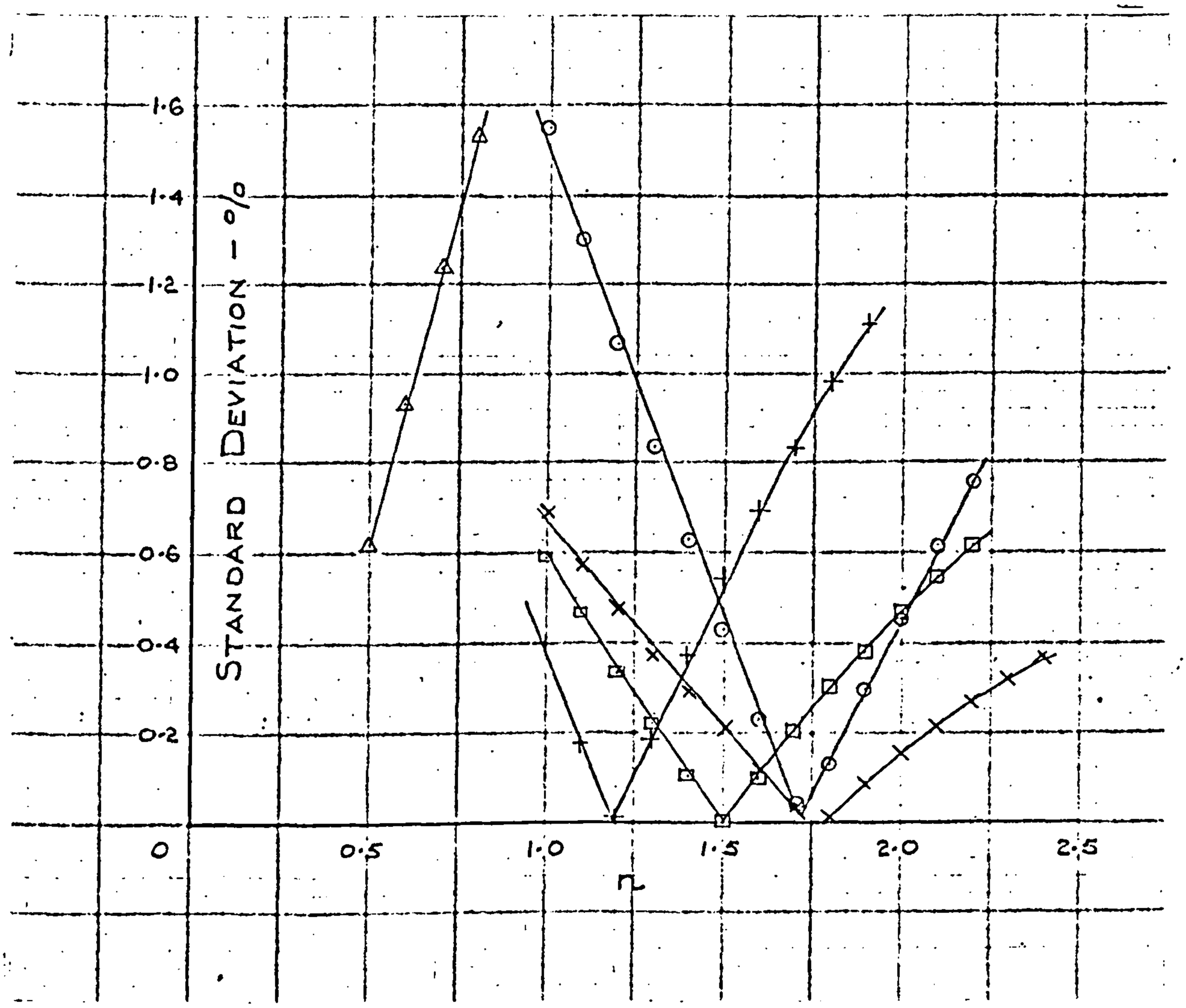

SYMBOL	b/t	MATERIAL	
×	1·74	NK 2	MEDIUM STEEL
+	1·52	NK 3	HARD STEEL
⊙	1·52	NK 4	Ni.Cr. STEEL (HOT ROLLED)
⊡	1·75	NK 5	Ni.Cr. STEEL (HEAT TREATED)
△	1·27	NK 6	CAST IRON

FIGURE 31a. NISHIHARA AND KAWAMOTO DATA.

COMPARISON WITH EQUATION 7.2.

STANDARD DEVIATION v n.

n = 0·5 TO 2·5

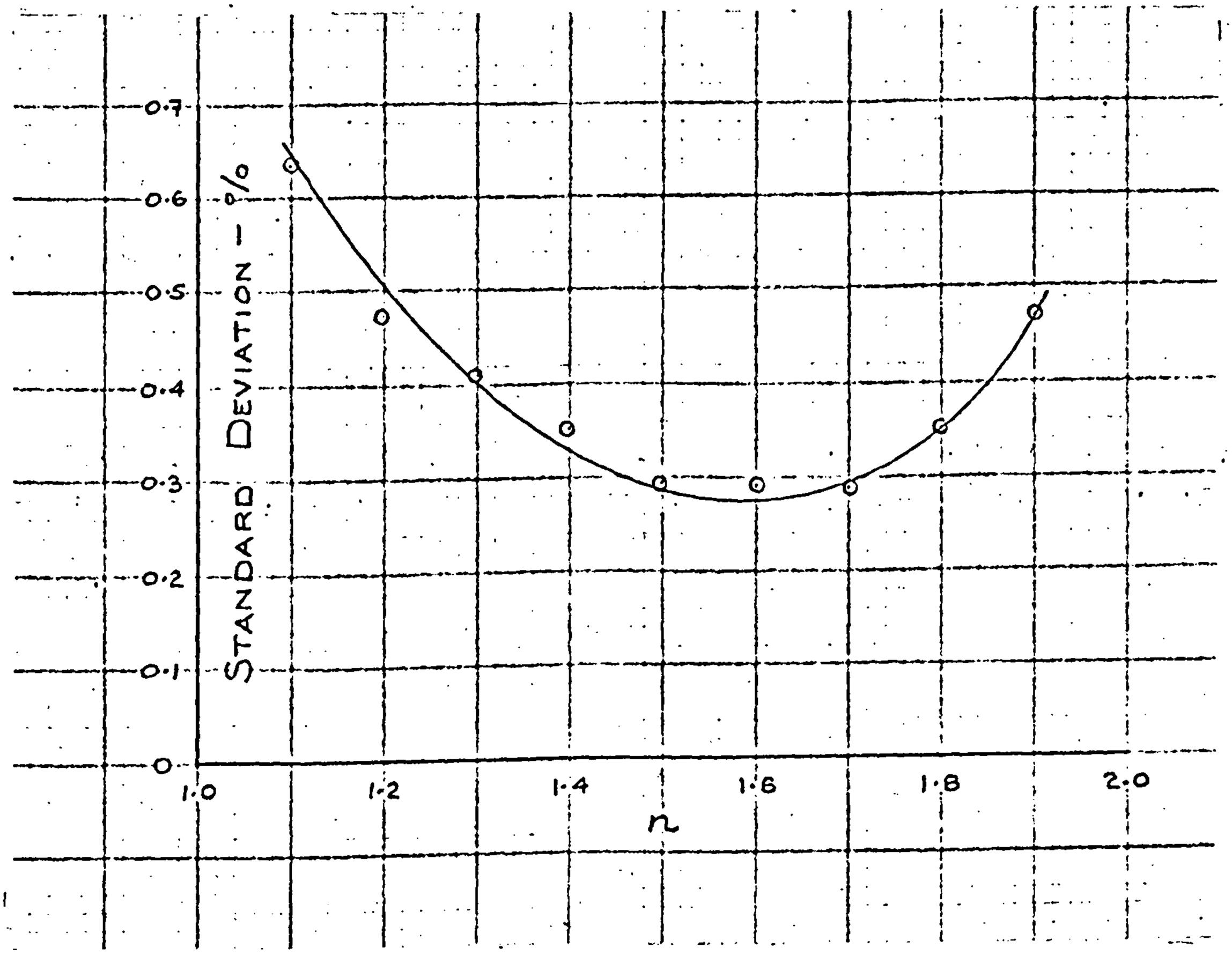

FIGURE 31b. NISHIHARA AND KAWAMOTO DATA

COMPARISON WITH EQUATION 7.2.

STANDARD DEVIATION v n.

MEAN VALUES.

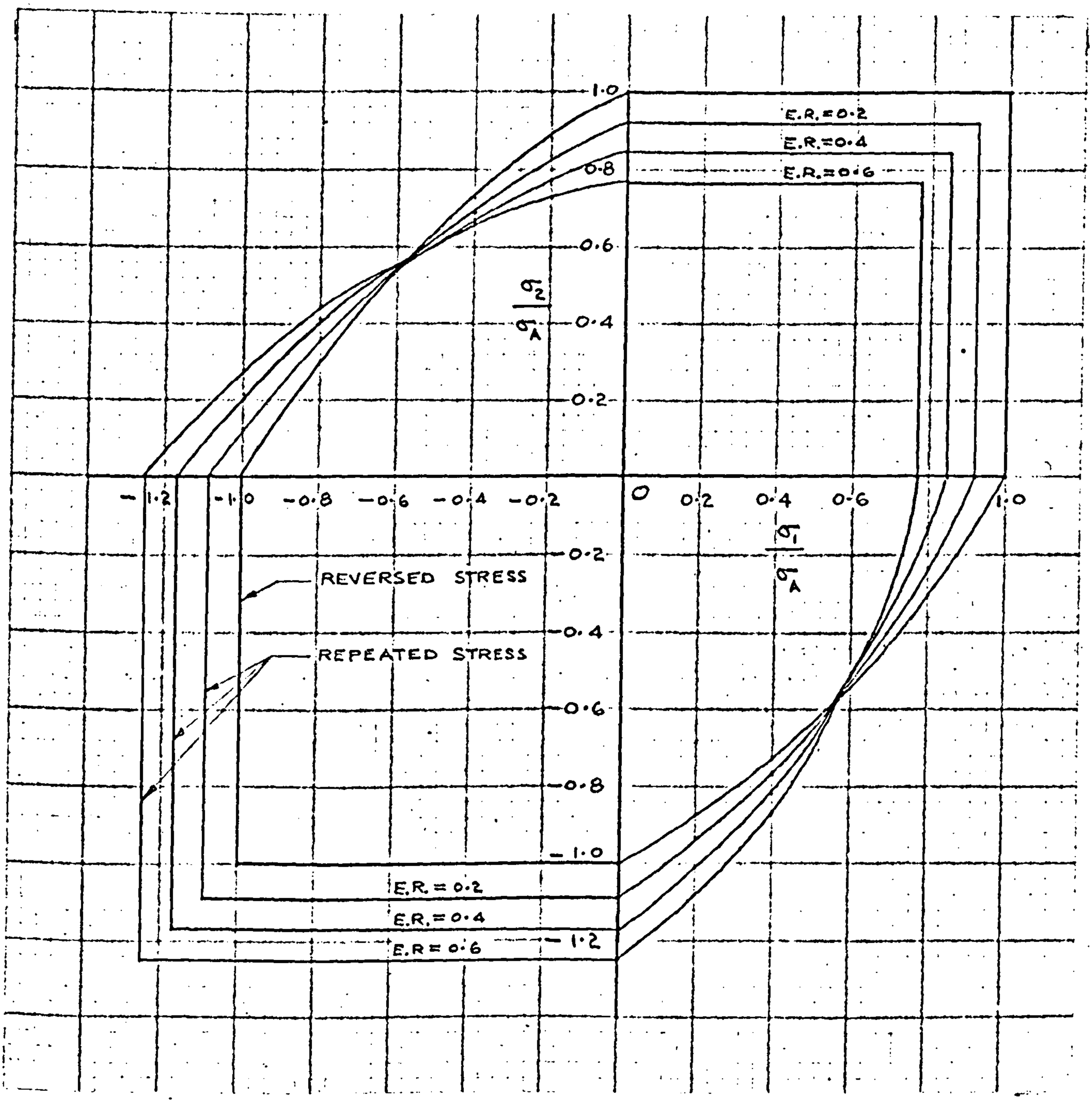

σ_1, σ_2 = LIMITING BIAXIAL PRINCIPAL STRESSES

σ_A = UNIAXIAL REVERSED FATIGUE STRENGTH

E.R. = ENDURANCE RATIO, σ_A/σ_U

FIGURE 32. LIMITING REVERSED AND REPEATED BIAXIAL STRESSES FOR ISOTROPIC DUCTILE MATERIALS AS PREDICTED BY EQUATIONS 7.14 AND 7.19.

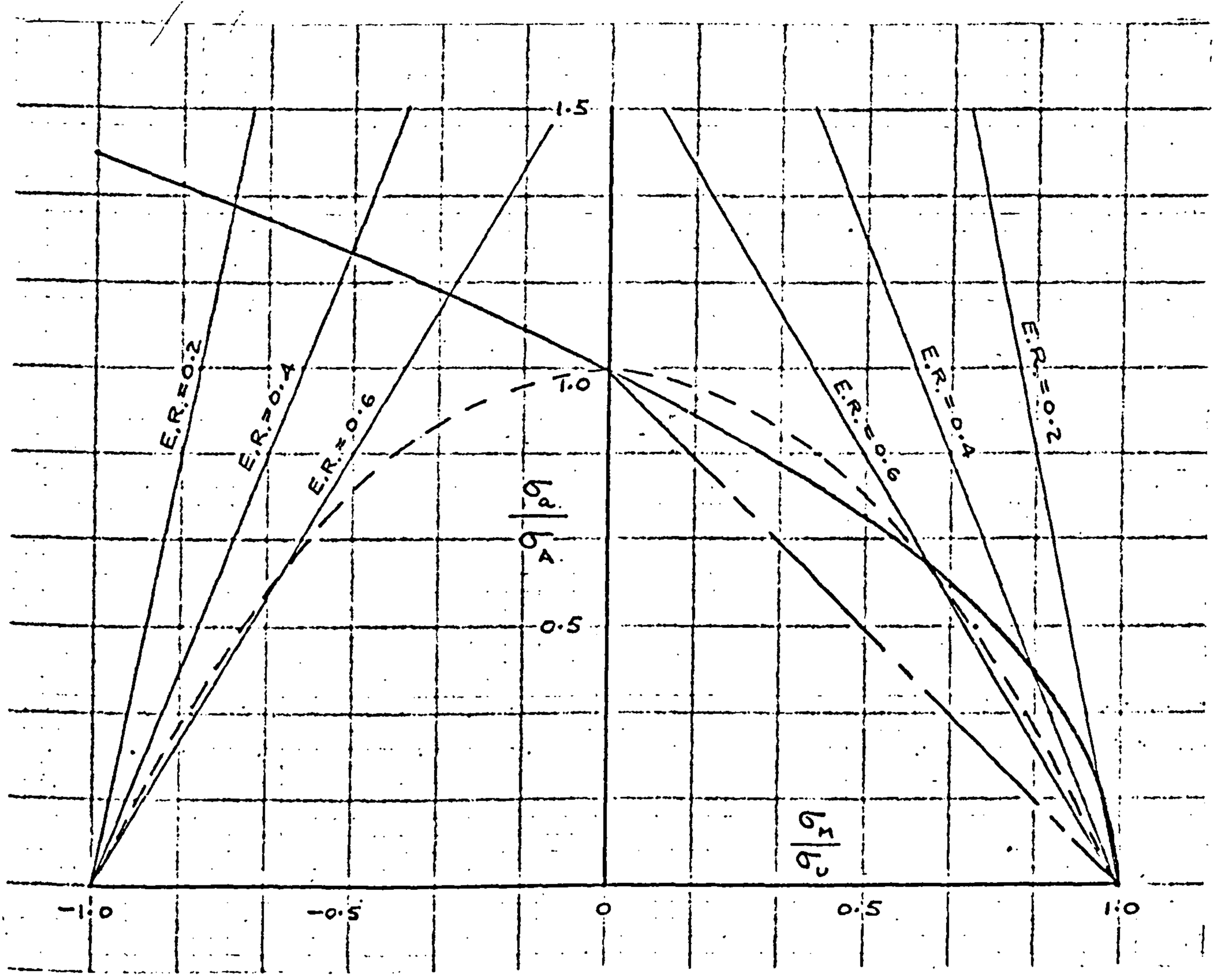

σ_a = STRESS AMPLITUDE

σ_A = REVERSED FATIGUE STRENGTH

σ_m = MEAN STRESS

σ_u = ULTIMATE TENSILE STRENGTH

E.R. = ENDURANCE RATIO, σ_A/σ_u

——— $\left[\frac{\sigma_a}{\sigma_A}\right]^2 + \frac{\sigma_m}{\sigma_u} = 1$ BOOTH EQUATION

- - - - $\frac{\sigma_a}{\sigma_A} + \left[\frac{\sigma_m}{\sigma_u}\right]^2 = 1$ GERBER PARABOLA

——— - $\frac{\sigma_a}{\sigma_A} + \frac{\sigma_m}{\sigma_u} = 1$ MODIFIED GOODMAN LINE

FIGURE 33. COMPARISON OF UNIAXIAL MEAN STRESS EQUATIONS.

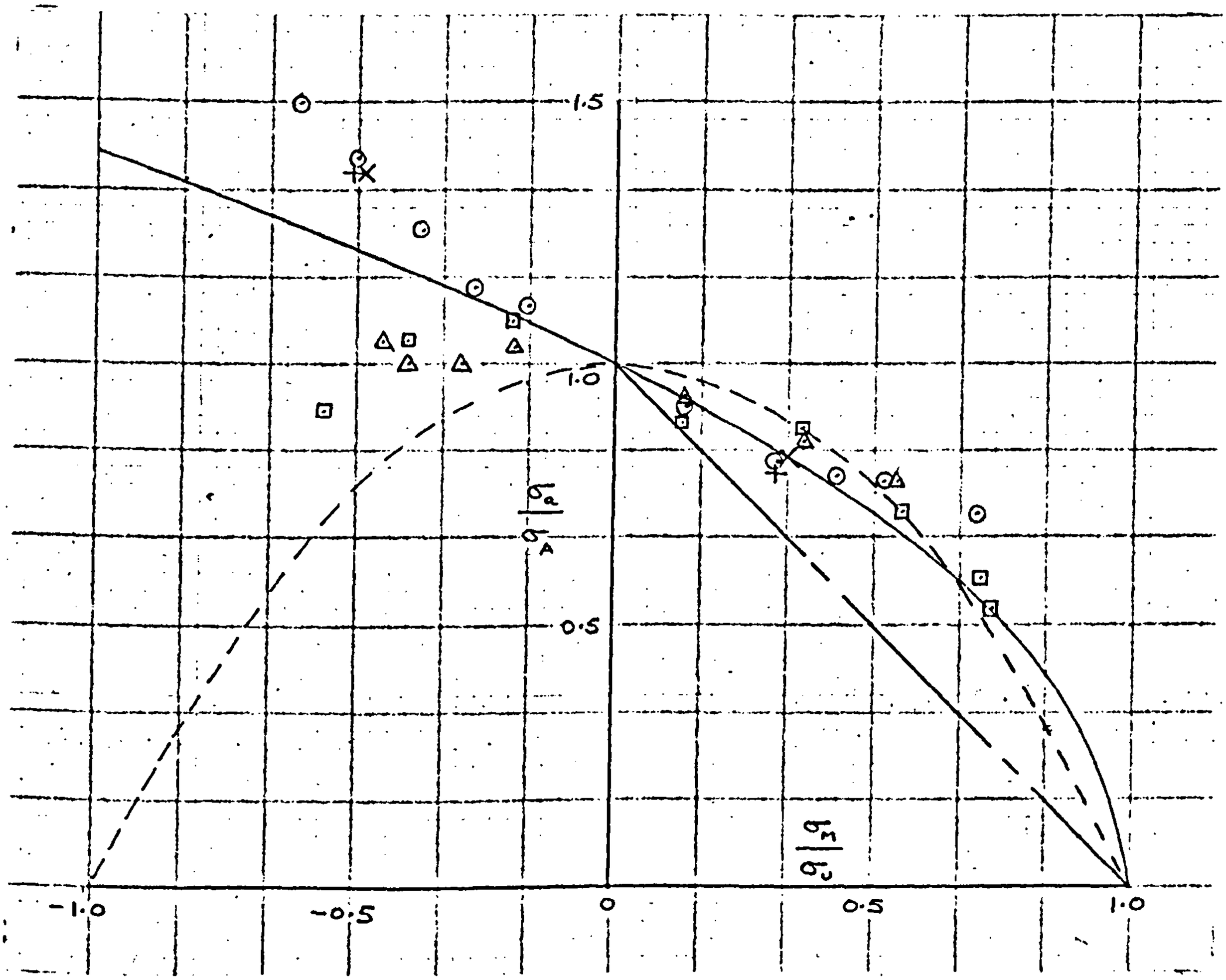

⊙ 0·41 % C. STEEL
× 0·44 % C. STEEL
\+ 0·65 % C. STEEL
NISHIHARA AND SAKURAI (91)

△ Ni. Cr. Mo. STEEL — WHITE, CROSSLAND, MORRISON (47)

⊡ Ni. Cr. Mo. STEEL — O'CONNOR, MORRISON (92)

——— BOOTH EQUATION

– – – – – GERBER PARABOLA

———– MODIFIED GOODMAN LINE

FIGURE 34. EFFECT OF MEAN STRESS ON THE FATIGUE STRESS AMPLITUDE OF UNNOTCHED STEELS.

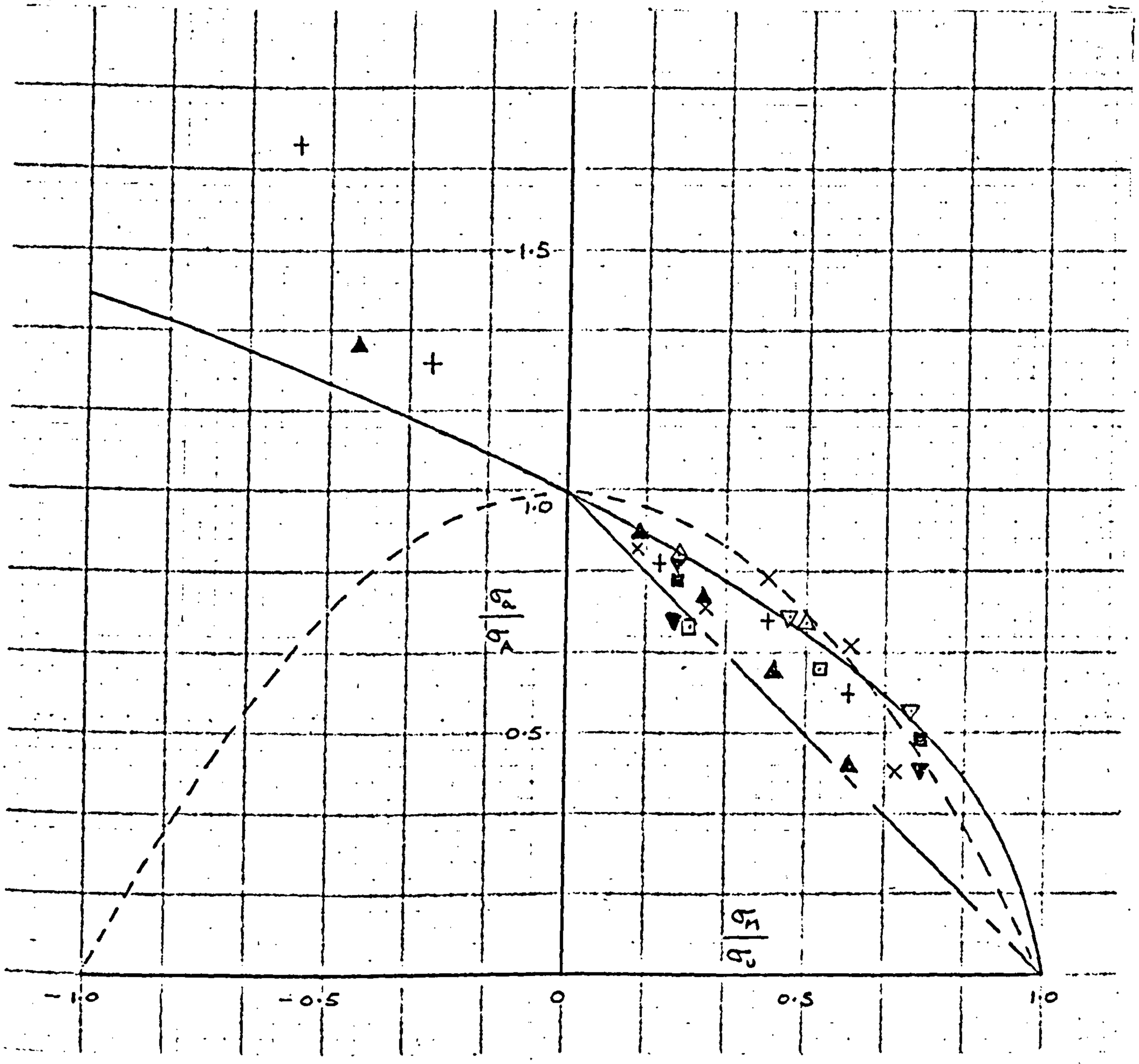

△ NS 4-½ H
▽ HE 20 WP
□ NP 4 M
▲ HE 15 W
▼ NP 5/6 M
X HE 15 WP
■ HE 10 WP
\+ HE 15 WP

WOODWARD, GUNN, FORREST (93) ALUMINIUM ALLOYS AT 10^7 CYCLES

——— BOOTH EQUATION

— — — — GERBER PARABOLA

——— — MODIFIED GOODMAN LINE

FIGURE 35. EFFECT OF MEAN STRESS ON THE FATIGUE STRESS AMPLITUDE OF UNNOTCHED ALUMINIUM ALLOYS.

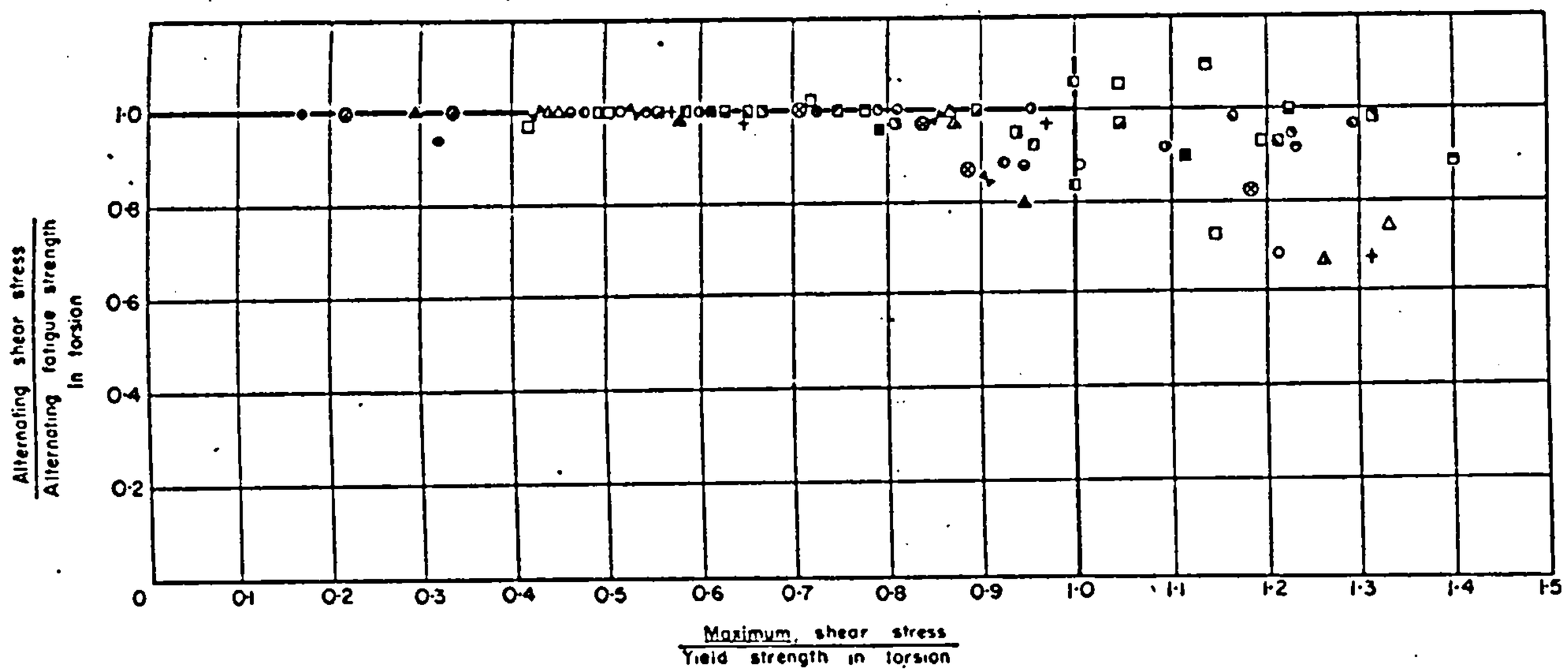

FIG. 55. Non-dimensional alternating shear stress–maximum shear stress diagram for ductile metals in torsion. (Smith [189])

+ Cr-Ni Steel, Quenched-Tempered	P. Ludwik and J. Krystok	Malleable Iron, Untempered	A. Pomp and M. Hempel
⊛ Siemens-Martin Steel		Malleable Iron, Tempered	
⊙ Baustahl, Soft		Beryllium Bronze, 97·6% Be–2·38% Cu	
□ Schmieder Bronze A, as rolled		0·9% C Steel, Quenched-Tempered	J. B. Johnson
△ Aluminium Alloy 17ST	Aluminium Co. of America	Cr-V Steel, Quenched-Tempered	
△ Aluminium Alloy 27ST		SAE 3140 Steel, Quenched-Tempered	
△ Aluminium Alloy 53ST		SAE 3140 Steel, as Hot-Rolled	J. O. Smith
▨ Mild Steel, Hot-Rolled		Tobin Bronze, Cold-Rolled	
◫ 0·6% C Steel, Quenched-Tempered	G. A. Hankins	1·2% C Steel, Normalized	
○ Si-Mn Steel, Quenched-Tempered		3·5% Ni Steel, Special Treatment "A"	H. F. Moore and T. M. Jasper
⊖ Cr-V Steel, Quenched-Tempered		3·5% Ni Steel, Special Treatment "D"	
◐ Brass, 60 Cu–40 Zn, as Rolled	H. F. Moore and R. E. Lewis	0·49% C Steel, Normalized	
⊖ Copper, Commercially Pure, Cold Rolled		0·46% C Steel, Quenched-Drawn	D. J. McAdam, Jr.
◑ Duralumin, as Rolled			

REPRODUCED FROM FORREST (64)

FIGURE 36. ALTERNATING SHEAR STRESS - MAXIMUM SHEAR STRESS DIAGRAM FOR DUCTILE MATERIALS IN TORSION.

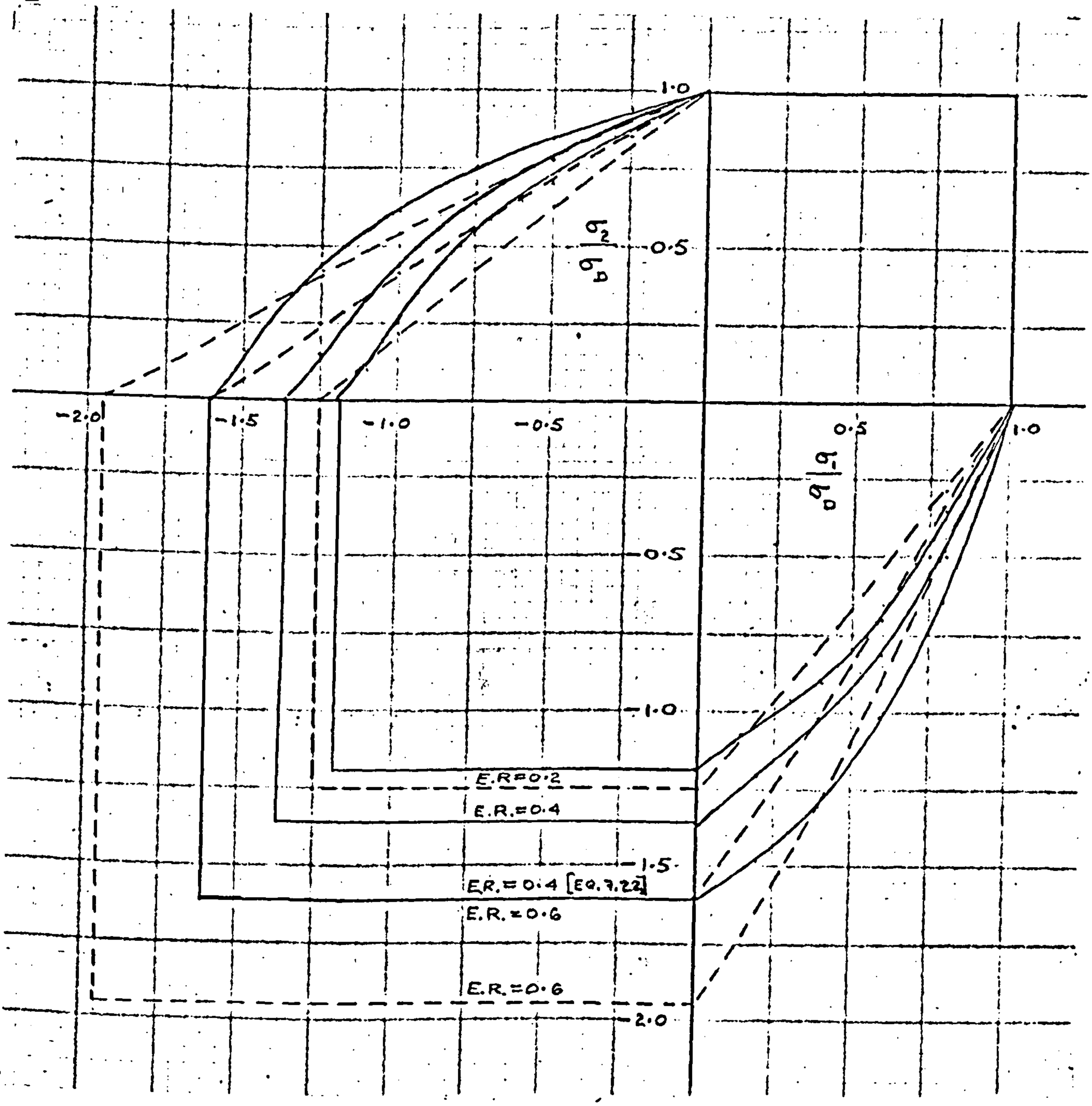

σ_1, σ_2 = LIMITING BIAXIAL PRINCIPAL STRESSES

σ_D = UNIAXIAL REPEATED TENSILE FATIGUE STRENGTH

E.R. = ENDURANCE RATIO, σ_A/σ_U

——— LIMITING STRESSES PREDICTED BY EQUATION 7.19.

- - - - LIMITING STRESSES PREDICTED BY EQUATION 7.22.

FIGURE 37. LIMITING REPEATED BIAXIAL STRESSES FOR ISOTROPIC DUCTILE MATERIALS AS PREDICTED BY EQUATIONS 7.19. AND 7.22.

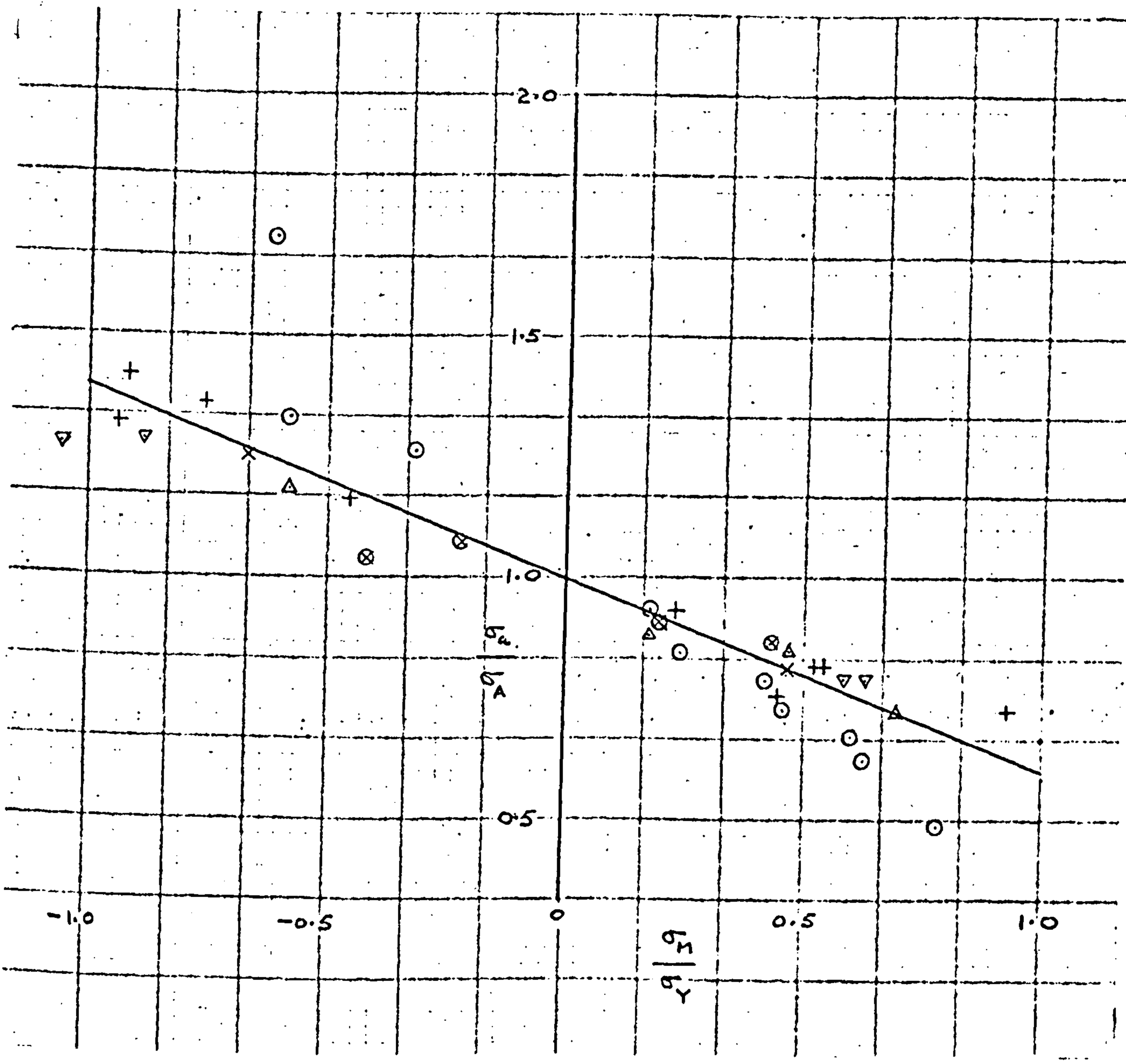

⊙	ALUMINIUM ALLOYS	WOODWARD ET AL (93)
⊗	Ni. Cr. Mo. STEEL	O'CONNAR AND MORRISON (92).
+	C. STEELS	NISHIHARA AND SAKURAI — FROM (6)
△	DURALUMIN	NISHIHARA AND KOJIMA — FROM (6)
▽	MILD STEEL	ROS AND EICHINGER — FROM (6)
×	ALUMINIUM ALLOY 24S-T	NEWMARK ET AL — FROM (6)

REPRODUCED FROM FORREST (84).

FIGURE 38. EFFECT OF MEAN STRESS ON FATIGUE STRESS AMPLITUDE OF STEELS AND ALUMINIUM ALLOYS IN TERMS OF YIELD STRESS

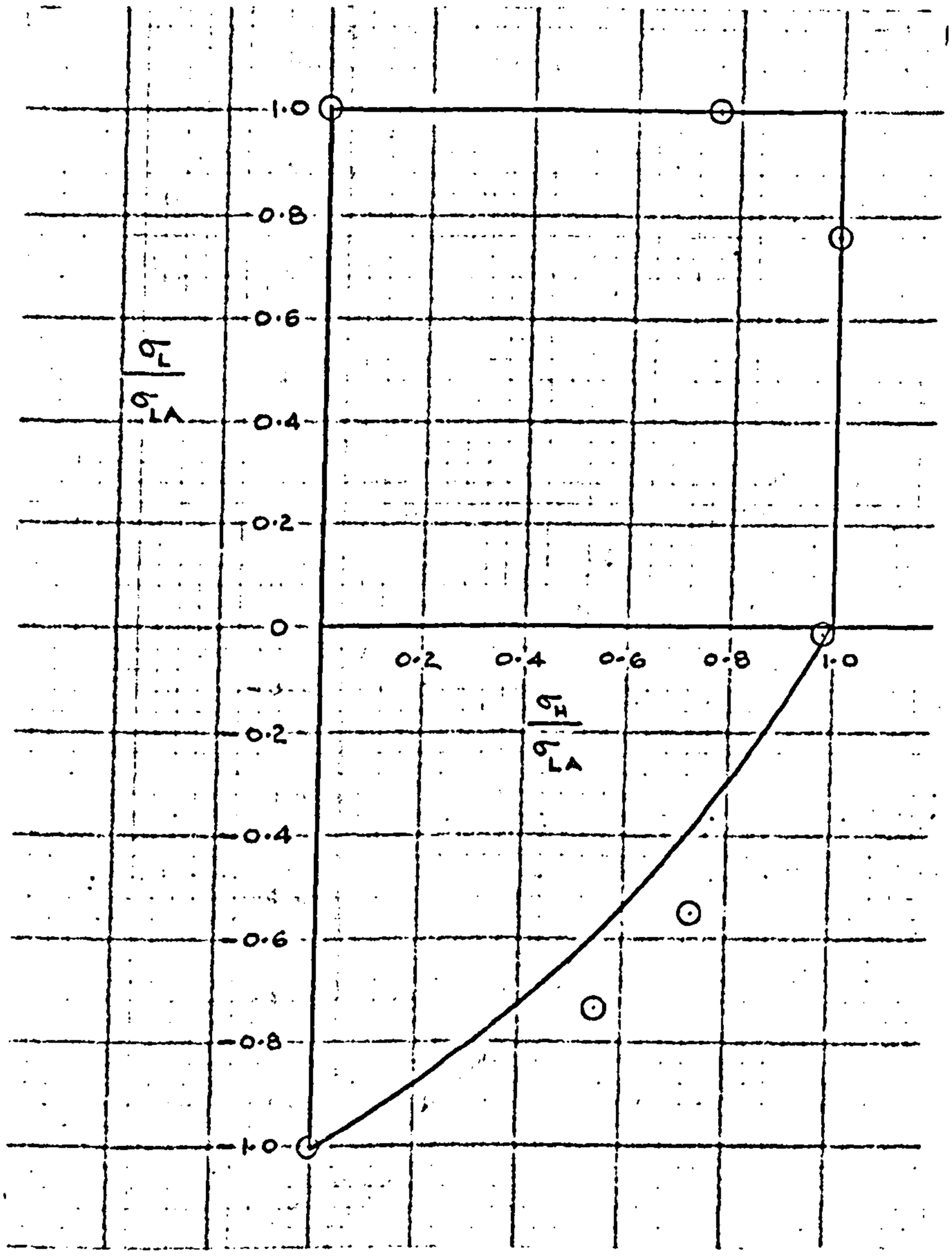

ROTVEL (39) – 0·35% C. STEEL – FATIGUE LIMIT

σ_L = LONGITUDINAL STRESS

σ_H = HOOP STRESS

σ_{LA} = REVERSED LONGITUDINAL FATIGUE STRENGTH

——— LIMITING STRESSES PREDICTED BY PROPOSED EQUATION 7.14.

FIGURE 39a. RESULTS FROM TESTS CARRIED OUT BY ROTVEL (39) ON THIN CYLINDERS COMPARED WITH THE PROPOSED EQUATION 7.14.

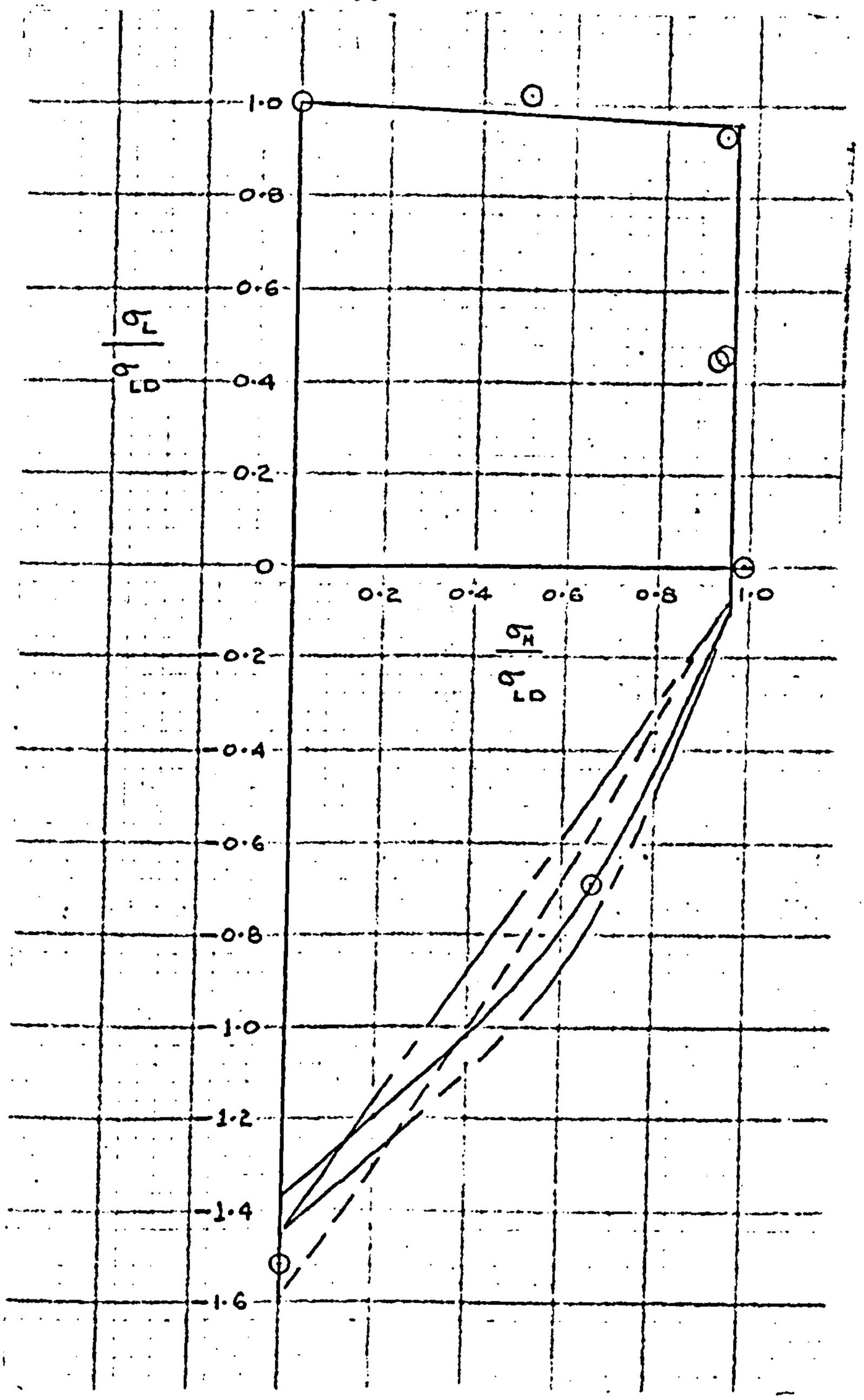

ROS AND EICHINGER (34) - TUBE STEEL.

σ_L = LONGITUDINAL STRESS

σ_H = HOOP STRESS

σ_{LD} = REPEATED TENSILE LONGITUDINAL FATIGUE STRENGTH

LIMITING STRESSES PREDICTED BY:

——— — BOOTH EQUATION 8.4.

——— - - BOOTH EQUATION 8.2.

— — — — — PROPOSED EQUATION 7.22

——————— PROPOSED EQUATION 7.19.

FIGURE 39b. RESULTS FROM TESTS CARRIED OUT BY ROS AND EICHINGER (34) ON THIN CYLINDERS COMPARED WITH THE PROPOSED EQUATIONS 7.19. AND 7.22 AND THE BOOTH EQUATIONS 8.2, 8.4.

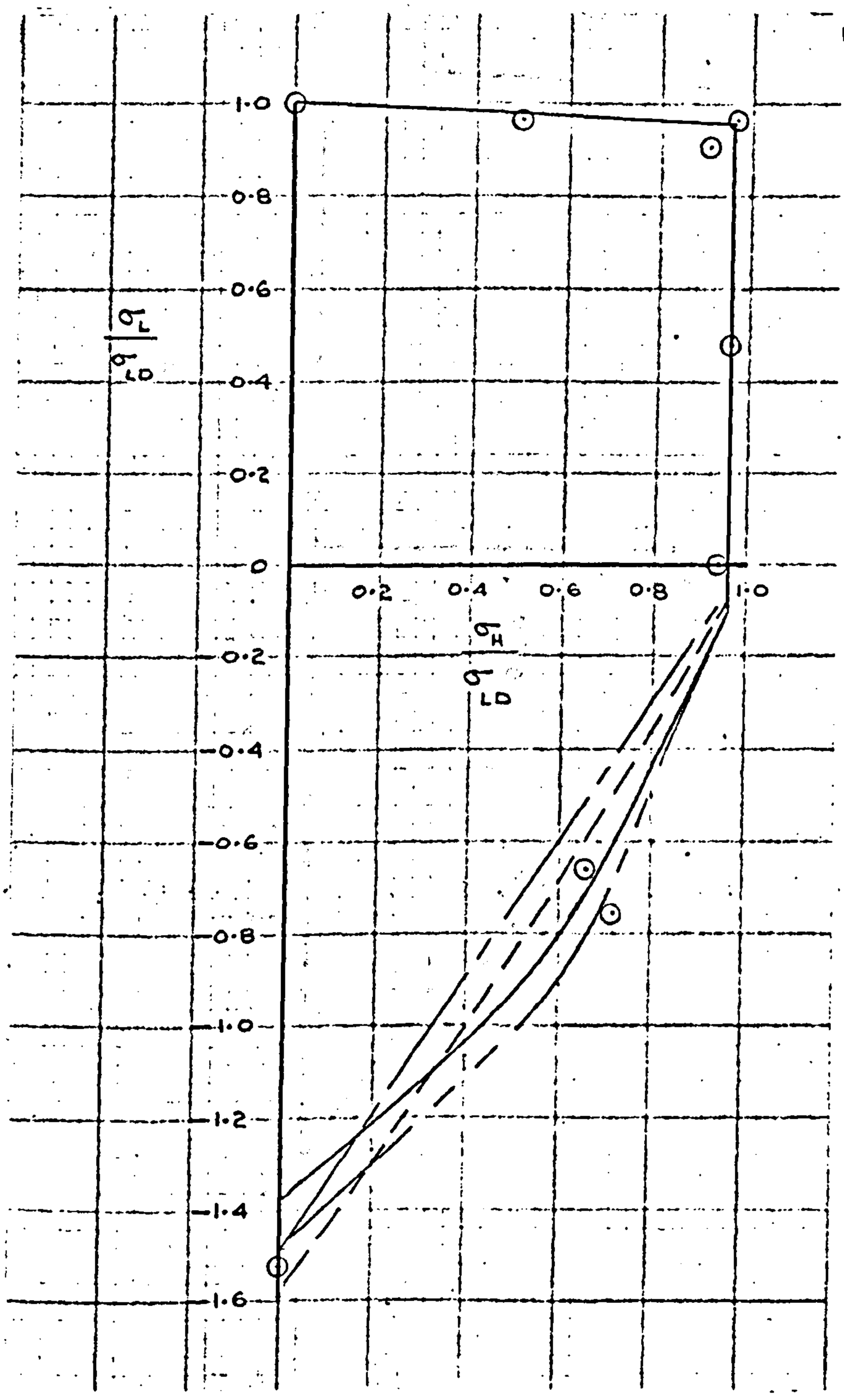

ROS AND EICHINGER (34) – CAST STEEL

σ_L = LONGITUDINAL STRESS

σ_H = HOOP STRESS

σ_{LD} = REPEATED TENSILE LONGITUDINAL FATIGUE STRENGTH

LIMITING STRESSES PREDICTED BY:

——— – BOOTH EQUATION 8.4.

—— – – BOOTH EQUATION 8.2.

– – – – – PROPOSED EQUATION 7.22

——— PROPOSED EQUATION 7.19.

FIGURE 39c. RESULTS FROM TESTS CARRIED OUT BY ROS AND EICHINGER (34) ON THIN CYLINDERS COMPARED WITH THE PROPOSED EQUATIONS 7.19. AND 7.22. AND THE BOOTH EQUATIONS 8.2., 8.4.

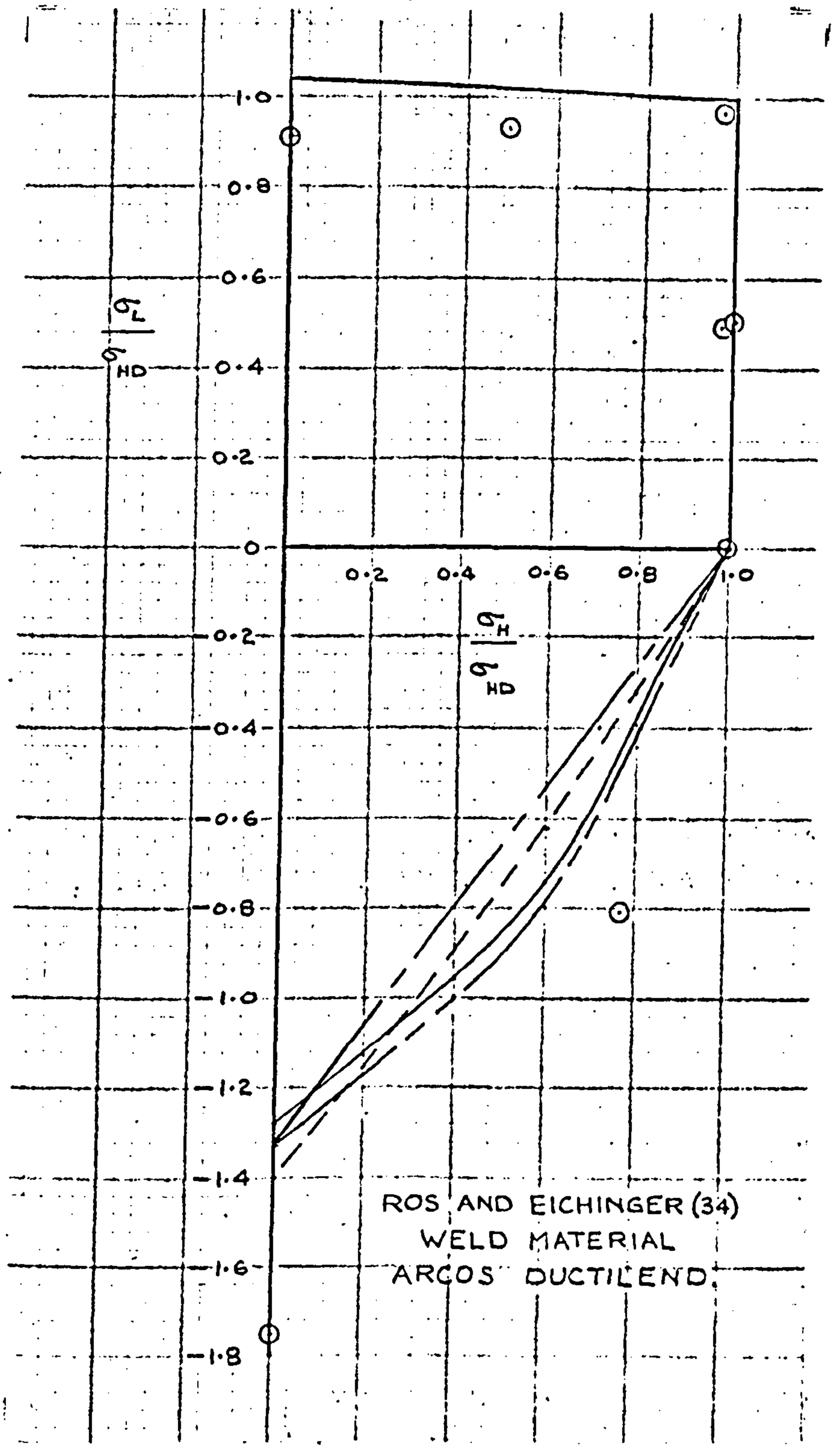

σ_L = LONGITUDINAL STRESS

σ_H = HOOP STRESS

σ_{HD} = REPEATED TENSILE HOOP FATIGUE STRENGTH.

LIMITING STRESSES PREDICTED BY:

——— — BOOTH EQUATION 8.4.

——— — — BOOTH EQUATION 8.2.

— — — — — PROPOSED EQUATION 7.22

——————— PROPOSED EQUATION 7.19.

FIGURE 39d. RESULTS FROM TESTS CARRIED OUT BY ROS AND EICHINGER (34) ON THIN CYLINDERS COMPARED WITH THE PROPOSED EQUATIONS 7.19. AND 7.22. AND THE BOOTH EQUATIONS 8.2, 8.4.

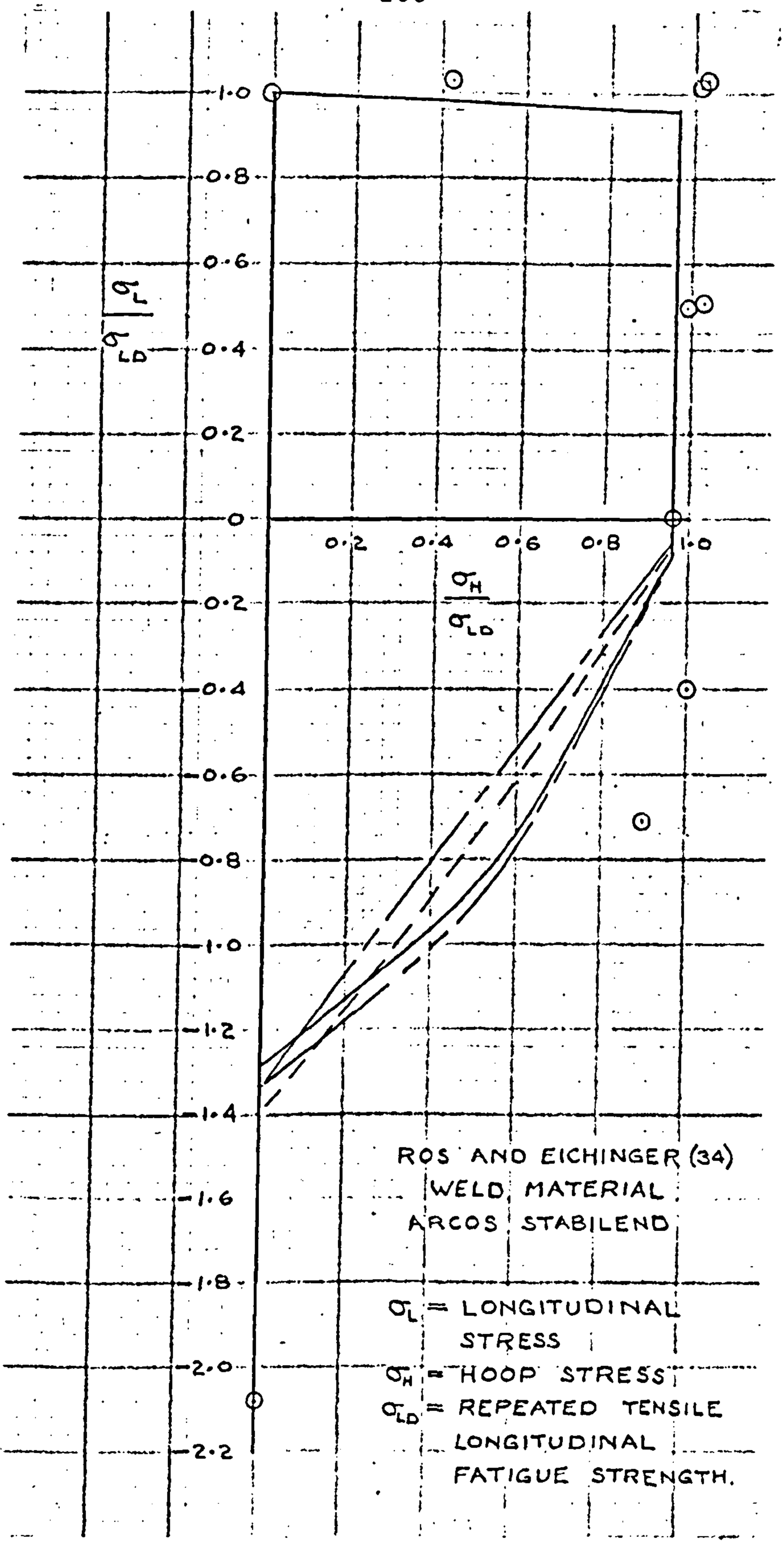

FIGURE 39e. RESULTS FROM TESTS CARRIED OUT BY ROS AND EICHINGER (34) ON THIN CYLINDERS COMPARED WITH THE PROPOSED EQUATIONS 7.19. AND 7.22. AND THE BOOTH EQUATIONS 8.2., 8.4.

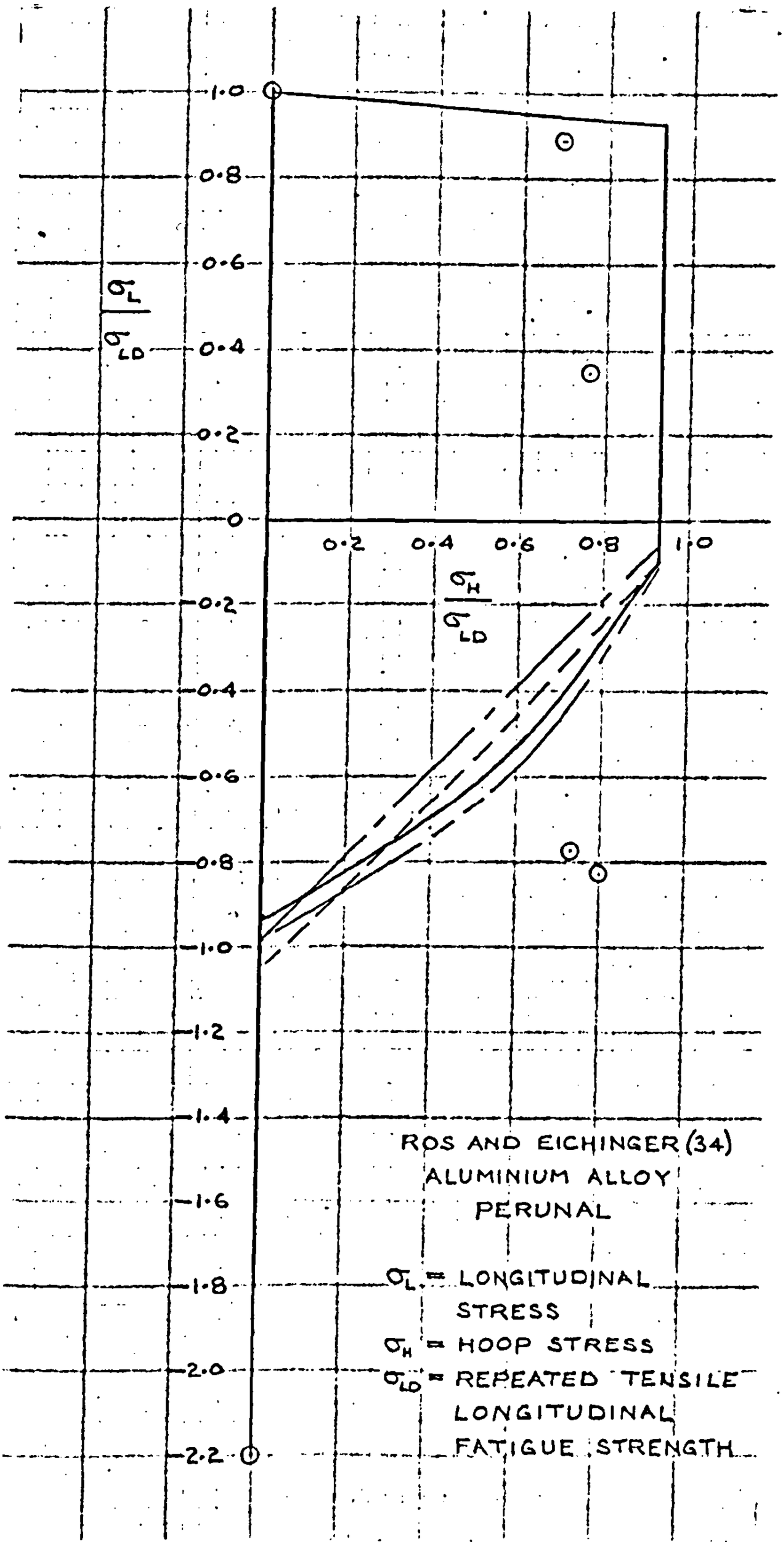

FIGURE 39f. RESULTS FROM TESTS CARRIED OUT BY ROS AND EICHINGER (34) ON THIN CYLINDERS COMPARED WITH THE PROPOSED EQUATIONS 7.19. AND 7.22. AND THE BOOTH EQUATIONS 8.2. 8.4.

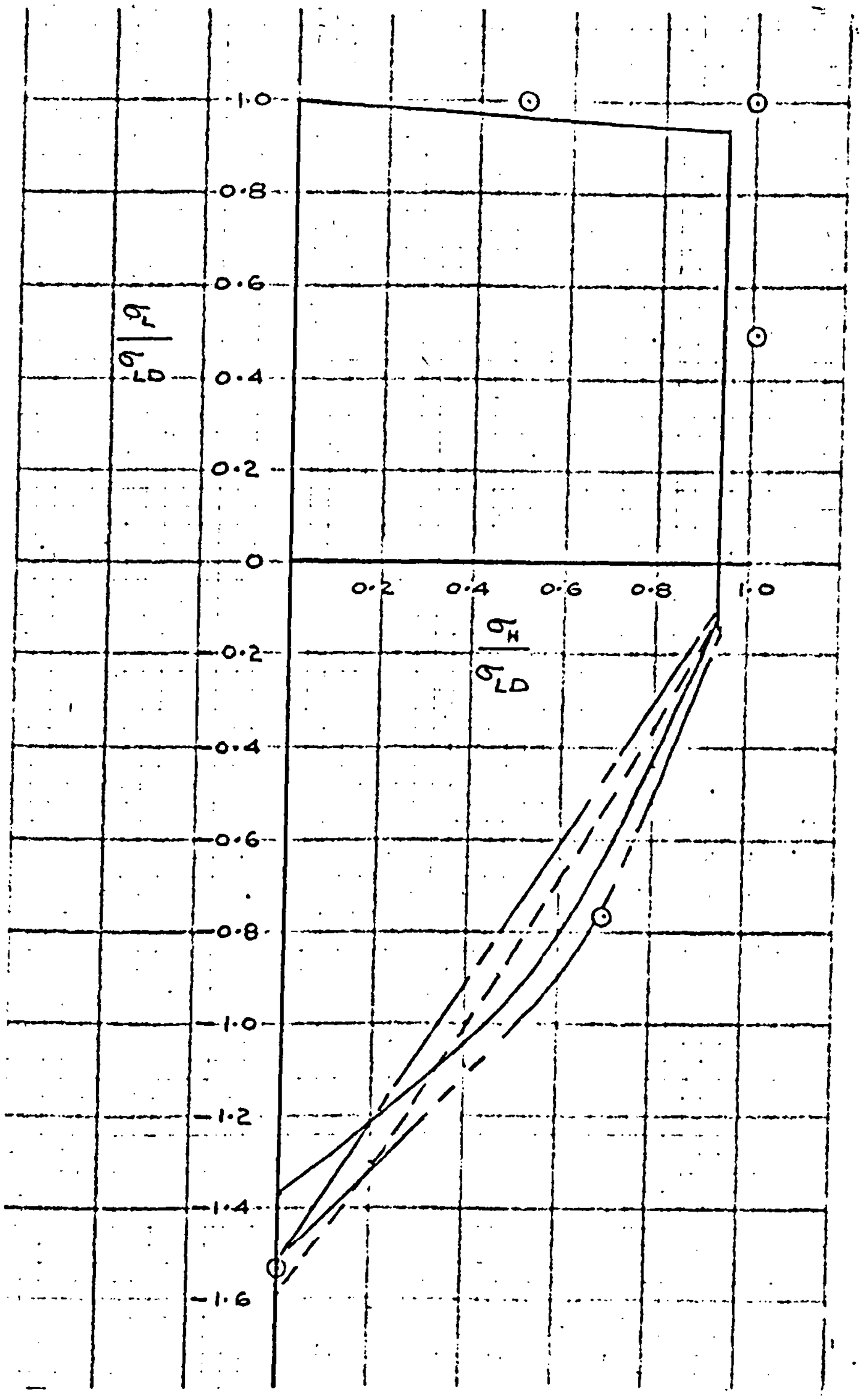

ROS AND EICHINGER(34) - REINEALUMINIUM

σ_L = LONGITUDINAL STRESS

σ_H = HOOP STRESS

σ_{LD} = REPEATED TENSILE LONGITUDINAL FATIGUE STRENGT

LIMITING STRESSES PREDICTED BY:

———— — BOOTH EQUATION 8.4.

———— — — BOOTH EQUATION 8.2.

— — — — — — PROPOSED EQUATION 7.22.

———————— PROPOSED EQUATION 7.19.

FIGURE 39g. RESULTS FROM TESTS CARRIED OUT BY ROS AND EICHINGER (34) ON THIN CYLINDERS COMPARED WITH THE PROPOSED EQUATIONS 7.19. AND 7.22. AND THE BOOTH EQUATIONS 8.2., 8.4.

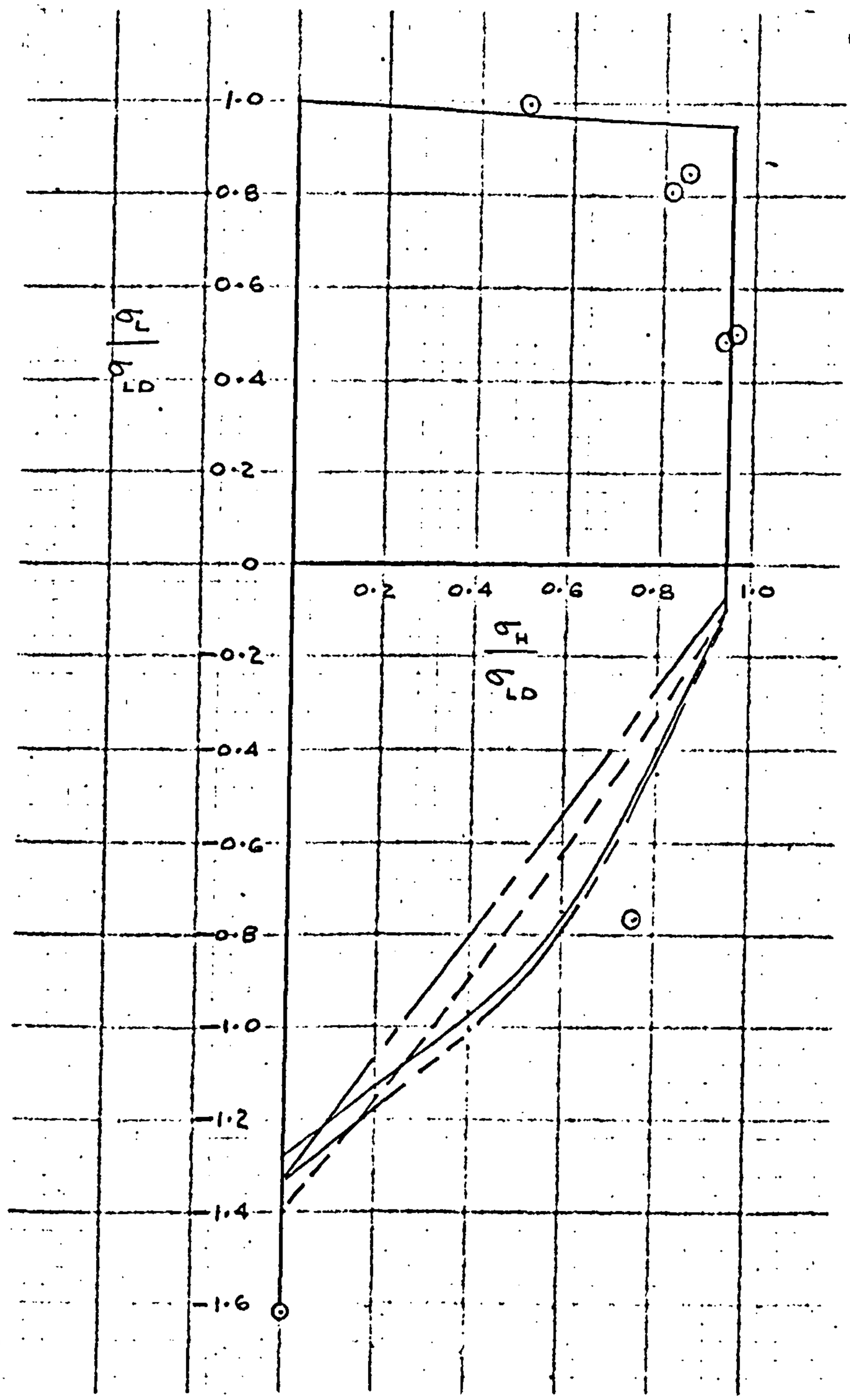

ROS AND EICHINGER (34) - AVIONAL

σ_L = LONGITUDINAL STRESS

σ_H = HOOP STRESS

σ_{LD} = REPEATED TENSILE LONGITUDINAL FATIGUE STRENGTH

LIMITING STRESSES PREDICTED BY:

———— — BOOTH EQUATION 8.4.

———— — — BOOTH EQUATION 8.2.

— — — — — PROPOSED EQUATION 7.22.

———— PROPOSED EQUATION 7.19.

FIGURE 39h. RESULTS FROM TESTS CARRIED OUT BY ROS AND EICHINGER (34) ON THIN CYLINDERS COMPARED WITH THE PROPOSED EQUATIONS 7.19. AND 7.22. AND THE BOOTH EQUATIONS 8.2. 8.4.

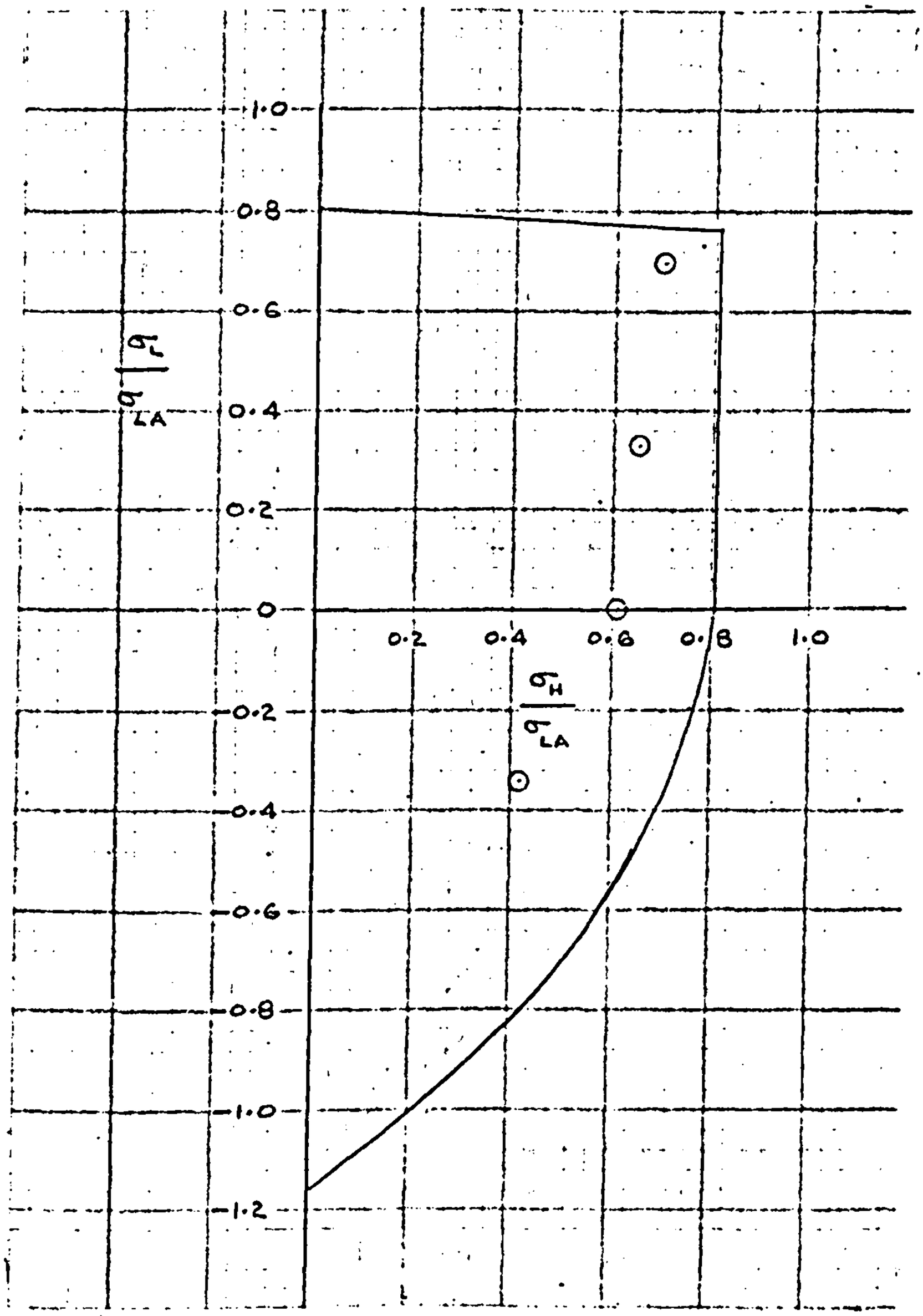

MAJORS ET AL (35) - SAE 1020 STEEL - FATIGUE LIMIT.

σ_L = LONGITUDINAL STRESS

σ_H = HOOP STRESS

σ_{LA} = REVERSED LONGITUDINAL FATIGUE STRENGTH

——— LIMITING STRESSES PREDICTED BY THE PROPOSED EQUATION 7.19.

FIGURE 39j. RESULTS FROM TESTS CARRIED OUT BY MAJORS ET AL (35) ON THIN CYLINDERS COMPARED WITH THE PROPOSED EQUATION 7.19.

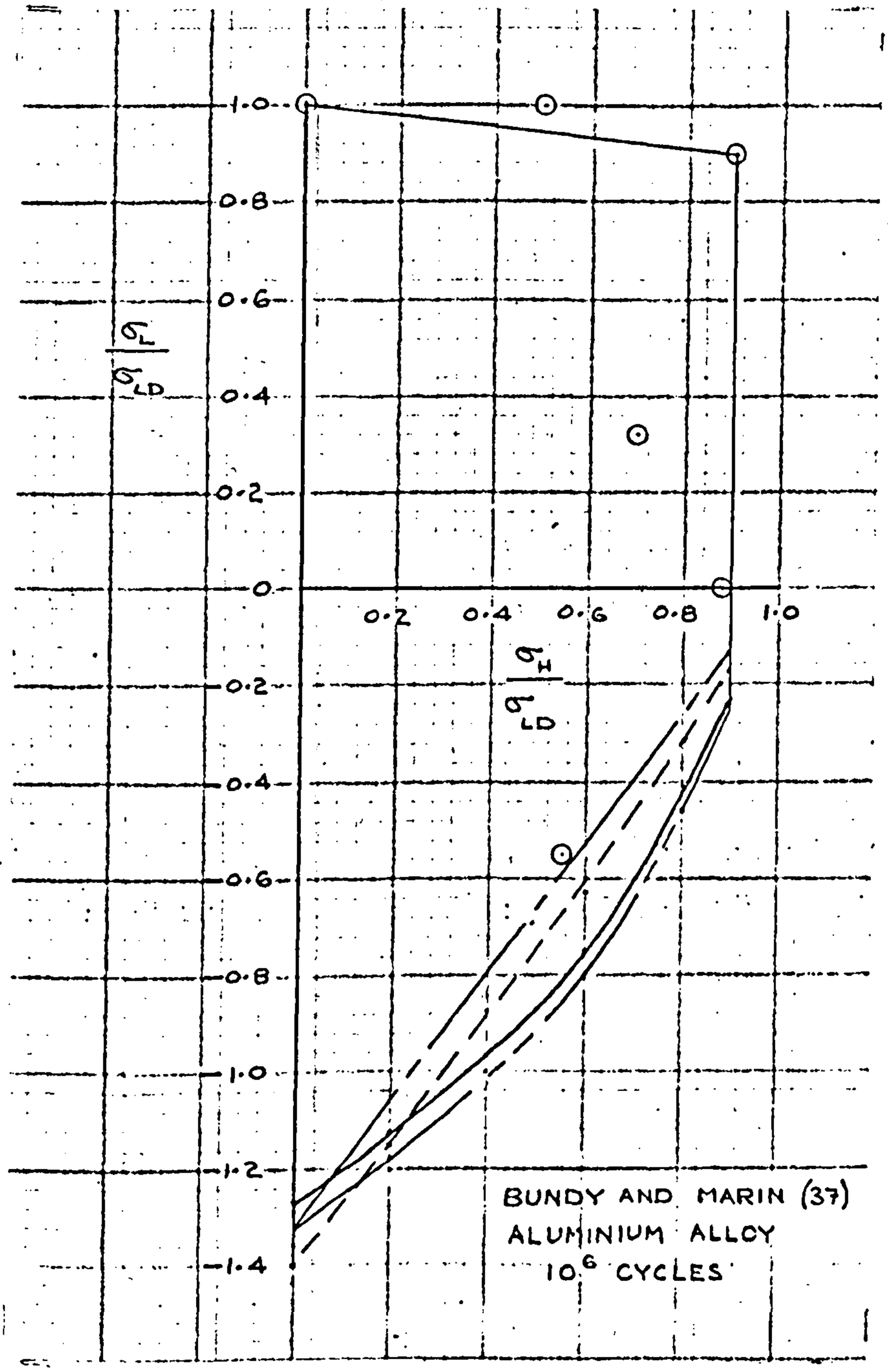

σ_L = LONGITUDINAL STRESS

σ_H = HOOP STRESS

σ_{LD} = REPEATED TENSILE LONGITUDINAL FATIGUE STRENGTH

LIMITING STRESSES PREDICTED BY:

———— BOOTH EQUATION 8.4.

———— – – BOOTH EQUATION 8.2.

– – – – – PROPOSED EQUATION 7.22.

———— PROPOSED EQUATION 7.19.

FIGURE 39k. RESULTS FROM TESTS CARRIED OUT BY BUNDY AND MARIN (37) ON THIN CYLINDERS COMPARED WITH THE PROPOSED EQUATIONS 7.19. AND 7.22. AND THE BOOTH EQUATIONS 8.2., 8.4

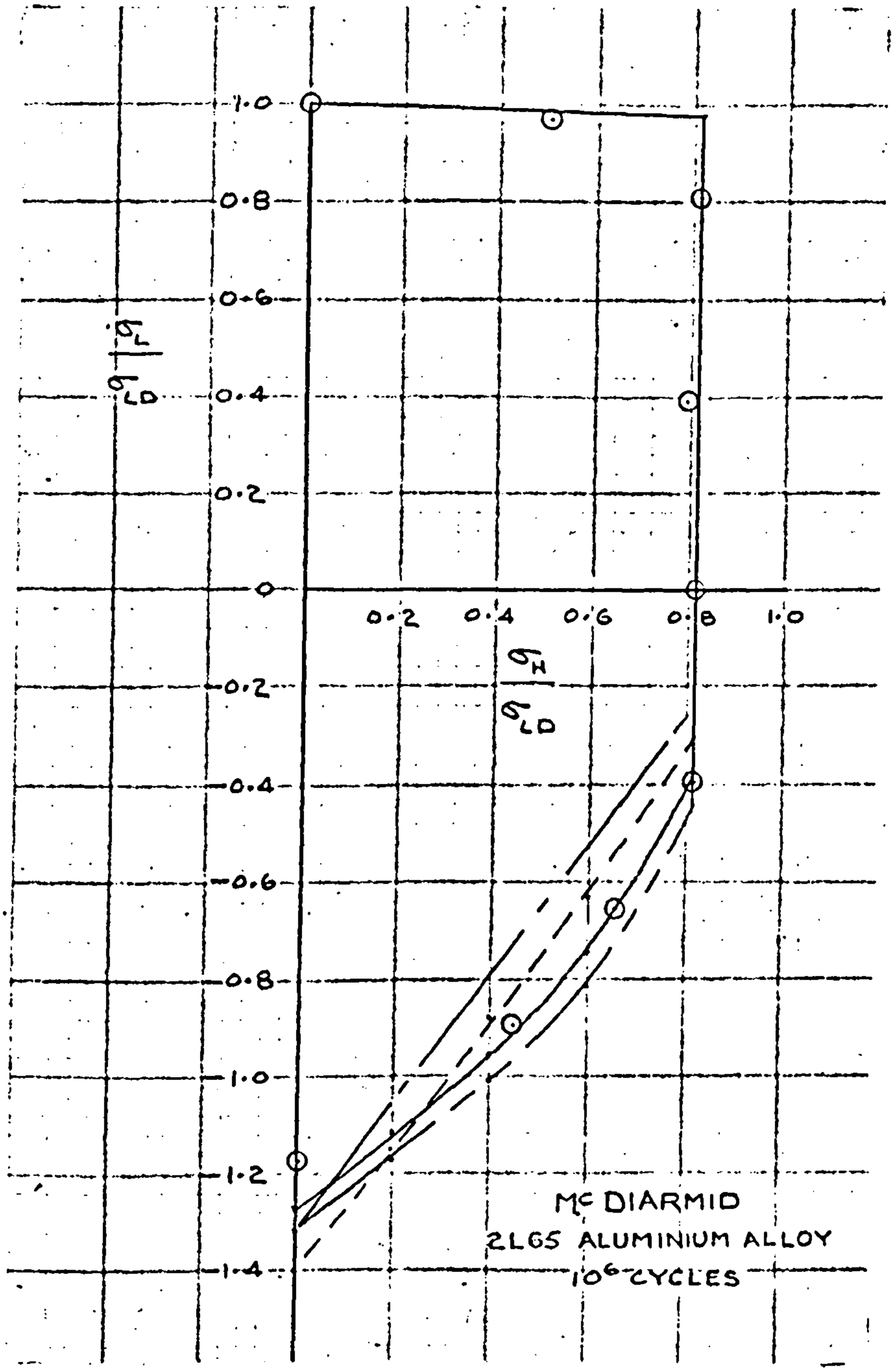

σ_L = LONGITUDINAL STRESS

σ_H = HOOP STRESS

σ_{LD} = REPEATED TENSILE LONGITUDINAL FATIGUE STRENGTH

LIMITING STRESSES PREDICTED BY:

———— — BOOTH EQUATION 8.4.

———— — — BOOTH EQUATION 8.2.

— — — — — PROPOSED EQUATION 7.22.

———— PROPOSED EQUATION 7.19.

FIGURE 40. RESULTS FROM PRESENT TESTS ON THIN CYLINDERS COMPARED WITH THE PROPOSED EQUATIONS 7.19. AND 7.22. AND THE BOOTH EQUATIONS 8.2. AND 8.4.

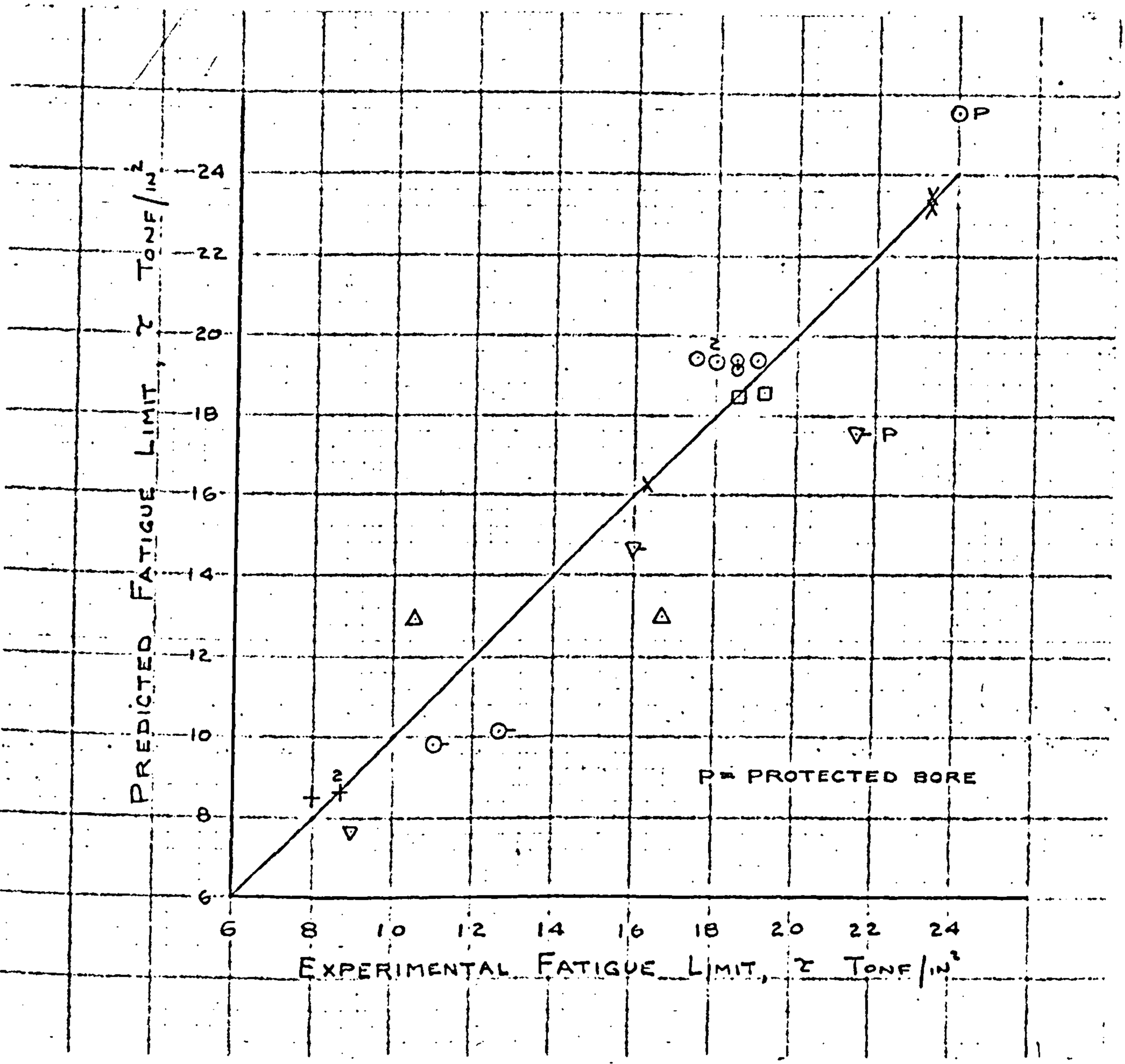

τ = RANGE OF PULSATING SHEAR FATIGUE STRENGTH AT 10^7 CYCLES.

SYMBOL	MATERIAL	
⊙	EN 25 STEEL (SOFT)	MORRISON (48)
X	EN 25 STEEL (HARD)	
⊡	HYKRO STEEL	
+	0·15 % C. STEEL	
△	18/8 Ti. STAINLESS STEEL	
▽	DTD 364 ALUMINIUM ALLOY	
⊙-	TITANIUM	
▽-	EN 26 STEEL	HASLAM (54)

FIGURE 41. RESULTS FROM TEST DATA IN THE LITERATURE ON THICK-WALL TUBES COMPARED WITH THE PROPOSED EQUATIONS 8.9. AND 8.11.

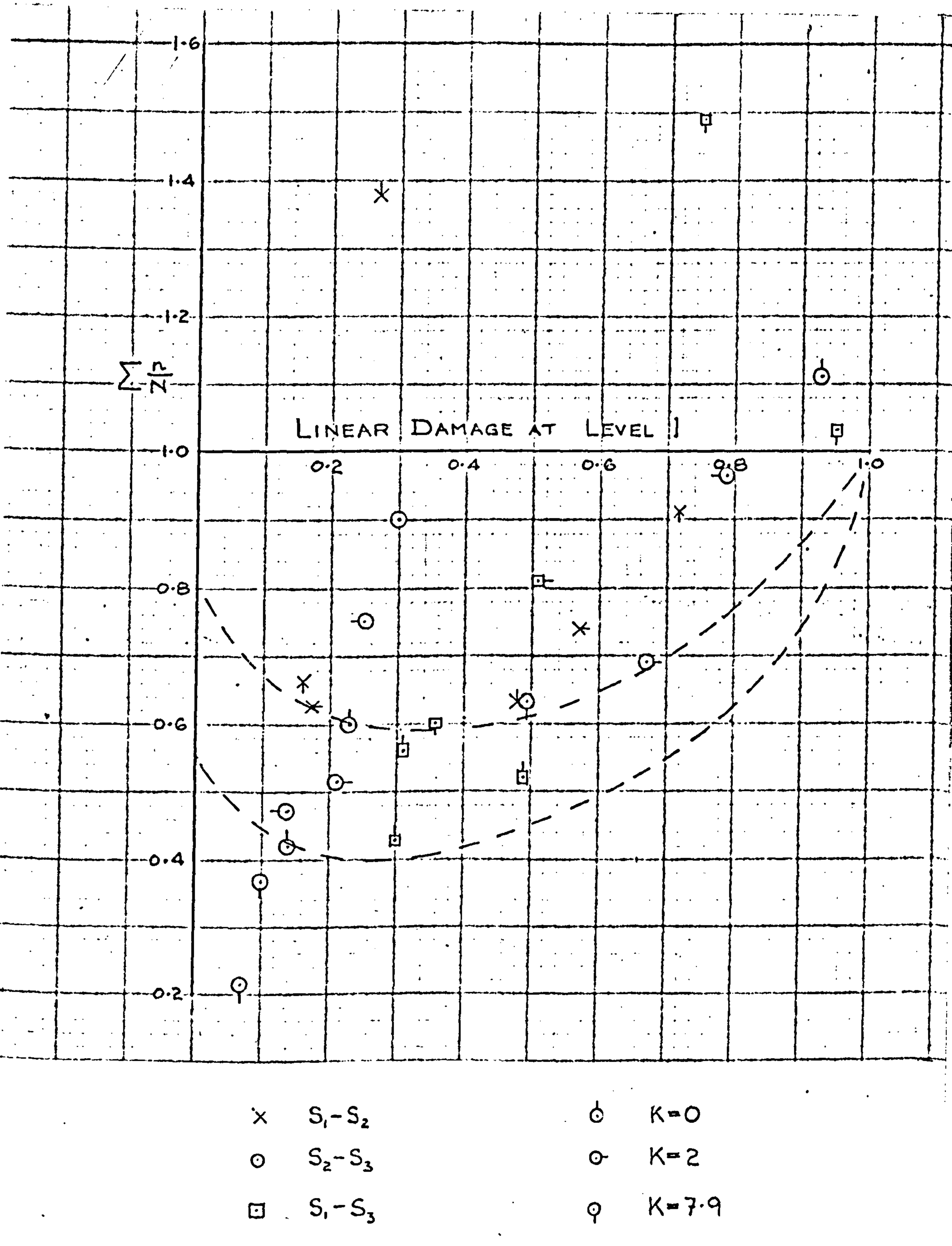

FIGURE 42. COMPARISON OF CUMULATIVE DAMAGE TEST RESULTS WITH THE STRESS DEPENDENCE THEORY OF EDWARDS (78).

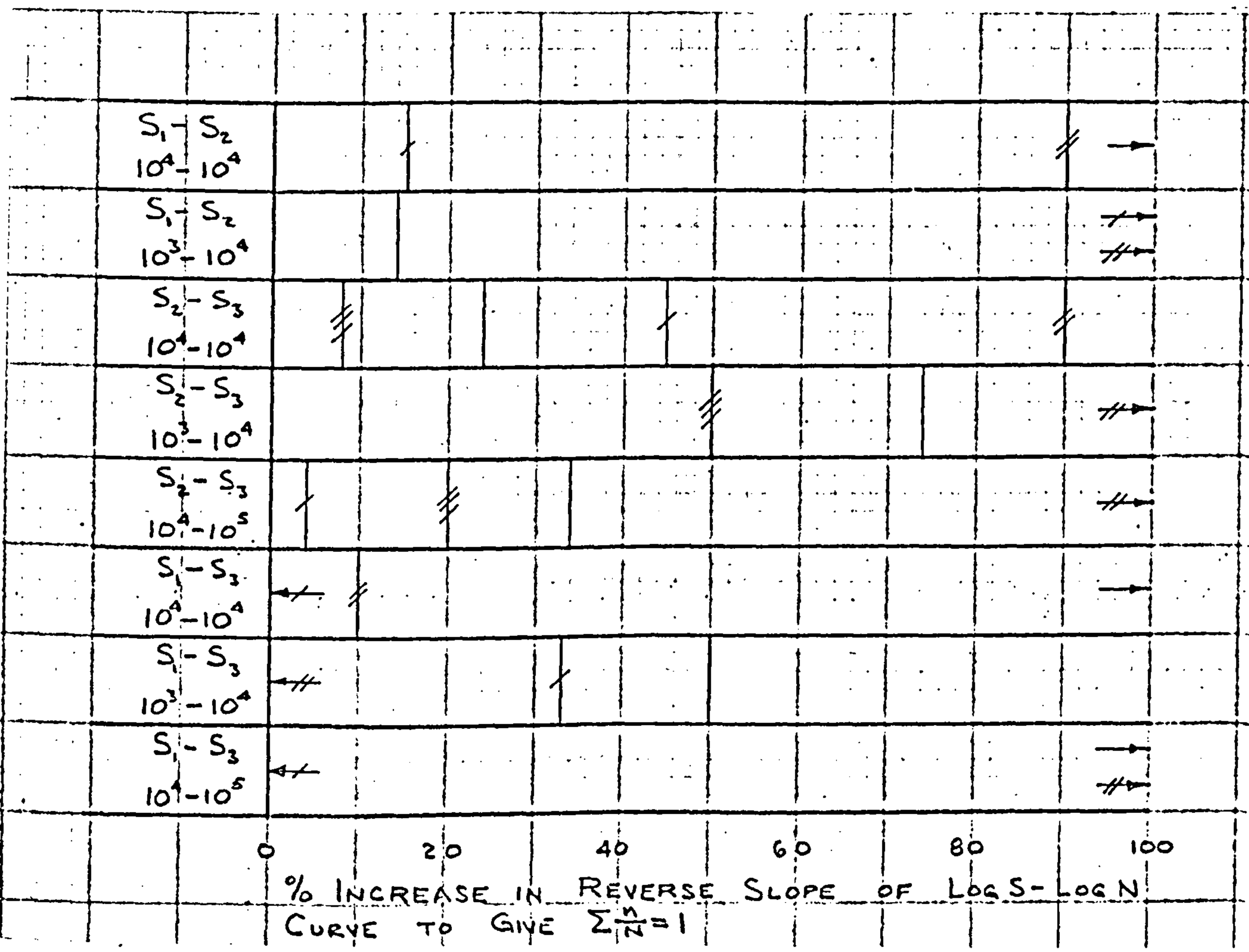

FIGURE 43. COMPARISON OF CUMULATIVE DAMAGE

TEST RESULTS WITH INTERACTION THEORY

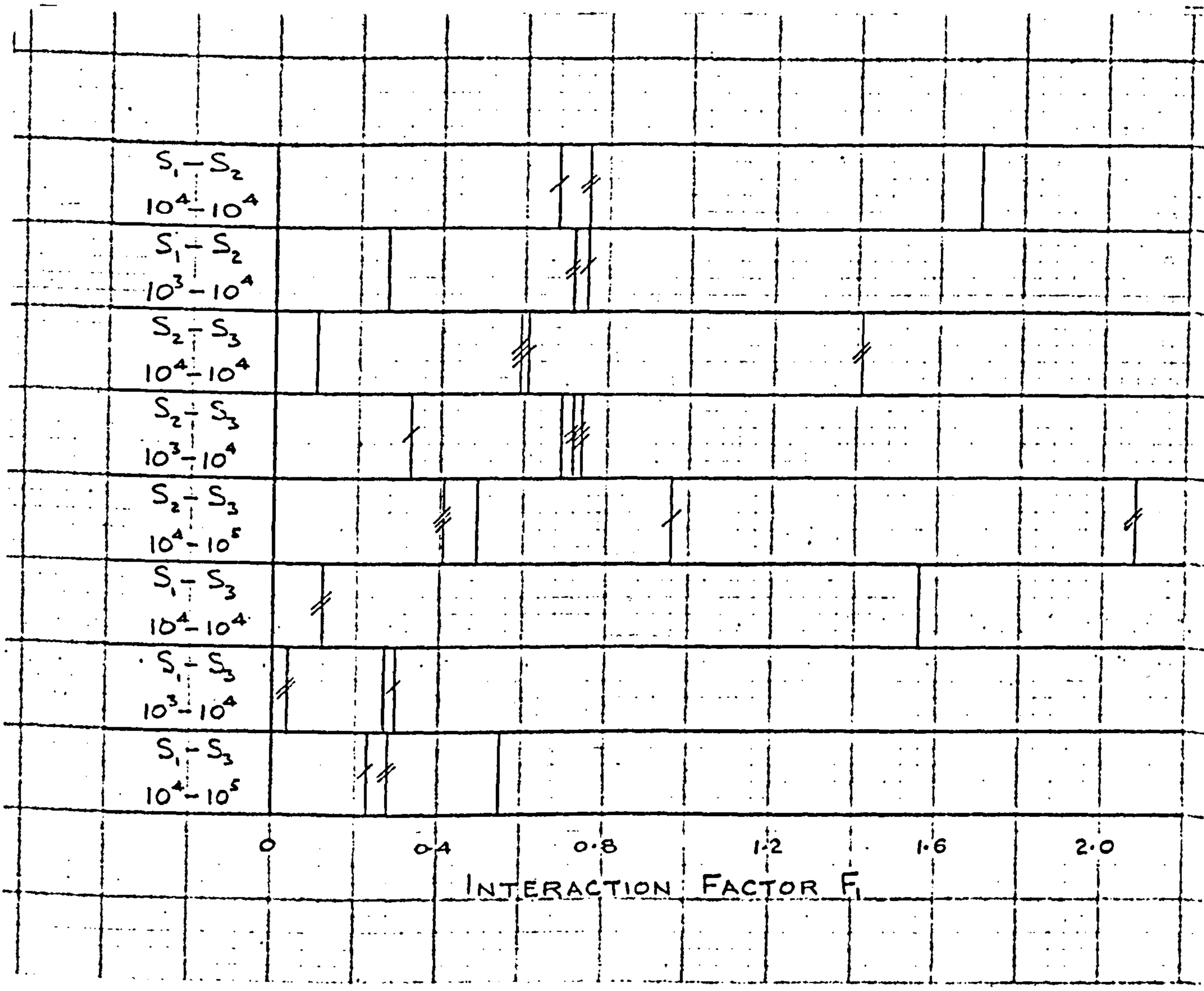

FIGURE 44a. COMPARISON OF CUMULATIVE DAMAGE TEST RESULTS WITH INTERACTION FACTOR F_1

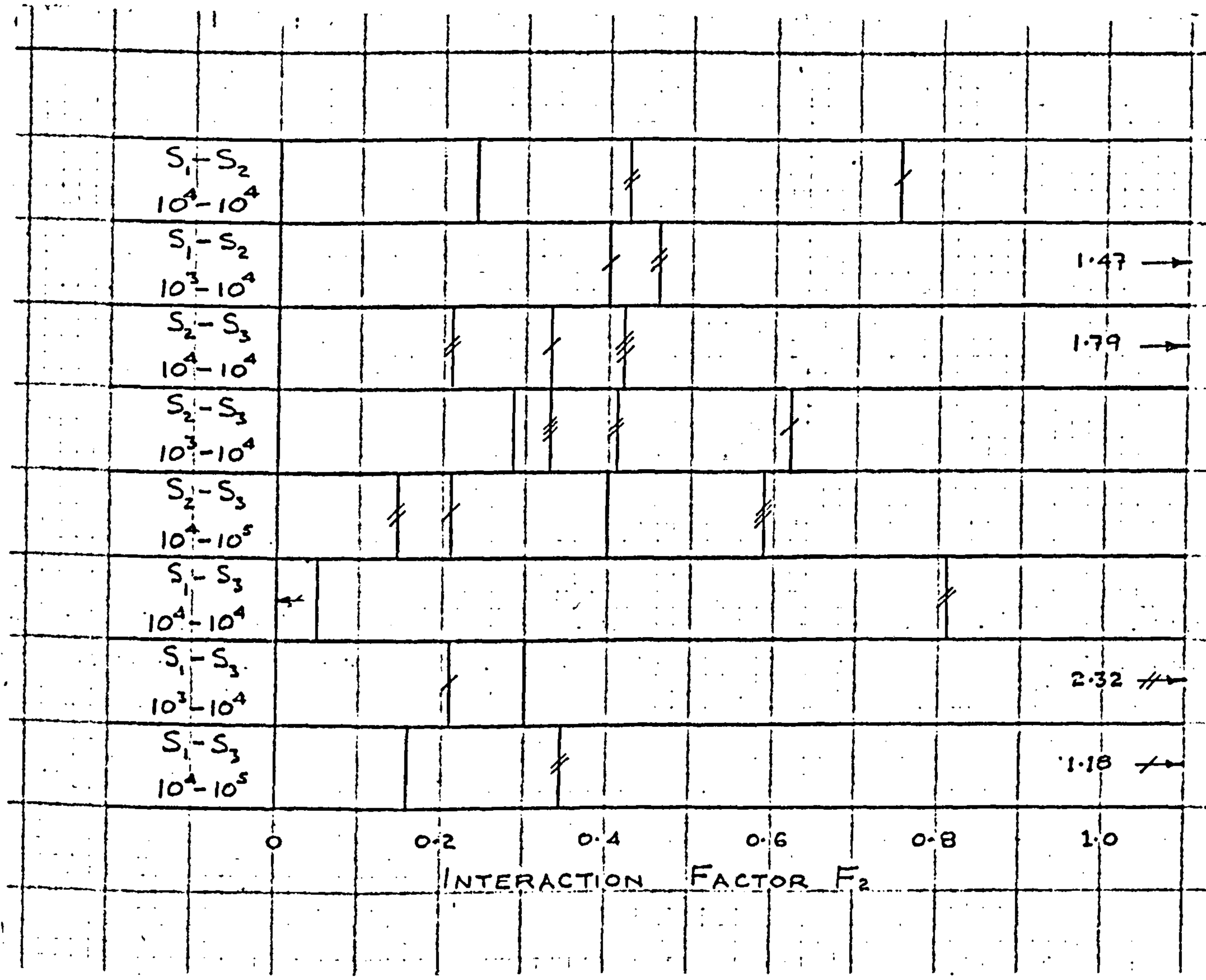

| . K=0

/ K=2

/. K=7.9

/// K=-1

FIGURE 44b. COMPARISON OF CUMULATIVE DAMAGE TEST RESULTS WITH INTERACTION FACTOR F_2.

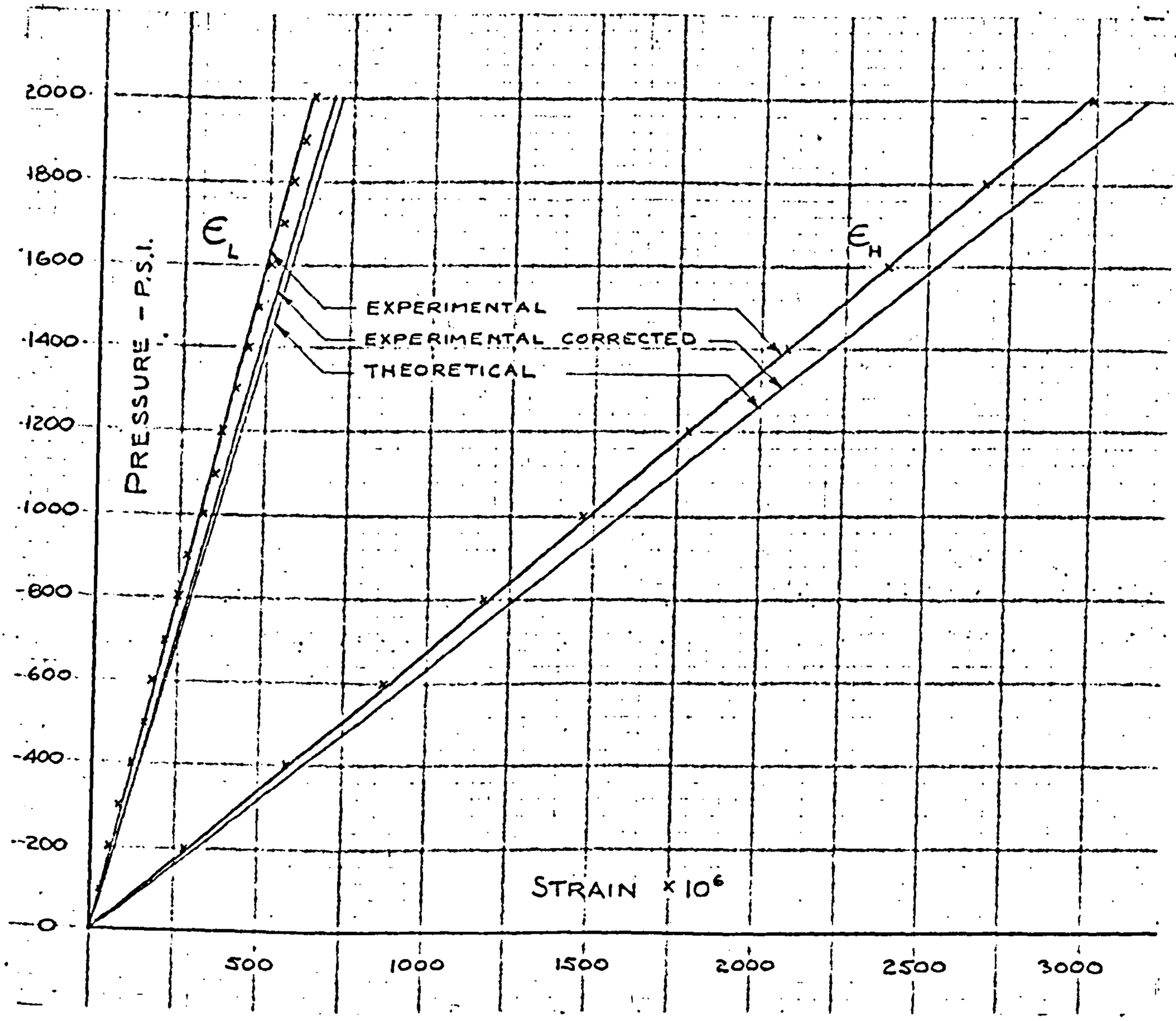

INTERNAL PRESSURE ONLY.
NO PISTON FITTED
MEAN OF SPECIMEN T2 AND T16 RESULTS

FIGURE 45a. PRESSURE - STRAIN CALIBRATION.

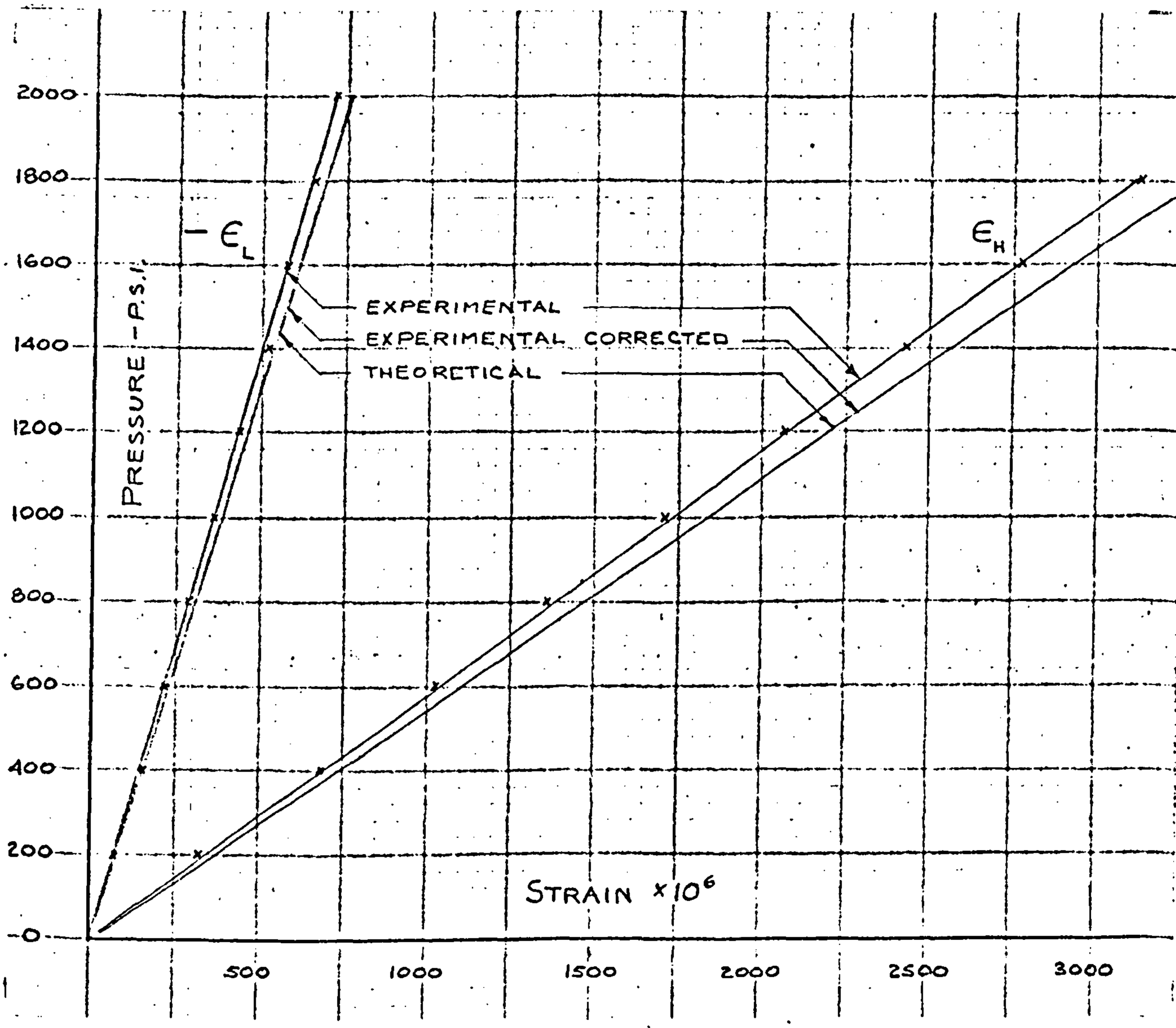

INTERNAL PRESSURE ONLY.
PISTON FITTED.
MEAN OF SPECIMEN T2 AND T16 RESULTS.

FIGURE 45b. PRESSURE - STRAIN CALIBRATION.

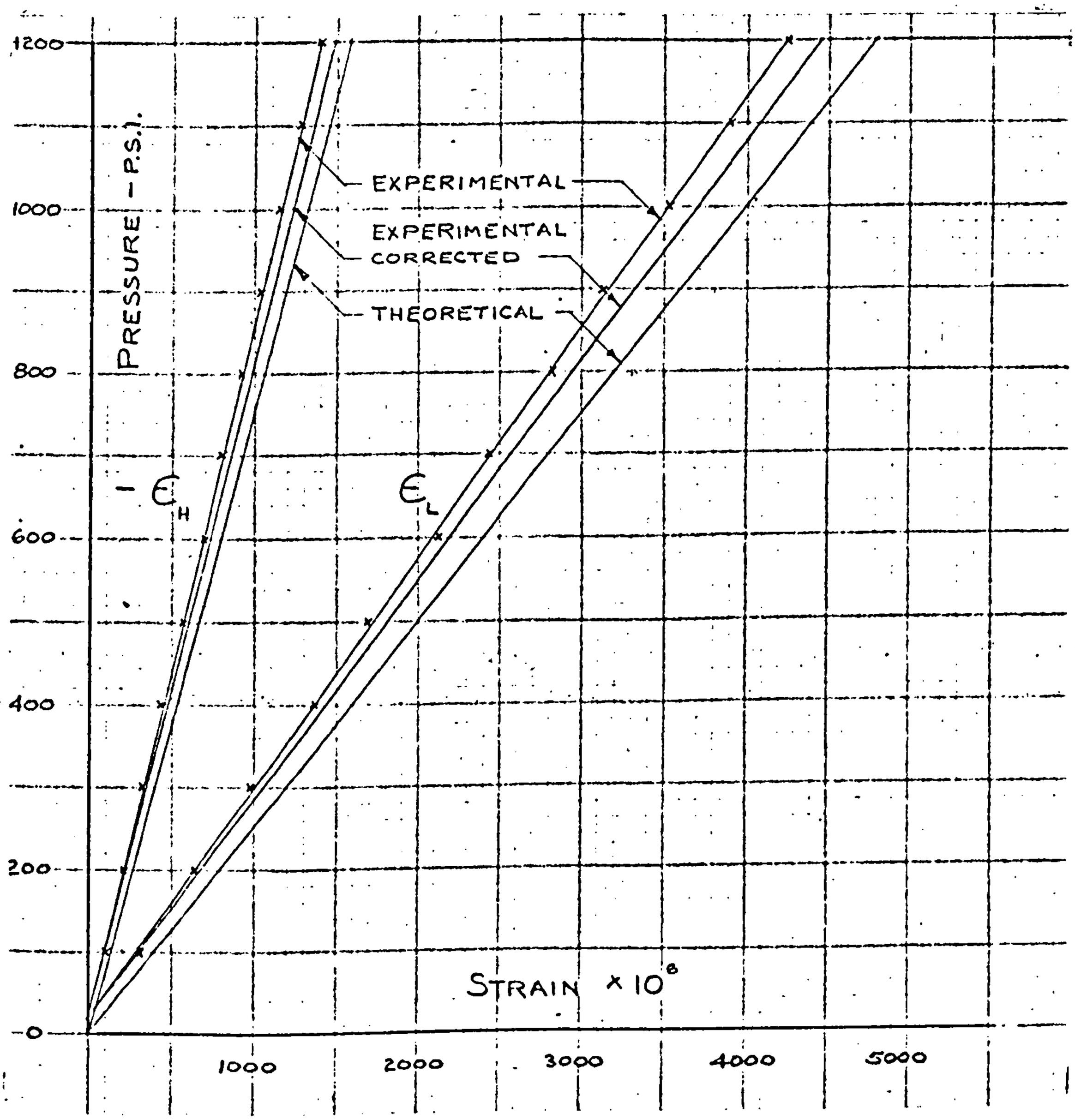

PULL PRESSURE ONLY.

MEAN OF SPECIMEN T2 AND T1G RESULTS.

FIGURE 45c. PRESSURE - STRAIN CALIBRATION.

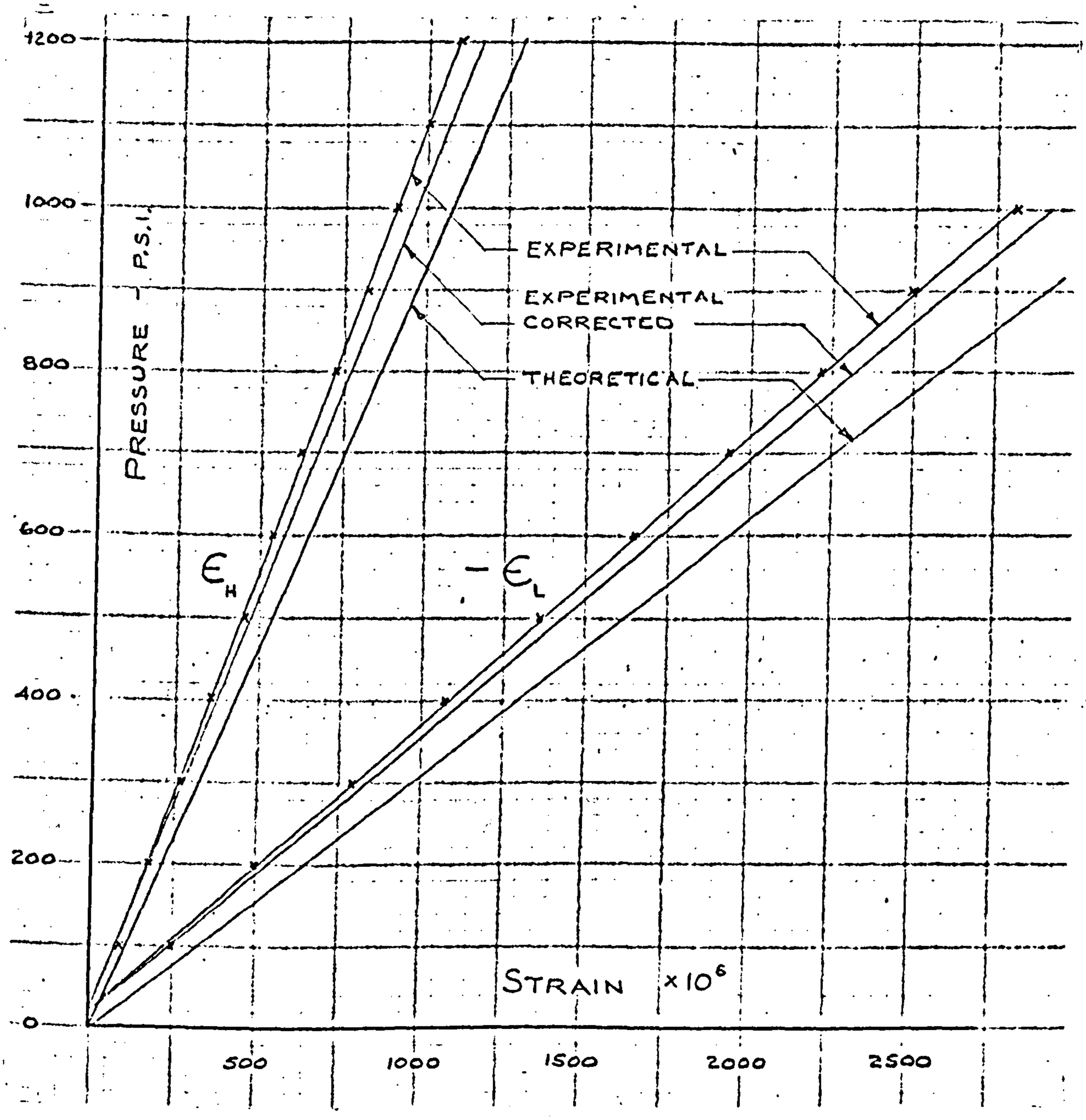

PUSH PRESSURE ONLY

MEAN OF SPECIMEN T2 AND T16 RESULTS

FIGURE 45d. PRESSURE - STRAIN CALIBRATION.

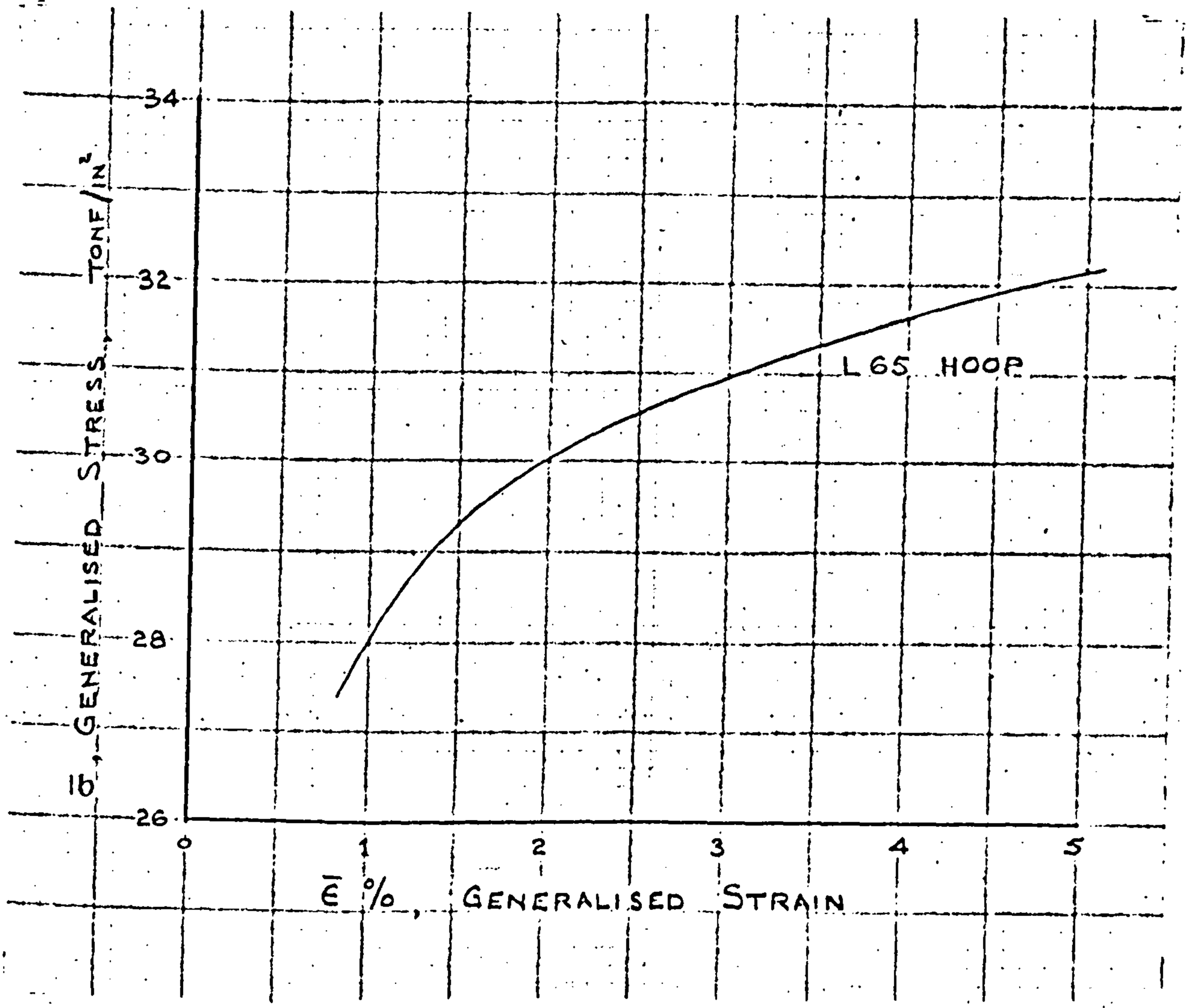

$\bar{\epsilon}$ = EQUIVALENT TOTAL STRAIN

$$= \sqrt{\frac{2}{3}}\left[(\epsilon_1-\epsilon_2)^2+(\epsilon_2-\epsilon_3)^2+(\epsilon_3-\epsilon_1)^2\right]^{\frac{1}{2}}$$

$\bar{\sigma}$ = GENERALISED STRESS

$$= \frac{1}{\sqrt{2}}\left[(\sigma_1-\sigma_2)^2+(\sigma_2-\sigma_3)^2+(\sigma_3-\sigma_1)^2\right]^{\frac{1}{2}}$$

REPRODUCED FROM CROSBY ET AL (43).

FIGURE 46. GENERALISED STRESS STRAIN CURVE FOR 2L65 ALUMINIUM ALLOY.

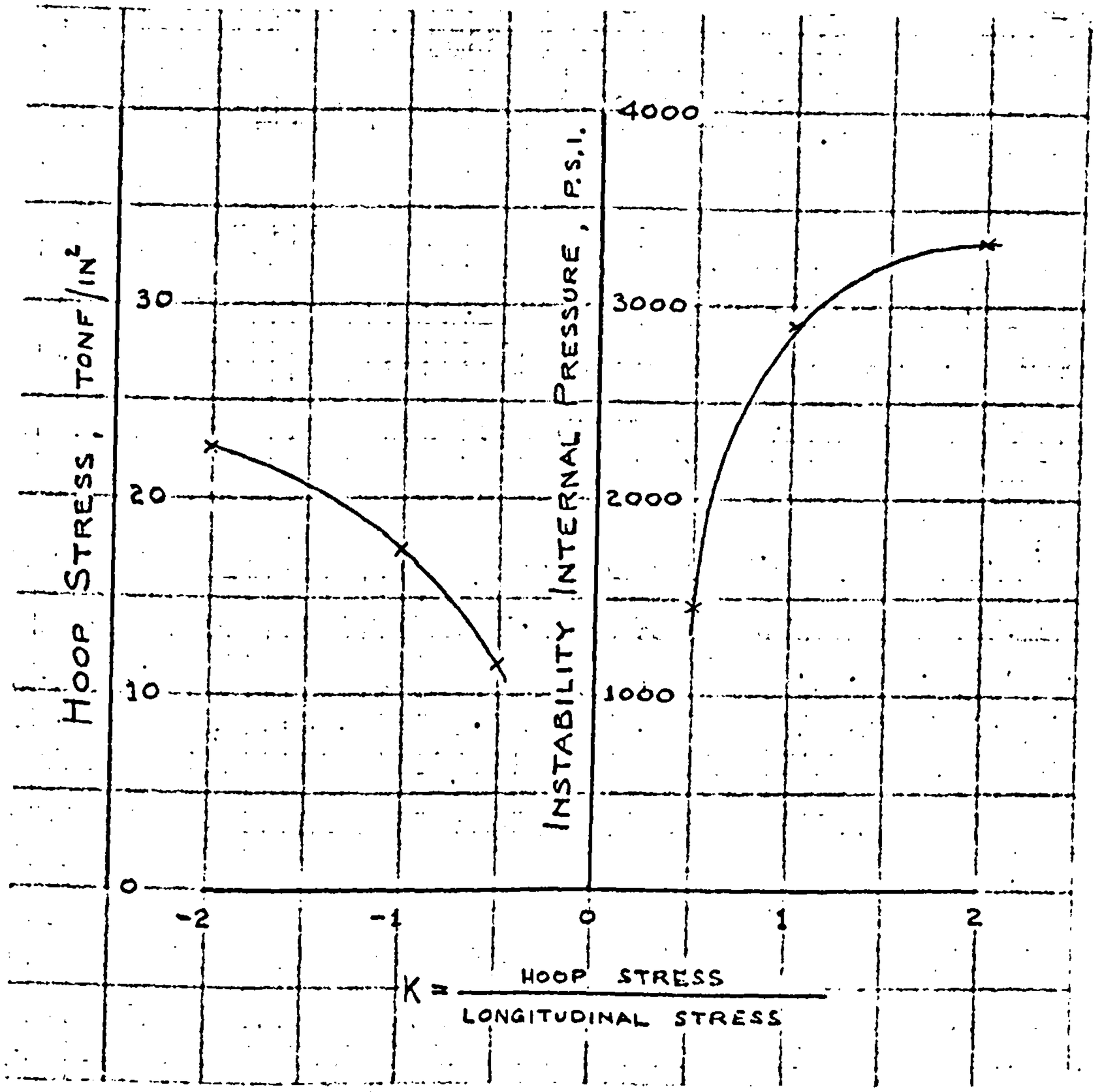

2L65 ALUMINIUM ALLOY TUBE

OUTSIDE DIAMETER 0·915 INCH.
WALL THICKNESS 0·020 INCH.

FIGURE 47. THEORETICAL INSTABILITY PRESSURE FOR THIN WALL TUBE

APPENDIX 1

STRESSES IN ECCENTRIC THIN WALLED CYLINDERS

1. Introduction

In order to minimise additional stress effects due to variations in the wall thickness of the specimens it had been hoped to maintain the wall thickness to 0.020 ± 0.0002 inch. For the first 90 specimens the mean and maximum variations in wall thickness were ± 0.00034 inch and ± 0.0007 inch respectively. The variation was due to difficulties in maintaining the bore of the specimen concentric with the outside diameter. In all cases, with the exception of the closed end case (K = 2), the specimen was in effect fixed at each end and thus no bending could take place. In the closed end case, the specimen was tested without the piston assembly but with an end cap on the top and thus was free to bend. When calculating the required loading for particular test cases, the longitudinal stress was calculated using the minimum mean thickness at the transverse stations considered and the hoop stress was calculated from the Lame equation using the minimum wall thickness and the outside diameter at this station. The outside diameter was used in these calculations as it could be measured more accurately than the inside diameter.

The accuracy of these assumptions is considered in the following calculations.

2. Closed end case (K = 2)

The resultant longitudinal force due to internal pressure acts along the axis of the bore and as the eccentricity, K, increases, the neutral axis of the cross-section moves away from the axis of the bore and so the bending moment $P(e + \bar{y})$ increases with increasing eccentricity. The expression for the maximum longitudinal stress due to the combined effects of end load and bending is found as follows:

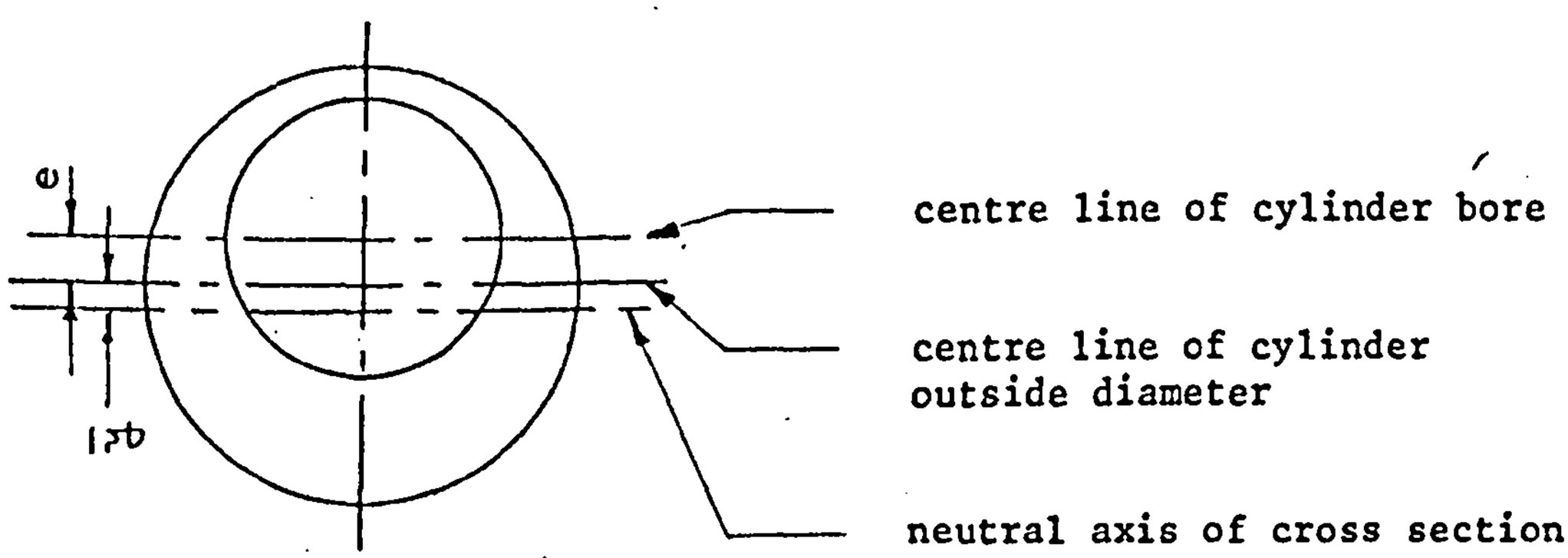

Let P = resultant longitudinal force due to internal pressure

d_1 = bore diameter

d_2 = outside diameter of cylinder

A = cross sectional area of cylinder

I_{NA} = second moment of area of section about neutral axis

e = eccentricity, half the difference between the maximum and minimum wall thicknesses

$\bar{y}$ = distance between the neutral axis and the centre line of the cylinder outside diameter

$\sigma_D = P/A$ = longitudinal direct stress

σ_B = bending stress

Taking moments of area about the neutral axis,

$$\bar{y} \cdot \frac{\pi}{4} d_2^2 = (\bar{y} + e) \cdot \frac{\pi}{4} d_1^2$$

and hence

$$\bar{y} = e \frac{d_1^2}{d_2^2 - d_1^2} \qquad (1)$$

Using the parallel axis theorem,

$$I_{N.A.} = \frac{\pi}{64} d_2^4 + \frac{\pi}{4} d_2^2 \bar{y}^2 - \left[\frac{\pi}{64} d_1^4 + \frac{\pi}{4} d_1^2 (\bar{y} + e)^2\right] \qquad (2)$$

The maximum bending stress occurs at the point furthest from the neutral axis and will be tensile in this case, thus

$$\sigma_B = \frac{P(e + \bar{y})}{I_{N.A.}} \left(\frac{d_2}{2} + \bar{y}\right) \qquad (3)$$

The maximum longitudinal stress is

$$\frac{P}{A} + \sigma_B = \frac{P}{A} + \frac{P(e+\bar{y})}{I_{N.A.}} \left(\frac{d_2}{2} + \bar{y}\right) \qquad (4)$$

Using equation (4) to evaluate the maximum longitudinal stress for the case where d_2 = 0.915 inch, d, = 0.875 inch and e = 0.0007" we find that σ_D = 17.8P and σ_B = 0.66P and thus in the worst possible case σ_B = 3.7% σ_D. For the mean value of e = 0.00034 inch then σ_B = 0.32P and hence σ_B = 1.8% σ_D. In general, for closed end (K = 2) tests, specimens of the least eccentricity were used. Thus the error in the longitudinal stress, due to neglecting the effect of bending, is of the order of 2%. Also, the fatigue strength is a function of the maximum fluctuating shear stress, which in this case is a function of the hoop and radial stresses; the longitudinal stress

being the intermediate principal stress.

In the case of hoop stress the exact solution for eccentric cylinders was first given by Jeffrey (66) and is taken here from Coker and Filon (67). In the case where the distance between the centres of the outside and inside diameters is less than half the internal radius, the maximum hoop stress at the internal surface occurs at the minimum wall thickness and can be calculated from

$$p\left[\left(\frac{2r_2^2}{r_2^2+r_1^2}\right)\left(\frac{r_2^2+r_1^2-e^2-2r_1e}{r_2^2-r_1^2-e^2-2r_1e}\right)-1\right] \qquad (5)$$

where p = internal pressure

r_2 = radius of outside diameter

r_1 = radius of inside diameter

e = eccentricity, distance between centres

$$e < \frac{r_1}{2}$$

The Lamé equation for the maximum hoop stress at the internal surface of a cylinder is given by

$$p\left[\frac{r_2^2+r_1^2}{r_2^2-r_1^2}\right] \qquad (6)$$

In the case of zero eccentricity equation (6) gives a maximum hoop stress of 22.4p. Using equation (6) to evaluate the maximum hoop stress where r_2 = 0.4575", r_1 = 0.4382" and e = 0.0007 inch we obtain max. σ_H = 23.2p, an increase of 3.5% on the nominal max. σ_H. Using equation (5) where r_2 = 0.4575 inch, r_1 = 0.4375" and e = 0.0007 inch we obtain max. σ_H = 23.7p, an increase of 5.8% on the nominal max. σ_H. For the case of e = 0.00034 inch, equations (6) and (5)

give increases of 1.8% and 4.2% respectively, on the nominal max. σ_H. Thus the equation used (6) gives a more conservative estimate of the increase in hoop stress due to eccentric effects. This seems reasonable as the eccentric effects quoted are the worst obtained across any measured cross section of the specimens i.e. the specimens do not have truly eccentric bores. In the worst case possible the maximum error in the value of hoop stress is unlikely to be greater than 1.5%. The above consideration of hoop stress applies to all test cases where internal pressure is applied i.e. all cases except those of longitudinal stress only.

3. Summary

For the specimens used bending stresses due to eccentric bore effects could be neglected. It was satisfactory to calculate longitudinal stresses using the minimum mean wall thickness. The calculation of hoop stress using the Lamé equation based on outside diameter and minimum wall thickness was likely to be accurate within 1.5%.

APPENDIX 2

CALIBRATION OF BIAXIAL FATIGUE TEST MACHINE

1. Introduction and Initial Calibration

The initial static calibration was carried out using four strain gauged specimens, each specimen having four strain gauges mounted at 90° to one another at the centre of the test portion. Two specimens had four longitudinal gauges and two had two gauges each in the longitudinal and transverse directions. The strain readings were obtained using a Boulton-Paul Transducer Meter. This proved to give rather a cumbersome procedure in switching from one strain gauge to the next, recording the strain and ensuring that the pressure in the specimen remained constant at the required level. Further, at the higher strain levels it was difficult to read the meter scale within an accuracy of 3%. In this way static pressure was calibrated against specimen strain for the different machine configurations used. With the use of the appropriate filter the transducer meter strain signals were displayed on an oscilloscope screen to give a calibration of static strain signal against specimen pressure. Similarly via pressure transducers the pressure signals were displayed on the oscilloscope. Thus static pressure and static strain were calibrated and could be displayed on the 4 trace oscilloscope. This calibration was used to check that in the dynamic pressure cases the full equivalent strain ranges were obtained. This proved to be the case within the $\pm$ 1½% degree of accuracy in reading the oscilloscope. A check showed that the strains produced by the longitudinal and internal pressure circuits were out of phase, when displayed on the oscilloscope. This was corrected by adjusting the phase relationship in the output controls of the oscillator.

2. Details of Static Calibration

Towards the end of the constant amplitude tests oil leaks from the seals, particularly the piston shaft seal, became unacceptable. It was decided to conduct a complete static pressure re-calibration to compare the effects of seal friction on the worn out seals, before they were discarded, and the new seals to be fitted. Another reason for re-calibration was that a data logging system with typewriter print-out had become available and this provided a quicker and more accurate means of strain recording.

As some difficulty had been experienced on previous calibration specimens due to the hydraulic oil unavoidably coming into contact with the strain gauge adhesive, two new calibration test specimens (T2 and T16) were prepared. These specimens had identical wall thickness dimensions of 0.0203 inch ± 1%. Specimen T2 was fitted with two longitudinal and two transverse strain gauges and specimen T16 with four longitudinal strain gauges. All gauges were coated with a thin layer of protective coating.

2.1 Calibration Cases

The calibration cases to be considered were

1. Specimen gauge calibration in tensile test machine.
2. Internal pressure only - no piston fitted.
3. Internal pressure only - piston fitted.
4. Pull pressure (tension on test specimen).
5. Push pressure (compression on test specimen).

2.1.1 Specimen gauge calibration

A 30 tonf capacity Amsler static testing machine was used for this purpose. As this machine was to be used over the low load

range of up to 1 tonf the machine calibration was checked using dead weights, themselves accurate to 0.02%, from zero to 400 lbf and found to be within 0.1%.

Tensile tests on both specimens showed the strain readings to be 5% low. This could be due to one or more of the following causes:

1. Inaccuracy in wall thickness measurement.
2. Variation in wall thickness of specimens.
3. Inaccuracy in the value of Young's Modulus used.
4. Possible error of $\pm$ 1½% in strain gauge readings.
5. The effect of the protective coating on the strain gauges.

Bending stresses of $\pm$ 3½% found in both specimens were allowed for.

Thus strain gauge readings have to be multiplied by 1.05.

2.1.2 Internal pressure only - no piston fitted

In this case the piston assembly is not fitted; the specimen being capped at the upper end.

For specimens of 0.875 inch I.D. and 0.0203 inch wall thickness

$$\sigma_L = 10.50\ p_{INT}\ \text{lbf/in}^2$$

and $\sigma_H = 20.15\ p_{INT}\ \text{lbf/in}^2$ (using the Lamé equation)

at the outer wall

where p_{INT} = internal pressure in lbf/in^2

Thus $$\epsilon_L = \frac{p_{INT}}{10.6 \times 10^6} \left[10.50 - 0.328 \times 20.15\right] = + 0.367 \times 10^6\ p_{INT}$$

$$\epsilon_H = \frac{p_{INT}}{10.6 \times 10^6} \left[20.15 - 0.328 \times 10.50\right] = +1.578 \times 10^6 \, p_{INT}$$

For specimen T16, at a pressure of 2000 lbf/in^2 the mean measured longitudinal strain was 647 x 10^{-6} giving a corrected value of 680 x 10^{-6} compared with a theoretical value of 734 x 10^{-6}. Small differences in the values of σ_L and σ_H can make an appreciable difference to the value of ϵ_L.

For specimen T2, at a pressure of 2000 lbf/in^2, the mean measured hoop strain was 3000 x 10^{-6} giving a corrected value of 3150 x 10^{-6} compared with a theoretical value of 3160 x 10^{-6}.

If the maximum differences in strain readings obtained in each case are assumed to be caused entirely by bending effects then the bending stresses occurring are 2.2% and 4.0% of the mean stresses for specimens T16 and T2 respectively.

The mean measured strains are shown plotted against internal pressure in Fig. 45a.

2.1.3 Internal pressure only with piston fitted

For this case

$$\sigma_L = +2.79 \, p_{INT} \text{ lbf/in}^2$$

and $$\sigma_H = +20.15 \, p_{INT} \text{ lbf/in}^2$$ (using the Lamé equation)

at the outer wall.

Thus $$\epsilon_L = \frac{p_{INT}}{10.6 \times 10^6} \left[2.79 - 0.328 \times 20.15\right] = -0.360 \times 10^{-6} \, p_{INT}$$

$$\epsilon_H = \frac{p_{INT}}{10.6 \times 10^6} \left[20.15 - 0.328 \times 2.79\right] = +1.818 \times 10^{-6} \, p_{INT}$$

For specimen T16, at a pressure of 2000 lbf/in^2, the mean measured longitudinal strain was 728 x 10^{-6} giving a corrected value

of 765 x 10^{-6} compared with a theoretical value of 720 x 10^{-6}, i.e. 6% greater than expected.

For specimen T2, at a pressure of 2000 lbf/in^2, the mean measured hoop strain was 3604 x 10^{-6} giving a corrected value of 3780 x 10^{-6} compared with a theoretical value of 3636 x 10^{-6}, i.e. 4% greater than expected.

If it is assumed that the longitudinal stress is only 90% effective due to the effect of seal friction in the shaft seal then we have

$$\epsilon_L = -0.387 \times 10^{-6}\ p_{INT}$$

and $$\epsilon_H = +1.825 \times 10^{-6}\ p_{INT}$$

For specimen T16 the corresponding longitudinal strain values become 765 x 10^{-6} as measured and 774 x 10^{-6} as predicted, while for specimen T2 the corresponding hoop strain values become 3660 x 10^{-6} as measured and 3650 x 10^{-6} as predicted. Thus the discrepancy found can be explained by the effect of seal friction.

The bending effects found in this case, again assuming bending to be the sole cause of differences in strain readings, are 1.5% and 3.5% for specimens T16 and T2 respectively.

The mean measured strains are shown plotted against internal pressure in Fig. 45b.

2.1.4 Pull pressure (full bore side of piston pressurised)

In this case

$$\sigma_L = +42.12\ p_{BORE}\ \text{lbf/in}^2$$

where p_{BORE} = pressure on full bore side of piston in lbf/in^2

Thus $$\epsilon_L = \frac{p_{BORE}}{10.6 \times 10^6} \times 42.12 = +3.980 \times 10^{-6}\ p_{BORE}$$

and $$\epsilon_H = \frac{-p_{BORE}}{10.6 \times 10^6} \times 42.12 \times 0.328 = -1.302 \times 10^{-6}\, p_{BORE}$$

For specimen T16, at a pressure of 1200 lbf/in^2, the mean measured longitudinal strain was 4226×10^{-6} giving a corrected value of 4450×10^{-6} compared with a theoretical value of 4780×10^{-6}, i.e. 7% less than expected.

For specimen T2, at a pressure of 1200 lbf/in^2, the mean measured longitudinal strain was 4218×10^{-6} giving a corrected value of 4440×10^{-6} compared with a theoretical value of 4780×10^{-6}, again 7% less than expected.

With the same assumptions as before the bending effects found were 1.4% and 3.4% for specimens T16 and T2 respectively.

Thus piston seal friction was found to account for 7% of the pull load so that the actual tensile load on the specimen is 0.93 of the applied pressure load.

The mean measured strains are shown plotted against pull pressure in Fig. 45c.

2.1.5 Push pressure (annulus side of piston pressurised)

In this case

$$\sigma_L = -34.33\, p_{ANN} \text{ lbf/in}^2$$

where p_{ANN} = pressure on annulus side of piston in lbf/in^2

Thus $$\epsilon_L = \frac{-p_{ANN}}{10.6 \times 10^6} \times 34.33 = 3.240 \times 10^{-6}\, p_{ANN}$$

and $$\epsilon_H = \frac{p_{ANN}}{10.6 \times 10^6} \times 34.33 \times 0.328 = +1.060 \times 10^{-6}\, p_{ANN}$$

For specimen T16, at a pressure of 1200 lbf/in^2, the mean

measured longitudinal strain was 3338 x 10^{-6} giving a corrected value of 3500 x 10^{-6} compared with a theoretical value of 3890 x 10^{-6}, i.e. 10% less than expected.

For specimen T2, at a pressure of 1200 lbf/in^2, the mean measured longitudinal strain was 3300 x 10^{-6} giving a corrected value of 3465 x 10^{-6} compared with a theoretical value of 3890 x 10^{-6}, i.e. 10.5% less than expected.

The bending effects found in this case were a maximum of 1.5% and 2.8% in the cases of specimen T16 and T2 respectively.

Thus piston seal friction was found to account for 10% of the push load so that the actual compressive load on the specimen is 0.90 of the applied pressure load.

The mean measured strains are shown plotted against push pressure in Fig. 45d.

3. Discussion

The seal friction effects found above have been allowed for when calculating stresses in the test specimens. It should be noted from Figs. 45c and d that the seal friction effect is not a constant percentage of the applied pressure load.

For specimens T16 and T2 the maximum bending effect found was 4% of the applied stress and this on the assumption that no other effect, such as variation in wall thickness, was present. With threaded ends on the specimens it is virtually impossible to completely eliminate bending effects. It is likely that bending effects in this work have been controlled to a possible limit of the order of 2%.

The strain readings recorded for cases 2.1.3, 4 and 5 were 1% greater in the case of the worn seals compared with those found with the new seals installed. The new seals had to be 'run-in' by hand on the bench before installation.

Test stresses calculated using the initial calibration figures were corrected according to the details of the calibration using specimens T16 and T2 as described here.

APPENDIX 3

SUMMARY OF SETTING-UP PROCEDURE FOR A PROGRAMME FATIGUE TEST

1. Test specimen assembled in test rig.
2. Pressure cocks to specimen closed.
3. Switch all systems to active.
4. Switch hydraulic pump on.
5. Set oscillator cycling frequency.
6. Run pressure systems at suitable pressure ranges for 20 minutes in order to warm up oil.
7. Check calibration of both pressure circuits using test pressure gauge and four trace oscilloscope.
8. Open pump house access flap.
9. Set programmer to 'controller'.
10. Set 'static' and 'dynamic' controls, in both pressure circuit, on controller to allow approximately twice the required dynamic pressure range, noting the control setting numbers.
11. Adjust pressure switch to required pressure.
12. Switch programmer from 'controller' to 'programmer'.
13. Using the programmer controls (mean and dynamic) set up the required mean and dynamic pressure ranges required. Note that the dynamic pressure range required, in this condition of test specimen isolated from pressure, in order to achieve the full required pressure range when the pressure cocks to the specimen are opened has been pre-determined using a thicker walled specimen.

14. Switch off 'dynamic' pressure at controller.

15. Set up programme by (a) resetting the cycle counter (b) switch cycle counter to on (c) reset internal cycle counter (d) reset programme levels (c) set cycle block lengths (f) set number of blocks and (g) switch on first block.

16. Set up mean pressures (controller settings already noted).

17. Switch pressure switch to 'active'.

18. Open pressure cocks to test specimen.

19. Switch on 'dynamic' pressures at the controller (settings already noted).

20. Trim pressure controls.

APPENDIX 4

INSTABILITY OF THIN WALL TUBES UNDER INTERNAL PRESSURE AND END LOAD

When a thin walled cylinder of ductile material is subjected to an internal pressure and an end load which are in phase, there is a particular pressure and corresponding generalised strain at which gross localised plastic strain (i.e. instability) occurs with no further increase in pressure. Fracture may occur before instability in the case of a material of low ductility or which contains flaws.

Crosby et al (43) in a study of the effects of stress biaxiality on the high-strain fatigue behaviour of BS L65C aluminium alloy, the same alloy as used in the present work, investigated such instability conditions for stress ratios K = ½, 1, 2 and -2. They found that instability occurred before fracture. For a thin walled cylinder of infinite length subjected to a constant ratio of hoop to longitudinal stress, its instability pressure and strains can be related to a particular point on the generalised stress-strain for the material (97). This theory and the generalised stress-strain curves shown in Fig. 46 were used to calculate instability pressures which were compared with experimental data. The effect of anisotropy was allowed for by using the generalised stress-strain curves for longitudinal and transverse specimens to calculate upper and lower bounds, respectively, for the instability pressure. Good agreement was found between theoretical and experimental instability pressures when the transverse generalised stress-strain curve was used. It was also noted that the effect of finite length on the instability behaviour of cylinders, subjected to internal pressure only, has been considered

by Weil (98) and that his analysis suggested that the length to radius ratio of the cylinders used will have an insignificant effect on their instability behaviour. This can also be assumed for the cylinders used in the present work.

The transverse generalised stress-strain curve of Fig. 46 has been used to calculate the theoretical instability pressure values for the thin walled cylinders used in the present work, again using the theory of reference (97). The results are shown in Fig. 4.7. Instability effects experienced during the experimental work are discussed in Chapter 6.4.